Machine Learning-Enhanced Sensing Capability of Graphene Oxide and Reduced Graphene Oxide Embedded in a Nano-cellulose Matrix

Ghazaleh Ramezani

A Thesis

In the Department

of

Department of Mechanical, Industrial and Aerospace Engineering

Presented in Partial Fulfillment of the Requirements

For the Degree of

Doctor of Philosophy

at Concordia University

Montréal, Québec, Canada

January 2026

© Ghazaleh Ramezani, 2026

CONCORDIA UNIVERSITY

SCHOOL OF GRADUATE STUDIES

This is to certify that the thesis prepared

By: **Ghazaleh Ramezani**

Entitled: **Machine Learning-Enhanced Sensing Capability of Graphene Oxide and Reduced Graphene Oxide Embedded in a Nano-cellulose Matrix**

and submitted in partial fulfillment of the requirements for the degree of

DOCTOR OF PHILOSOPHY ([Your Department])

complies with the regulations of the University and meets the accepted standards with respect to originality and quality.

Signed by the final examining committee:

_____ Chair
[*Chair's Name]*

_____ External Examiner
[*Examiner's name]*

_____ Examiner
[*Examiner's name]*

_____ Examiner
[*Examiner's name]*

_____ Examiner
[*Examiner's name]*

_____ Thesis Supervisor
[*Supervisor's name]*

Approved by _____

[Graduate Program Director]

[Month/day/year] _____

[Dean's Name]

[Faculty Name]

Abstract

Machine Learning-Enhanced Sensing Capability of Graphene Oxide and Reduced Graphene Oxide Embedded in a Nano-cellulose Matrix

Ghazaleh Ramezani, Ph.D.

Concordia University, 2026

This thesis addresses the critical need for sustainable, high-performance materials by exploring eco-friendly nanocomposites composed of graphene oxide (GO) and reduced graphene oxide (rGO) within a nanocellulose matrix. Nanocellulose, in the form of cellulose nanocrystals and nanofibers, is preferred due to its nanoscale dimensions that provide a high surface area, enhanced flexibility, and superior mechanical and chemical reactivity, making it an ideal matrix for integrating functional nanomaterials. GO and rGO complement each other: GO's oxygen-containing groups facilitate surface modification and dispersion in aqueous media, while rGO restores electrical conductivity necessary for biosensing and flexible electronics. In this work, GO and rGO were synthesized and reduced using green agents like citric and L-ascorbic acids, offering scalable and safer alternatives to conventional methods.

Experimental studies on nanocellulose/GO and nanocellulose/rGO films demonstrated exceptional electrical conductivity, mechanical strength, and environmental stability, vital for wearable electronics and biosensors. Spectroscopic, microscopic, and electrochemical analyses revealed the roles of hydrogen bonding, π–π interactions, and composite architecture in performance. Predictive modeling using Lasso regression and neural networks established robust composition–property relationships with high accuracy ($R^2 > 0.99$).

Overall, this research confirms that nanocellulose composites with GO and rGO are renewable, recyclable, and functional under ambient conditions, presenting promising applications in biosensing, smart packaging, and health monitoring. The study advances our understanding of why nanocellulose and GO/rGO-based hybrids are uniquely suited, fostering progress in sustainable functional materials at the nanoscale.

Acknowledgments

I would like to express my deepest and most sincere gratitude to my thesis supervisors, Professor Ion Stiharu and Professor Theo G.M. van de Ven, for their unwavering guidance, intellectual generosity, and continuous encouragement throughout every stage of my doctoral journey. Professor Stiharu's expertise in mechanical engineering and MEMS, his meticulous attention to experimental rigor, and his constant availability for discussion have shaped the way I approach scientific problems. Professor van de Ven's profound knowledge of cellulose chemistry, his creativity in research, and his remarkable ability to connect fundamental science with practical application have left a lasting impression on my thinking as a researcher. Together, their complementary expertise provided me with a truly interdisciplinary foundation that made this work possible. I also wish to thank Professor Vahe Nerguizian for his helpful contributions and collaborative involvement in several of the publications comprising this thesis.

I am thankful to the Department of Mechanical, Industrial, and Aerospace Engineering at Concordia University for providing me with an exceptional academic environment, access to state-of-the-art facilities, and the support necessary to carry out this research.

Finally, and above all, I owe an immeasurable debt of gratitude to my family — my beloved mom and dad, and my dear brother Hossein — for their unconditional love, endless patience, and selfless sacrifices throughout this long and demanding journey. The distance between us made every word of encouragement all the more precious, and knowing you were always there, even from across the world, has been my greatest source of strength. This achievement belongs to all of us.

Dedication

To my beloved family,

for their endless love, support, and encouragement.

Table of Contents

List of Figures

List of Tables

List of Symbols/Abbreviations/Glossary/Equations/Other

Abbreviation	Full Form
2D	Two-dimensional
AI	Artificial Intelligence
ANN	Artificial Neural Network
CNC	Cellulose Nanocrystals
CNF	Cellulose Nanofibers
CNT	Carbon Nanotubes
CPF	Chlorpyrifos
CVD	Chemical Vapor Deposition
DIC	Digital Image Correlation
DSC	Differential Scanning Calorimetry
ECC	Engineered Cementitious Composites
FLG	Few-Layer Graphene
FTIR	Fourier Transform Infrared Spectroscopy
GNP	Graphene Nanoplatelets
GO	Graphene Oxide
GOQD	Graphene Oxide Quantum Dots
GQD	Graphene Quantum Dots
HNC	Hairy Nanocrystalline Cellulose
HNT	Halloysite Nanotubes
IoT	Internet of Things
LCA	Life Cycle Analysis
LED	Light-Emitting Diode
MFC	Microfibrillated Cellulose
MXene	A Class of 2D Transition Metal Carbides, Nitrides, or Carbonitrides
NFC	Nanofibrillated Cellulose
PHBV	Poly(3-hydroxybutyrate-co-3-hydroxyvalerate)
PSO	Particle Swarm Optimization
PVA	Polyvinyl Alcohol
PVP	Polyvinylpyrrolidone
RSM	Response Surface Methodology
SA	Starch Acetate
SEM	Scanning Electron Microscopy
SNEDDS	Self-Nanoemulsifying Drug Delivery System

Abbreviation	Full Form
TGA	Thermogravimetric Analysis
TEM	Transmission Electron Microscopy
UTS	Ultimate Tensile Strength
UV	Ultraviolet

Chapter 1: Introduction to Nanomaterials

1.1 The Need for Nanomaterials and Their Environmental Context

Over the past decades, nanomaterials have emerged as transformative enablers of technologies that combine performance, miniaturization, and sustainability. Their defining characteristic—high specific surface area coupled with tunable physical, chemical, and electronic properties—has enabled progress across the fields of energy storage, catalysis, electronics, filtration, sensing, and medicine. The necessity for nanomaterials arises from global imperatives: reducing the material intensity of advanced technologies, improving functional efficiency, and transitioning toward environmentally benign processes. At the same time, the environmental burden associated with nanomaterial synthesis, dispersion, and recycling must be critically addressed. Persistent nanoparticles, heavy-metal-based systems, and poorly degradable carbon nanostructures pose ecological and health risks if unregulated. Consequently, the design of sustainable and biodegradable nanomaterials has become an essential direction driving current research.

1.2 Impact on Biological Systems and the Environment

While nanomaterials offer revolutionary potential, their high reactivity and biological accessibility necessitate careful evaluation of environmental and physiological interactions. Inhalable or ingestible nanoscale particles may cause oxidative stress or membrane disruption in organisms, highlighting the importance of studying bioaccumulation and ecotoxicity pathways. Research trends now prioritize *green-by-design* nanomaterials, where both synthesis and end-of-life processes align with the circular economy. Using renewable sources such as biomass-derived cellulose for producing nanostructures presents one of the most promising strategies to reconcile technological advancement with sustainability.

1.3 Capabilities and Classification of Nanomaterials

Nanomaterials can be broadly grouped into inorganic (metal-based, metal–oxide, layered 2D) and organic (biopolymeric, carbon-based) categories. Inorganic nanostructures often provide exceptional electrical and mechanical performance, while organic nanomaterials exhibit biodegradability and compatibility with living systems. Among inorganic systems, graphene derivatives—graphene oxide (GO) and reduced graphene oxide (rGO)—have attracted exceptional attention for their remarkable electrical conductivity and mechanical strength. In comparison, emerging carbon allotropes such as fullerenes and warped graphene nanosheets offer prospective electronic and catalytic functionalities that remain under intensive exploration. These advanced materials, while beyond the direct scope of this thesis, deserve attention as future candidates capable of revolutionizing electronic transport, charge storage, and drug delivery efficiencies.

1.4 Organic Nanomaterials: The Case of Nanocellulose

On the other end of the spectrum, organic nanomaterials such as nanocellulose (NC) represent an abundant, renewable, and environmentally compatible alternative. Derived from cellulose, the most widespread natural polymer on Earth, nanocellulose exists mainly as cellulose nanocrystals (CNCs), hairy nanocelluloses (HNCs), cellulose nanofibrils (CNFs), and bacterial cellulose (BC). CNCs feature high crystallinity and stiffness; HNC offer ease of chemical modification; CNFs exhibit flexibility and network-forming capability; BC offers exceptional purity and mechanical resilience. Production typically involves environmentally conscious pathways such as acid hydrolysis, mechanical fibrillation, or biosynthesis. These routes consume minimal toxic reagents and generate biodegradable products. Owing to their large surface area, film-forming ability, and modifiable surface chemistry, nanocellulose materials are increasingly recognized as prime candidates for flexible and biodegradable electronic and sensing devices.

1.5 Synergy Between Inorganic and Organic Nanostructures

Combining 2D inorganic nanomaterials (GO, rGO) with organic nanofibrous matrices such as CNC or CNF leads to hybrid structures that unite sustainability with advanced functionality. Graphene derivatives provide exceptional mechanical reinforcement and electrical conductivity, while the nanocellulose network offers stability, flexibility, and biodegradability. This synergy addresses key limitations of non-recyclable conventional composites, producing multifunctional films that maintain structural integrity, conductivity, and biocompatibility. The resulting nanocomposites not only minimize environmental impact but also open avenues for recyclable, low-energy manufacturing of sensors, flexible electronics, and smart packaging systems.

1.6 Scope and Structure of the Thesis

This doctoral thesis is rooted in the need to merge high-performance two-dimensional (2D) nanomaterials with environmentally sustainable organic matrices. The work is uniquely structured around four published research articles that collectively form the core of the dissertation. These articles present the original methodologies, experiments, and key findings produced during the PhD research. The remaining two chapters draw extensively on published literature and additional results, synthesizing them with insights gained from the primary publications to provide comprehensive context, advanced discussion, and future perspectives.

Altogether, the thesis demonstrates a highly productive research program, comprising the publication of eight papers, with continued work leading to further contributions in the field. Chapter 1 establishes the conceptual framework, discussing environmental motivation, material selection, and the sustainability of nanomaterials. Chapter 2 summarizes recent advances in integrating 2D materials like graphene oxide with cellulose for diagnostics and biosensing. Chapters 3 and 4 focus on the design, fabrication, and optimization of nanocellulose-based hybrid systems, addressing challenges in scalability, environmental impact, and biomedical applications through original results and multi-objective optimization. The final chapters consolidate this knowledge base, offering scientific reflection, a synthesis of findings, and directions for future study.

These chapters together form a coherent narrative connecting environmental responsibility with innovative, functional nanotechnology. The thesis highlights how sustainable material synthesis, rigorous optimization, and cross-disciplinary research converge to build the next generation of recyclable, high-performance hybrid nanomaterials, underlining both academic impact and real-world applications.

Closure

This chapter set out to establish the conceptual and scientific foundation on which the rest of the thesis rests. The central argument (that the global need for miniaturized, high-performance, and environmentally responsible technologies demands a new generation of nanomaterials) was developed through several converging perspectives. The environmental burden of conventional nanoparticle systems was acknowledged alongside the opportunities that renewable, biodegradable alternatives now offer. The main material families were introduced and classified: inorganic nanostructures such as graphene oxide and reduced graphene oxide stand out for their exceptional electrical and mechanical properties, while organic nanomaterials, in particular nanocellulose in its various forms (CNC, CNF, HNC, BC), offer biocompatibility, surface versatility, and sustainability. The rationale for combining these two families was made explicit: the resulting hybrids inherit the conductivity and mechanical strength of graphene derivatives while retaining the renewability and film-forming capacity of the cellulose matrix. This synergy directly motivates the experimental and analytical work that follows. The chapter also defined the structure of the thesis, identifying how each subsequent chapter contributes to a coherent account of material design, characterization, optimization, and application. Together, these introductory arguments frame the research not merely as a materials study but as a contribution to sustainable nanotechnology.

Chapter 2: GO/rGO and Nanocellulose Materials—Properties, Fabrication, and Characterization

This chapter is a published paper in **Micromachines (2024), Vol. 15, Issue 1, Article 82**, titled "Advancement in Biosensor Technologies of 2D Material Integrated with Cellulose—Physical Properties."[1]

Advancement in Biosensor Technologies of 2D Material Integrated with Cellulose; Physical Properties

Abstract: This paper provides an in-depth analysis of recent advancements in integrating two-dimensional (2D) materials with cellulose to enhance biosensing technology. The incorporation of 2D materials such as graphene and transition metal dichalcogenides, along with nanocellulose, improves the sensitivity, stability, and flexibility of biosensors. Practical applications of these advanced biosensors are explored in fields like medical diagnostics and environmental monitoring. This innovative approach is driving research opportunities and expanding the possibilities for diverse applications in this rapidly evolving field.

2.1. Introduction

This paper discusses the recent advancements in biosensor technologies, focusing on how integrating two-dimensional (2D) materials with cellulose improves biosensing functionality. The primary focus is on applications in medical diagnostics and environmental monitoring. By exploring the unique properties of 2D materials like graphene and transition metal dichalcogenides, as well as their synergistic effects when combined with nanocellulose, this highlights the practical applications of these advanced biosensors. It also addresses gaps in existing literature and suggests directions for future research to expand possibilities in this field.

2.1.1. Background: The Emergence of 2D Materials in Biosensor Technologies

The use of two-dimensional (2D) materials in biosensor technologies has revolutionized the field. Materials like graphene, transition metal dichalcogenides (MoS_2 and WS_2), hexagonal boron nitride (h-BN), and black phosphorus have a nanoscale thickness and distinct physical properties that might greatly enhance biosensor performance [2].

Graphene, with its exceptional electrical conductivity and mechanical strength, is widely recognized for its versatility in biosensors. Its planar structure and high electron mobility improve sensitivity and specificity, making it an ideal component [3].

Transition metal dichalcogenides, such as MoS_2 and WS_2, possess unique semiconductor properties due to their layered structure. These materials can interact with light and electrical fields, making them particularly suitable for biosensor applications that require precise electrical

characteristics [4]. Also, studies enhance the role of 2D materials in cancer biosensors: a MoS2/Cu2O sensor for lung cancer detection [5], PEC biosensors for esophageal cancer [6], and a lab-on-chip design for broad cancer cell detection [7]. These highlight advancements in material use and detection techniques, aiding early cancer diagnosis.

Emerging as other 2D materials with unique optical and electronic properties, black phosphorus and hexagonal boron nitride (h-BN) offer new possibilities for expanding the range of biosensor functionalities [5]. In Figure 2.1, we review well-known 2D material-based sensors such as graphene, TMDs, h-BN, MXenes, and BP [8].

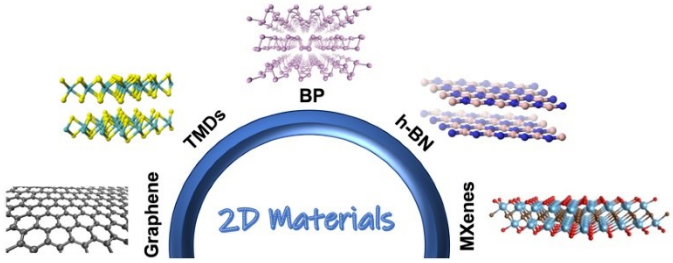

Figure 2.1. Major classes of 2D materials considered in this review: Graphene, TMDs, BP, h-BN, and MXenes[8]. @copyright https://www.sciencedirect.com/science/article/pii/S2214180422000691 with permission.

In addition, we review the synthesis and alteration procedures for these materials, which are crucial for customizing their characteristics to suit specific biosensor applications. These techniques include chemical vapor deposition, exfoliation, and functionalization. This knowledge provides a basis for comprehending the significant influence these materials have had on advancements in biosensor technology. Also, nanocellulose, derived from cellulose, has emerged as a promising material in biosensor technology and is discussed in the next section.

2.1.2. Overview of Nanocellulose

Nanocellulose, derived from cellulose, is a promising material in biosensor technology due to its biocompatibility and large surface area. This section offers a comprehensive overview of different forms of nanocellulose, including cellulose nanocrystals, cellulose nanofibers, and bacterial cellulose. Furthermore, it explores the diverse applications of nanocellulose in the development of biosensors.

Cellulose nanocrystals: CNCs are produced through acid hydrolysis and have high crystallinity, strength, and rigidity, which enhance the structural integrity of sensors [9].

Cellulose nanofibers: CNFs are made using mechanical or enzymatic methods and offer flexibility and a high aspect ratio, which are important for creating reactive surface areas in sensors [10].

Hairy nanocellulose (HNC): This form of nanocellulose is obtained by cleaving the amorphous regions in CNF, resulting in rod-shaped nanoparticles with “hairy” structures on their ends,

facilitating further chemical modification, enhancing its compatibility with other materials, and increasing its accessible surface area, which is advantageous in applications like catalysis and adsorption [11]. In Figure 2.2, a schematic representation of cellulose structures from resources to the molecular level is depicted [12].

Bacterial cellulose: BC is prized for its purity and unique mechanical properties. It is synthesized by bacteria without plant-based impurities such as hemicellulose and lignin [13].

The surface chemistry of nanocellulose plays a vital role in the functionality of biosensors. Its hydroxyl groups can be chemically modified, allowing for the attachment of sensing molecules or nanoparticles. HNCs can contain aldehyde, carboxyl, amine, or other groups in their hair. Moreover, utilizing nanocellulose from renewable sources highlights its environmental sustainability and its potential for creating eco-friendly biosensor designs [14].

Cellulose is a versatile raw material that can be converted into numerous products for various applications, including sensors. However, its full potential is often not realized due to challenges associated with its reduced chemical reactivity, and the limitations of cellulose reactivity are primarily due to its structural characteristics and the strong intermolecular hydrogen bonds that make it a recalcitrant polysaccharide [15].

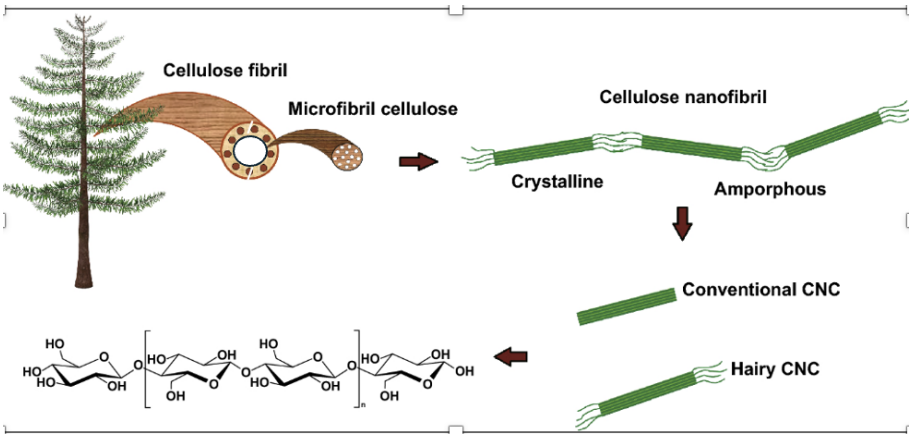

Figure 2.2. Schematic representation of cellulose structures from resources to molecular level. Adapted from [12].

2.1.2.1. Reactivity Issues

Dissolution difficulty: Dissolving cellulose is important for creating high-value cellulosic products and functional materials. However, the stiffness of its chains and the numerous hydrogen bonds make it difficult to dissolve cellulose, as they prevent the chains from interacting with each other [16].

Hydroxyl group accessibility: The dissolved state of cellulose allows for the full availability of hydroxyl groups, which are essential for introducing functional groups into the cellulose structure. Nonetheless, the hierarchical structure and crystalline nature of cellulose in plant cell walls limit accessibility to these hydroxyl groups, restricting their use [12].

Chain degradation and side reactions: When chemically modifying cellulose, there is a risk of chain degradation and the occurrence of side reactions. This can reduce the yield and quality of the modified product [9].

Enzymatic hydrolysis limitations: The enzymatic hydrolysis rate of cellulose decreases with conversion, which limits its commercial use. Factors such as changes in crystallinity, accessibility, reactivity, and the hydrolysable fraction of cellulose contribute to this decline due to chemical modification [17].

2.1.2.2. Approaches to Enhance Reactivity

Additives to improve solubility: The dissolution of cellulose in aqueous NaOH can be enhanced with additives to stabilize the solution against gelation [18].

Surface functionalization: Techniques such as TEMPO-oxidation can be used to study and quantify cellulose reactivity. Raman spectroscopy provides insights into the structural changes during functionalization by analyzing chemical bonds at the molecular level, enhancing our understanding of cellulose solubility and reactivity [12].

Linkers for functionalization: Aminopropyltriethoxysilane has been utilized as a linker for cellulose-based functional materials, offering the potential to create enhanced properties [11].

Ionic conductive hydrogels: Carboxymethyl cellulose-based ionic conductive hydrogels are used in highly sensitive, stable, and durable sensors for various applications [11].

Functionalizing cellulose with other functionalities or sensor scaffolds is indeed a challenging task due to the complex structure of cellulose and the difficulty in achieving high yields [19]. Here are some examples of attempts to functionalize cellulose and the challenges encountered:

Copper nanoparticles-induced trimesic acid-grafted cellulose: This approach was used to create a multifunctional textile with low chemical induction. However, the process is complex and requires careful control to ensure the successful grafting of trimesic acid onto the cellulose [19].

Graft copolymers of poly (ethyl acrylate) and cellulose: This approach was used to develop reactive metal ion sorbents. However, the details of the process and its challenges are not available in the search results [20].

Carboxymethyl cellulose (CMC) modified to have covalently tethered hydrazide groups: This approach was used to create adhesive joints between wet cellulose surfaces. However, wet

adhesion was dominated by polyelectrolyte complexation, and the presence of hydrazone linkages had little influence on wet adhesion [21].

In terms of chemosensors, there are examples of chemosensors being used for the tracking of metal ions, such as the "off-on"-based fluorescent chemosensor for Cu^{2+} in aqueous media and living cells. Another example is the use of supramolecular chemosensors for enzyme assays, which can specifically signal analytes with fluorescence-based read-out methods. However, these examples do not specifically involve the functionalization of cellulose [22].

In conclusion, while there are various attempts to functionalize cellulose with other functionalities or sensor scaffolds, achieving high yields and 100% functionalization remains a significant challenge due to the complex structure of cellulose and the difficulty in controlling the grafting process.

Cellulose-based implants are gaining attention in the field of bone tissue engineering due to their biocompatibility, mechanical strength, and ability to support cell differentiation [23]. The various cellulose-based scaffold materials are summarized in Table 2.1, which outlines their key components, properties, and relevant references. Here are some examples of cellulose-based scaffold materials:

Cellulose-acetate-based composite: This composite is used as a coating for biodegradable magnesium implants. The composite includes fillers such as hydroxyapatite and magnesium particles, which have shown positive effects on biocompatibility and surface analysis [24].

Cellulose-based materials crosslinked with epichlorohydrin: These materials have improved thermal stability, surface area, and swelling degree of hydrogels, making them suitable for implant applications [25].

Wood-derived composite scaffold: This scaffold is developed from natural wood treated with an alkaline solution, resulting in a cellulose skeleton with high elasticity. The scaffold is further modified with chitosan quaternary ammonium salt (CQS) and dimethyloxalylglycine (DMOG) to enhance antibacterial, osteogenic, and angiogenic activities [26].

Silk fibroin/cellulose hydrogels: These hydrogels are created by dissolving silk fibroin and cellulose together, resulting in a porous structure that supports the differentiation of MC3T3 cells into osteoblasts, making them a suitable scaffold for bone tissue engineering [27].

Cellulose-acetate-based composite coatings on Mg_3Nd alloys: These coatings are used to reduce the biodegradation rate and modify the surface properties of Mg_3Nd alloys to increase osteointegration [28].

HDPE/Chitosan composites: These composites contain chitosan, a bio-based polymer with biocompatibility and antimicrobial properties, and are used for bone replacement applications [29].

Here is a summary table 2.1 of the mentioned cellulose-based implants:

Table 2.1. Summary of Cellulose-Based Scaffold Materials and Their Properties.

Implant Type	Key Components	Key Properties	Reference
Cellulose-Acetate-Based Composite	Hydroxyapatite, Magnesium particles	Biocompatibility, Surface analysis	[24]
Cellulose-Based Materials Crosslinked with Epichlorohydrin	Epichlorohydrin	Thermal stability, Surface area, Swelling degree	[25]
Wood-Derived Composite Scaffold	Chitosan quaternary ammonium salt (CQS), Dimethyloxalyl glycine (DMOG)	Antibacterial, Osteogenic, and Angiogenic activities	[26]
Silk Fibroin/Cellulose Hydrogels	Silk fibroin, Cellulose	Supports cell differentiation to osteoblasts	[27]
Cellulose Acetate-Based Composite Coatings on Mg3Nd Alloys	Cellulose acetate	Reduces biodegradation rate, Increases osteointegration	[28]
HDPE/Chitosan Composites	Chitosan	Good mechanical properties, Antimicrobial activity	[29]

2.1.3. Applications and Case Studies

The integration of 2D materials with nanocellulose has greatly expanded the application and advancement of biosensors in various fields. In this section, we will explore case studies and applications that demonstrate the practical implications and benefits of these advancements.

Recent Research and Advancements

Monoelemental 2D materials, such as Xenes (e.g., graphyne, silicene, germanene), have been extensively researched for their potential use in biosensors. These materials possess desirable characteristics, including high optical response capability, excellent electrical-optical properties, a large specific surface area, and easy modification of potential [30].

The utilization of cellulose, a carbohydrate biopolymer, has brought significant advancements to the field of biosensors through the development of portable paper-based biosensors and microfluidic paper-based analytical devices (μPADs) [31]. These innovative devices offer exceptional sensitivity and cost-effectiveness, making them a promising alternative to

conventional advanced analytical instruments. With their applications in emergency medical situations, point-of-care health diagnostics, and early cancer screening, rPBBs and μPADs present exciting opportunities for improving healthcare outcomes [32].

Paper and cellulose-based biosensors have gained relevance during the COVID-19 pandemic due to their rapid production capabilities and suitability for use by untrained personnel. These biosensors are used in low-cost point-of-care diagnosis, including viral genomic material detection, viral antigen identification, and serological antibody testing [33].

2.2. Advantages of 2D Materials and Cellulose in Biosensors

The use of 2D materials in biosensor applications provides several advantages, including excellent mechanical, optical, and electrical properties. These properties are essential for the development of wearable biosensors that enable real-time monitoring of human health information and accurate measurement of vital signs [34]. Integrating 2D materials into wearable biosensors has expanded opportunities for early detection of life-threatening diseases and continuous health tracking.

In addition to 2D materials, cellulose-based biosensors also offer significant benefits. They are cost-effective, highly sensitive, and compatible with portable sensing devices used in biomedical applications. One major advancement in this field is the functionalization of cellulose papers with antibodies, nucleic acids, and nanomaterials in PBBs (paper-based bioassays) and μPADs (microfluidic paper-slip devices) [34].

Hence, the application of 2D materials and cellulose in medical diagnostics and biosensors has shown great potential. These materials have unique properties that make them suitable for various applications, including disease detection, real-time monitoring, and point-of-care diagnostics. However, further research is needed to fully utilize their capabilities and address any challenges associated with their use.

The use of biosensors has significantly advanced the detection of biomarkers, particularly in early cancer diagnosis. In a recent study, a biosensor incorporating graphene as a 2D material demonstrated improved sensitivity and selectivity for tumor markers. This innovative biosensor was able to detect biomarkers at concentrations as low as 1 ng/L, representing a significant advancement in early cancer detection methods [35].

Biosensors that incorporate nanocellulose have shown promising potential for the early detection of cancer biomarkers in blood samples. These biosensors are highly sensitive and capable of detecting biomarkers even at very low concentrations [36]. The use of 2D materials, such as nanocellulose-based materials, has also attracted significant research interest due to their unique properties, including high conductivity, hydrophilicity, and biocompatibility . These properties make them suitable for various biomedical sensing applications [37].

In recent developments in bioelectronics, 2D carbon networks arranged into high-order 3D nanotube arrays on flexible microelectrodes have emerged as implantable probes. These probes enable the in-situ detection of cancer tissues by differentiating them from normal tissues [38]. Their electrochemical sensing capabilities allow for the detection of H_2O_2 biomarkers secreted by various cancer cells and tissues—a crucial factor in cancer diagnosis and evaluation [39].

Moreover, electrochemical biosensors utilizing graphene and other 2D materials have shown great potential for detecting biomarkers associated with hematological malignancies like leukemia, lymphoma, and multiple myeloma. These biosensors offer a wide linear range, a low detection limit, high sensitivity, excellent selectivity, and cost-effectiveness [40].

In addition to that, metal nanoparticles have been employed on 2D platforms to enhance the detection of electrochemical biomarkers. This approach has demonstrated remarkable sensitivity, selectivity, fast response time, ease of use at a low cost, and simple fabrication procedures [41].

There have also been advancements in designing phosphorene-based nanosensors for the detection of formaldehyde as an essential lung cancer biomarker. These sensors exhibit exceptional sensitivity in detecting formaldehyde levels [42].

An electrochemical biosensor has been developed using reduced graphene oxide-modified and reduced-molybdenum disulfide multi-layered nanosheets for detecting neuron-specific enolase, a biomarker for lung cancer [43]. The sensor exhibits a wide linear range of detection and remains unaffected by other interfering species commonly found in human serum.

2.2.1. Medical and Diagnostic Applications

Glucose monitoring is essential for managing health conditions such as diabetes. Recent advancements in the construction of glucose-monitoring biosensors have focused on utilizing 2D materials and cellulose [34]. However, further research is needed to enhance their performance and explore their potential in clinical practice.

The use of 2D materials has proven beneficial in glucose sensing applications, resulting in improved sensor properties including stability, large surface area, and affordability [43].

Cellulose has been utilized in the development of wearable, self-powered glucose biosensors. A flexible biosensor was created using cellulose fibers coated with multi-wall carbon nanotubes and reduced graphene oxides, resulting in a porous electrode with excellent flexibility, conductivity, and electroactive surface area for urine glucose detection [34].

In a recent study, researchers investigated the potential of combining reduced graphene oxide (rGO) with gold nanoparticles in cellulose-nanofiber matrices to create a transducer layer for an environmentally friendly and flexible glucose sensor [39].

Furthermore, metal-organic frameworks such as 2D isomorphic Co/Ni-Metal-Organic Frameworks have demonstrated promise as materials for detecting glucose. These MOFs exhibit higher sensitivity, a wider linear range, and lower detection limits compared to other MOF-based glucose sensors.

Biosensors for DNA detection are crucial in genetic testing and disease diagnosis, utilizing the high surface area of nanocellulose and the electrical conductivity of 2D materials like molybdenum disulfide [43]. A recent study showed that such biosensors achieved a sequencing error rate below 0.1% and improved sequencing speed, enhancing the precision and reliability of DNA sequencing [44].

Graphene-like 2D materials and cellulose were utilized to develop biosensors for DNA detection. One study investigated the interaction of a two-dimensional metal oxide with single-stranded DNA (ssDNA) as a potential method for detecting viral infections [45]. Spectroscopic measurements confirmed strong interactions between ssDNA and the metal oxide, suggesting its efficacy in detecting viral infections. Another study focused on an electrochemical biosensor using $BiSbTeSe_2$, an intrinsic topological insulator, which demonstrated high sensitivity in detecting target DNA with a low detection limit of 1.07×10^{-15} M [41].

The potential of 2D materials and cellulose in biosensors is demonstrated by examples such as the development of a photoelectrochemical aptasensor for detecting SARS-CoV-2 spike glycoprotein using a two-dimensional (2D) metal-organic framework and the synthesis of TEMPO-oxidized cellulose nanocrystal-capped gold nanoparticles for colorimetric detection of unamplified pathogenic DNA oligomers. These applications show their efficacy in detecting viral infections, HIV gene determination, and SARS-CoV-2 spike glycoprotein [41], [46].

Advanced biosensors incorporating 2D materials and nanocellulose have indeed shown promise in managing cardiovascular diseases by detecting and quantifying cholesterol. These biosensors demonstrate high sensitivity and accuracy, with a notable study achieving a detection limit of 0.1 mg/dL and a response time under 5 min [20]. The innovative design utilizes graphene oxide as a 2D material to enhance performance in clinical applications. Furthermore, cellulose-based biosensors have been successfully employed for monitoring various biomolecules, including glucose, urea, cells, amino acids, proteins, lactate, and hydroquinone [46].

However, while these advancements are promising, there are still areas that require further research and development. For instance, while 2D materials like graphene and MoS_2 have been widely used in biosensors, there is a need to explore other 2D materials to discover novel properties that may contribute to the construction of high-performance electrochemical biosensors [15].

A critical factor in the future of electrochemical biosensing is the creation of highly sensitive biosensors through affordable and simple fabrication processes. These sensors must offer excellent sensitivity, selectivity, reliability, and stability. Cellulose-based biosensors have shown promise

but may require additional chemical treatments due to their hydrophilic nature being incompatible with certain molecular sensors [47]. Moreover, there is a need for advancements in miniaturizing cholesterol and dopamine biosensors for lab-on-chip devices to overcome existing technical limitations and enable convenient use by patients at home [45].

In conclusion, while advanced biosensors incorporating 2D materials have shown significant promise in managing cardiovascular diseases, there are still challenges to be addressed and potential directions for future research. These include exploring different 2D materials, enhancing fabrication procedures, addressing the hydrophilic nature of cellulose, and improving biosensor miniaturization.

Cellulose-based biosensors have also been developed specifically for glucose and urea detection. Their accurate readings enable effective management of conditions such as diabetes or kidney disease. These sensors employ immobilized enzymes on a cellulose substrate to generate an electrical signal proportional to the concentration of glucose or urea [46].

Cellulose-based biosensors have found applications in the detection of specific diseases by identifying cells and proteins associated with certain conditions. In cancer diagnostics, they can detect specific cancer-associated proteins or cancer cells, enabling early disease diagnosis and monitoring [47].

Furthermore, cellulose-based biosensors have shown usefulness in pathogen detection for diagnosing infectious diseases. By detecting specific biomarkers associated with pathogens, these biosensors facilitate rapid and accurate diagnoses [48].

2.2.2. Environmental Monitoring

Water quality analysis: Graphene-based biosensors offer a potential solution for real-time environmental monitoring and pollution control by detecting trace amounts of heavy metals in water sources. Graphene and other 2D materials have been studied for their potential in analyzing and treating water quality. Graphene, especially graphene nanoflakes, has been used to create hydrogels for biosensors, showing promise as a material for water quality analysis. Furthermore, graphene microfiber membranes have been developed to remove nano-sized pollutants from water. The effectiveness of these membranes has been improved through surface functionalization that adjusts the interlayer separation in 2D membranes, enhancing their sieving capabilities. The combination of graphene oxide and cellulose acetate creates a unique adsorbent for efficient phosphate removal from water [49]. The presence of hydroxyl groups on the modified surface of cellulose acetate aids in the process [50]. Moreover, field-effect transistors made from 2D materials find application in water-related sensing. For instance, MoS_2 nanosheets can be inkjet-printed into ultrathin semiconducting channels to fabricate FET-based water sensors. These sensors demonstrate high selectivity towards Pb2+ even at low concentrations (as low as 2 ppb), highlighting the potential use of 2D materials in assessing water quality.

Cellulose and 2D materials have displayed promising potential in water quality analysis, treatment, pollutant removal, biosensing, and monitoring. These filters can capture specific aquatic impurities for which antibodies can be produced and attached to the filters [51].

The utilization of two-dimensional nuclear magnetic resonance (2D NMR) techniques has allowed for the qualitative analysis of substructures of water-soluble organic compounds in atmospheric aerosols. This includes identifying spectral signatures associated with anhydrosugars present in cellulose. In terms of air quality monitoring, both 2D materials and cellulose offer high sensitivity for detection. A study demonstrated the use of a sensor composed of reduced graphene oxide (rGO) and graphene oxide on a cellulose-acetate composite membrane, which exhibited excellent sensitivity to minute changes in air quality. Furthermore, one notable advantage is their flexibility and adaptability for various applications. The same study emphasized that the film's flexibility makes it suitable for wearable electronic devices or other applications that require flexible substrates.

Recent research has investigated the utilization of cellulose-based materials for analyzing indoor air quality. These innovative thermal insulation materials, obtained from recycled cellulosic and/or animal waste, were thoroughly examined [52].

Another study focused on developing a highly sensitive, flexible sensor. The sensor was created using an electro-spun composite membrane with abundant mesopores. This sensor exhibited exceptional sensitivity at low strains, making it ideal for potential use in wearable electronic devices.

In a separate investigation, researchers studied the effectiveness of composite membranes containing a 2D material and carbon nanotubes in solar steam generation and desalination processes. These composite membranes demonstrated self-floating capabilities on the air-water interface and minimized the accumulation of salt during de-salination due to their hydrophobic nature [53].

The application of 2D materials and cellulose In air quality monitoring exhibits great potential due to their flexibility and sensitivity. Recent studies have demonstrated their versatility and innovative possibilities in various fields, including thermal insulation and wearable electronic devices [54]. The application of 2D materials and cellulose in various fields, including thermal insulation, wearable electronic devices, and air quality monitoring, indeed exhibits great potential due to their flexibility and sensitivity. However, several challenges need to be addressed to fully realize their potential.

A major hurdle in developing wearable electronic devices using 2D materials and cellulose is finding the right balance between mechanical stretchability and electronic performance. For example, stretchable electronics, which are crucial for wearable devices, require substrates that can withstand stretching while maintaining their electronic functionality. PDMS is commonly used

due to its ease of fabrication and low cost; however, enhancing its mechanical stretchability without compromising electronic performance remains a significant challenge [55].

The fabrication methods also present considerable challenges. Modern electronic devices are designed for 2D planar substrates, which are generally ill-suited for the intricate 3D structures of textiles. Consequently, there is an urgent need to develop fabrication techniques specifically tailored for e-textiles to advance wearable electronics [56].

The development of efficient, flexible, and scalable energy storage solutions remains a significant challenge for powering wearable electronic textiles. Additionally, technical breakthroughs are needed for manufacturing state-of-the-art 2D layered nanomaterial-supported flexible/stretchable sensors and power devices, which are crucial to the development of wearable biomedical sensors and power devices [57]. Lastly, strain engineering presents opportunities and challenges for creating flexible nanoelectronics and optoelectronic devices. Most of these devices utilize chemical vapor deposition or mechanical exfoliation of ultrathin 2D TMD materials, which may limit their application in wearable and implantable devices with higher train tolerance [58].

In summary, while 2D materials offer promising opportunities in various applications, there are significant challenges related to mechanical stretchability, electronic performance, fabrication methods, energy storage, and strain engineering that need to be addressed to advance this field.

2.2.3. Food Safety

Pathogen Detection in Food Products: One approach involves the use of enzyme-based paper biosensors for monitoring food freshness and predicting spoilage. For instance, a biosensor has been developed to measure the release of hypoxanthine, an indicator of meat and fish degradation. This is accomplished through enzymatic conversion facilitated by XOD within a sol-gel biohybrid on paper that retains the reaction products [59].

The unique optical properties of 2D materials like graphene and transition metal dichalcogenides enhance biomolecule detection in optical biosensors. These materials can be modified to improve sensitivity and detection limits and are commonly used alongside techniques such as surface plasmon resonance, fluorescence resonance energy transfer, and evanescent waves for detecting biomolecules. Nanomaterials like carbon nanotubes, magnetic nanoparticles, gold nanoparticles, dendrimers, graphene nanomaterials, and quantum dots are widely used in biosensors due to their unique properties. One application is the use of fiber-optic surface plasmon resonance sensors based on 2D materials for detecting different types of cells by measuring peak power loss changes [60].

Intelligent packaging technology is emerging to directly monitor food quality, eliminating the need for complex processes. This can be leveraged to detect microorganisms that cause foodborne illnesses visible on the food package itself [61].

Achieving high-quality sensing performance, including sensitivity and stability, relies heavily on maintaining stable biosensor interfaces. To improve interface properties, nanomaterials like chitosan and cellulose are often combined with polymers [62].

In order to detect pathogens in food products, researchers are employing a combination of 2D materials and cellulose-based biosensors. By integrating different materials, methods, and technologies with their respective advantages and challenges, this approach aims to enhance the sensitivity and stability of these biosensors.

2.2.4. Agricultural Applications

Soil Health Monitoring: Incorporating nanocellulose and 2D materials into biosensors allows for monitoring soil nutrients and pH levels to support sustainable farming practices. The use of these materials in sensor technology has been explored in various contexts, such as health monitoring and environmental sensing, but there is limited documentation on their specific application for soil health monitoring [63].

2.2.5. Health Monitoring

Cellulose-based sensors have been developed for health monitoring purposes. A plantar wearable pressure sensor utilizing hybrid lead zirconate-titanate/microfibrillated cellulose piezoelectric composite films has been proposed for measuring plantar pressure. Similarly, a high-performance humidity sensor based on GO/ZnO/plant cellulose film has been developed for respiratory monitoring [64], [65].

The utilization of 2D materials in health monitoring wearable devices is another area where they have found applications. Carbon black and MoS_2, as 1D and 2D nanomaterials, respectively, have been extensively studied as core sensing components for flexible strain sensors that are used to monitor the vital signs of patients [66], [67]. Furthermore, 2D materials are being employed in enzymatic and nonenzymatic glucose sensing applications. Additionally, a GaSe-based fiber optic sensor has been specifically designed for lactate sensing in human sweat as an indicator of a potential heart attack [68].

Regarding soil health monitoring sensors, the search results provided limited evidence on the specific utilization of 2D materials and cellulose. Although there is a wireless subsoil health sensor developed for detecting volumetric water content, it does not make use of these materials. Further research is required to explore their potential in soil health monitoring applications.

Wearable health devices offer continuous health monitoring through the integration of flexible and biocompatible biosensors. These biosensors, composed of 2D materials and cellulose derivatives, can track vital health parameters such as heart rate and blood oxygen levels in real-time [69].

Graphene and other 2D materials have seen extensive use in developing wearable biosensors, which can be integrated into various wearable platforms like wristbands, headbands, and smart

garments. These materials offer exceptional mechanical, optical, and electrical properties that make them ideal for such applications [70]. Additionally, certain advancements have been made in utilizing cellulose-a biomass material, in the fabrication of wearable biosensor devices [71]. Most notably, nanocellulose's high specific surface area, biodegradability, cost-effectiveness, and sustainability are key factors behind these developments. For instance, a self-powered glucose biosensor was created from a flexible textile matrix made of cellulose fibers [72]. The sensor featured a porous three-dimensional electrode with excellent flexibility, surface conductivity, and electroactive surface area achieved by coating multi-wall carbon nanotubes and reduced graphene oxides onto the cellulosic textile matrix [73].

Wearable biosensors made from 2D materials and cellulose have gained attention in health monitoring for providing real-time data on vital signs. They are utilized in glucose monitoring, biomarker detection, and remote healthcare monitoring. These biosensors provide a versatile approach to personalized healthcare delivery with their design, fabrication, performance, sensitivity, and various health monitoring applications [74]. These materials offer flexibility, wearability, and responsiveness to external stimuli, which makes them well-suited for wearable health monitoring applications [75]. For example, a smart fabric based on MXene can be created by depositing Ti_3C_2Tx nanosheets onto cellulose fiber non-woven fabric. This fabric has a sensitive and reversible response to humidity, making it suitable for wearable respiration monitoring applications. It also has the potential to be used as a low-voltage thermotherapy platform due to its fast and stable electro-thermal response [76], [77]. Furthermore, cellulose nanofibrils and Ti_3C_2 MXene can be combined through 3D printing to create smart fibers and textiles with responsiveness to various external stimuli. These materials have shown potential as strain sensors .

In addition, a plant-based substrate called "sporosubstrate" has been developed using natural pollen that is non-allergenic. This substrate allows for the creation of flexible shapes with customizable properties and performance characteristics. It finds application in electronic healthcare devices and wearable wireless heating systems [78], [79].

Flexible and lightweight biosensors have been developed using 2D graphene oxide and Ti_3C_2 nanosheet-based supercapacitors. These sensors exhibit high sensitivity and a wide detection range and can be integrated into wearable monitoring systems for tracking physical status during various activities. The use of a cellulose-blend cloth substrate further enhances the versatility of these biosensors in wearable health applications [80].

2.2.6. Integration of 2D Materials and Nanocellulose in Biosensor Technologies

Integrating 2D materials with cellulose in biosensors enhances their properties, such as sensitivity, stability, and flexibility. Graphene and transition metal dichalcogenides like MoS_2 and WS2 have unique physical properties that improve the performance of biosensors. The electrical conductivity and mechanical strength of graphene enhance sensitivity and specificity, while the layered

structure of transition metal dichalcogenides provides precise electrical characteristics for biosensor applications [81].

Combining 2D materials with nanocellulose improves biosensor performance by leveraging the high surface area of nanocellulose and the electrical properties offered by 2D materials. This combination results in highly sensitive sensors. Additionally, incorporating cellulose into 2D materials enhances the mechanical strength, biocompatibility, and environmental stability of biosensors [82]. The integration of graphene and molybdenum disulfide with cellulose creates flexible and stretchable electronic devices suitable for wearable electronics and sensors. The biocompatibility of nanocellulose contributes positively to biosensor functionality, while its mechanical strength enhances stability [83].

Integrating cellulose with 2D materials in biosensors enhances device strength, biocompatibility, and environmental stability. This integration is driving research opportunities and expanding the applications in this rapidly advancing field.

The most common properties tested in biosensors include:

Electrical properties: These materials are significant contributors to the performance of biosensors. Graphene, with its high electrical conductivity achieved through wet-chemical methods, is essential for device performance. Similarly, materials like MoS_2 and WS_2 possess exceptional electrical properties due to their strong covalent and van der Waals interactions. Notably, the covalent functionalization of these atomic-thin materials with a large surface-to-volume ratio is critical to optimizing biosensor functionality [84]. Graphene's high electrical conductivity, achievable through wet-chemical methods, is integral to device performance. MoS_2 and WS_2, with their strong covalent and van der Waals interactions, exhibit notable electrical properties. The covalent functionalization of these materials is vital due to their atomic thinness and large surface-to-volume ratio [85].

Mechanical properties: Methods such as mechanical exfoliation and chemical vapor deposition yield 2D materials with distinct mechanical characteristics, which play a crucial role in biosensing applications. Techniques like mechanical exfoliation and chemical vapor deposition enable the production of 2D materials with unique mechanical attributes for biosensor applications, thanks to their atomic thinness and extensive surface area [86].

Chemical properties: To enhance the functionality of biosensors, it is important to consider the chemical properties of nanocellulose. Nanocellulose contains hydroxyl groups that can be chemically modified, allowing for the attachment of sensing molecules or nanoparticles [87].

Optical properties: The optical properties of 2D materials such as graphene and transition metal dichalcogenides improve biomolecule detection in optical biosensors. These materials can be modified to enhance sensitivity and detection limits [88].

Thermal properties: In addition to other properties, certain biosensors also measure thermal conductivity. For instance, a study examined the heat transfer capabilities of polypyrrole/carbon black composite-coated cellulose (cotton) yarn. The objective was to gain insights into the behavior and performance of these materials in terms of their ability to conduct heat [89].

Sensitivity and specificity: The use of graphene and transition metal dichalcogenides in biosensors has significantly improved their sensitivity and specificity. These materials have a large surface-to-volume ratio, allowing for better interaction with analytes and enhanced detection capabilities [90]. Biosensors employing 2D materials and cellulose have shown increased sensitivity and specificity in applications such as early cancer diagnosis, biomarker detection, glucose monitoring, and DNA detection. These materials demonstrate exceptional electrical properties and high surface area, contributing to their enhanced performance [91].

Stability: The mechanical strength of nanocellulose significantly enhances the stability and durability of biosensors. This improvement is primarily due to several key properties of nanocellulose:

High Surface Area: This characteristics of nanocellulose facilitates greater enzyme immobilization in biosensors. This is crucial because it allows for higher protein loadings, which in turn improves the sensor's response and stability [92].

High Young's Modulus: This property indicates that nanocellulose is a stiff material. In the context of biosensors, a higher Young's modulus translates to improved structural integrity, making the biosensors less prone to deformation under stress [93].

Biodegradability and renewable nature: These environmentally friendly properties of nanocellulose make it an ideal material for sustainable biosensor development [94].

Tunable surface chemistry: The ability to modify the surface of nanocellulose allows for better integration with other materials in biosensors, potentially leading to enhanced performance and specificity [95].

Synergistic effects with other materials: When combined with other materials, like in the case of rice starch-based edible films, nanocellulose not only enhances mechanical strength but also can impart other desirable properties to the composite material. This synergy can be leveraged in biosensors to create more robust and efficient devices [96].

In summary, the incorporation of nanocellulose into biosensors offers a multitude of benefits, primarily due to its strong mechanical properties, high surface area, and customizable nature. These characteristics contribute to the development of more stable, durable, and potentially more sensitive biosensing devices.

Flexibility: Combining the unique properties of nanocellulose with flexible and durable 2D materials makes them an ideal choice for developing wearable biosensors suitable for real-time health monitoring [97].

Cost-effectiveness: Portable paper-based biosensors and microfluidic paper-based analytical devices (μPADs) are cellulose-based biosensors that offer high sensitivity and affordability. These innovative devices provide a viable alternative to conventional advanced analytical instruments [98].

Environmental sustainability: By utilizing nanocellulose from renewable sources, the environmental sustainability of biosensors can be emphasized while also highlighting their potential for being eco-friendly as products and technologies.

In cellulose nano-whisker/graphene nano-platelet composite films, the sensing capabilities of a biosensor depend on its design and functionalization [99]. Biosensors can be designed to detect substances such as glucose, cholesterol, lactate, DNA, RNA, proteins, and various types of cells through a reaction with a specific enzyme or molecule that is attached to the sensor, causing a detectable change in the sensor's properties [100].

Graphene and its hybrid materials are currently utilized in the development of high-performance electrochemical biosensors. They serve as advanced electrodes due to their large accessible surface area, electrical conductivity, and capacity for immobilizing enzymes [101]. For example, a glucose biosensor can be functionalized with glucose oxidase, an enzyme that reacts with glucose to produce hydrogen peroxide and gluconolactone. The hydrogen peroxide can then be detected electrochemically. Similarly, a DNA biosensor might be functionalized with a specific sequence of DNA that binds to the target DNA sequence, which causes a detectable change in the sensor's properties [102].

Composite materials, such as the ones mentioned, have been extensively researched in various fields, including wearable electronics, energy storage, sensing devices, and environmental monitoring. Wearable biosensors made from 2D materials and cellulose have demonstrated potential in health monitoring by collecting real-time data on vital signs, glucose levels, biomarker detection, and remote healthcare monitoring [103].

2.2.7. Biosensor Functionality

The electrical and mechanical properties of these advanced materials significantly contribute to biosensor functionality. For instance, in plasmonic biosensing and photoelectrochemical (PEC) biosensing, the sensitivity of biosensors is notably enhanced by 2D nanomaterials [104].

2.2.8. Comparison with Other Technologies

Biosensors utilizing 2D materials and cellulose offer numerous advantages compared to traditional biosensors and other advanced analytical instruments. These include unique electrical and optical

properties, high specific surface area, excellent mechanical properties, good thermal and chemical stability, high catalytic activities, facile synthesis process, and large surface areas for toxin detection improvement with increased selectivity and sensitivity due to their outstanding electrical signal amplification capabilities [105].

The performance of these biosensors can vary in terms of sensitivity, specificity, and stability compared to traditional biosensors and other advanced analytical instruments. Further research is needed to optimize their performance and address any associated challenges with their use.

2.2.9. Theoretical Foundations

The theoretical foundations related to the integration of 2D materials with cellulose in biosensors and other applications primarily revolve around the principles of quantum mechanics, band structure engineering, and strain engineering.

Band structure engineering: Band theory, an approximation to the quantum state of solids, has been instrumental in the development of modern integrated solid-state electronics. The emerging 2D layered materials, with their unique electrical, magnetic, optical, and structural properties, provide a platform to implement quantum-engineered devices. These materials allow for the exploration of advanced quantum mechanical effects, such as band-to-band tunnelling, spin–orbit coupling, spin–valley locking, and quantum entanglement, which are crucial for energy-efficient electronics and optoelectronics [106]. Band structure engineering is a key theoretical foundation for manipulating the electronic properties of 2D materials. This involves modifying the energy bands of these materials to control their electronic and optical properties. Techniques for band structure engineering include localized chemical doping, dual gating, liquid gating, thickness modulation, and constructing heterojunctions [107].

Strain engineering: Strain engineering is a promising approach to tuning the electrical, electrochemical, magnetic, and optical properties of 2D materials. This involves applying mechanical strain to these materials to alter their properties, a technique that has the potential for high-performance 2D-material-based devices. Strain engineering can fundamentally change the electronic and optoelectronic properties of 2D materials, leading to novel functional device applications[108], [109].

These theoretical foundations provide the basis for understanding and manipulating the properties of 2D materials when integrated with cellulose, thereby enhancing their performance in various applications, including biosensors.

The incorporation of 2D materials into biosensor technology significantly enhances their performance by leveraging various physical properties at the nanoscale. Specific examples include graphene and molybdenum disulphide, which exhibit exceptional physical, mechanical, and optical characteristics that render them ideal for nanoelectronic devices and sensors [110]. These materials can be combined with cellulose-based compounds to form blends with enhanced

attributes for applications in energy storage, optoelectronics, and biological control. By integrating nano-sized substances into Na-CMC blends through strain engineering techniques, it becomes possible to manipulate the band structure of 2D materials for continuous tuning purposes [111], [112]. Consequently, this integration facilitates the development of high-performance biosensors characterized by improved sensitivity, selectivity, and stability.

High surface-to-volume ratios: The large surface-to-volume ratio of 2D materials offers significant advantages in various applications, including adsorption, sensing, and catalysis. These materials have shown potential as effective adsorbents for environmental decontamination due to their high surface area, specific binding capability, and chemical stability [113].

2.2.10. Electrical Conductivity and Electron Mobility

The integration of cellulose with 2D materials has demonstrated promising potential for improving electrical conductivity and electron mobility across various applications, including wearable electronics, energy storage, and sensing devices. For example, the use of cellulose-based ion gels in fabricating aerosol-jet-printed electrolyte-gated indium oxide thin-film transistors resulted in devices with electron densities surpassing $7 \times 1014\ cm^{-2}$ and mobilities exceeding $11\ cm^2\ V^{-1}\ s^{-1}$. Furthermore, stretchable thermal sensors for wearable electronics were developed using polypyrrole-coated threads that maintained consistent electrical conductivity even under tensile strains above 100% [114].These instances emphasize the advantageous prospects of combining cellulose with 2D materials.

Mechanical properties: Integration of 2D materials with cellulose has been found to enhance the stability and durability of biosensors, offering the potential for functionalization and integration with various biomolecules. The mechanical properties of cellulose integrated with specific 2D materials are influenced by the fabrication process and modifications applied . Research has shown that graphene and molybdenum disulphide can be incorporated into cellulose to create flexible and stretchable electronic devices suitable for wearable electronics and sensors. For example, a flexible capacitor was fabricated using a few-layer MoS_2 grown on aluminum foil as electrodes and cellulose paper as a dielectric material, demonstrating enhanced capacitance upon strain due to its piezoelectric property.

Various approaches have been used to study the tensile properties of all-cellulose composites. The assessment of tensile properties can be done using nominal stress and strain equations, considering factors such as force, cross-sectional area, displacement, and initial length [115].

A study demonstrated that modifying the surface properties of natural cellulose fibers through chemical methods improves the mechanical properties of graphene/cellulose conductive paper. The study found that the carboxyl content in cellulose had a significant impact on the mechanical properties of graphene/oxidized-cellulose conductive paper. When the carboxyl content was low,

graphene/oxidized-cellulose conductive paper achieved an elastic modulus value of 1572 MPa, which was 27.4% higher compared to cellulose/graphene conductive paper [116], [117].

Cellulose, a readily available and cost-effective natural material, offers impressive mechanical properties and structural stability. It has the potential to replace carbon fiber/epoxy composites with cellulose/epoxy composites that deliver excellent performance at an affordable price [118].

In summary, the integration of 2D materials with cellulose presents promising prospects for various applications, particularly in flexible and wearable electronics. However, specific properties may vary depending on the choice of 2D materials used, fabrication processes employed, and modifications applied to cellulose.

2.2.11. Environmental and Economic Aspects

The environmental cost as well as the economic cost are factors of major influence when establishing the acceptance of technology. The environmental cost includes aspects such as the toxicity of the extraction process, fabrication, usage, and disposal. Cellulose provides great benefits in all the above categories. Below, some of the environmental and economic-related aspects are discussed.

2.2.12. Environmental Aspects

2D materials, including graphene and other 2D metal-organic frameworks, can be synthesized in a cost-effective and environmentally friendly manner. These materials have great potential for use in advanced electrical devices and integrated circuits. Cellulose, an abundant renewable resource on earth, serves as the foundation for these 2D materials. It possesses excellent properties such as biocompatibility, environmental friendliness, and chemical stability .

In the field of all-solid-state flexible supercapacitors, cellulose-based hybrid 2D material aerogels have been utilized. These aerogels are created through a supercritical CO_2 drying process using cellulose nanofibers to effectively disperse other 2D materials like molybdenum disulphide and reduced graphene oxide .

Additionally, cellulose has found utility in environmental applications such as industrial water decontamination. Its efficacy and affordability make it a desirable choice for this purpose. Selective oxidation of cellulose has been employed to produce novel high-performance materials with diverse applications in fields including bio-medical engineering, healthcare, energy storage, barriers, sensing technologies, and food packaging [119].

2.2.13. Economic Aspects

Combining 2D materials with cellulose provides notable economic advantages. This integration enables the development of self-powered sensors for various applications, such as biomedicine, environmental detection, human motion monitoring, energy harvesting, and smart wearable

devices. Additionally, combining cellulose with MXene results in the cost-effective manufacturing of green and highly efficient electromagnetic interference shielding materials. Furthermore, it allows for the production of all-solid-state flexible supercapacitors using cellulose-based hybrid 2D material aerogels [120].

To conclude, integrating 2D materials into cellulose offers significant environmental and economic benefits. This makes it a highly promising field for future research and development efforts.

2.3. Examples and Discussion

The unique electrical, mechanical, and chemical characteristics of two-dimensional (2D) materials and nanocellulose make them valuable in enhancing biosensor functionality across various domains in the field of biosensor technology [119], [120], [121].

2.3.1. Enhanced Sensitivity and Specificity

The utilization of 2D materials like graphene and transition metal dichalcogenides in biosensors has significantly enhanced their sensitivity and specificity. These materials possess a large surface-to-volume ratio, facilitating better interaction with analytes and improving detection capabilities. Graphene-based biosensors have demonstrated remarkable sensitivity in detecting glucose levels, which is advantageous for managing diabetes. Similarly, sensors based on MoS_2 exhibit increased specificity in differentiating various biomolecules, making them essential for analyzing complex biological samples [122].

2.3.2. Wearable and Flexible Biosensors

The combination of flexible and strong 2D materials with the lightweight and biocompatible nature of nanocellulose makes them ideal for wearable biosensors. These materials allow for the creation of sensors that can conform to the body, providing continuous monitoring of health without causing discomfort. For instance, a skin patch sensor can track sweat composition to provide insights into hydration levels and electrolyte balance. This application demonstrates how material properties directly impact user comfort and sensor effectiveness. Figure 2.3a illustrates an overview of the rGO-paper ring in different positions on a bent or extended finger, with the inner ring securely attached to the knuckle while allowing flexibility for bending or straightening along with finger movements. A few remarkable applications of cellulose and 2D materials are presented below.

Figure 2.3a depicts the rGO-paper ring and its placement on a bent and extended finger. These wearable sensors are made from reduced graphene oxide (rGO) arranged on paper substrates, making them highly responsive to deformations such as bending and folding. Figure 2.3b shows the response of rGO-paper rings when various fingers are bent or extended. In a practical application shown in Figure 2.3c, real-time control of a 3D-printed robotic hand is demonstrated

using intelligent rGO-paper rings. The changes in compressive and tensile resistances of these rings serve as inputs to control specific motions, such as those performed by the middle finger and thumb.

To detect different human motions involving knee and wrist joints with skin stretching up to 55%, intricately designed rGO-paper strain sensors were prepared. These sensors were made using flexible paper substrates and a precise digital craft cutter. They featured parallel rGO lines and conductive silver connections patterned on a stretchable paper kirigami through the multilayer masking method. The sensor was designed with alternating concave and convex bends in the paper strips to ensure that the strain-sensitive rGO patterns remained effective. Silver lines were used to connect these patterns (Figure 2.3d). When the knee or wrist sensor is bent, the rGO-patterned paper strips produce positive or negative signals depending on the direction of bending. The response behaviour of this wearable pressure sensor was demonstrated for various motions such as knee bending, walking, and wrist bending (Figure 2.3e–h). These sensors also allow for real-time pulse reading, as shown in Figure 2.3i,j. Wearable electronics that do not hinder body movement have gained attention due to their versatility across multiple applications. In addition, rGO-paper sensors are highly sensitive to folding and bending while also being easy to manufacture. This allows for greater freedom in creative design within a wide sensing range. One potential application of incorporating rGO-paper sensors is in paper keyboards, where they can effortlessly detect when keys are touched. The detected signals can then be processed according to predefined instructions. To demonstrate the feasibility of this concept, we used the multilayer masking method to create U-shaped rGO patterns and silver connecting lines on paper cantilevers. Figure 2.3k shows both the top and bottom sides of an rGO-paper keyboard, with various LEDs illuminated by utilizing the signals from individual keys as shown in Figure 2.3,m. To detect a wide range of human motions involving skin stretching up to 55% in knee and wrist joints, they fabricated intricately designed rGO-paper strain sensors on flexible paper substrates using a digital craft cutter. Using the multilayer masking technique, parallel rGO lines and conductive silver connections were patterned onto a stretchable paper kirigami. This design allowed for proper detection and differentiation of various motions by selectively patterning strain-sensitive rGO on specific paper strips, preventing signal nullification caused by opposite bending directions. The interconnected rGO patterns were joined by silver lines (Figure 2.3d), generating positive or negative signals based on the direction of bending as the knee or wrist is stretched uniformly by all the rGO-patterned paper strips. These rGO-paper sensors have proven to be effective in detecting and distinguishing various movements such as knee bending, walking, and wrist flexion (Figure 2.3e–h). They are also capable of accurately measuring pulse rates in real-time (Figure 2.3i,j). Wearable electronics that can monitor body motion without impeding movement have gained significant attention across a wide range of applications. The high sensitivity to bending and folding exhibited by rGO-paper sensors makes them ideal for fabrication purposes. Additionally, their versatility allows for the development of innovative designs for various sensing applications. Apart from being used as wearable electronics, the remarkable sensitivity of these

sensors makes them suitable for creating paper keyboards that can detect key touches. The detected signals can then be processed according to specific instructions.

To validate this concept, U-shaped reduced graphene oxide (rGO) patterns and silver connecting lines were patterned on paper cantilevers using a multilayer masking technique. The design of an rGO-paper keyboard is showcased in Figure 2.3k, which shows both the top and bottom sides. Figure 2.3,m demonstrates how individual keys are used to illuminate different LEDs accordingly [123].

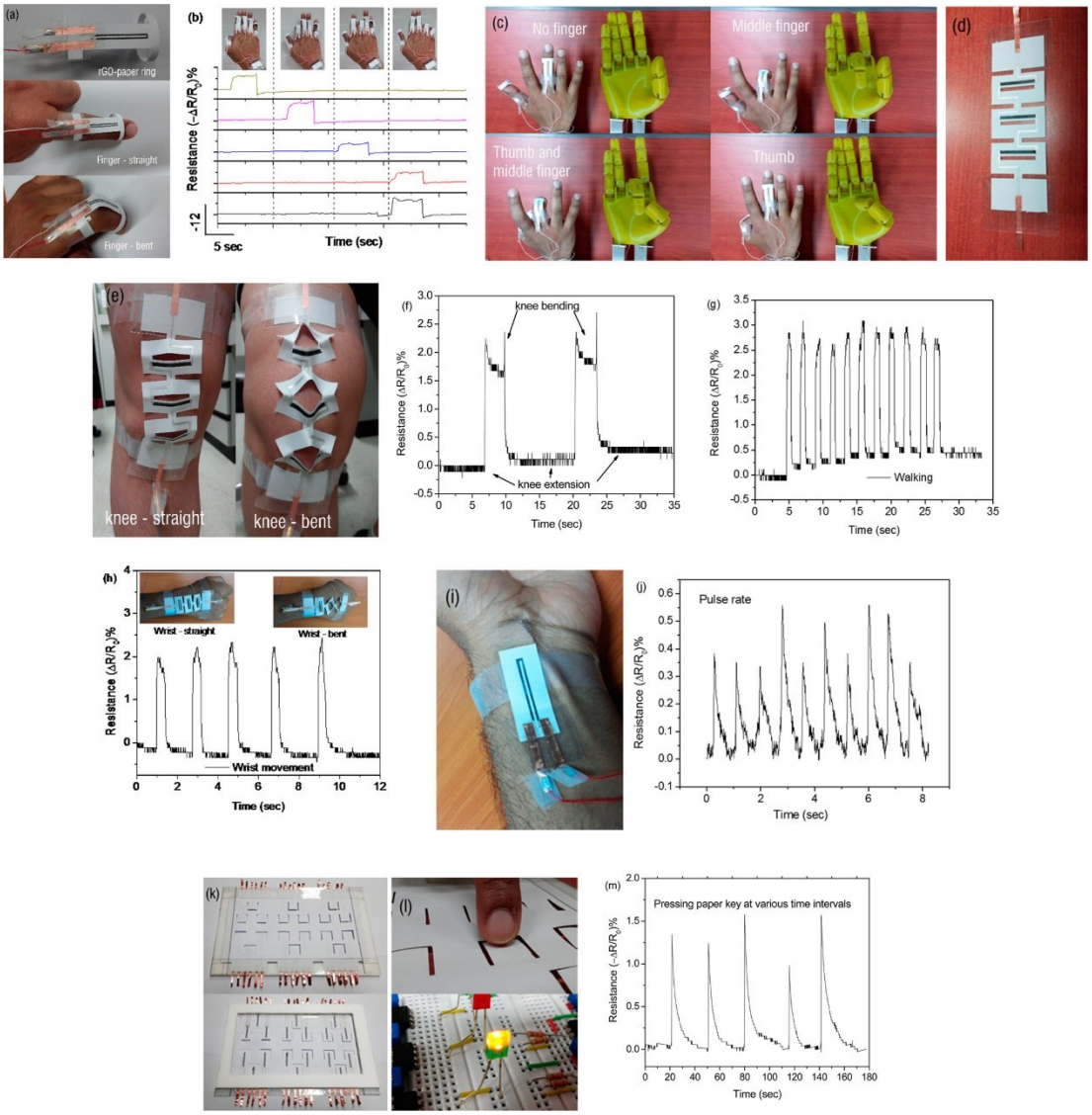

Figure 2.3. The rGO-paper rings demonstrate flexibility in different positions. (**a**) Photos show an rGO-paper ring in extended and bent positions. (**b**) Response signals from five independent rGO-paper rings monitoring various finger positions are depicted. Photographs of the hand in four different positions, corresponding to the plotted signals, are included. (**c**) The middle finger and

thumb of a 3D-printed robotic hand can be controlled using rGO-paper rings. (**d**) An intricate kirigami pattern is created through a multilayer masking process using rGO-paper. (**e**) Positions while wearing rGO-paper sensors. Observing changes in the resistance of an rGO-paper sensor on a knee during (**f**) sitting and (**g**) walking. (**h**) Response curve from wrist movement. (**i**) rGO paper sensor for pulse detection on the wrist, (**j**) and its corresponding signal data display. (**k**) Laminated paper keyboard with images of both sides (top and bottom view). (**l**,**m**) By touching a paper key, an LED illuminates and generates the corresponding signal [123]. @copyright 2017American Chemical Society. @ Highly Sensitive Bendable and Foldable Paper Sensors Based on Reduced Graphene Oxide | ACS Applied Materials & Interfaces—with permission.

2.3.3. Environmental Monitoring Applications

The high sensitivity of materials like graphene oxide makes them valuable in environmental monitoring. They can detect minute chemical changes and trace amounts of heavy metals and pollutants in water, showcasing their potential to address global environmental challenges [124].

In addition to monitoring human physiological signals, 2D materials can also be used for visualizing other physical signals, such as pressure and strain. Pressure sensors based on piezoresistive, capacitive, and triboelectric effects have been developed using various types of 2D materials. The integration of 2D MoS_2 into high-k Al_2O_3 layers has enabled a large-scale tactile sensor to effectively detect pressures ranging from 1 to 120 kPa. This sensor exhibits high sensitivity ($\Delta R/R_0$: 0.011 kPa^{-1}) and a fast response time (180 ms), as illustrated in Figure 2.4A(i–iv), addressing the interference challenges associated with traditional passive pressure sensors. These findings imply potential applications in multitouch perception and handwriting recognition. Furthermore, previous studies have highlighted the piezoresistive properties of compressible and flexible carbon aerogels incorporating carbon nanotubes, graphene, and other 2D nanomaterials. These materials are well-suited for use in wearable bioelectronics and electronic skins to detect tactile contacts with exceptional sensitivity. To enhance the interaction between nanomaterials and improve the performance of sensors, a solution is to use bacterial cellulose as a binding agent. By connecting Ti_3C_2 nanosheets, lightweight CECAs (Compressible and elastic carbon aerogels) can be created for electronic devices. These CECAs exhibit continuous lamellae with wave-like or oriented patterns that provide excellent compression properties, maintaining elasticity even under strains up to 99% for over 10,000 cycles (Figure 2.4B(ii, iii)). The results demonstrate that this device displays remarkable sensitivity across a wide range of pressures, from 0 kPa to 10 kPa, with exceptional linearity up to a strain of 95%. Additionally, it exhibits increased sensitivity to small changes in strain and pressure conditions [125].

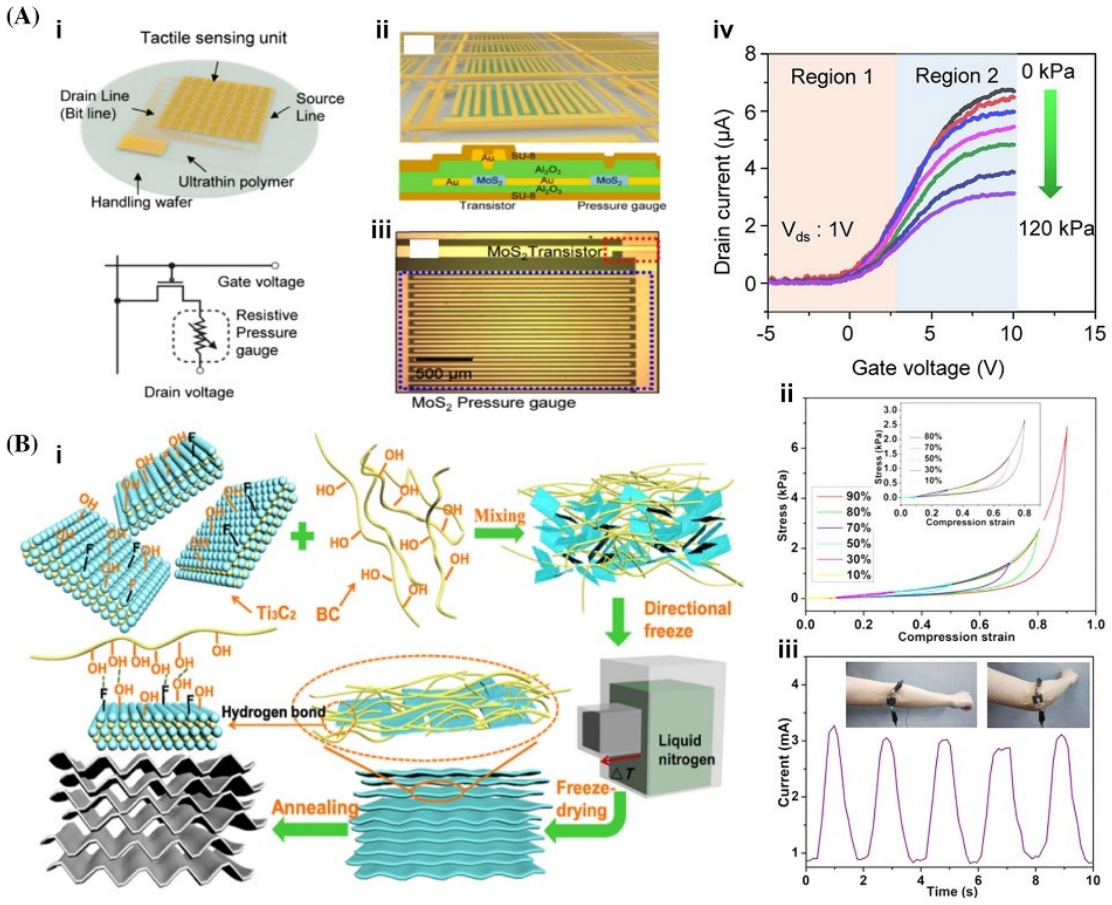

Figure 2.**4.** (**A**) (**i**–**iii**) The schematic structure and images of the MoS2 sensor. (**iv**) Pressure-transfer parameters of the MoS2 sensor from 0 to 120 kPa. (**B**) (**i**) Illustration of fabricating C-MX/BC-x carbon aerogel, where C, MX, BC, and x represent carbonization, Ti3C2, bacterial cellulose, and the mass ratio of BC to Ti3C2, respectively. (**ii**) Stress–strain curves at various compression strains with current signals from (**iii**) elbows [125]. @copyright Structures, properties, and challenges of emerging 2D materials in bioelectronics and biosensors - Chen - 2022 - InfoMat - Wiley Online Library—with permission.

2.3.4. Medical and Diagnostic Applications

The use of biosensors made with 2D materials has greatly advanced biomarker detection in the medical field. These sensors have transformed the development of efficient diagnostic tools, allowing for accurate and rapid detection of cardiac biomarkers from small blood samples . This enables prompt diagnosis in emergencies. Additionally, these biosensors are biocompatible and minimize the risk of adverse reactions, making them suitable for long-term implantable devices [126].

The regulation of glucose levels is crucial to managing diabetes on a global scale. To meet the growing demand for affordable and versatile sensing systems, an amperometric sensor was proposed to detect glucose using patterns of reduced graphene oxide (rGO). The method involves depositing patterned graphene oxide on substrates through filtration techniques such as stamping, followed by reducing it to rGO to ensure conductivity.

An effective biosensor for electrochemical enzymatic determination of glucose can be developed using graphene-based patterns modified with glucose oxidase . The biosensor has a response time of 0.37 s, a sensitivity of 11.2 μA mM^{-1} cm^{-2}, and a linear range from 1.0 to 25.0 mM. It also demonstrates a low detection limit of 0.32 mM while maintaining reproducibility, stability, selectivity, and resistance against interference in glucose analysis. The electrochemical mechanism of glucose oxidation at rGO/GOx is depicted in Figure 2.5. [127]. These results suggest that this platform has the potential to accurately measure glucose levels in human serum and find practical applications in various (bio)sensing systems during sample testing scenarios.

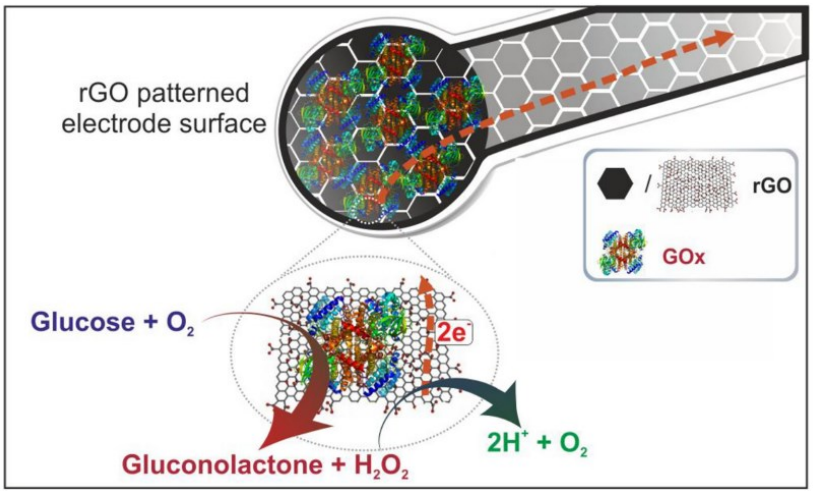

Figure 2.5. The electrochemical mechanism of glucose oxidation at reduced graphene oxide (rGO)/glucose oxidase is a significant area of study [127]. @copyright Simply patterned reduced graphene oxide as an effective biosensor platform for glucose determination - ScienceDirect with permission.

2.3.4.1. Innovations and Limitations

Recent advancements in biosensor technologies have successfully integrated 2D materials with cellulose, leading to significant improvements in functionality. The ultra-thin nature and extensive surface area of these materials have proven to be pivotal in enhancing the sensitivity of biosensors used for applications such as plasmonic and photoelectrochemical biosensing [128].

By combining nanocellulose with 2D materials, researchers have achieved synergistic enhancements in the performance of biosensors. Nanocellulose offers excellent biocompatibility,

a large surface area, and chemical versatility, while 2D materials contribute their unique electrical properties [138]. This combination results in highly sensitive biosensors that can detect even trace amounts of analytes. Furthermore, the mechanical strength provided by nanocellulose ensures the long-term stability and durability of these devices [129].

Various methods are utilized in material synthesis and processing, each offering distinct advantages and posing specific challenges. For example, Graphene Quantum Dots can be synthesized through top-down and bottom-up approaches, affecting their ultimate properties. Techniques like plasma-enhanced chemical vapour deposition are key in synthesizing MoS_2 and WS_2, enabling the creation of consistent, large-area structures. A critical area of research is the integration of bipolar exfoliated reduced graphene oxide with microelectrodes, addressing synthesis and deposition challenges. However, this field faces complexities. The synthesis and processing of these materials, especially when integrating 2D materials with nanocellulose, can influence biosensor performance, impacting sensitivity, specificity, and stability. Advancements in this field necessitate further research to optimize the performance of these sophisticated biosensors. This consistently emphasizes the primary advantage of these materials: enhanced sensitivity. It's also important to consider factors like repeatability and the fabrication process, which significantly influence the properties of 2D materials. Despite substantial contributions to the field, uncertainties remain, particularly regarding the relationship between material properties, fabrication methods, and the intricacies within these methods.

2.3.4.2. Challenges and Future Directions

The challenges of integrating two-dimensional (2D) materials with cellulose for applications such as biosensors are complex and multifaceted. Here are some of the key challenges that need to be addressed:

Material compatibility and scalability

Chemical interaction: The chemical compatibility between 2D materials and cellulose is critical. There may be challenges in achieving a stable chemical interaction that does not compromise the unique properties of the 2D materials or the integrity of the cellulose.

Mechanical stability: The integrated structure must be mechanically stable, which is particularly important for flexible applications like electronic skin (E-skin).

Large-scale synthesis: Scaling up the synthesis of 2D materials while maintaining their quality and uniformity over large areas is a significant challenge.

Integration Techniques: Developing scalable integration techniques that can handle the delicate nature of 2D materials without damaging them is difficult.

Degradation and sensitivity: Over time and under real-world conditions, there could be degradation of materials or loss of sensitivity, which are crucial for the practical implementation of biosensors.

Cost and accessibility

Synthesis and integration costs: The cost associated with the synthesis and integration of 2D materials and nanocellulose into biosensors might be high, potentially limiting their widespread use.

Limited Access: Access to advanced materials and fabrication techniques could be limited, posing a barrier to adoption.

Biocompatibility and safety

Toxicity and immune responses: A comprehensive analysis of biocompatibility and safety is essential, especially for medical applications, to understand potential toxicity or immune responses.

Performance standardization

Inconsistencies in performance: Variations in fabrication methods and materials could lead to inconsistencies in biosensor performance. Standardization protocols are needed for reliable and reproducible results.

Challenges in integration with AI and IoT

Seamless integration: The challenges associated with seamless integration, data processing, and real-time communication between biosensors and Artificial intelligence (AI) and Internet of things (IoT) technologies need to be addressed [139].

In summary, the integration of 2D materials with cellulose for biosensor applications involves overcoming challenges related to material compatibility, scalability, long-term stability, cost, biocompatibility, performance standardization, and integration with advanced technologies. These challenges must be addressed to ensure the successful development and implementation of these advanced biosensors.

In future research, efforts are focused on developing more sustainable synthesis methods and exploring novel material combinations for broader applications, including screen-printed carbon electrodes modified with graphene quantum dots, MoS_2, laccase as a caffeic acid biosensor; reduced graphene oxide/molybdenum disulfide/polyaniline nanocomposite-based electrochemical aptasensor for the detection of aflatoxin B1 fabrication [140–142].

2.4. Conclusions

This paper highlights the recent advancements in biosensor technologies, with a specific focus on integrating two-dimensional materials and nanocellulose. These innovations have resulted in improved sensitivity, specificity, flexibility, and biocompatibility of biosensors. Moreover, the devices created produce a minimal environmental footprint, and they are easy to recycle. The use

of these advanced materials has expanded their applications in medical diagnostics, environmental monitoring, and personal health devices.

These developments have transformed the capabilities of biosensors by enabling more precise and early detection of biomarkers. This is particularly important for medical diagnostics and environmental monitoring, where accurate detection is crucially needed. Additionally, the increased flexibility and biocompatibility have paved the way for wearable biosensors that are revolutionizing personal healthcare monitoring.

The potential for advancements in biosensors is immense, and the field is still in its infancy. Ongoing research focuses on improving synthesis techniques, expanding material options, and integrating with artificial intelligence and Internet of Things technologies. These developments will address current challenges and enable innovative applications. The collaboration between material science, bioengineering, and technology plays a vital role in driving the progress of biosensor technologies.

In conclusion, significant advances in material properties have had a profound impact on biosensors. These breakthroughs offer great promise for significant improvements in healthcare and environmental monitoring practices.

Closure

This chapter examined the current state of knowledge on integrating two-dimensional materials with nanocellulose for biosensing and related applications, drawing on the published paper in *Micromachines* (2024). The discussion opened with an account of the physical characteristics that make 2D materials — graphene, transition metal dichalcogenides, hexagonal boron nitride, and black phosphorus — attractive platforms for signal transduction, then turned to the complementary role of nanocellulose as a biocompatible, high-surface-area scaffold. The reactivity challenges inherent to cellulose — chain rigidity, limited hydroxyl group accessibility, enzymatic hydrolysis limitations — were reviewed alongside practical strategies to overcome them, including TEMPO-oxidation and silane-based functionalization. Application domains were surveyed in depth: medical diagnostics, glucose and DNA detection, environmental monitoring of water and air, food safety, and wearable health devices. In each domain, the combination of 2D material conductivity and nanocellulose structural integrity proved to deliver improvements in sensitivity, selectivity, flexibility, and cost-effectiveness that neither component achieves alone. The chapter also addressed theoretical underpinnings — band structure engineering, strain engineering, and the high surface-to-volume ratio of 2D systems — as well as economic and environmental considerations. Taken together, the material reviewed here provides the scientific context and application rationale that informed the experimental choices made in the following chapters.

Chapter 3: GO/rGO Modification—Methods, Models, and Application Results

This chapter is a published paper in **Encyclopedia (2024), Vol. 4, Issue 4, pp. 1827–1856**, titled "Optimizing Graphene Oxide Content in Cellulose Matrices: A Comprehensive Review on Enhancing Structural and Functional Performance of Composites." [130]

Optimizing Graphene Oxide Content in Cellulose Matrices: A Comprehensive Review on Enhancing Structural and Functional Performance of Composites

Abstract:

The incorporation of graphene into cellulose matrices has emerged as a promising strategy for enhancing the structural and functional properties of composite materials. This comprehensive provides a critical analysis of recent advances in optimizing graphene content in cellulose matrices and its impact on composite performance. Various optimization techniques, including response surface methodology, particle swarm optimization, and artificial neural networks, have been employed to identify optimal graphene concentrations and processing conditions. Quantitative analyses demonstrate significant improvements in mechanical properties, with notable increases in tensile strength and Young's modulus reported for graphene/microfibrillated cellulose composites. Substantial enhancements in thermal stability have been observed in lysozyme-modified graphene nanoplatelet/cellulose composites. Electrical conductivity has been achieved at low graphene loading levels. Additionally, barrier properties, biocompatibility, and functionality for applications such as energy storage and environmental remediation have been substantially improved. The paper explores case studies encompassing the optimization of thermal conductivity, viscosity, durability behaviors, pollutant removal, and various other properties. Despite promising results, challenges remain, including uniform dispersion, scalability, cost-effectiveness, and long-term stability. Strategies such as surface functionalization, solvent selection, and protective coatings are discussed. Future research directions, including novel processing techniques like 3D printing and electrospinning, as well as the incorporation of additional functional materials, are outlined. This paper synthesizes current knowledge, identifies emerging trends, and provides a roadmap for future research in the rapidly evolving field of graphene-cellulose composites.

3.1. Introduction

The integration of graphene oxide (GO) into cellulose matrices has emerged as a promising frontier in materials science, offering unprecedented opportunities to enhance the structural and functional properties of composite materials. This synergistic combination leverages the unique characteristics of GO—a two-dimensional carbon-based material with abundant oxygen-containing functional groups, high specific surface area, and excellent dispersibility in aqueous solutions—with the abundant, renewable, and biodegradable nature of cellulose [131], [132]. Unlike pristine graphene, GO's oxygen-rich surface chemistry facilitates stronger interactions with

cellulose, making it particularly suitable for composite applications . A study by Luo et al. (2018) reported the fabrication of bacterial cellulose/graphene oxide hydrogels using layer-by-layer assembly, resulting in extremely enhanced mechanical properties [133]. Another study by Song et al. (2017) demonstrated the creation of nanofibrillated cellulose (NFC)/reduced graphene oxide (RGO) hybrid films using layer-by-layer assembly, achieving a high tensile strength of 107 MPa along with outstanding flexibility [134]. Another study explored the synergistic effects of GO and CNC on the properties of poly(3-hydroxybutyrate-co-3-hydroxyvalerate) (PHBV) nanocomposites. The researchers prepared ternary nanocomposites consisting of PHBV and CNC-GO nanohybrids using a simple solution casting method .The study found that the ternary nanocomposites displayed significantly improved properties compared to neat PHBV and binary nanocomposites. Specifically, the ternary nanocomposites with 1 wt% covalent bonded CNC-GO exhibited excellent barrier properties, along with enhanced thermal stability, mechanical properties, and antibacterial activity [135]. These studies underscore the versatility of GO-cellulose composites in addressing challenges in materials engineering and environmental sustainability.

The optimization of GO content within cellulose matrices remains a critical challenge that significantly influences the final properties and performance of these composites. Factors such as the degree of oxidation of GO, the method of incorporation, and the processing conditions all play crucial roles in determining the overall efficacy of the composite. To address this challenge, researchers have employed various sophisticated optimization techniques. For instance, Basha et al. (2022) utilized response surface methodology (RSM) to optimize the adsorption of methylene blue dye using sulfonated graphene oxide impregnated cellulose acetate floated beads, demonstrating the effectiveness of statistical approaches in tailoring composite properties [136]. Building on this work, Khiam et al. (2022) applied particle swarm optimization (PSO) in conjunction with artificial neural networks (ANN) to optimize GO content in graphene oxide/chitosan composites for methylene blue adsorption, highlighting the potential of machine learning techniques in materials design [136]. Furthermore, Balasubramani et al. (2020) employed a similar ANN-PSO approach to model and optimize the removal of an antidepressant using graphene oxide/cellulose nanogel composites, further emphasizing the growing importance of these techniques in environmental applications [137].

Advancements in understanding the fundamental mechanisms underlying the enhanced properties of GO-cellulose composites have also been made. Recent advancements in understanding the fundamental mechanisms underlying the enhanced properties of graphene oxide (GO)-cellulose composites have provided significant insights into their remarkable performance and potential applications. These composites have garnered considerable attention due to their synergistic combination of the exceptional properties of GO and the abundant, renewable nature of cellulose. The enhanced properties of GO-cellulose composites can be largely attributed to the strong interfacial interactions between the two components. Recent studies have elucidated the nature of these interactions, revealing a complex interplay of hydrogen bonding, electrostatic interactions,

and mechanical interlocking [138]. The presence of oxygen-containing functional groups on both GO and cellulose surfaces facilitates the formation of an extensive hydrogen bonding network, which significantly contributes to the improved mechanical properties of the composites [139], [140]. Furthermore, molecular dynamics simulations have provided valuable insights into the nanoscale mechanisms of reinforcement. These simulations have demonstrated that the incorporation of GO into cellulose-based matrices can enhance the Young's modulus and tensile strength by up to 32.1% and 23.8%, respectively. This remarkable improvement is attributed to the formation of hydrogen bonds and the presence of Ca2+ ions near the interface, which play a crucial role in improving interfacial adhesion and facilitating load transfer between GO and the cellulose matrix [141].

Recent research has also highlighted the multifunctional nature of GO-cellulose composites, particularly in environmental remediation applications. These composites have shown exceptional performance in the removal of heavy metals, organic compounds, dyes, and microbial contaminants from wastewater [142]. The high surface area, superior mechanical strength, and notable biodegradability of nano-cellulose composites, when combined with GO, create a powerful platform for addressing complex environmental challenges [141].

In the context of water treatment, GO-cellulose composites have demonstrated remarkable adsorption capacities for various pollutants. The integration of GO with cellulose-based materials has been shown to enhance the stability and processability of the composites, making them more suitable for large-scale industrial applications [143]. Moreover, these composites exhibit excellent regeneration potential, further enhancing their economic viability and sustainability in wastewater treatment processes [144]

D’Amora et al. (2023) conducted an extensive molecular dynamics study to elucidate the complex interfacial interactions between graphene oxide (GO) and cellulose nanofibrils [145]. Their research employed advanced simulation techniques to model the behavior of GO sheets and cellulose nanofibrils at the molecular level. The study revealed that hydrogen bonding plays a crucial role in the mechanical reinforcement of GO-cellulose composites. Specifically, they observed that the oxygen-containing functional groups on GO surfaces formed strong hydrogen bonds with the hydroxyl groups of cellulose chains. This interaction significantly enhanced the interfacial adhesion between GO and cellulose, leading to improved mechanical properties of the composite. Furthermore, the simulations demonstrated that the density and distribution of oxygen-containing groups on GO surfaces directly influenced the strength of these interfacial interactions. This finding provides valuable insights for optimizing GO functionalization to maximize its reinforcing effect in cellulose matrices.

Many studies explored on developed an innovative 3D printing methods for fabricating GO-cellulose aerogels with hierarchical porous structures . Their approach utilized a custom-designed extrusion-based 3D printer capable of precisely depositing a GO-cellulose nanofiber (CNF) ink.

The ink formulation was carefully optimized to achieve the right viscosity and shear-thinning behavior necessary for successful printing. The researchers employed a freeze-drying process post-printing to create the aerogel structure. The resulting 3D-printed GO-cellulose aerogels exhibited remarkable mechanical strength, with compressive moduli up to 150% higher than conventionally prepared composites. Additionally, the hierarchical porous structure, consisting of macropores from the printed architecture and mesopores within the GO-CNF network, led to enhanced electrical conductivity. The authors demonstrated the potential of these 3D-printed aerogels in various applications, including as high-performance supercapacitor electrodes and efficient oil absorption materials for environmental remediation.

Biswas et al. (2023) conducted a comprehensive study on the use of GO-cellulose nanocrystal (CNC) composites as efficient drug carriers for controlled release applications [146]. The researchers developed a novel synthesis method that involved the in-situ reduction of GO in the presence of CNCs, resulting in a uniform dispersion of reduced GO (rGO) within the CNC matrix. They investigated the drug loading and release characteristics of these composites using doxorubicin, a common anticancer drug, as a model compound. The study revealed that the GO-CNC composites exhibited a remarkably high drug loading capacity of up to 85%, significantly higher than pure CNCs or GO alone. The researchers attributed this enhanced loading to the synergistic effects of π-π stacking interactions between the drug and rGO sheets, as well as hydrogen bonding with the CNC surface. Furthermore, the drug release profiles showed a sustained release behavior over 72 hours, with the ability to modulate the release rate by adjusting the GO content in the composite. In vitro cytotoxicity studies demonstrated that the drug-loaded GO-CNC composites effectively inhibited the growth of cancer cells while showing minimal toxicity to healthy cells. The authors also conducted in vivo studies using a mouse tumor model, which showed improved tumor reduction compared to free doxorubicin administration. This comprehensive study highlights the potential of GO-cellulose nanocomposites in developing advanced drug delivery systems for cancer therapy.

Another study made significant strides in developing GO-cellulose nanofiber composite electrodes for high-performance supercapacitors [147]. Their research focused on optimizing the GO content and the nanostructure of the composite to maximize energy storage capacity and cycling stability. The team employed a layer-by-layer assembly technique to create highly ordered GO-CNF nanostructures with precisely controlled thickness and composition. They investigated the effect of GO content (ranging from 5 to 30 wt%) on the electrochemical performance of the composites. The study revealed that a GO content of 20 wt% resulted in the optimal balance between electrical conductivity and ion accessibility. These optimized GO-CNF electrodes exhibited an exceptionally high specific capacitance of 412 F/g at a current density of 1 A/g, which is among the highest reported for cellulose-based supercapacitors. Moreover, the electrodes demonstrated remarkable cycling stability, retaining 95% of their initial capacitance after 10,000 charge-discharge cycles. The researchers attributed this outstanding performance to the synergistic effects

of GO's high electrical conductivity and the CNF's porous structure, which facilitated rapid ion transport and provided a large surface area for charge storage.

To further demonstrate the practical applicability of their GO-CNF supercapacitors, Kasprzak et al. fabricated a flexible, all-solid-state device using a gel electrolyte [148]. This device maintained excellent capacitive behavior under various bending conditions, showcasing its potential for use in wearable electronics and flexible energy storage systems.

These case studies illustrate the diverse and promising applications of GO-cellulose composites, highlighting the importance of continued research in this field to unlock their full potential in various technological domains.

From a chemical and physical perspective, graphene can be categorized into two primary classes: CVD-prepared graphene and oxidized graphene. CVD-prepared single- or multilayer graphene exhibits well-defined aromatic structures with minimal defects, as illustrated in Figure 3.1C (a and b). While these graphene sheets possess highly reactive surfaces suitable for bioelectrode applications, their poor solubility limits their use in nanomedicine or as nanocarriers. In contrast, graphene oxide (GO), depicted in Figure 3.1C (c), is a highly oxidized form of graphene that combines hydrophobic sp2- and sp3-bonded carbon with numerous hydrophilic functional groups, resulting in an amphiphilic colloid with enhanced dispersibility in aqueous and polar solvents. GO's unique structure enables π-π interactions, weak hydrogen bonding, and strong electrostatic interactions, making it suitable for various chemical modifications and interactions with biological systems. Reduced graphene oxide (RGO), shown in Figure 3.1C (d), offers a balance between the properties of graphene and GO, while graphene quantum dots (GQDs) and graphene oxide quantum dots (GOQDs), illustrated in Figure 3.1C (e and f), are nanometer-sized fragments with unique optical properties, opening up new possibilities for biological applications such as cell imaging and bioelectrodes [149].

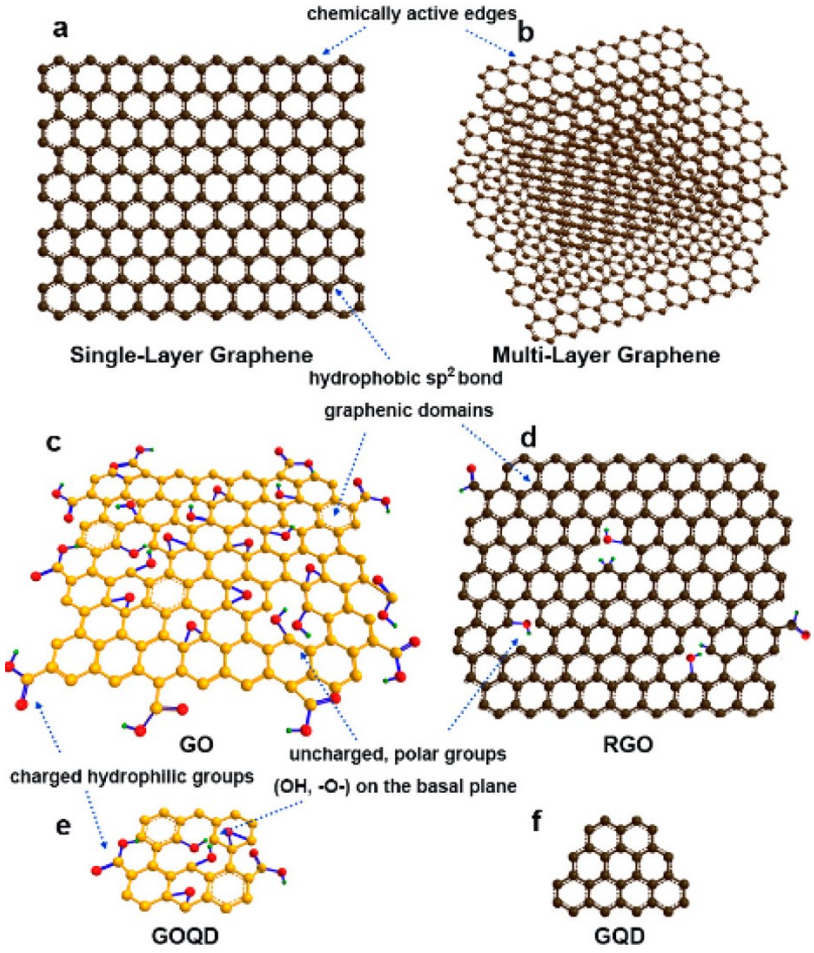

Figure 3.1. The forms of graphene and its derivatives that have been used for the construction of bioactive architectures: (a) single-layer graphene, (b) multilayer graphene, (c) GO, (d) RGO, (e) GOQD, (f) GQD. [150]. Copyright with permission [Functional Graphene Nanomaterials Based Architectures: Biointeractions, Fabrications, and Emerging Biological Applications | Chemical Reviews]

3.2. Rheological Impact of Graphene on Polymeric Matrices

The incorporation of graphene into polymeric matrices induces profound rheological changes, fundamentally altering the physicochemical properties of the resulting nanocomposites. These modifications stem from the unique characteristics of graphene, particularly its high aspect ratio and surface area, which create a complex interplay with the polymer chains. The rheological impact manifests primarily through viscosity enhancement, non-Newtonian behavior, and altered viscoelastic properties, all of which are intricately connected and dependent on factors such as graphene concentration, polymer-graphene interactions, and processing conditions[151].

The addition of graphene typically leads to a significant increase in viscosity, attributed to the formation of a percolated network within the polymer matrix. This network restricts the mobility of polymer chains, resulting in a more viscous material. Concurrently, the nanocomposites exhibit pronounced non-Newtonian behavior, characterized by shear-thinning properties. This phenomenon is often described by models such as the Cross-Williams-Landel-Ferry (Cross-WLF), which capture the complex flow behavior of these materials. The shear-thinning nature arises from the alignment of graphene sheets and polymer chains under applied stress, facilitating easier flow at higher shear rates [151].

Viscoelastic properties, as indicated by storage modulus (G') and loss modulus (G''), undergo substantial changes with graphene incorporation. The enhanced storage modulus observed in many graphene-polymer systems signifies improved elastic behavior and structural integrity. These rheological modifications are intrinsically linked to the concentration of graphene, with studies showing that even small additions (0.5-1.0 wt%) can induce substantial changes in viscosity and viscoelasticity. As concentration increases, a more pronounced network structure forms, leading to more significant rheological alterations [152], [153].

The nature and strength of polymer-graphene interactions play a crucial role in determining the rheological behavior of nanocomposites. Strong interfacial interactions, often evidenced by Fourier Transform Infrared (FTIR) spectroscopy studies, contribute to more effective stress transfer and enhanced rheological properties. These interactions are influenced by the processing conditions during nanocomposite preparation, including extrusion temperature, shear rate during mixing, and cooling rates, all of which affect graphene dispersion and, consequently, the rheological behavior of the composite [154], [155]. The rheological changes induced by graphene incorporation have far-reaching implications for both material properties and processing considerations. The increased viscosity and enhanced viscoelastic response often correlate with improvements in mechanical properties, such as tensile strength, modulus, and hardness. These enhancements are attributed to the effective load transfer between the polymer matrix and the well-dispersed graphene sheets. Furthermore, the rheological modifications frequently coincide with enhanced thermal stability, as evidenced by shifts in melting temperatures and decomposition onset temperatures observed in thermogravimetric analysis (TGA) and differential scanning calorimetry (DSC) studies [27].

While the increased viscosity of graphene-polymer nanocomposites can pose challenges for conventional processing techniques, it also presents opportunities for novel processing methods. The shear-thinning behavior, for instance, can be advantageous in extrusion-based additive manufacturing processes, allowing for improved flow through nozzles at high shear rates while maintaining structural integrity at rest. This characteristic exemplifies how the rheological impacts of graphene incorporation can be harnessed to enhance both material performance and processability [151].

Figure 3.2a-f presents a comprehensive analysis of the molecular characteristics, chemical structure, rheological behavior, and mechanical properties of PVBVA/graphene conductive patterns. Raman spectroscopy (2a) reveals the presence of graphene through characteristic D, G, and 2D bands, with a low ID/IG ratio indicating minimal structural defects. FTIR spectroscopy (2b) demonstrates hydrogen bonding between PVBVA and graphene, evidenced by a shift in hydroxyl peaks. Rheological studies (2c,d) show that the PVBVA/graphene ink exhibits higher viscosity and storage/loss moduli compared to pure PVBVA, resulting in improved printability and pattern precision. Tensile tests (2e,f) indicate significant enhancements in ultimate tensile strength and tensile modulus of the PVBVA/graphene patterns compared to pure PVBVA, with improvements of 98.7% and 177% respectively. These results are contextualized within existing literature, highlighting the exceptional mechanical reinforcement achieved with a relatively low graphene concentration [156].

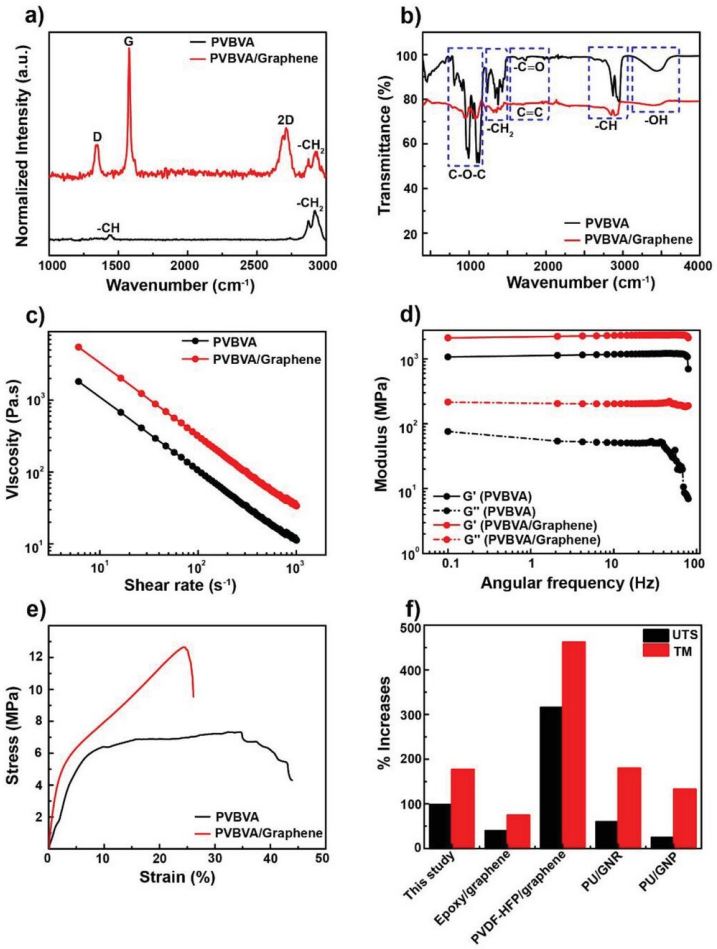

Figure 3.2. a) Structural analysis of the PVBVA/graphene-based conductive ink using Raman spectra. b) FTIR spectra indicating the interactions between the PVBVA polymer gel and graphene. Rheological behavior of the PVBVA/graphene-based conductive ink: c) dynamic viscosity and d) storage (G′) and loss moduli (G″) at various shear rates. e) Tensile properties of the

PVBVA/graphene-based conductive ink patterns: f) comparison of the percentage increment in the ultimate tensile strength (UTS) and tensile modulus (TM) of the PVBVA/graphene-based nanocomposites with those reported in previous studies [156] Reprinted with permission from ref. [156] Copyright 2023 Advanced Materials Technologies.

3.3. Theory

3.3.1. Theoretical Framework

Nanocomposite theory provides a fundamental framework for understanding the complex interactions between graphene and cellulose matrices at the nanoscale level. This theory elucidates how the unique properties of graphene, particularly its nanoscale dimensions and high aspect ratio, profoundly influence the overall characteristics of the cellulose matrix. Recent advancements in research have shed light on the intricate mechanisms underlying nanocomposite theory in graphene-cellulose systems, offering deeper insights into their behavior and potential applications [152]. At the core of nanocomposite theory in graphene-cellulose systems are the interfacial interactions between the two components. These interactions, primarily hydrogen bonding and π-π interactions, occur between the oxygen-containing functional groups on the graphene oxide surface and the hydroxyl groups of cellulose nanofibrils. The significance of these interfacial interactions lies in their ability to facilitate efficient stress transfer between the cellulose matrix and graphene sheets, which is crucial for improving the overall mechanical strength and stiffness of the composite. Islam et al. (2024) conducted an extensive study using molecular dynamics simulations to investigate these interactions at the molecular level, revealing that the strength and nature of these bonds directly influence the composite's mechanical properties [157]. This understanding is crucial for optimizing the composite's performance, as it allows researchers to tailor the interfacial chemistry to achieve desired mechanical characteristics. Also, The strength of these interfacial interactions directly influences the formation of percolation networks within the composite, another critical aspect of nanocomposite theory. He et al. (2022) made a significant breakthrough in this area by demonstrating that the percolation threshold in graphene-cellulose composites occurs at lower graphene concentrations than previously believed [158]. This finding has profound implications for the electrical properties of these composites, as the formation of a continuous pathway of graphene sheets throughout the cellulose matrix dramatically enhances electrical conductivity. The lower percolation threshold means that significant improvements in electrical conductivity can be achieved with smaller amounts of graphene, making these composites more economically viable and potentially expanding their range of applications. This discovery opens up new possibilities for developing lightweight, conductive materials for applications in flexible electronics, sensors, and electromagnetic shielding. Also, the mechanical reinforcement of cellulose matrices by graphene is a complex process involving several interrelated mechanisms, all of which are underpinned by the principles of nanocomposite theory. Jayatilaka et al. (2021) made significant strides in quantifying the stress transfer mechanism using in-situ Raman spectroscopy, allowing for direct measurement of stress transfer from the cellulose

matrix to individual graphene sheets during mechanical loading [159]. Their findings revealed that the efficiency of stress transfer is highly dependent on the quality of interfacial bonding and the orientation of graphene sheets within the matrix, further emphasizing the importance of the interfacial interactions. This understanding is crucial for optimizing the composite's mechanical properties, as it allows researchers to design materials with enhanced load-bearing capabilities by controlling the orientation and distribution of graphene sheets within the cellulose matrix.

The recent breakthrough in visualizing crack propagation in graphene-cellulose composites in real-time has been facilitated by advanced imaging techniques such as Digital Image Correlation (DIC). DIC has proven to be a powerful method for studying failure and crack propagation in advanced composite materials, including fibre-reinforced polymer (FRP) composites. This technique allows for the determination of material deformation and damage, providing valuable insights into the behavior of composites under stress. In parallel, research on cellulose nanocrystal (CNC) matrices has shown that polymer nanocomposites containing self-assembled CNCs are ideal for applications requiring both strength and toughness, as the helicoidal structure of CNCs can deflect crack propagation while the polymer matrix dissipates impact energy [160]. Their study demonstrated the effectiveness of graphene sheets in deflecting cracks and enhancing fracture toughness by forcing cracks to follow a more tortuous path around the graphene sheets. This mechanism works in tandem with the pull-out mechanism studied by Ilyaei et al. (2021), who developed a novel method to quantify the pull-out energy of individual graphene sheets from the cellulose matrix [161]. The pull-out mechanism is a crucial energy dissipation process during fracture, contributing significantly to the overall toughness of the composite. These findings have important implications for designing materials with enhanced damage tolerance and resistance to crack propagation, which is particularly relevant for applications in structural materials and protective coatings. Also, by integrating these various mechanisms, Zhu et al. (2024) introduced an innovative concept of hierarchical reinforcement in graphene-cellulose composites [162]. This multi-scale approach involves using graphene to reinforce cellulose nanofibrils, which in turn reinforce the bulk cellulose matrix. The hierarchical structure allows for efficient stress transfer across multiple length scales, resulting in exceptional improvements in mechanical properties. This approach demonstrates how a comprehensive understanding of nanocomposite theory can lead to novel design strategies for high-performance materials. By leveraging the synergistic effects of reinforcement at different scales, researchers can develop materials with unprecedented combinations of strength, toughness, and lightweight characteristics.

Surface modification of graphene and cellulose plays a crucial role in enhancing their compatibility and tailoring the properties of the resulting composites, further expanding the applications of nanocomposite theory [163]. Cruz-Benítez et al. (2023) developed a green approach for covalent functionalization of graphene oxide with cellulose nanocrystals using enzyme-mediated coupling [164]. This method resulted in improved dispersion of graphene in the cellulose matrix and enhanced mechanical properties of the composite. The covalent bonds formed between graphene

oxide and cellulose nanocrystals create strong interfacial interactions, leading to more efficient stress transfer and better overall mechanical performance. This approach not only improves the composite's properties but also addresses environmental concerns by utilizing green chemistry principles. Also, Complementing this covalent approach, Han et al. (2022) explored the use of bio-inspired polydopamine for non-covalent functionalization of graphene [165]. This approach led to improved interfacial adhesion between graphene and cellulose, resulting in enhanced thermal conductivity in the composites. The non-covalent nature of this functionalization method allows for the preservation of graphene's intrinsic properties while still improving its compatibility with the cellulose matrix. This research highlights the importance of balancing the degree of functionalization with the preservation of graphene's unique properties to achieve optimal composite performance.

Further advancing our understanding of surface modification, Nekooei et al. (2023) investigated the use of cellulose derivatives for polymer wrapping of graphene [166]. Their study provided new insights into the molecular mechanisms of polymer adsorption on graphene surfaces, offering a way to improve the dispersion of graphene in cellulose matrices while potentially preserving the unique properties of graphene. This research highlights the importance of understanding molecular-level interactions in optimizing nanocomposite properties and demonstrates the potential for using cellulose-based materials to enhance the compatibility between graphene and cellulose matrices. Mohamed et al. (2018) developed a novel, environmentally friendly surfactant derived from cellulose for stabilizing graphene dispersions [167]. This approach led to improved colloidal stability and enhanced properties in the resulting composites. The use of cellulose-derived surfactants represents a sustainable approach to graphene functionalization, addressing concerns about the environmental impact of traditional synthetic surfactants while also improving the processing and fabrication of graphene-cellulose composites. This research demonstrates the potential for developing fully bio-based composites with enhanced properties, aligning with the growing demand for sustainable materials in various industries.

Computational approaches, including molecular dynamics simulations and finite element analysis, have become increasingly important in predicting and optimizing the properties of graphene-cellulose composites. Naddeo et al. (2018) proposed a hierarchical multiscale model that combined molecular dynamics simulations, micromechanical models, and finite element analysis to predict the mechanical properties of graphene-cellulose nanocomposites across multiple length scales [168]This comprehensive approach demonstrates the power of computational techniques in advancing our understanding of these complex materials and provides a valuable tool for materials design and optimization. Petry et al. (2022) developed a machine learning model based on artificial neural networks to predict the thermal conductivity of graphene-cellulose aerogels [169]. Their model showed excellent agreement with experimental data and could be used to design composites with tailored thermal properties, highlighting the potential of data-driven approaches in materials

design. This research demonstrates the growing importance of artificial intelligence and machine learning in materials science, offering new avenues for rapid materials discovery and optimization.

3.3.2. Theoretical Modelling and Simulation of Graphene-Cellulose Composites

The integration of graphene into cellulose matrices to form advanced composite materials has garnered significant attention in recent years due to the exceptional properties exhibited by these hybrid structures. To elucidate the complex interactions and resultant characteristics of graphene-cellulose composites, researchers have increasingly turned to sophisticated theoretical modelling and simulation techniques. These computational approaches offer invaluable insights across multiple scales, ranging from molecular-level interactions to macroscopic property predictions, thereby facilitating the rational design and optimization of experimental protocols.

3.3.3. Molecular Dynamics Simulations

Molecular dynamics (MD) simulations have been instrumental in understanding the interfacial interactions between graphene and cellulose at the atomic level [170]. Alqus et al. (2015) conducted MD simulations to study the interactions between hydrophobic and hydrophilic faces of ordered cellulose chains and a single layer of graphene in explicit aqueous solvent [171]. Their findings revealed that the hydrophobic cellulose face forms a stable complex with graphene, with the interface remaining solvent-excluded over the course of simulations. This study provided valuable insights into the amphiphilic nature of cellulose and its interactions with graphene in aqueous environments. Figure 3.3 shows time series snapshots from a 300 ns molecular dynamics simulation of the graphene-cellulose (GC100) interface. Panel (a) provides a side view of the full system, illustrating the layered structure of cellulose on the graphene surface. Panels (b) and (c) offer top views of the graphene/layer 1 and graphene/layer 4 interfaces, respectively. These images demonstrate the stability of the hydrophobic cellulose face interacting with graphene, particularly in layer 1, while showing some flexibility in the more solvent-exposed layer 4. This figure highlights the strong complementarity between the hydrophobic cellulose face and graphene, which is crucial for understanding the behaviour and properties of graphene-cellulose composites [171]

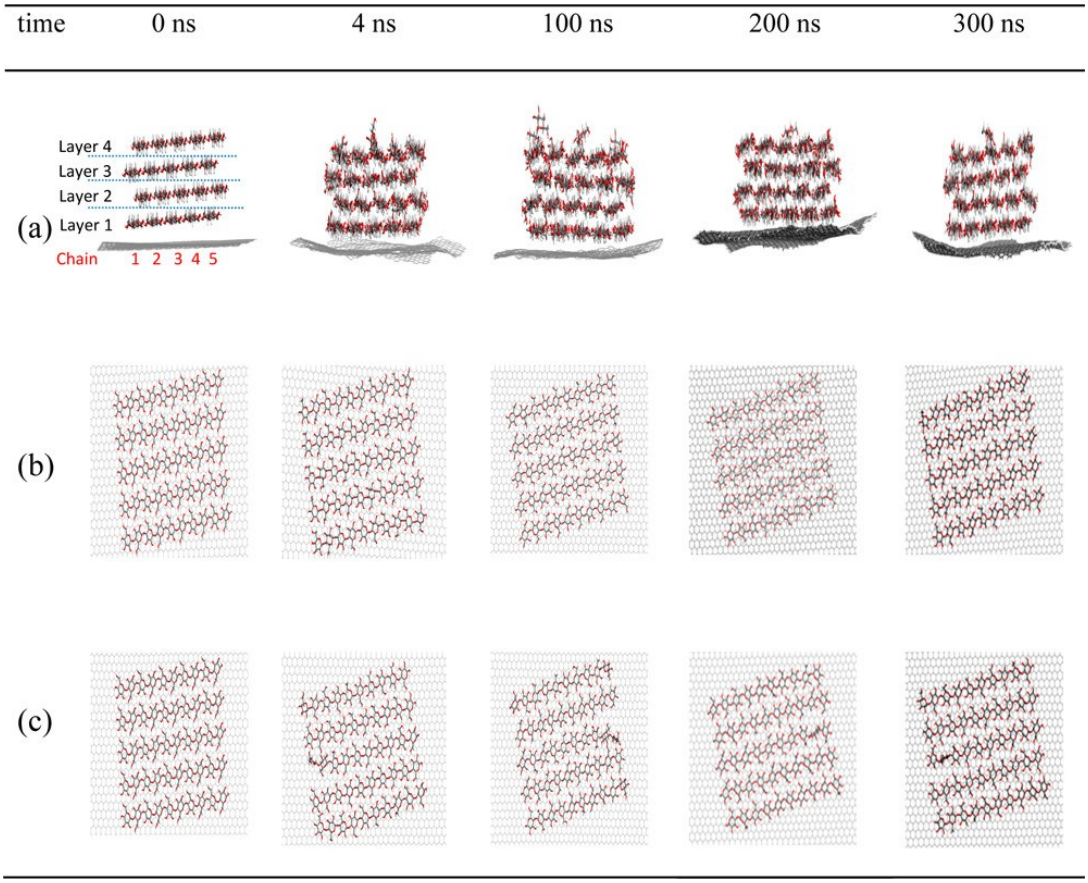

Figure 3.3: Time series of configurations sampled from 300 ns MD simulation of GC100. Structures shown of (a) full system (side view, and top views of (b) graphene/layer 1 and (c) graphene/layer Reprinted from ref. [171].

3.3.4. Finite Element Analysis

The field of finite element analysis (FEA) for graphene-cellulose composites is an emerging area of research that combines the unique properties of graphene with the abundant and renewable nature of cellulose. While direct studies on FEA of graphene-cellulose composites are limited, recent advancements in related areas provide valuable insights into potential developments in this field. S. Wang et al. (2023) demonstrated the application of FEA to graphene-reinforced composites by studying the properties of Ag-GNP silver-graphene composites and analyzing the electrical contact coupling field[172]. This approach could potentially be adapted for graphene-cellulose systems. In a related study, Wei et al. (2023) developed a simplified finite element method for analyzing the resistance response of graphene composites, considering size distribution and agglomeration [173]. This method could be valuable for modelling graphene-cellulose composites. Also, Nukala et al. (2023) conducted a simulation of wood polymer composites using finite element analysis [174]. This study is particularly relevant as wood is a cellulosic material, and the techniques used could be adapted for graphene-cellulose composites. Advancements in

FEA for related composite materials have also been made. For instance, Wu et al. (2023) developed a size-dependent FEM for analyzing the 3D free vibration of functionally graded graphene platelets-reinforced composite cylindrical micro shells [175]. Similarly, Tayebi et al. (2023) applied a full layerwise finite element method to analyze the free vibration of functionally graded composite rectangular plates reinforced with graphene nanoplatelets [176]In the realm of cellulose-based composites, Sathishkumar et al. (2023) conducted numerical buckling analysis of cellulose microfibril-reinforced polymer composites [177]. This study demonstrates the application of FEA to cellulose-based materials, which could be extended to include graphene reinforcement.

3.3.5. Multiscale Modelling

Multiscale modelling has emerged as a powerful approach for understanding and predicting the properties of complex materials like graphene-cellulose composites across different length scales. This hierarchical modelling strategy aims to bridge the gap between atomic-scale interactions and macroscopic properties. For instance, Rafiee and Rafiee et al. (2020) used multiscale modelling to predict Young's modulus in agglomerated graphene/polymer composites, focusing on capturing the agglomeration phenomenon [178]. C. Zhu et al. (2018) explored cellulose nanofiber-graphene oxide biohybrids, using advanced microscopy and ReaxFF simulations to study self-assembly and copper-ion adsorption, providing insights into the interactions at the molecular level [179].

3.3.6. Density Functional Theory (DFT)

Density Functional Theory (DFT) calculations have indeed enriched recent studies on cellulose-graphene composites, providing valuable insights into their interactions and properties at the molecular level [180]. A study utilized DFT to investigate the electronic properties of graphene quantum dots with various substitutional impurities, which could be relevant for cellulose-graphene nanocomposites [181]. Another study on cellulose acetate/graphene oxide composites used DFT simulations to understand the adsorption mechanisms between these materials, finding that hydrogen bonding from hydroxyl groups facilitates the adsorption process [49]. Research by Tachikawa et al. used DFT to investigate hydrogen storage mechanisms in alkali-doped graphene nanoflakes, which could potentially be applied to cellulose-graphene systems [182]. A study on dialdehyde cellulose/graphene oxide films used DFT calculations along with molecular docking to investigate their potential antimicrobial activity against COVID-19 [183].

3.3.7.. Machine Learning Models

Recent advancements in artificial intelligence have led to the development of machine learning models for predicting and optimizing the properties of graphene-cellulose composites. For example, Petry et al. (2022) explored the use of machine learning to analyze the microscopic interactions between graphene oxide and cellulose, enhancing the understanding of binding strengths [169]. Balasubramani et al. (2023) applied machine learning models to optimize

processes involving graphene oxide and microcrystalline cellulose, focusing on pharmaceutical applications [184]. Additionally, Champa-Bujaico et al. (2023) utilized support vector machines to predict properties of bionanocomposites made from crystalline nanocellulose and graphene oxide, demonstrating the potential of machine learning in material design and optimization [185]. These studies highlight the transformative impact of AI in advancing the capabilities of graphene-cellulose composites.

3.4. Optimization of Graphene Content

Determining the optimal graphene content in cellulose matrices is crucial for achieving the desired structural and functional performance. Excessive or insufficient graphene loading can lead to suboptimal properties, making it essential to identify the optimal graphene concentration. Several studies have employed various optimization techniques, including response surface methodology (RSM), particle swarm optimization (PSO), and artificial neural networks (ANN), to identify the optimal graphene content and processing conditions [186], [187], [188].

3.4.1. Response Surface Methodology (RSM)

RSM is a widely used statistical technique for optimizing multiple variables simultaneously. In the context of graphene-cellulose composites, RSM has been employed to optimize various properties and processing conditions [136]. Figure 3.4 illustrates the effects of various experimental parameters on chlorpyrifos (CPF) removal using magnetic graphene oxide-carboxymethyl cellulose (MGOC) composite. The 3D plots show: A) CPF concentration and contact time: Higher CPF concentrations decreased removal efficiency due to increased competition for adsorption sites. B) CPF concentration and MGOC dosage: Increasing adsorbent dosage improved removal efficiency by providing more adsorption sites. C) MGOC dosage and contact time: Removal efficiency increased with contact time, reaching equilibrium at 45 minutes. D) Solution pH: Lower pH improved CPF removal due to electrostatic interactions between the positively charged MGOC surface and the negatively charged CPF molecules [189].

The adsorption mechanism involves diffusion, electrostatic interactions, hydrogen bonding, surface complexation, and π-π interactions between CPF and MGOC composite.

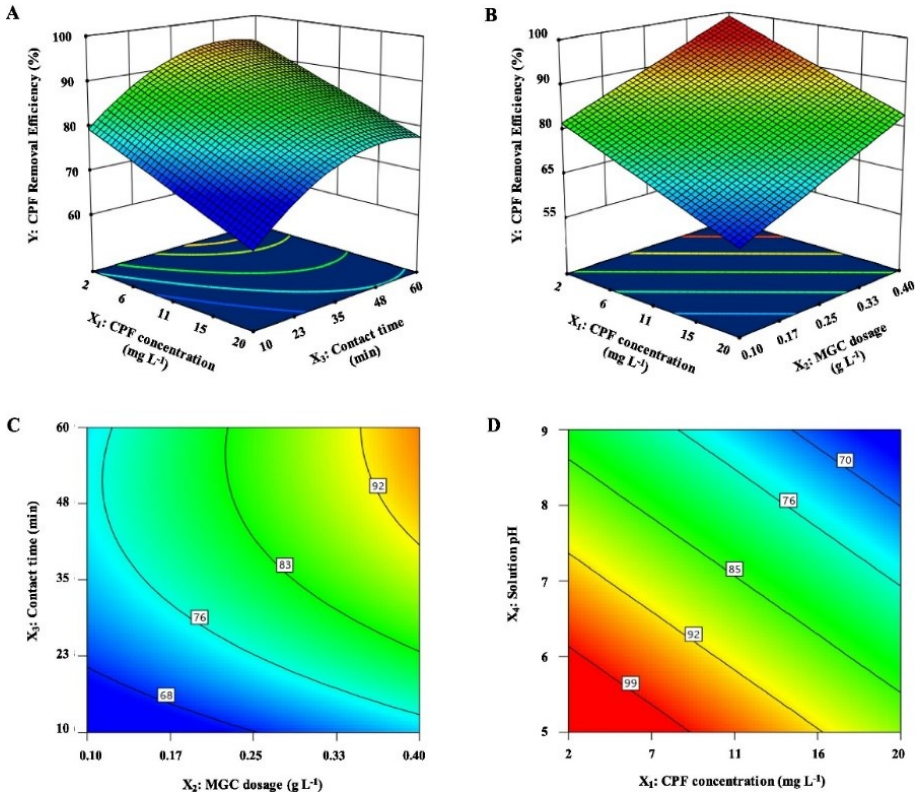

Figure 3.4: CPF removal efficiency as a function of (A) CPF concentration and contact time, (B) CPF concentration and MGOC dosage, (C) contact time and a MGOC dosage, and (D) solution pH and CPF concentration; (the operating parameters set at their center points: CPF concentration of 11 mg/L, adsorbent dosage of 0.25 g/L, contact time of 35 min, and solution pH of 7) [189]. [with permission Adsorption characteristics in the removal of chlorpyrifos from groundwater using magnetic graphene oxide and carboxy methyl cellulose composite - ScienceDirect]

3.4.1.1. Optimization of Thermal Conductivity and Viscosity

A study employed RSM to optimize the thermal conductivity and viscosity of hybrid nanofluids containing graphene nanoplatelets (GNPs) and cellulose nanocrystals (CNCs). The researchers utilized a central composite design (CCD) to investigate the effects of temperature, volume concentration, and nanofluid type on the thermal properties. The results demonstrated that the optimal thermal conductivity and viscosity values were achieved at specific combinations of these factors, highlighting the effectiveness of RSM in optimizing the graphene content and processing conditions. Another study employed RSM to optimize the durability behaviours of engineered cementitious composites (ECC) by incorporating graphene oxide (GO) and polyvinyl alcohol (PVA) fibers. The researchers used a CCD to establish thirteen mixtures with varying GO and PVA concentrations and evaluated eight response variables, including compressive strength, weight loss, and rapid chloride permeability. The analysis of variance effectively designed and

evaluated response models, with high R^2 values ranging from 84% to 99%, indicating a good fit between the experimental data and the predicted values [190], [191], [192].

PSO is a computational optimization technique inspired by the social behaviour of bird flocking or fish schooling. In the context of graphene-cellulose composites, PSO has been employed in conjunction with ANN to optimize various properties and applications [193], [194]. One notable application of PSO in this field is the optimization of antidepressant removal from water using graphene oxide/cellulose nanogel composites. Researchers have employed PSO-based ANN modelling to fine-tune the composition and processing parameters of these composites, resulting in more efficient removal of antidepressants like Flupentixol from aqueous[195]. The researchers employed a combination of Particle Swarm Optimization (PSO) and Artificial Neural Network (ANN) modelling to optimize the removal process. This study presents a comprehensive approach to developing and optimizing a graphene oxide/cellulose nanogel composite for antidepressant removal. The researchers employed an Artificial Neural Network (ANN) model to predict the composite's adsorption capacity, which was further enhanced through Particle Swarm Optimization (PSO) to fine-tune input parameters. By optimizing process variables, including graphene oxide content, the team achieved improved removal efficiency for Flupentixol. The successful application of the PSO-ANN methodology in tailoring graphene content demonstrates its potential for enhancing antidepressant removal in various applications, highlighting the synergy between advanced materials development and computational optimization techniques in environmental remediation efforts.

3.4.1.2. Optimization of Dye Removal

Another study by Khiam et al. utilized PSO and ANN to optimize the removal of methylene blue dye from aqueous solutions using a graphene oxide/cellulose nanocrystal composite. The researchers employed PSO to optimize the input parameters of the ANN model, which predicted the adsorption capacity of the composite. The optimized composite exhibited excellent dye removal efficiency, demonstrating the effectiveness of the PSO-ANN approach in optimizing the graphene content for environmental remediation applications [196]. A study concluded that the developed carboxymethyl cellulose-graphene oxide (CMC-GA-GO) biobased composite demonstrated high efficiency in removing methylene blue from wastewater, with maximum dye removal percentages ranging from 93-98%. The optimal conditions for maximum removal were found to be 20% GO weight percent in the composite, 25 minutes adsorption time, 25°C adsorption temperature, 10-30 ppm initial MB concentrations, pH 7.0, and 0.2 g adsorbent dose. The adsorption process followed the Langmuir isotherm model and pseudo-second order kinetics, indicating monolayer adsorption and chemisorption, respectively. Thermodynamic analysis revealed the process was exothermic and spontaneous, working best at lower temperatures. The composite also showed good reusability, retaining 86% of its MB dye removal capacity after 10

cycles. Overall, the study concluded that the CMC-GA-GO composite shows promise as an inexpensive, reusable adsorbent for removing organic cationic dyes like methylene blue from industrial wastewater [143]. Another study employed ANN-PSO modeling to optimize methylene blue adsorption using graphene oxide/chitosan composites [197]. This approach allowed for precise prediction and optimization of the adsorption process.

Sulfo-functional 3D porous cellulose/graphene oxide composites have been developed as an innovative solution for water purification, specifically targeting the removal of methylene blue and tetracycline pollutants. These advanced materials leverage a three-dimensional structure to maximize surface area and enhance adsorption capabilities. The incorporation of sulfo-functional groups further augments the composites' affinity for the target contaminants. This dual-action approach enables the efficient elimination of both dye (methylene blue) and antibiotic (tetracycline) pollutants from water, showcasing the potential of these composites in addressing complex water treatment challenges [198]. Recent research in environmental remediation is exploring multifaceted approaches to pollutant removal [199]. Scientists are developing composites capable of simultaneously addressing multiple contaminants, including toxic metals and organic pollutants like phenol. These advanced materials, often incorporating graphene oxide, chitosan, and cellulose derivatives, demonstrate versatility in tackling various environmental challenges [200]. Additionally, the field is witnessing a growing integration of artificial intelligence and experimental design methodologies to optimize removal processes, signalling a shift towards more sophisticated and efficient pollution control strategies [201].

3.4.2. Artificial Neural Networks (ANN)

ANN is a machine learning technique that can model complex nonlinear relationships between input and output variables. In the context of graphene-cellulose composites, ANN has been used in combination with PSO to optimize various properties and applications[137]. Figure 3.5 shows the optimal values of PSO parameters obtained by conducting a sensitivity analysis for a maximum iteration of 1000[137].

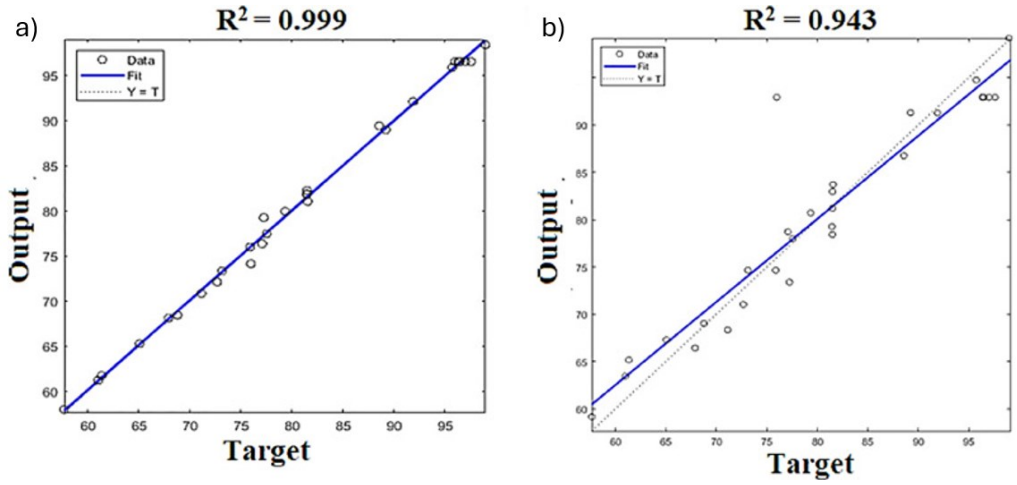

Figure 3.5: Regression plot for testing data a) GO: S*pop* value of 50 and 4-8-1 network configuration b) GOC: S*pop* value of 50 and 4-8-1 network configuration [137][with permission of Efficient removal of antidepressant Flupentixol using graphene oxide/cellulose nanogel composite: Particle swarm algorithm based artificial neural network modelling and optimization - ScienceDirect]. In the study by Xiang et al., ANN was used in combination with PSO to optimize the removal of antidepressants using a graphene oxide/cellulose nanogel composite. The ANN model was trained on experimental data, and PSO was employed to optimize the input parameters, including the graphene oxide content, leading to improved adsorption performance [202]. This synergistic approach demonstrates the potential of ANN and PSO in optimizing the graphene content for specific applications. The optimization of dye removal processes has been extensively studied using various advanced techniques. One notable approach involves the use of response surface methodology (RSM) to optimize the adsorption of methylene blue dye using sulfonated graphene oxide impregnated cellulose acetate floated beads [136]. This method allows for the systematic evaluation of multiple parameters affecting dye removal efficiency. In another study, researchers developed a cost-effective and sustainable lemongrass membrane for dye removal, demonstrating excellent adsorption capabilities for methylene blue dye [203]. The kinetic study of this process revealed that the methylene blue adsorption followed a pseudo second-order model, providing valuable insights into the adsorption mechanism. Additionally, the incorporation of graphene oxide into the lemongrass membrane was explored, although the pure lemongrass membrane showed comparable dye adsorption performance [203]. These findings highlight the potential of using naturally sustainable materials in conjunction with advanced optimization techniques to enhance dye removal processes, offering promising solutions for wastewater treatment.

This flowchart (Figure 3.6) outlines the various optimization techniques used to determine the optimal graphene content in cellulose matrices. It includes the following key techniques and their specific applications:

RSM (Response Surface Methodology): Used for optimizing thermal conductivity, viscosity, and durability behaviors. The flowchart highlights two branches of RSM applications: one for thermal properties using graphene nanoplatelets (GNPs) and cellulose nanocrystals (CNCs), and another for durability in engineered cementitious composites (ECC) with graphene oxide (GO) and polyvinyl alcohol (PVA) fibers [204], [205].

PSO & ANN (Particle Swarm Optimization and Artificial Neural Networks): Employed together to enhance the removal efficiencies of pollutants such as antidepressants and dyes from aqueous solutions. These techniques optimize parameters in conjunction with ANN models that predict the adsorption capacity of graphene-cellulose composites.

This diagram visually communicates the strategic applications of these techniques in optimizing material properties and enhancing functional performance [206].

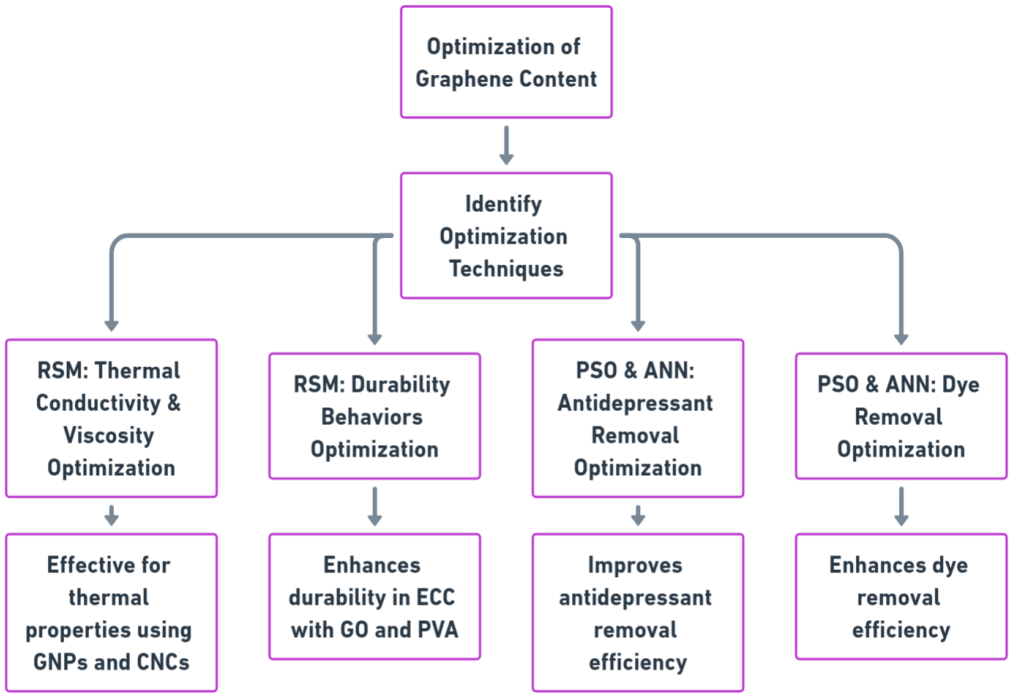

Figure 3.6: Optimization Techniques for Graphene Content.

3.5. Quantitative Analysis of Structural and Functional Performance

The optimization of graphene content in cellulose matrices has been shown to significantly enhance the structural and functional performance of the resulting composites. Several studies have quantitatively analyzed the improvements in mechanical properties, thermal stability,

electrical conductivity, barrier properties, and other relevant characteristics achieved through the incorporation of optimized graphene content [207], [208].

3.5.1. Mechanical Properties

The addition of graphene to cellulose matrices has been demonstrated to improve the mechanical properties of the composites, such as tensile strength, Young's modulus, fracture toughness, and elongation at break [209]. Recent studies have demonstrated significant improvements in tensile properties of cellulose-based composites reinforced with graphene and its derivatives [210]. A study on cellulose acetate/graphene oxide (CA/GO) films revealed that the addition of just 0.5 wt% GO led to a 64% increase in tensile strength and an 85% enhancement in strain-to-failure compared to pure cellulose acetate films. This remarkable improvement was attributed to the strong interfacial interactions between GO and the cellulose matrix, facilitated by hydrogen bonding. Research has shown that carboxymethyl cellulose (CMC) functionalization can effectively improve the dispersion of graphene-based materials in polymer matrices. A study on epoxy nanocomposites reinforced with CMC-functionalized graphene nanoplatelets (GNPs) demonstrated enhanced tensile properties, with CMC-GNP reinforced composites exhibiting superior tensile strength compared to those reinforced with carbon nanotubes (CNTs) [210].

The incorporation of graphene-based materials has also been shown to enhance the compressive strength of cellulose composites. A recent study investigating the effects of graphene oxide (GO) and graphene nanoplatelets (GNPs) on cement-based composites found that the incorporation of 0.02 wt% GO and GNPs enhanced the flexural strength by 16.3% and 11.6%, respectivel [138]. The researchers attributed this improvement to the ability of GO and GNPs to fill cracks and form a more compact microstructure in cement mortars. The addition of graphene-based materials has been shown to significantly increase the Young's modulus of cellulose composites. A molecular dynamics simulation study on calcium silicate hydrate (C-S-H) composites, which are the main products of cement hydration, revealed that the incorporation of GO enhanced the Young's modulus by 32.1% [138]. This improvement was attributed to the formation of hydrogen bonds and the presence of Ca^{2+} ions near the interface, which improved interfacial adhesion and load transfer between GO and C-S-H. Graphene reinforcement has been shown to enhance the fracture toughness of cellulose-based composites. A study on chitosan-based composites containing optimized amounts of graphene oxide (GO) and cellulose nanocrystals (CNCs) observed a 216% improvement in toughness compared to pristine chitosan [211]. This significant enhancement was attributed to the synergistic effects of GO and CNCs, as well as their strong interfacial interactions with the chitosan matrix. The addition of graphene-based materials has been shown to improve the elongation at break of cellulose composites. A study on graphene oxide/polyacrylamide/ carboxymethyl cellulose sodium (GO/PAM/CMC) nanocomposite hydrogels demonstrated improved elongation at break with the incorporation of GO [212]. The researchers found that hydrogen bonding between the oxygen-containing groups of GO and the N-H bonds of PAM resulted in a dense structure, leading to enhanced mechanical properties.

Figure 3.7 illustrates the mechanical properties of Cellulose Nanofiber-Graphene Oxide hybrid (CNGO) hybrid filaments: (a) The stress-strain curves demonstrate how the addition of graphene oxide (GO) affects the mechanical behavior of the filaments. As the GO concentration increases, the curves generally show higher stress values but lower strain at failure, indicating increased strength but reduced ductility. (b) This graph displays the relationship between GO concentration and two key mechanical properties: Young's modulus and tensile strength. Both properties show a similar trend, increasing significantly as GO content rises up to 5 wt%, then slightly decreasing at 7 wt%. This suggests an optimal GO concentration around 5 wt% for maximizing mechanical performance. (c) This plot compares the tensile strength of the CNGO hybrid filaments produced in this study to other reported values in literature, with respect to filament diameter. It demonstrates that the CNGO filaments achieve competitive strength values, especially considering their relatively large diameter. The graph also indicates a general trend of increasing strength as filament diameter decreases, likely due to improved molecular alignment in thinner fibers [207].

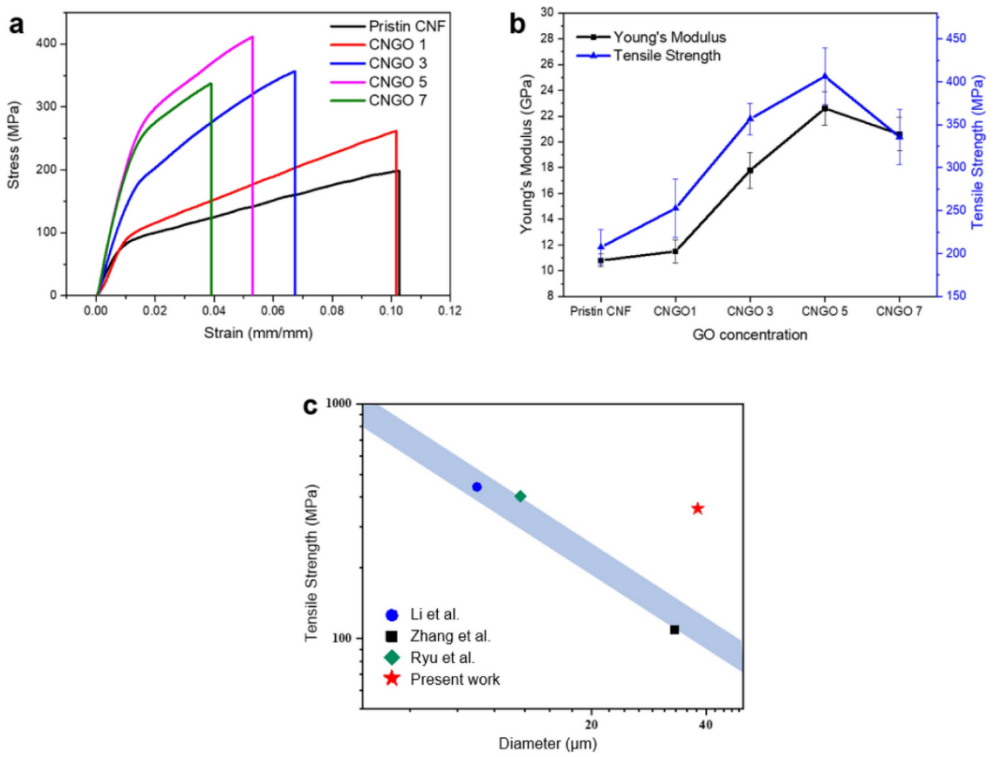

Figure 3.7: Mechanical properties of CNGO hybrid filaments: (a) stress–strain curves, (b) variations of Young's modulus and tensile strength with the GO concentration, (c) comparison of tensile strength with other reports in terms of filament diameter [213][High-strength cellulose nanofiber/graphene oxide hybrid filament made by continuous processing and its humidity monitoring | Scientific Reports (nature.com)]Open Access

3.5.2. Thermal Stability

Graphene has been shown to improve the thermal stability of cellulose matrices by acting as a barrier to heat transfer and enhancing the char formation during thermal degradation. A study by Phiri et al. demonstrated that the incorporation of graphene into microfibrillated cellulose (MFC) composites resulted in a 22% enhancement in thermal stability at 9 wt% graphene loading. The researchers observed that the graphene sheets formed a network structure within the MFC matrix, effectively hindering the movement of polymer chains and delaying the onset of thermal degradation. Another study by Shen et al. demonstrated that the incorporation of lysozyme-modified graphene nanoplatelets (LmGNP) into cellulose-based composites significantly enhanced the thermal conductivity, with a 297.3% increase observed for composites containing 8 wt% LmGNP compared to pure cellulose [214]. The researchers attributed this enhancement to the high thermal conductivity of graphene and the effective heat transfer pathways provided by the well-dispersed LmGNP in the cellulose matrix. Recent work by NI et al. investigated the thermal properties of unsaturated polyester composites reinforced with kenaf core fiber and hybrid nanofillers of cellulose nanocrystals (CNC) and graphene nanoplatelets. The study revealed that the incorporation of these nanofillers significantly improved the thermal stability of the composites. The maximum degradation temperature (T) increased to 387.8°C for samples containing both CNC and GNP, compared to the control samples without nanofillers [215].

Figure 3.8 presents the TG and DTG curves for NFC/GO-C and NFC/GO-E composites. The thermogravimetric analysis up to 800°C shows a final weight loss of approximately 32.0% to 34.0%, primarily due to the decomposition of NFC and GO, including cellulose/hemicellulose and oxygen-containing functional groups (C=O, C-O-C, C-O-H). Above 500°C, the weight-loss peak becomes less distinct due to biochar formation and the breakdown of C-C and C-H bonds. For NFC/GO-C composites, minor and major mass losses occur at 200°C and 307°C, while NFC/GO-E composites exhibit shoulder peaks at 205°C and 241°C. The thermal degradation process can be divided into two stages: 100-220°C and 220-380°C [216]

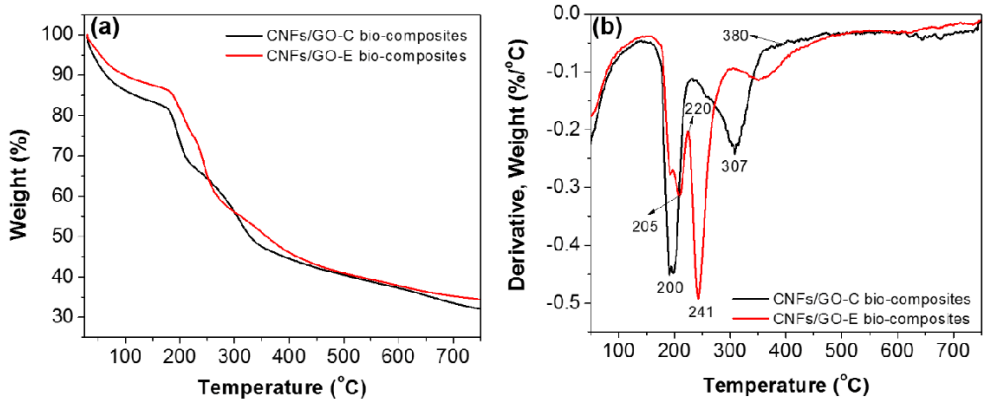

Figure 3.8:Thermogravimetric curves (TG), (a) and differential thermogravimetric curves (DTG), (b) of NFC/GO composites [216].Copyright with permission[PEER-REVIEW ARTICLE]

An innovative application of graphene-cellulose composites in thermal energy storage was explored by Hekimoğlu et al. The researchers developed a shape-stabilized microcrystalline cellulose/methyl stearate/graphene nanoplatelet composite for thermal energy storage applications . The addition of graphene nanoplatelets not only enhanced the thermal conductivity of the composite but also improved its thermal stability and energy storage/release performance. The thermal stability of graphene-cellulose composites is significantly influenced by the concentration and dispersion of graphene within the cellulose matrix, as well as the interfacial interactions between these components. While increasing graphene content generally enhances thermal stability, an optimal concentration exists beyond which further additions may not yield substantial improvements or may even result in detrimental effects due to agglomeration. Recent research has focused on developing innovative methods to improve graphene dispersion and strengthen interfacial interactions, such as surface modification techniques, the use of compatibilizers, and chemical functionalization of graphene or cellulose surfaces. These strategies aim to optimize the thermal stability of the composite by ensuring uniform distribution of graphene and maximizing the synergistic effects between the graphene and cellulose components [217].

3.5.3. Electrical Conductivity

The incorporation of graphene into cellulose matrices can impart electrical conductivity to the otherwise insulating materials. The graphene/microfibrillated cellulose (MFC) composite films demonstrated enhanced electrical, thermal, and mechanical properties. These composites were prepared using a simple method of co-exfoliation of graphite in an MFC suspension by high-shear exfoliation, resulting in homogeneously dispersed pristine graphene in the MFC matrix without chemical treatment. The composites achieved a high electrical conductivity of 2.4 S/m, although the specific graphene loading for this conductivity was not mentioned. At 0.5 wt% graphene loading, the specific surface area of the composites increased from 218 to 273 m^2/g, while the tensile strength and Young's modulus improved by 33% and 28%, respectively [218]. A review by Pottathara et al. explored the potential of graphene-based composites for flexible electronics, highlighting their superior mechanical strength, conductivity, and extraordinary thermal stability. The researchers discussed various strategies for incorporating graphene into polymer matrices, such as solution mixing, in-situ polymerization, layer-by-layer assembly, and their impact on the electrical and mechanical properties of the resulting composites [219]. The incorporation of graphene into cellulose matrices yields composites with markedly increased electrical conductivity compared to pure cellulose fibers. In this study, reduced graphene oxide (rGO) was introduced to cellulose fibers and the resulting electrical properties analyzed as a function of rGO content. The dependence of conductivity on rGO concentration was quantitatively described using a percolation model, $\sigma = \sigma_0(p - p_c)^t$, where $p$corresponds to the mass fraction of rGO (p = rGO wt%/100). Figure 3.9 displays the fitted conductivity data and the derived percolation parameters. The observed percolation threshold (2.4 wt%) is higher than that reported for cellulose-GO composites and likely reflects the enhanced fiber alignment and morphology of the spun fibers. The fitted

conductivity of the rGO phase ($\sigma_0 = 73.3$ S/cm) and critical exponent ($t = 3.5$) are consistent with literature values, while a critical exponent above the theoretical value for 3D networks may arise from non-uniform filler dispersion and anisotropic orientation within the fiber matrix.These results support the notion that morphological control and filler dispersion are crucial to optimizing conductivity in cellulose/graphene composites. Comparison to related works—such as those based on microfibrillated cellulose or other nanocellulose matrices—reveals similar improvements in conductivity, mechanical strength, and thermal stability, with percolation parameters largely dictated by processing technique and composite structure [220].

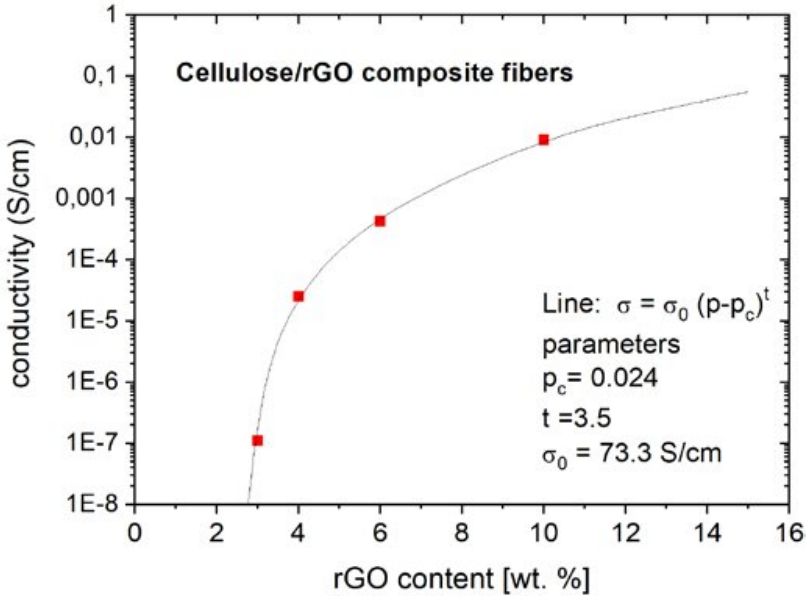

Figure 3.9: Dependence of electrical conductivity on rGO content (wt%) in cellulose fibers. The experimental data are fitted by the percolation model $\sigma = \sigma_0(p - p_c)^t$, where σ is conductivity, σ_0 the conductivity of rGO, p the mass fraction of rGO ($p =$ rGO wt% / 100), p_c the percolation threshold, and t the critical exponent. Fit parameters: $p_c = 0.024$ (2.4 wt%), $t = 3.5$, $\sigma_0 = 73.3$ S/cm [220]. Copy right with permission [Regenerated-Cellulose-Graphene-Composite-Fibers-with-Electroconductive-Properties.pdf] Open Access

3.5.4. Barrier Properties

Graphene and its derivatives have been shown to improve the barrier properties of cellulose matrices, particularly against water vapor and gas permeation. In the study by Santillo et al. , the researchers demonstrated that the presence of graphene oxide slightly increased the water barrier properties of chitosan-based composites, while the incorporation of CNCs and borate significantly reduced the water vapor permeability by about 50% compared to pristine chitosan. The researchers attributed this enhancement to the tortuous path created by the impermeable GO and CNC fillers,

which hindered the diffusion of water vapor through the composite. Another study by Qing et al. investigated the barrier properties of graphene oxide (GO)/cellulose nanofiber (CNF) composites for food packaging applications. The researchers found that the incorporation of GO significantly improved the oxygen barrier properties of the CNF films, with a 50% reduction in oxygen permeability observed for composites containing 1 wt% GO. The researchers attributed this enhancement to the high aspect ratio and impermeable nature of GO, which created a tortuous path for gas diffusion [221].

3.5.5. Biocompatibility and Tissue Engineering Applications

The biocompatibility and biodegradability of cellulose-based composites make them attractive candidates for tissue engineering applications. A review by Oprea et al. explored the potential of cellulose composites with graphene for tissue engineering, highlighting their ability to promote cellular attachment, growth, proliferation, and stem cell differentiation. The study discussed the preparation methods and biological performance of various cellulose-based composites, including cellulose paper, bacterial cellulose, and cellulose derivatives, with graphene, graphene oxide, and reduced graphene oxide. These composites have shown promising results in developing multifunctional scaffolds for cell culture, bone, and neural tissue regeneration. A study by Y et al. investigated the potential of graphene oxide (GO)/cellulose nanofiber (CNF) composites for bone tissue engineering applications. The researchers found that the incorporation of GO into CNF scaffolds enhanced the attachment, proliferation, and osteogenic differentiation of human mesenchymal stem cells (hMSCs). The GO/CNF composites exhibited improved mechanical properties, electrical conductivity, and biocompatibility, making them promising candidates for bone tissue regeneration. A notable study conducted in 2024 focused on the development of an injectable carboxymethyl chitosan (CMC)/hydroxyethyl cellulose (HEC)/β-tricalcium phosphate (β-TCP)/graphene oxide (GO) hydrogel for bone tissue engineering applications. The researchers employed a hydrothermal method to synthesize GO-functionalized bacterial cellulose, which was subsequently crosslinked with CMC and HEC. This innovative approach resulted in hydrogels with exceptional swelling properties and improved mechanical characteristics, particularly with the addition of 1 mg/mL GO. The study also investigated the osteogenic differentiation of rat bone marrow mesenchymal stem cells (rBMSCs), demonstrating significant promotion of osteogenesis, with the best effect observed at a GO concentration of 2 mg/mL [222].

The biocompatibility of these hydrogels was thoroughly evaluated through cell viability and proliferation assays. The results demonstrated good cell viability and proliferation, indicating the potential of these materials for tissue engineering applications. Furthermore, the hydrogels exhibited promising characteristics for bone tissue engineering, suggesting their potential use in clinical settings [222]. Another significant study in 2024 explored the development of polymer nanocomposites based on carbon nanotubes, graphene, and cellulose for fused deposition modeling

(FDM) applications [223]. This research aimed to enhance the properties of FDM-printed parts by incorporating various nanofillers. The study highlighted the astonishing properties, biocompatibility, and ability to tailor the final performance of FDM-printed nanocomposite parts using these nanofillers. The researchers provided a comprehensive review of the processing, characterization, and potential applications of these nanocomposites in industrial settings[224]. The potential applications of graphene oxide in medical implants have also been the subject of recent research. A comprehensive review published in 2024 examined the use of nanomaterials, including graphene, in various medical implant applications [225]. The review focused on the advancements and challenges in employing nanomaterials to enhance the functionality of medical implants. Graphene, due to its unique electronic properties, was found to be particularly promising for applications such as electrical stimulation in neural implants. The study highlighted the potential improvements in mechanical strength, biocompatibility, and drug delivery capabilities of implants incorporating nanomaterials like graphene [225] . In the realm of biosensors, a 2024 study utilized graphene oxide in the development of an electrochemical biosensor for the early detection of pancreatic cancer [226]. The researchers coated a gold working electrode with graphene oxide nano colloidal solution to create a nanoengineered biosensor capable of detecting pancreatic cancer-specific biomarkers. This innovative approach demonstrates the potential of graphene-based materials in advancing medical diagnostics and early disease detection [226].

3.5.6. Energy Storage and Environmental Remediation Applications

Graphene-cellulose composites are used to create high-performance supercapacitor electrodes. These composites offer high electrical conductivity and capacitance, making them suitable for flexible energy storage systems. For instance, chemically bonded polypyrrole/bacterial cellulose/graphene composites have demonstrated high volumetric and gravimetric capacitance with excellent cycling stability [227]. These composites serve as host matrices in lithium-sulfur batteries, enhancing the electrochemical performance by providing a stable structure and improving conductivity [228]. Flexible electrodes made from graphene-cellulose composites are used in lithium-ion batteries. They provide mechanical support and improved electrical conductivity, contributing to the overall efficiency and flexibility of the battery [229]. The morphology and characteristics of the self-supporting LFP/G/NFC electrode are vividly presented in Figure 3.10, offering a comprehensive view of its structure and properties. Figure 3.10(a) reveals the intricate composition of the electrode, where $LiFePO_4$ particles, graphene sheets, and nanofibrillated cellulose (NFC) fibers are clearly discernible. The graphene and filamentous NFC have combined to form a porous conductive framework, within which the homogeneous $LiFePO_4$ particles are well-dispersed, albeit slightly aggregated.

A cross-sectional view of the flexible electrode is provided in Figure 3.10(c), showcasing a clear and neat morphology. The absence of significant structural defects in this cross-section indicates stable binding between the components. This arrangement has resulted in a mesh-like three-dimensional structure with good electronic conductivity, which enhances the electronic contact at

the electrode/electrolyte interface. The surface characteristics of the prepared LFP/G/NFC electrode are displayed in Figure 3.10(b). Notably, the surface appears smooth and free from any flaws or peeling, suggesting a well-integrated structure. The electrode's flexibility is demonstrated in Figure 3.10(d), where it exhibits high resilience through repeated bending. The electrode maintains its integrity even when bent to a curvature radius below 5 mm for 100 cycles, a testament to the sturdy frame provided by the graphene and NFC components. Figures 3.10(e) and 10(f) offer insight into the wettability of the electrode. These images compare the water contact angles of pure LiFePO4 (68.9°) and the flexible LFP/G/NFC electrode (47.2°). The noticeably lower contact angle of the LFP/G/NFC electrode indicates superior electrolyte wettability compared to conventional LiFePO4 electrodes. This enhanced wettability, combined with the electrode's flexibility and stable structure, suggests promising performance potential for this self-supporting LFP/G/NFC electrode in lithium-ion battery applications [229].

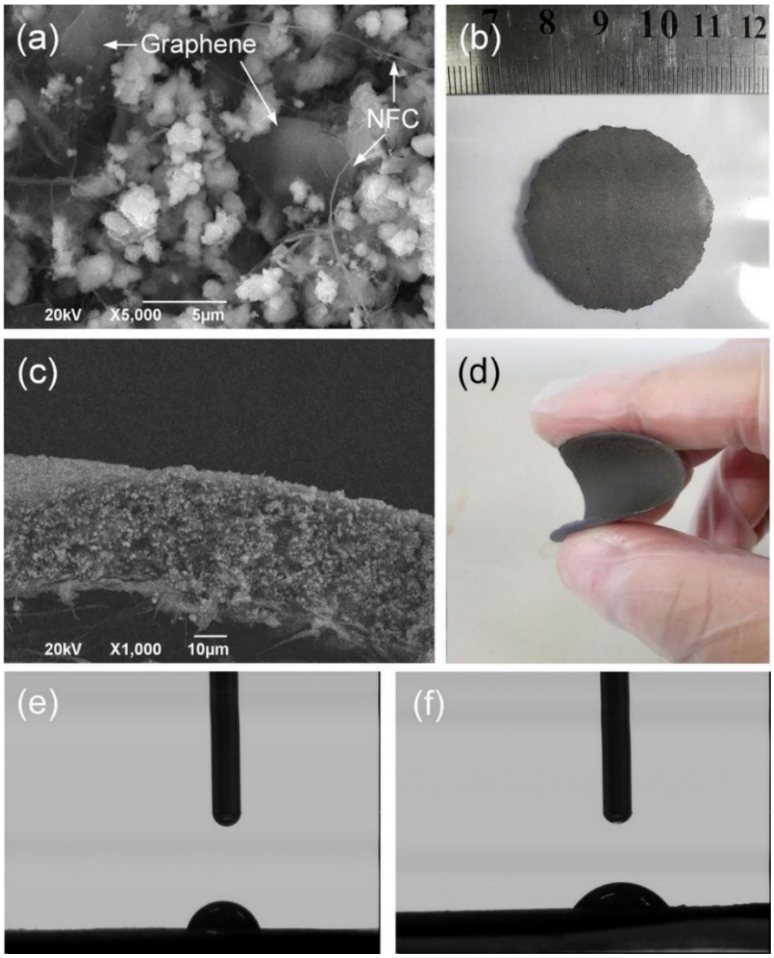

Figure 3.10: SEM images of (a) the surface and (c) the cross-section of flexible LFP/G/NFC electrode; The photos of (b) flattened and (d) bent flexible LFP/G/NFC electrode; Images of water contact angle on (e) pure $LiFePO_4$ and (f) flexible LFP/G/NFC electrode [229]. Copyright with

permission [Preparation and characterization of flexible lithium iron phosphate/graphene/cellulose electrode for lithium ion batteries - ScienceDirect]

The high adsorption capacity and nanoporous structure of graphene-cellulose composites make them effective in filtering and purifying water. They can remove contaminants and pollutants efficiently due to their large surface area and reactivity. These composites are used in phase change materials for solar energy applications. They enhance thermal conductivity and flexibility, which are crucial for efficient thermal energy storage and management [230].

3.6. Challenges and Future Perspectives

While the incorporation of graphene into cellulose matrices has shown promising results in enhancing structural and functional properties, several challenges remain to be addressed. One of the main challenges is the uniform dispersion and prevention of agglomeration of graphene or its derivatives within the cellulose matrix. Agglomeration can lead to non-uniform property enhancements and potentially compromise the overall performance of the composite. Various strategies have been explored to address this challenge, including surface functionalization, solvent selection, and the use of dispersing agents or surfactants . A study by Liu et al. investigated the effect of surface functionalization on the dispersion of graphene oxide (GO) in cellulose nanofiber (CNF) matrices. The researchers found that the introduction of carboxyl and hydroxyl groups on the GO surface improved its dispersion and interfacial interactions with the CNF matrix, resulting in enhanced mechanical and thermal properties of the composites. Apart from graphene oxide a large family of graphene derivatives bearing other functional groups - amines, thiols, sulfates, etc. - are known to date and being employed, particularly for composite fabrication [231], [232]. Another study by Li et al. explored the use of different solvents for the dispersion of graphene in microfibrillated cellulose (MFC) matrices. The researchers found that the use of N,N-dimethylformamide (DMF) as a solvent resulted in better dispersion and exfoliation of graphene, leading to improved mechanical and electrical properties of the composites compared to those prepared using water as the solvent [233].

Another challenge is the scalability and cost-effectiveness of the production processes. Many of the reported studies have been conducted on a laboratory scale, and the translation of these processes to industrial-scale production may require further optimization and cost considerations . A study by Xie et al. explored the scalable production of graphene-cellulose composites using a continuous flow reactor[234]. The researchers developed a cost-effective and environmentally friendly method for the large-scale production of graphene-cellulose composites, which could potentially facilitate their commercialization and industrial applications. Another study by Mendez et al. reported a cost-effective and scalable method for the production of graphene oxide (GO) using a modified Hummers method. The researchers demonstrated that the use of a more environmentally friendly oxidizing agent and the recycling of the oxidizing solution could

significantly reduce the production cost of GO, making it more accessible for various applications, including the development of graphene-cellulose composites [235].

The long-term stability and durability of graphene-cellulose composites under various environmental conditions, such as temperature, humidity, and UV exposure, need to be thoroughly investigated to ensure their suitability for practical applications . A study by Zhu et al. investigated the long-term stability and durability of graphene-cellulose composites under accelerated aging conditions. The researchers subjected the composites to elevated temperatures, humidity, and UV exposure to simulate long-term environmental conditions. The results showed that while the mechanical properties of the composites remained relatively stable, there was a gradual decrease in electrical conductivity over time, which was attributed to the degradation of the graphene network within the cellulose matrix. To address the issue of long-term stability and durability, researchers have explored the use of protective coatings on graphene-cellulose composites. A study by Xu et al. investigated the application of a polyurethane coating on graphene-cellulose composites for outdoor applications. The researchers found that the polyurethane coating effectively protected the composites from UV radiation, moisture, and other environmental factors, maintaining their mechanical and electrical properties over an extended period [236].

Despite the challenges, the field of graphene-cellulose composites holds immense potential for future research and development. The exploration of novel processing techniques, such as 3D printing, electrospinning, and layer-by-layer assembly, could lead to the fabrication of composites with unique architectures and tailored properties for specific applications. A study by Mohan et al. explored the 3D printing of graphene-cellulose composites for the fabrication of complex structures with tailored mechanical and electrical properties. The researchers developed a novel 3D printing technique that allowed for the precise control of the graphene distribution within the cellulose matrix, enabling the creation of composites with anisotropic properties and customized functionalities. Another study by Jiang et al. investigated the electrospinning of graphene-cellulose nanofiber composites for tissue engineering applications. The researchers demonstrated that the incorporation of graphene into the electrospun cellulose nanofibers enhanced the mechanical properties, electrical conductivity, and biocompatibility of the resulting scaffolds, making them suitable for applications such as neural tissue regeneration and biosensing [237].

Furthermore, the incorporation of other functional materials, such as metal nanoparticles, carbon nanotubes, or conductive polymers, into graphene-cellulose composites could result in multifunctional materials with enhanced properties and expanded application potential [238].A study by Zhu et al. explored the incorporation of silver nanoparticles into graphene-cellulose composites for antimicrobial applications. The researchers found that the synergistic effect of graphene and silver nanoparticles resulted in composites with enhanced mechanical properties, electrical conductivity, and antimicrobial activity, making them suitable for applications such as wound dressings and biomedical devices. One notable study focused on the development of graphene oxide-functionalized bacterial cellulose–gelatin hydrogels for wound dressing

applications. Ullah et al. (2023) created composite hydrogels by blending gelatin and graphene oxide-functionalized bacterial cellulose (GO-f-BC), using tetraethyl orthosilicate (TEOS) as a crosslinker. These hydrogels demonstrated impressive swelling capabilities in various media, with maximum swelling rates of 1903% in aqueous media, 1547% in PBS, and 1367% in electrolyte solutions. The composites also exhibited excellent hemocompatibility, with hemolysis rates below 0.5%, and showed antimicrobial activity against both Gram-positive and Gram-negative bacteria. Notably, cell viability and proliferation improved with increasing graphene oxide content, with optimal results observed in hydrogels containing 0.04 mg GO [239]. Another innovative approach was demonstrated by Xu et al. (2023), who developed a novel core-shell composite using pine needles-derived carbon fibers (PNCFs) and graphene for electromagnetic interference (EMI) shielding. This study showcases the potential of combining biomass-derived carbon materials with graphene for advanced applications. The researchers created pore-rich PNCFs through KOH activation and integrated graphene using plasma-enhanced chemical vapor deposition (PECVD). The resulting composite achieved impressive electrical conductivity of 4.97 S cm^{-1} and excellent EMI shielding effectiveness, exceeding 70 dB over the X-band frequency range. Furthermore, the material showed promise for stealth applications due to its high absorption loss, which accounted for 90.8% of the total loss. This research underscores the potential of integrating biomass-derived carbon fibers with graphene to create high-performance EMI shielding materials [240].

3.7. Conclusions

The optimization of graphene content in cellulose matrices has proven to be a promising approach for enhancing the structural and functional performance of composite materials. Various optimization techniques, including RSM, PSO, and ANN, have been employed to identify the optimal graphene concentration and processing conditions. Quantitative analyses have demonstrated significant improvements in mechanical properties, thermal stability, electrical conductivity, barrier properties, and biocompatibility when the optimized graphene content is incorporated into cellulose matrices. These findings highlight the potential of graphene-cellulose composites for a wide range of applications, including structural materials, thermal insulation, conductive materials, tissue engineering, energy storage, and environmental remediation. However, challenges such as uniform dispersion, scalability, cost-effectiveness, and long-term stability need to be addressed to facilitate the practical implementation of these composites. Future research directions may include the exploration of novel processing techniques, the incorporation of additional functional materials, and the development of multifunctional composites with tailored properties for specific applications. Additionally, the investigation of long-term stability and durability under various environmental conditions, as well as the development of protective coatings or encapsulation strategies, could further enhance the practical applicability of these composites. Overall, the field of graphene-cellulose composites presents exciting opportunities for innovation and the creation of high-performance, sustainable, and multifunctional materials. Interdisciplinary collaborations among researchers, engineers, and industry partners will be crucial

in overcoming the existing challenges and unlocking the full potential of these advanced composite materials.

Closure

This chapter, based on the paper published in *Encyclopedia* (2024), focused on the practical and theoretical dimensions of incorporating graphene oxide into cellulose matrices, with particular attention to how the amount and distribution of GO govern composite performance. It began by reviewing nanocomposite theory as it applies to graphene–cellulose systems: interfacial interactions between the oxygen-containing groups of GO and the hydroxyl groups of cellulose (primarily hydrogen bonding and π–π stacking) determine the quality of stress transfer and the onset of electrical percolation. Recent evidence showing that the percolation threshold in these composites occurs at lower graphene concentrations than previously assumed was discussed as an important practical insight. Surface modification strategies , both covalent (enzyme-mediated coupling) and non-covalent (polydopamine coating), were reviewed as tools to improve interfacial compatibility without sacrificing the intrinsic properties of graphene. Optimization approaches surveyed included response surface methodology, particle swarm optimization, and artificial neural networks, each offering a different balance of experimental efficiency and predictive power. The chapter documented quantitative gains in tensile strength, Young's modulus, thermal stability, and electrical conductivity that result from well-controlled graphene loading, while also acknowledging persistent challenges in uniform dispersion, scalability, and long-term stability. These insights directly informed the experimental design and modeling methodology adopted in Chapter 5.

Chapter 4: Advancements in Hybrid Cellulose-Based Films

This chapter is a published paper in the **Journal of Functional Biomaterials (2024), Vol. 15, Issue 4, Article 93,** titled "Advancements in Hybrid Cellulose-Based Films: Innovations and Applications in 2D Nano-Delivery Systems." ***Add authors***

Advancements in Hybrid Cellulose-Based Films: Innovations and Applications in 2D Nano-Delivery Systems

Abstract: This paper delves into the realm of hybrid cellulose-based materials and their applications in 2D nano-delivery systems. Cellulose, recognized for its biocompatibility, versatility, and renewability, serves as the core matrix for these nanomaterials. The paper offers a comprehensive overview of the latest advancements in the creation, analysis, and application of these materials, emphasizing their significance in nanotechnology and biomedical domains. It further illuminates the integration of nanomaterials and advanced synthesis techniques that have significantly improved the mechanical, chemical, and biological properties of hybrid cellulose-based materials.

4.1. Introduction

In the contemporary era of sustainable material development, there is an increasing focus on products derived from cellulose, the most abundant organic compound on Earth. Cellulose's unique combination of biocompatibility, flexibility, and sustainability has not only entrenched it as a fundamental component in traditional sectors like textiles and paper production but has also placed it at the forefront of more advanced fields. Specifically, the rise of nanotechnology and biomedical engineering has led to new advancements in cellulose-based materials, including hybrid films [14], [241]. Figure 4.1 provides a schematic representation of cellulose structures from resources to the molecular level.

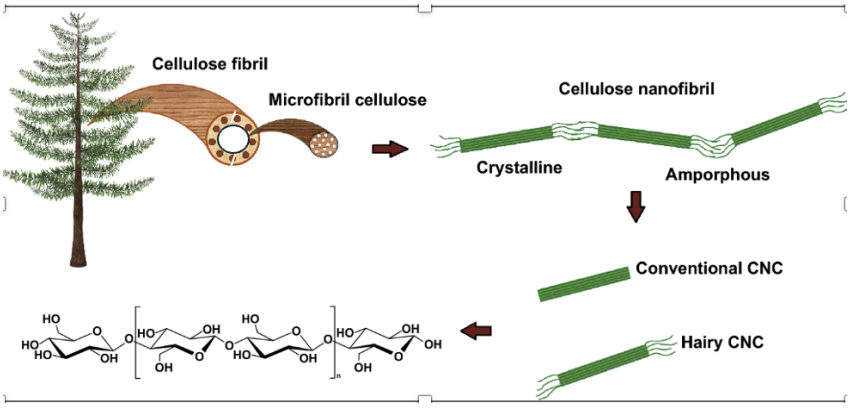

Figure 4.1. Schematic representation of cellulose structures from resources to the molecular level [241]. Copyright with permission [A Review on Surface-Functionalized Cellulosic

Nanostructures as Biocompatible Antibacterial Materials|Nano-Micro Letters (springer.com)].
Adapted from[[241]***]***

However, despite the promising potential of these materials, there are still challenges and limitations in the current research. For instance, the structure of pure cellulose has inherent shortcomings such as poor plasticity and dimensional stability and lack of antibacterial activity [242]. Moreover, the effectiveness of cellulose-based nano-delivery systems may be limited by their inability to cross the blood–brain barrier, essential for drug resistance in, e.g., epilepsy [243]. Though this paper discusses the potential of hybrid cellulose-based films for applications in drug delivery, tissue engineering, and other biomedical areas, it is important to note that the materials and systems described herein are at various stages of research and development. Many of these applications are still in the experimental phase and have not yet been approved by regulatory agencies such as the Food and Drug Administration (FDA) for clinical use. The transition from laboratory research to clinical application involves extensive testing, regulatory approval, and compliance with safety and efficacy standards. Therefore, readers are cautioned that the use of these materials in medical and pharmaceutical treatments requires thorough investigation, validation, and regulatory approval before they can be considered for clinical applications. This paper aims to provide an overview of current research and potential future directions in the field, rather than to suggest immediate clinical implementation.

This paper explores the progress in hybrid cellulose-based films—a novel category of materials that enhance traditional cellulose products through integration with nanotechnology and chemical modifications. These breakthroughs have resulted in materials with improved mechanical properties and functionalities that can potentially be applied across various domains. Our focus lies in their crucial role in nano-delivery systems—an area experiencing significant interest for revolutionizing drug delivery, tissue engineering, and other biomedical applications [244].

Hybrid cellulose-based films possess distinctive properties such as controlled release of embedded active materials, targeted delivery capabilities, and biodegradability. They are anticipated to make a substantial impact on nano-delivery systems. This paper presents an extensive overview of recent developments, current challenges, emerging trends, and future perspectives in this arena of hybrid cellulose-based films. It provides valuable insights for researchers, industry professionals, and policymakers who are actively involved in or keenly positioned vis-à-vis sustainable nanotechnology policy. The term ‘hybrid’ is used to describe cellulose-based films that have been enhanced through the incorporation of various nanomaterials. This integration aims to leverage the unique properties of both cellulose and nanomaterials to create films with superior mechanical, electrical, thermal, and biological properties. The ‘hybrid’ aspect refers to the combination of organic cellulose with inorganic or other organic nanomaterials, such as nanoparticles, nanotubes, and graphene, resulting in composite materials that exhibit enhanced functionalities. These hybrid films are designed for specific applications in drug delivery, environmental sensing, and biomedical engineering, among others, where their controlled release, targeted delivery

capabilities, and biodegradability are crucial. The use of the term ‘hybrid’ in this context emphasizes the synergistic effects achieved by merging cellulose with nanomaterials, creating a new class of materials that are distinct from their individual components. [242], [245], [246].

4.2. Synthesis Methods for Cellulose-Based Hybrid Films

Advanced synthesis techniques like electrospinning, chemical vapor deposition, and sol-gel processes have produced hybrid cellulose-based films with improved properties.

Electrospinning is a versatile technique that can produce nanofibers from various materials, such as polymers and composites. In one study, co-electrospinning was utilized to create a composite membrane of cellulose acetate/thermoplastic polyurethanes . This process involved optimizing parameters, including the materials’ weight percentages, the solvents’ volume ratio, and the applied voltage. The resulting composite membrane demonstrated enhanced properties, rendering it suitable for applications such as photodynamic antibacterial usage [247].

Chemical vapor deposition is another method for synthesizing hybrid films. Researchers synthesized an ultrathin, uniform organic–inorganic hybrid dielectric film using initiated CVD in a study. This hybrid dielectric was created from tetrakis-dimethyl-amino-zirconium and 2-hydroxyethyl methacrylate—a high-k inorganic material and a soft organic material, respectively. The resulting film demonstrated a high dielectric constant, low leakage current density, and high breakdown field, indicating its suitability for advanced flexible electronic applications [248], [249].

The sol-gel process is a method for producing solid materials from small molecules. It was used to create photocatalytic coatings on cellulose fabrics through the pad-dry-cure process, using a composition that included a bifunctional anchoring agent, a crosslinking agent, and a catalyst for epoxy group polymerization. These coatings showed improved resistance to wet treatments and enhanced photocatalytic performance [250].

Additionally, advanced techniques like matrix-assisted pulsed laser evaporation (MAPLE) have been employed for synthesizing biopolymer thin films. The method has successfully produced thin films of polysaccharides such as dextran doped with iron oxide nanoparticles and levan. MAPLE has proven effective in obtaining thin films of sensitive materials without inducing thermal decomposition or irreversible degradation meso-porous silica particles as efficient carriers for drug delivery[251].

Advanced synthesis techniques contribute to the enhanced properties of hybrid cellulose-based films, including increased mechanical strength, improved drug-loading capacity, and enhanced biodegradability. However, further research is needed to optimize these methods and expand their applications [252], [253]. The term ‘hybrid’ is used to emphasize the integration of cellulose with various nanomaterials, such as nanoparticles, nanotubes, and graphene, through advanced synthesis techniques like electrospinning, chemical vapor deposition, sol-gel processes, and

matrix-assisted pulsed laser evaporation (MAPLE). This integration results in the formation of hybrid cellulose-based films that exhibit enhanced properties compared to pure cellulose films.

Table 4.1 offers a comprehensive overview of cellulose-based 2D materials, highlighting their foundational material characteristics, recent advancements, and spectrum of applications. It outlines the challenges faced in the development and commercialization of these materials, alongside the anticipated future directions that could propel their utilization across various industries. Additionally, the table compares cellulose-based 2D materials with other nanomaterials, underlining their distinctive benefits in terms of sustainability and application diversity. Finally, it addresses real-world applications and regulatory considerations, presenting a holistic view of the potential and constraints of cellulose-based 2D materials in advancing technological and environmental solutions.

Table 4.1. Key insights on cellulose-based 2D materials: properties, applications, and perspectives**.**

Aspect	Details
Material Base	Cellulose, recognized for its biocompatibility, versatility, and renewability.
Advancements	Integration with nanomaterials like nanoparticles, nanotubes, graphene, and advanced synthesis techniques.
Applications	Drug delivery, tissue engineering, environmental sustainability, and smart drug delivery systems.
Challenges	Scalability, compatibility with a broad range of compounds, regulatory hurdles, and environmental impact assessment.
Future Directions	Development of stimuli-responsive materials, integration with IoT for healthcare, and exploration of new synthesis methods to enhance properties.
Comparative Analysis	Relative to graphene and MXenes, cellulose-based 2D materials offer unique advantages in sustainability, biodegradability, and potential for diversification in applications.
Real-World Applications	Pharmaceutical industry, environmental remediation, biomedical scaffolds, energy storage, and water purification.
Regulatory and Commercialization Considerations	FDA approval process, market availability, liability issues, and environmental concerns.

4.3. Integration of Nanomaterials

The integration of nanomaterials into cellulose films, indeed, signifies a crucial development in the creation of hybrid structures. These hybrid structures are formed by combining cellulose with a second type of nanomaterial, such as nanoparticles, nanotubes, or graphene. This combination enhances the intrinsic properties of cellulose films and introduces new functionalities, making them suitable for a wide range of applications, including nano-delivery systems. The term ’hybrid’

in this context aptly describes the synergistic effects achieved by merging nanocellulose with other nanomaterials to enhance performance and achieve tailored functionalities[254], [255].

The incorporation of various nanomaterials into cellulose films is detailed in the following sections.

4.4. Surface Modification Techniques

Surface modification techniques encompass a range of chemical and physical approaches designed to tailor the interfacial properties of cellulose-based materials for enhanced performance in advanced applications. The major categories of these techniques are outlined below.

4.4.1. Grafting of Polymers

Polymer grafting onto cellulose films can significantly change their properties. For example, starch acetate has been utilized as a microencapsulating agent in creating controlled-release microcapsules containing gliclazide. These gliclazide microcapsules were fabricated using an emulsion solvent evaporation technique, with varying core coat ratios. In vitro studies on drug release indicated sustained release for up to 24 h from the microcapsules, depending on factors such as the size of the microcapsules, coat thickness, and SA concentration [256].

4.4.2. Coating with Bioactive Substances

Coating cellulose films with bioactive substances can enhance their biocompatibility and functionality. Biocompatible polymers such as polylactic-co-glycolic acid, poly(ε-caprolactone), polylactic acid, poly(3-hydroxybutyrate-co-3-hydroxyvalerate), chitosan, and cellulose have been used in various biomedical applications. These polymers can be processed into films using techniques such as augmentation, film processing, injection molding, blow molding techniques, controlled/implantable drug delivery devices, biological grafting, and nanotechnology. The resulting films exhibit improved biocompatibility with non-toxicity under mild processing conditions while reducing immunological reactions and minimizing side effects [257], [258], [259], [260].

4.4.3. Other Chemical Modifications

Other chemical modifications can be used to customize the properties of cellulose films. For example, chitosan nanocomposites have been applied in biomedical fields such as drug delivery, tissue regeneration, and wound healing. The biomedical effectiveness of chitin and chitosan compounds is closely related to the production process conditions. The use of chitosan nanocomposites in these applications has led to improved biocompatibility and functionality [261]. In summary, functionalization and surface modification strategies play a crucial role in customizing the properties of hybrid cellulose films for specific applications. These strategies can

significantly enhance the performance of these films in nano-delivery systems, making them suitable for various biomedical uses.

Table 4.2 outlines the diverse surface modification techniques applied to cellulose films, detailing the methods employed, their resultant enhancements, and the corresponding scientific references. These modifications significantly alter the physical and chemical properties of cellulose films, improving their applicability in biomedical and technological fields. The table is segmented into three primary modification strategies, each aiming to enhance the biocompatibility, functionality, and overall performance of the cellulose films in various applications: grafting of polymers, coating with bioactive substances, and other chemical modifications.

Table 4.2. Enhancement strategies for cellulose films via surface modification**.**

Surface Modification Technique	Description	Outcomes	References
Grafting of Polymers	Utilization of starch acetate for creating controlled-release microcapsules containing gliclazide using an emulsion solvent evaporation technique.	Sustained drug release up to 24 h, dependent on microcapsule size, coat thickness, and SA concentration.	[256], [262]
Coating with Bioactive Substances	Use of biocompatible polymers (e.g., polylactic-co-glycolic acid, poly(ε-caprolactone), polylactic acid, poly(3-hydroxybutyrate-co-3-hydroxyvalerate), chitosan, cellulose for biomedical applications.	Improved biocompatibility, non-toxicity, reduced immunological reactions and side effects.	[257], [258], [259], [260], [263], [264]
Other Chemical Modifications	Application of chitosan nanocomposites in drug delivery, tissue regeneration, and wound healing.	Enhanced biocompatibility and functionality.	[261]

4.5. Recent Studies and Publications

This section highlights recent advancements and key publications related to cellulose nanostructures and their emerging applications.

4.5.1. Customization of Cellulose Nanostructures for Specific Delivery Challenges

Recent research has indicated the potential of cellulose nanostructures for targeted drug delivery. One-dimensional nanostructures, like nanorods, nanofibers, or nanotubes, have high drug-loading capacities and improved targeting due to their high surface-to-volume ratios. These structures can be tailored to target different cells by altering the ligands used. Moreover, they can react to changes in the target environment, enabling drug release only at the specific site [265].

4.5.2. Cellulose-Based Systems for Hydrophobic Drug Delivery

4.5.2.1. Antibacterial Cellulose-Based Materials

Research has led to the development of antibacterial nanocrystalline cellulose through a novel functionalization process. This process involves the integration of aldehyde groups into hairy nanocrystalline cellulose, enabling the direct attachment of natural antibacterial agents such as lysozyme and nisin. The effectiveness of this method has been demonstrated through its ability to maintain the antibacterial activity of these agents over extended periods, signifying a promising approach for antibacterial applications [266]. Figure 4.4 presents a schematic illustration of the synthesis process of conventional nanocrystalline cellulose from cellulose nanofibrils via acid hydrolysis, highlighting its application in the development of antibacterial cellulose-based materials. This novel functionalization process involves integrating aldehyde groups into hairy nanocrystalline cellulose, facilitating the direct attachment of natural antibacterial agents such as lysozyme and nisin. The method's effectiveness is underscored by its capability to preserve the antibacterial activity of these agents over extended periods, offering a promising avenue for enhanced antibacterial applications [266].

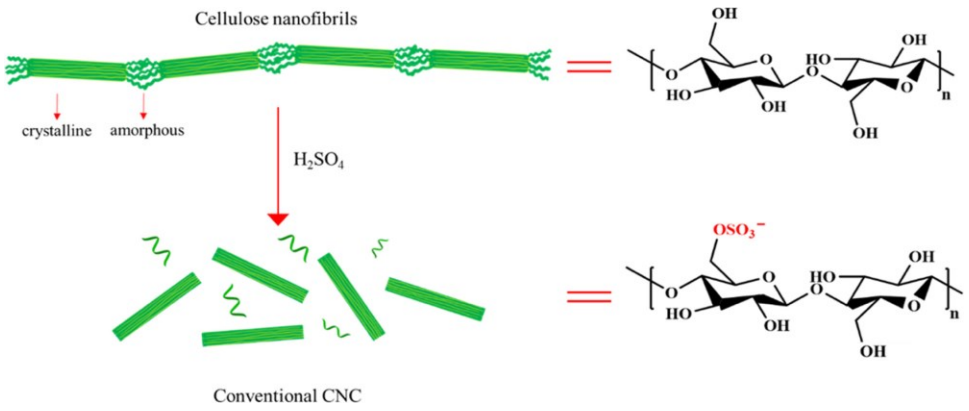

Figure 4.2. Schematic illustration of the synthesis of the conventional cellulose nanocrystalline from cellulose nanofibrils under acid hydrolysis [266]. Copyright with permission [Biotemplated Hollow Mesoporous Silica Particles as Efficient Carriers for Drug Delivery|ACS Applied Bio Materials].

4.5.2.2. Antibacterial and Biofilm-Disrupting Hydrogels

Innovations in cellulose for wound-dressing applications have resulted in the creation of highly absorbent antibacterial and biofilm-disrupting hydrogels. These hydrogels are produced by covalently bonding ε-poly-L-lysine to carboxyl-modified cellulosic hydrogels, exhibiting significant bactericidal efficacy and compatibility with mammalian cells. This breakthrough suggests a potent solution for wound-dressing materials (Figure 4.3) [267].

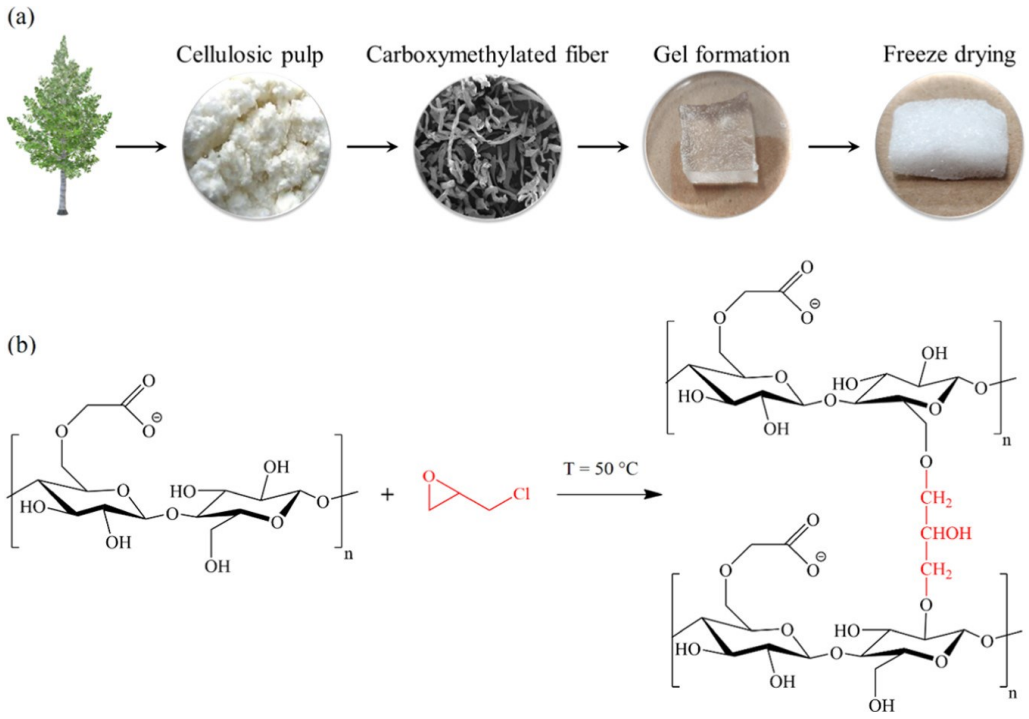

Figure 4.3. (**a**) Representative images of different stages of the gel formation. (**b**) Schematic of the reaction of carboxymethyl cellulose fiber and epichlorohydrin to form the gel [267]. Copyright with permission [Highly Absorbent Antibacterial and Biofilm-Disrupting Hydrogels from Cellulose for Wound Dressing Applications|ACS Applied Materials & Interfaces].

4.5.2.3. Antibacterial Pickering Emulsions

Further exploration into antibacterial cellulose-based materials has given rise to antibacterial Pickering emulsions stabilized by bifunctional hairy nanocellulose. These emulsions utilize cellulose nanocrystals modified with aldehyde and carboxylic acid groups, offering stability without surfactants and demonstrating enhanced antibacterial properties when combined with essential oils like carvacrol [268].

4.5.2.4. Green Extraction of Antibacterial Cellulose-Based Nanofibers

Figure 4.4 illustrates the chemical modification process of cellulose to enhance its antibacterial properties through a green extraction methodology. Initially, cellulose reacts with sodium periodate to produce dialdehyde-modified cellulose (DAMC). Subsequently, it undergoes a reaction with sodium chlorite to synthesize dialdehyde-dicarboxylate-modified nanofibrils. The process concludes with the isolation of bifunctional hairy nanocellulose (BHNC) through heat treatment. This schematic represents a significant advancement in the extraction of antibacterial cellulose-based nanofibers from natural sources like pine cones, using an eco-friendly thermo-oxidation method with H_2O_2, demonstrating potent antibacterial activity against common pathogens [6].

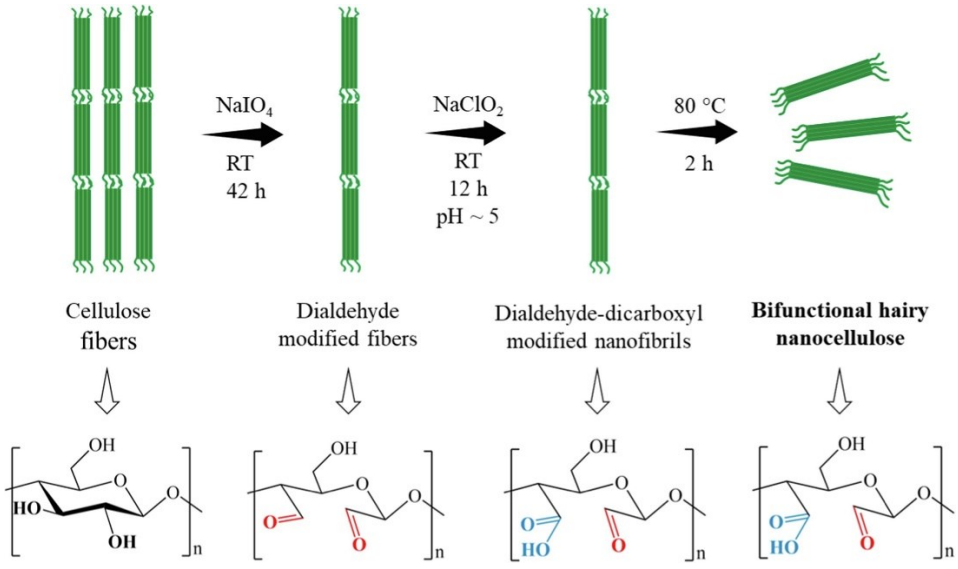

Figure 4.4. Schematic of cellulose reaction with sodium periodate to produce dialdehyde-modified cellulose (DAMC), followed by reaction with sodium chlorite to synthesize dialdehyde-dicarboxylate-modified nanofibrils, and finally BHNC isolation through heat treatment [245]. Copyright with permission [Antibacterial Pickering emulsions stabilized by bifunctional hairy nanocellulose—ScienceDirect].

4.5.2.5. Superhydrophobic and Antibacterial Cellulose-Based Fibers and Fabrics

Recent reviews have highlighted progress in the development of superhydrophobic and antibacterial cellulose-based fibers and fabrics. These advancements focus on enhancing antibacterial properties through surface structuring, chemical modifications, and the incorporation of antibacterial agents, aiming to balance biocompatibility and biodegradability [269].

4.5.2.6. Edible Carboxymethyl Cellulose Films with Natural Antibacterial Agents

Studies have also ventured into edible carboxymethyl cellulose films incorporated with natural antibacterial agents like lysozyme. These films not only demonstrate improved mechanical and water resistance properties but also exhibit significant antimicrobial efficacy against food-borne pathogens, showcasing the potential for food-packaging applications [270].

4.5.2.7. Cellulose-Based Hydrogels for Antibacterial Wound Dressing

Additionally, cellulose-based hydrogels have been identified as promising materials for antibacterial wound dressing, capable of mimicking the skin's microenvironment. The exploration of cellulose from diverse sources for hydrogel production emphasizes the importance of biocompatibility and biodegradability in creating effective wound-healing solutions.

These developments in hybrid cellulose-based films and materials underscore the versatile and significant potential of cellulose in crafting innovative and effective antibacterial solutions for a broad range of applications.

4.5.3. Drug Delivery

4.5.3.1. Biotemplated Hollow Mesoporous Silica Particles

Recent studies have introduced hollow-shaped porous silica materials, utilizing a biotemplate-directed method with cellulose nanocrystals as the template. These materials, including porous hollow silica nanorods and ultraporous sponge-like structures, have showcased their efficiency in drug delivery and dye removal applications. Notably, the ultraporous variants exhibit superior adsorption capacities, marking a significant stride in material design for therapeutic applications [271].

4.5.3.2. Stimuli-Responsive Chitosan

The versatility of chitosan has been explored through its responsiveness to both internal (pH, temperature, enzymes) and external (ultrasound, light, magnetic fields) stimuli. This adaptability positions chitosan as a formidable platform for controlled drug delivery, with current designs emphasizing the material's efficiency in releasing bioactive agents under specific conditions [272].

4.5.3.3. Hairy Nanocellulose-Based Supramolecular Architectures

Innovations in biopolymer-based nanosponges have led to the creation of trifunctional structures by cross-linking beta-cyclodextrin ethylene diamine with bifunctional hairy nanocellulose. These complexes, characterized by their unique morphological and structural properties, have demonstrated potential in capturing and sustaining the release of drug molecules like doxorubicin, with notable pH responsiveness [273].

4.5.3.4. Internally Bridged Nanosilica

Research has yielded monodisperse colloids with a distinctive sea urchin-like structure, internally bridged for hosting drugs within their framework. These pH-responsive nanocomposites have been tested for their biocompatibility as nanocarriers, presenting a novel approach to controllable drug delivery mechanisms [274].

4.5.3.5. Hollow Silica-Based Materials

Molecular dynamics simulations have been employed to investigate the transfer processes of drugs using hollow silica particles, focusing on the optimization of surface wettability, pore size, and flow velocity. This analytical approach provides critical insights into enhancing drug delivery efficiency through structural optimization [275].

4.5.3.6. Chitosan/Hyaluronic Acid Nanoparticles

The development of oxidative stress and pH-responsive nanoparticles from chitosan/hyaluronic acid has been reported. These nanoparticles excel in the encapsulation and controlled release of small molecules and proteins, triggered by specific endogenous conditions. Their high encapsulation efficiency underscores the potential for targeted therapeutic applications [276].

4.5.3.7. Reusable Green Adsorbent Aerogel for Dye Removal

A study explores the development of a reusable green adsorbent aerogel. This aerogel is made from crosslinked hairy nanocrystalline cellulose and modified chitosan, showcasing its effectiveness in dye removal. The research highlights the potential of this eco-friendly material in environmental applications, particularly in water purification [277].

4.5.3.8. Stimuli-Responsive Chitosan for Efficient Delivery of Bioactive Agents

In another study, the use of stimuli-responsive chitosan as a platform for drug delivery systems is reviewed. This material can respond to various internal and external stimuli, making it highly

suitable for controlled and targeted delivery of bioactive agents. The paper discusses the design of chitosan-based architectures that can efficiently load and release drugs at desired sites, emphasizing the potential of chitosan in biomedical applications [278].

4.5.3.9. Detection of Biomolecules

Cellulose-based systems have been effectively used for delivering hydrophobic drugs. For instance, one study showcased the use of cellulose nanocrystals derived from rubber wood as a delivery vehicle for hesperidin, a hydrophobic drug. The CNCs were modified and coated with a cationic surfactant to create a drug delivery system that exhibited promising drug release performance. Another study introduced a solid self-nanoemulsifying drug delivery system using innovative cellulose-based microparticles as adsorptive carriers for the lipophilic drug celecoxib. This system combined the benefits of liquid-SNEDDS with those of solid dosage forms, particularly stability, while preserving the in vitro release performance of the liquid formulation . Additionally, the exploration of theoretical models for optimizing antibody–antigen interactions opens new avenues in biomolecule detection, leveraging computational techniques to enhance the selectivity and functionality of antibody-based filtration systems [279].

4.5.3.10. Cellulose-Based Systems in Targeted Cancer Therapy

Cellulose-based systems have been explored for targeted cancer therapy. For instance, one-dimensional nanostructures have been used to encapsulate anticancer drugs into cellulose nanofibers, providing a novel approach for drug delivery systems . Also, DNA nanomaterials with advanced molecular recognition capabilities and biocompatibility have acted as carriers for the CRISPR/Cas gene-editing system in cancer therapy [280].

In conclusion, recent research has highlighted the potential of cellulose-based systems in drug delivery, particularly for hydrophobic drugs and targeted cancer therapy. These versatile systems tackle specific delivery challenges and present exciting prospects for future advancements in drug delivery research and development [281].

4.6. Emerging Trends and Challenges

In recent years, there has been a significant trend in the development of stimuli-responsive cellulose-based materials. These materials are designed to react to specific stimuli such as temperature, light, electrical signals, magnetic fields, and humidity. The choice of cellulose as a base material is favoured because of its sustainability and renewability. Cellulose-based materials that respond to stimuli have been used in a wide range of applications, including drug delivery. Bacterial cellulose fibers, for example, have shown promise as a sustainable platform for drug delivery. By designing these materials to react to specific stimuli within the body, they can enable

targeted and controlled release of drugs. This approach has the potential to enhance the effectiveness of drug therapies and minimize the side effects [282].

Additionally, the exploration of theoretical models for optimizing antibody–antigen interactions opens new avenues in biomolecule detection, leveraging computational techniques to enhance the selectivity and functionality of antibody-based filtration systems. However, the development and use of these materials pose several challenges. Scalability is one of the main challenges. Although they exhibit promise in laboratory settings, scaling up production to industrial levels can be difficult due to factors such as cost, complexity of production processes, and quality control [283].

Another challenge is compatibility with a broader range of pharmaceutical compounds. Although cellulose-based materials have been successfully used with specific drugs, further exploration of their compatibility with other pharmaceutical compounds is necessary. This is especially important for the delivery of protein-based therapeutics, which often require specific conditions for stability and activity [284].

Furthermore, the prospective integration of these materials with advanced technologies such as the Internet of Things (IoT) has yet to emerge as a present concern but might become critical in the future, contingent on the security of internet traffic. At this juncture, the full potential of the IoT in healthcare, particularly in drug delivery systems, remains largely untapped due to these security considerations. Without stringent security measures in place, IoT-enabled drug delivery could pose significant risks, likening it to a precarious situation akin to handling a loaded gun. Thus, the advancement of the IoT in drug delivery hinges on overcoming these security challenges to ensure it serves as a beneficial tool rather than a potential threat.

In conclusion, though stimuli-responsive cellulose-based materials exhibit considerable potential for targeted drug delivery and other applications, addressing the existing significant challenges remain imperative. To fully realize the vision of personalized medicine—creating specific formulations tailored to individual patients—further research and development are essential. This endeavor will not only require advancements in materials science and pharmaceutical sciences but also significant contributions from information technology and artificial intelligence. Collaboration across these diverse fields is crucial to harnessing the capabilities of cellulose-based materials for personalized therapeutic solutions, illustrating a comprehensive approach to overcoming the hurdles that currently impede progress.

4.7. Comparative Analysis of Cellulose-based 2D Materials and Other Nanomaterials

Cellulose-based 2D materials have been attracting significant attention due to their unique properties and potential applications in various fields. Derived from cellulose, one of the most abundant renewable materials, they are known for their mechanical robustness, biocompatibility, and biodegradability. In comparison to other nanomaterials, cellulose-based 2D materials offer

several advantages. They are low-cost, abundant, and environmentally friendly due to their biodegradability. Moreover, they exhibit a wide variety of fibers that can be manipulated at the nano-, micro-, and macroscales to produce synthetic cellulose-based active materials [285].

Cellulose-based 2D materials find various applications. For instance, they are utilized as potential CO2 adsorbents due to their high adsorption capacity. They have also been combined with MXenes, a group of 2D metal carbides and nitrides, to create composite electrodes for supercapacitors [286].

Graphene-based 2D nanomaterials have been extensively researched for their potential applications in various sectors due to their large surface area and anisotropic physicochemical properties, making them suitable for biomedical and agroecological applications. However, cellulose-based 2D materials have distinctive properties that distinguish them. For instance, they can be assembled into rod-like crystallites in either 2D or 3D forms, and modifications within the oligosaccharide core can impact molecular packing, resulting in the formation of unique structures .

Cellulose nanofibrils/nanofibers are a type of cellulose-based 2D material widely used in environmental science applications. They are favoured for their one-dimensional nanostructure, high specific surface area, excellent biodegradability, low cost, and sustainability. In conclusion, though both cellulose-based 2D materials and other nanomaterials like graphene have their unique properties and applications, their environmental friendliness, versatility, and ability to be manipulated at different scales make cellulose-based 2D materials stand out for various applications [287].

4.8. Case Studies and Potential Applications

Cellulose-based 2D nano-delivery systems have been explored in various fields such as pharmaceuticals, environmental applications, and biomedical engineering. Recent case studies demonstrate their practical applications.

Pharmaceutical Industry

Smart Acetaminophen Delivery: Core-shell nanoparticles were developed for smart drug delivery of acetaminophen using cellulose acetate and polyvinylpyrrolidone. These nanoparticles exhibited a biphasic release, offering rapid therapeutic action followed by sustained release over 30 h. This feature is beneficial for maintaining an effective blood drug concentration .

Environmental Applications

Eucalyptus Essential Oil Delivery: Nanofibrillated and microfibrillated cellulose-based materials were utilized to form 3D networks for encapsulating and delivering eucalyptus essential oil. These systems were tailored for dermic and respiratory applications, displaying precise and consistent release kinetics essential for long-lasting therapeutic effects .

Biomedical Engineering

Electrospun Nanofiber Scaffolds: Advances in electrospinning have led to the development of ultrafine nanofiber scaffolds from cellulose derivatives. These scaffolds are used in biomedical applications, including transdermal systems, antibacterial agents, wound dressing, cancer treatment, and as carriers for growth factors and stem cell delivery systems .

Thermosensitive Drug Delivery: A study on PNIPAM/Hexakis nanocomposites has highlighted their potential as thermosensitive drug delivery systems due to their ability to respond to temperature changes. This property is advantageous for achieving controlled drug release in biomedical and pharmaceutical applications [288], [289].

Marketed Nano-delivery Systems

Approved Therapeutic Nanoparticles: The pharmaceutical industry has witnessed the approval of a variety of therapeutic nanoparticles, including Epaxal®, an aluminum-free hepatitis 'A' vaccine, and Puricase®, designed for tophaceous gout. These products illustrate the successful implementation of nanoparticle-based drug delivery systems in the market [290], [291].

Optimization and Quality Control

Bacterial Nanocellulose Production: Research on bacterial nanocellulose has been focused on optimizing production and quality control for its use as a non-active pharmaceutical ingredient, to develop sustainable biomaterials to replace non-renewable sources in delivery systems.

Plant-Based Compound Delivery

Nano-Formulated Plant-Based Compounds: The development of nano vehicles for encapsulating plant-based compounds has been explored to combat bacterial infections. These nano-formulated compounds can disrupt cell membranes, inhibit enzyme activity, and interfere with biofilm formation. This displays the versatility of cellulose-based nano-delivery systems in pathogen treatment. These case studies illustrate the diverse applications of cellulose-based 2D nano-delivery systems across different sectors, highlighting their potential to revolutionize drug delivery and therapeutic strategies .

Biodegradable Medical Implants

A study on cellulose-acetate-based composites used as coatings for biodegradable magnesium implants for trauma showed promising results. The composite coating reduced the biodegradation rate of the magnesium implants, known to promote bone healing and exhibit adequate mechanical strength during their biodegradation in the bone-healing process [292]. Another study on Mg–Ca–Zn biodegradable alloys used as orthopedic implants demonstrated high biocompatibility and excellent mechanical properties, making them suitable for small bones of the feet and hands, ankles, or small joints [293], [294].

4.9. Environmental Impact

Cellulose-based 2D nanomaterials have demonstrated remarkable potential in reducing energy consumption for heat transfer operations, offering a sustainable alternative. Through environmental impact analysis, it has been revealed that these materials can be utilized on a large scale in the automobile industry and cooling processes .

The environmental impact of producing and disposing of hybrid cellulose-based films, especially in the context of 2D nano-delivery systems, can be assessed through life cycle analysis, carbon footprint evaluation, and comparison with traditional materials .

Carbon Footprint

The carbon footprint of a product refers to the total amount of greenhouse gases, including carbon dioxide and methane, emitted into the atmosphere during its production, use, and end-of-life phases. The increased use of fossil-based plastic in food packaging has contributed to higher levels of plastic waste, carbon footprints, and global warming. This has prompted the exploration of alternatives like cellulose-based hydrogels for biodegradable food packaging .

Comparison with Traditional Materials

Traditional packaging systems are often made of petroleum-based materials, which raise environmental concerns due to their limited biodegradability and the pollution they cause. In contrast, cellulose-based films are derived from renewable resources and are biodegradable, making them a more environmentally friendly alternative. However, these films often lack antioxidant and antimicrobial activities that are crucial for food preservation. To address this issue, researchers have developed active films by incorporating antioxidants and antimicrobial agents into the films .

Moreover, the drawbacks of petrochemical polymer-based packaging, such as extreme depletion of fossil resources, excessive carbon footprints of products, and environmental pollution from nonbiodegradable plastic packages have prompted scientists to develop novel packaging materials from nature-inspired biopolymers like cellulose. In conclusion, hybrid cellulose-based films can significantly reduce the environmental impact of production and disposal compared to traditional materials, making them a more sustainable choice .

Energy Storage

MXenes, a new class of advanced 2D nanomaterials, have become prominent among various types of electrode materials for electrochemical energy storage devices. Due to their distinctive layered structures, enhanced electrical and thermal conductivity, superior charge carrier mobility, and strong mechanical properties, these materials have introduced an intriguing opportunity in functional materials. Ongoing research aims to address the challenge of aggregation and nanosheet restacking that reduces the accessibility of the active surface sites of MXene materials for electrolyte ions [295], [296].

Water Purification

Cellulose nanofibrils/nanofibers are extensively utilized in environmental science applications, particularly for water purification. Their high specific surface area, excellent biodegradability, low cost, and sustainability make CNFs well-suited for the removal of metal ions, anions, organic dyes, oils, and bio-contents from water .

4D Printing

Cellulose-based materials have also been utilized in 4D printing. Printed cellulosic materials can transform from a 1D strand or 2D surface into a 3D shape in response to an external stimulus. This technology has potential applications in numerous fields, such as biomedicine, tissue engineering, wearable devices, and environmental science.

Here are some recent studies and publications that demonstrate the practical applications of these materials:

Dermic and Respiratory Applications

A study was conducted on the design, development, and optimization of drug delivery systems using nanofibrillated and microfibrillated cellulose-based materials as 3D networks encapsulating eucalyptus essential oil molecules for dermal and respiratory applications. The optimized porous structures retained the desired molecules, leading to controlled and uniform release kinetics over time—a crucial aspect in developing effective drug delivery systems in the biomaterials field.

Biomedical Applications of Chitosan Nanocomposite

Chitosan nanocomposites have found use in various biomedical applications, including drug delivery, tissue regeneration, and wound healing. The physicochemical properties of chitin and chitosan compounds are closely tied to the conditions of their production process, influencing their biomedical activity. These materials have also been studied for their potential to substitute non-renewable fiber sources in the creation of non-woven delivery systems .

Aerogels for Biomedical Applications

Cellulose nanofiber-based aerogels are widely utilized in the biomedical field because of their biocompatibility, renewability, and biodegradability. These aerogels find applications in sustainable antibiotic delivery for wound healing, preparation of scaffolds for tissue cultures, development of drug delivery systems, biosensing, and as an antimicrobial film for wound healing .

Thermosensitive Drug Delivery Systems

Thermosensitive drug delivery systems, like PNIPAM/Hexakis, have been the focus of research in nanobiotechnology due to their multifunctional properties. These systems show potential for a

variety of applications, including cell delivery, and have been investigated for their ability to enhance the delivery of biomolecules, genes, and drugs [297].

Electrospun Nanofiber in Drug Delivery Systems

Electrospun nanofiber scaffolds have been developed for drug delivery systems, offering benefits such as high specificity and a porous structure suitable for the delivery of biomolecules, genes, and drugs. These nanofibers have been applied in transdermal systems, antibacterial agents, wound dressing, cancer treatment, scaffolds for growth factor delivery, and carriers for stem cell delivery systems .

Biopolymeric Auto-Fluorescent Micro- and Nanogels

Multifunctional biopolymeric auto-fluorescent micro- and nanogels have been developed as a platform for biomedical applications, specifically in the field of theragnostics for advanced healthcare .

These real-world applications demonstrate the potential of hybrid cellulose-based films and related materials in addressing various challenges in drug delivery and biomedical applications. The case studies and practical insights illustrate that these materials are not only theoretically promising but are also actively being developed into products and solutions with significant potential impact on healthcare and medicine.

Cellulose-based 2D materials possess a variety of unique properties that make them appealing for a wide range of applications, such as those detailed below.

Biodegradability and Renewable Sourcing: Cellulose is one of the most abundant renewable materials on Earth, making it biodegradable and CO2-neutral in the long run. This status is conditional on sustainable practices, such as replanting trees to replace those harvested for cellulose production—ensuring CO2 neutrality as these new plantings mature. Cellulose is available in a wide variety of fibres globally, which contributes to the sustainability and potential environmental friendliness of cellulose-based materials .

Mechanical Robustness: Cellulose and cellulose-based composite materials are well known for their mechanical strength, which is especially advantageous in applications like biodegradable medical implants, where the material must retain its structural integrity under physiological conditions.

Unique Nanostructuring: Nanostructuring cellulose-based 2D materials can result in unique properties. For instance, cellulose nanofibrils/nanofibers possess a high specific surface area due to their one-dimensional nanostructure, which is advantageous for applications like water purification.

Electrical Conductivity: MXenes are a class of 2D nanomaterials with metal-like electrical conductivity, making them promising electrode materials for energy storage devices. When combined with cellulose, these materials can overcome common issues such as low mechanical strength and restacking, which are often associated with MXenes.

Optical Properties: Cellulose-based materials can exhibit unique optical properties. For instance, hemicellulose nanocrystals derived from industrial biowastes demonstrate excellent dispersibility in water and are suitable for use in applications involving one-dimensional (1D) carbon nanotube nano-inks as well as two-dimensional (2D) transition metal dichalcogenide nanozymes .

Thermal Stability: Cellulose-based materials, like the ones used in MXene/cellulose-based electrodes, are recognized for their thermal stability. This characteristic is essential for applications involving high temperatures or requiring materials to maintain their properties under thermal stress.

Hydrophilicity: Cellulose-based materials, like graphene oxide-cellulose nanocrystal hybrid membranes, exhibit improved surface hydrophilicity. This characteristic is advantageous for applications requiring water permeability, such as wastewater treatment [298].

Cellulose-based 2D materials possess unique properties that make them well-suited for a wide range of applications, including biodegradable medical implants, energy storage, and water purification. Ongoing research in this field is expected to unveil further potential applications and benefits of these materials.

4.9.1. Detailed Applications of Cellulose-Based 2D Materials

Cellulose-based 2D materials have been extensively researched for their potential in various biomedical applications. They possess unique properties such as customizable surface modification, favorable optical transparency, good hydrophilicity, excellent biocompatibility, and mechanical properties that are both remarkable and especially suited for the demands of various applications, especially in the biomedical field.

Drug Delivery

Cellulose-based materials are widely used in drug delivery to create sustained-release systems. For instance, novel cellulose-based microparticles have been utilized as adsorptive carriers to develop solid self-nano-emulsifying drug delivery systems. These systems aim to improve the oral bioavailability of poorly soluble lipophilic drugs while maintaining stability and release behaviors. Moreover, cellulose and its derivatives have been employed as excipients in controlled drug delivery systems, allowing them to modify the solubility and gelling behavior of drugs for controlling release profiles. Figure 4.5 illustrates various applications of MOF/cellulose composites, including their use as antibacterial materials and for protein immobilization. In Figure 4.5a-1, schematics depict the fabrication of MOF wood composite materials and their antibacterial mechanism. Figure 4.5a-2 shows an illustration of antibodies or enzymes immobilized by MOF

on a fabric substrate. Figure 4.5b demonstrates how MOF/cellulose hydrogel exhibits a colour transition upon sensing histamine (HI) vapour, along with a truth table of the logic analytical device for HI monitoring. Figure 4.5c features a photograph of a CNF@c-MOF double-layer supercapacitor device and an LED powered by devices in series under different deformations [299].

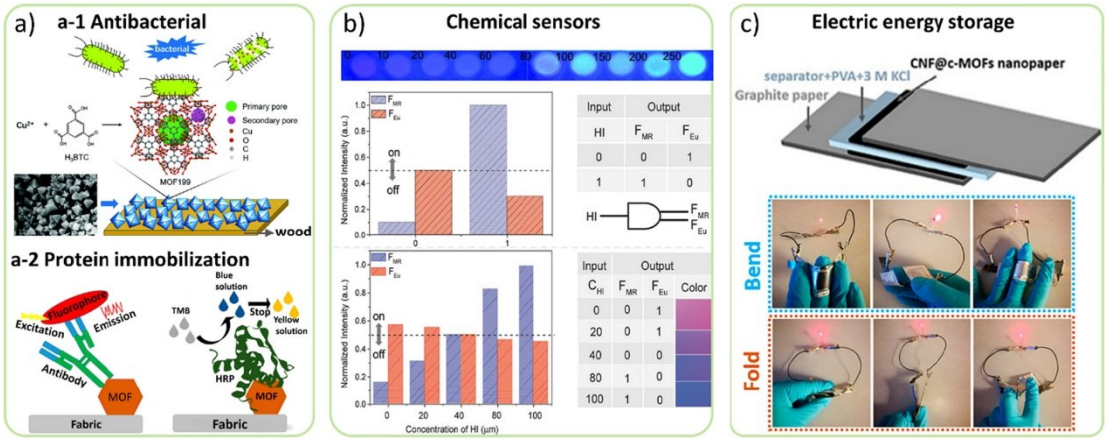

Figure 4.5. (**a**) Applications of MOF/cellulose composite as an antibacterial material and for protein immobilization. (**a-1**) Schematics of the fabrication of MOF wood composite materials and their antibacterial mechanism. (**a-2**) Illustration of an antibody or enzyme immobilized by MOF on a fabric substrate. (**b**) MOF/cellulose hydrogel exhibited a colour transition upon sensing histamine (HI) vapour, and the truth table of the logic analytical device for HI monitoring. (**c**) Photograph of a CNF@c-MOF double-layer supercapacitor device and an LED powered by devices in series under different deformations. Copyright with permission [Review on design strategies and applications of metal-organic framework-cellulose composites—ScienceDirect].

Gene Therapy

Nonviral cationic materials, such as dendrimers, have been investigated for gene therapy to deliver genetic material into diseased cells. Dendrimers are nanosized synthetic polymers with numerous peripheral functional groups that can bind cationic moieties. They provide an alternative to viral carriers because of their biocompatibility and degradability in vivo [300], [301].

Biosensing

Two-dimensional cellulose-based materials have also demonstrated potential in biosensing applications. For example, heterostructures of these materials have been utilized in biosensing to leverage their distinctive electronic and surface properties for detecting a range of biological substances. Additionally, thin films of 2D materials have been suggested for use in surface plasmon resonance sensors to detect concentrations of toxic gases such as NO2, highlighting the adaptability of these materials in sensing applications.

Case Studies and Real-World Examples

Cellulose-based 2D materials have real-world applications in the development of biosensors for environmental monitoring and healthcare diagnostics. For instance, cellulose nanocrystals and nanofibrils are being explored in hydrogels for biomedical uses like tissue engineering and regenerative biomedicine .

Two-dimensional materials have been utilized in cancer treatment for combination therapy, making use of their high drug-loading capacity and photothermal properties. These materials can be applied in multimodal therapy, encompassing drug delivery, photothermal therapy (PTT), and gene delivery, to enhance the effectiveness of cancer treatments.

When ground into homogeneous slurries, cellulose-based hydrogels could be readily injected in vivo at the tumour sites in mice. Illumination (1.0 W/cm^2, 5 min) of hepatocellular carcinomas was performed only twice (at day 1 and day 3) during a 2-week treatment period after the injection. The injected cellulose-based hydrogels included were DOX-loaded cellulose hydrogel (group 3, G3), neat cellulose hydrogel (group 4, G4), MXene-integrated cellulose hydrogel (group 5, G5), and DOX/MXene-containing cellulose hydrogel (group 6, G6). The MXene loading in G5 and G6 was fixed at 235.2 ppm. Two control groups were also investigated: saline (group 1, G1) and neat cellulose hydrogel combined with DOX (group 2, G2). Saline was administered by intravenous injection (G1). In G2, the neat cellulose hydrogel was intratumorally injected into mice, whereas the DOX solution was administered by intravenous injection. The anticancer activity of the hydrogels is further shown in Figure 4.6.

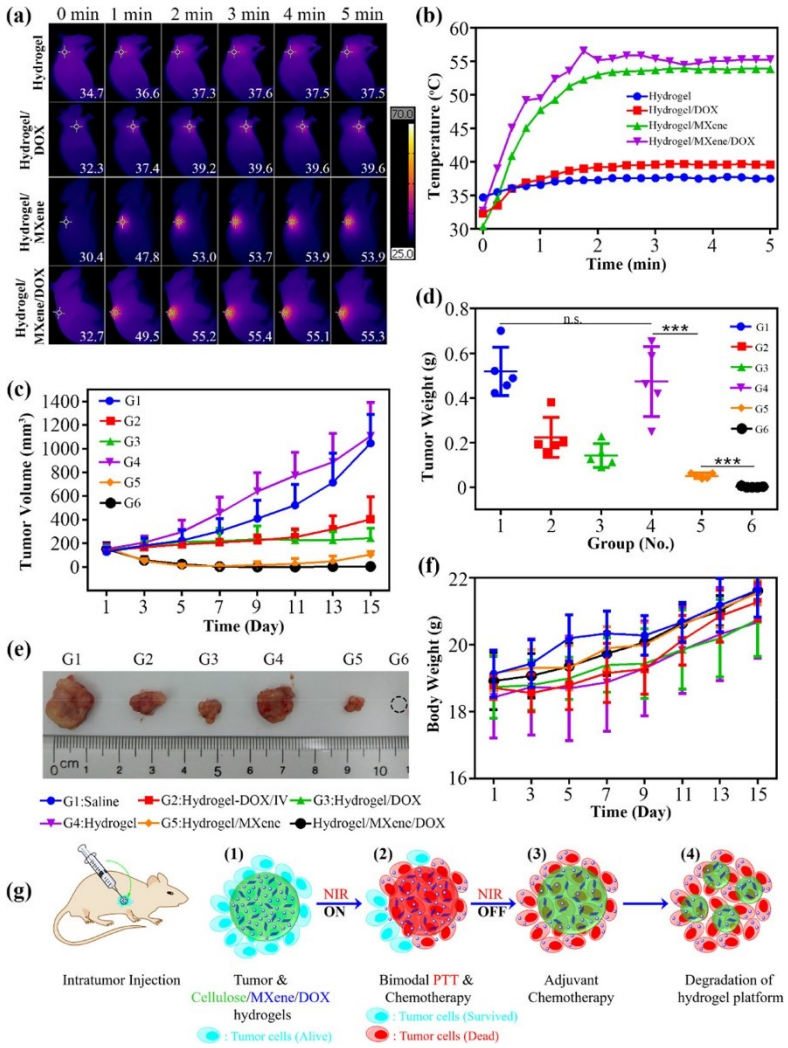

Figure 4.6. In vivo photothermal cancer therapy. (**a**) Graphic depiction of laser illumination and temperature at 0, 1, 2, 3, 4, and 5 min. (**b**) Temperature augmentation during laser illumination. (**c**) Tumor volumes during the observation period. (**d**) Tumor weights measured at day 15. Unpaired t test, $n = 5$, ***$p < 0.001$, ns stands for nonsignificant. Data are mean ± SD. (**e**) Representative images of tumors for each group. (**f**) Body weights of mice during different therapies. (**g**) Graphical representation of PTT/chemotherapy therapy. Intratumoral injection of cellulose/MXene/DOX hydrogels into mice followed by four steps: (1) cellulose/MXene/DOX hydrogels injected into the tumor site; (2) NIR irradiation on (PTT and chemotherapy); (3) NIR irradiation off (adjuvant chemotherapy); (4) degradation of the cellulose hydrogel platform [125]. Copyright with permission [Two-Dimensional MXene (Ti3C2)-Integrated Cellulose Hydrogels: Toward Smart Three-Dimensional Network Nanoplatforms Exhibiting Light-Induced Swelling and Bimodal Photothermal/Chemotherapy Anticancer Activity|ACS Applied Materials & Interfaces].

Figure 4.6a,b show that significant temperature increases were only detected for the hydrogels with incorporated MXene nanosheets (i.e., G5 and G6), demonstrating the outstanding photothermal properties of the MXene-integrated cellulose hydrogels in vivo. The FLIT values of cellulose/MXene hydrogel (G5) and DOX-loaded cellulose/MXene hydrogel (G6) reached temperatures in the range of 50–55 °C (Figure 4.6b), comparable to those obtained in Figure 6d for cellulose/MXene hydrogel with an MXene loading of 235.2 ppm. However, there were differences in both the temperature rise rate and plateau obtained in vivo (Figure 4.6b) compared with those measured in a cuvette (Figure 6d), possibly due to the different measurement methods employed. Figure 4.6c,d show the tumor growth curves and final tumor weights for each group. Figure 4.6e shows a representative tumor for all of the groups, and Figure 4.6f shows the body weight changes of the mice over the course of treatment. Notably, all six treatments had no significant influence on the body weight of mice.

A comprehensive analysis of Figure 4.6c–e confirms the effectiveness of the dual-modular cancer therapy. The similar tumor growth curves of group 1 (saline) and group 4 (hydrogel with NIR) imply that both saline and neat cellulose hydrogel were unable to inhibit tumor growth. The tumors in both group 2 (hydrogel combined with IV DOX) and group 3 (hydrogel/DOX) grew more slowly than the negative control (i.e., group 1 and group 4), indicating that both intravenously injected DOX and DOX released from the cellulose hydrogel can partially inhibit tumor growth but cannot effectively cure it. Similarly, comparing group 5 with group 4 showed that a single PTT can eliminate the vast majority of the tumor. Furthermore, the smaller tumors in group 5 compared to groups 2 and 3 suggested that PTT was more effective than DOX chemotherapy. However, tumors still relapsed after potent PTT (group 5 results). These results demonstrate that neither PTT nor chemotherapy alone was able to completely ablate the tumors and clear tumor cells. In contrast, tumors in group 6 were completely cleared and did not relapse, indicating that all the tumor cells were eradicated by the dual-modular PTT/chemotherapy. The noticeable relapse in group 5 but not in group 6 indicates that PTT could kill the majority of the tumor cells, but a small percentage of them may have survived (Figure 4.6g(2)), leading to tumor relapse, whereas the combined chemotherapy by DOX released from the hydrogel provided an adjuvant killing effect and a continuous inhibitory effect on the remaining tumor cells, achieving complete tumor clearance (Figure 4.6g(3)). Furthermore, as NIR illumination significantly accelerated the release rate of DOX in cellulose/MXene, more DOX may have been released into the tumor microenvironment during PTT, augmenting the effect of chemotherapy, resulting in a synergistic effect. Additionally, this cellulose-based platform can be partially disintegrated/degraded within 2 weeks, as shown in Figures 4.5g(4) and S3 in the Supporting Information [298].

In conclusion, cellulose-based 2D materials have a wide range of applications in the biomedical field due to their sustainable nature, biocompatibility, and versatile properties. Ongoing research is actively focused on developing these materials for drug delivery, gene therapy, and biosensing,

among other applications, to overcome challenges and enhance their performance in real-world scenarios.

4.9.2. Challenges and Limitations of Cellulose-Based 2D Materials

Cellulose-based 2D materials have promising applications in various fields, but their widespread use is hindered by several existing challenges and limitations that will be discussed below.

Scientific and Technological Challenges

One of the main scientific challenges involves the interaction of cellulose nanofibrils with bacteria and proteins, which leads to surface fouling. This interaction can cause the material to lose its integrity due to water-induced swelling . Technological challenges include the high reflectivity of sunlight and low efficiency of photothermal conversion, which can significantly hinder the application of cellulose-based materials in solar water evaporation [302], [303].

Economic and Scalability Challenges

Economic and scalability challenges are prevalent in cellulose-based 2D materials production. The cost of production is high now, and scaling up while maintaining material quality is a big challenge. Additionally, these materials are currently limited to fillers in epoxy resins and polyurethane-based coatings, narrowing their potential market. However, there is hope that as applications broaden, the demand will increase, potentially reducing costs and expanding market opportunities .

Potential Solutions and Ongoing Research

Ongoing research is currently focused on various strategies to overcome these challenges. For example, hybridization strategies are being explored to address the limitations of cellulose nanofibrils by combining multiple components that work together synergistically toward specific properties and applications .

Research is ongoing to enhance the efficiency of photothermal conversion by designing and optimizing the hierarchical structure of films through the addition of carbon materials during bacterial cellulose culture .

Research is currently focused on developing new methods for producing 2D materials such as graphene from sustainable microcrystalline cellulose at a low cost to address economic and scalability challenges. Furthermore, active research in the exploration of MXenes as nanofillers in polymer-based coatings is ongoing [304].

In conclusion, although cellulose-based 2D materials show great promise for various applications, there are still significant challenges that need to be addressed. Nevertheless, ongoing research focused on overcoming these hurdles is paving the way for wider adoption of these materials in the future.

4.9.3. Emerging Trends and Future Directions in Cellulose-Based 2D Materials

Integration with Smart Drug Delivery Systems

Cellulose-based 2D materials are increasingly being integrated with smart drug delivery systems due to their adaptable surface chemistry, high surface area, biocompatibility, and biodegradability. These nanocellulose-based composite materials can be transformed into drug delivery carriers and designed into multidimensional structures such as 1D (nanofibers, microparticles), 2D (films), and 3D (hydrogels, aerogels) materials for use as different drug carriers. The specific requirements of these materials for drug delivery include good drug-loading capacity, biocompatibility, and biodegradability to ensure that drugs are released at the correct concentrations and proper rate .

3D Bioprinting

An emerging trend is the use of cellulose-based 2D materials in 3D bioprinting. A bioink that combines the exceptional shear-thinning properties of nanofibrillated cellulose with the rapid cross-linking ability of alginate has been developed for printing living soft tissue with cells in 3D. This advancement has allowed for the printing of both 2D grid-like structures and complex 3D constructs, including anatomically shaped cartilage structures such as a human ear and sheep meniscus using MRI and CT images as references. The potential application of nanocellulose in the 3D bioprinting of living tissues and organs has been convincingly demonstrated [305].

4.10. Real-World Applications and Implications

This section highlights the practical applications of hybrid cellulose-based films and addresses key questions regarding their commercial and regulatory status.

FDA Approval: To date, several cellulose-based products have been approved by regulatory agencies such as the FDA for various applications, including wound dressings and food packaging. However, specific hybrid cellulose-based materials are still undergoing extensive testing and evaluation to meet safety and efficacy standards for medical and pharmaceutical applications.

Market Availability: Some cellulose-based materials, such as cellulose acetate and carboxymethyl cellulose, are commercially available and used in various industries. The development of hybrid cellulose-based materials with enhanced properties is an active area of research, with potential future commercialization .

Liability Issues: The liability for unintended consequences arising from the release of hybrid cellulose-based materials depends on regulatory compliance, product safety assessments, and the legal framework governing environmental protection and public health.

Environmental Implications

Cellulose-based 2D materials are sourced from renewable resources, offering an eco-friendly alternative to non-renewable materials. Cellulose is abundant, low-cost, biodegradable, and CO_2 neutral, with a wide variety of fibers available globally. The production of these materials often involves bio-derived pathways developed with the environmental impact in mind. For example, the fabrication of a 2D TiO_2/g-C_3N_4 heterojunction for generating 5-hydroxymethylfurfural (5-HMF) utilizes bio-derived pathways to access ionic liquids from natural renewable resources [306].

Lifecycle Analysis and Recycling Potential

Cellulose-based 2D materials have an eco-friendly lifecycle because they are biodegradable. They can be recycled and reused in various applications, such as CO_2 adsorption, where they exhibit high adsorption capacity. Following the adsorption process, the CO_2 molecules can be desorbed, captured, and stored for further applications, showcasing the recycling potential of these materials [307].

Moreover, the production of cellulose-based thermal insulation materials involves recycling cellulosic and/or animal waste. These materials have demonstrated good thermal insulating quality, which can contribute to energy efficiency in buildings. In conclusion, cellulose-based 2D materials offer a positive environmental impact because of their renewable nature, biodegradability, and the eco-friendly methods used in their production. Their lifecycle includes the potential for recycling, further enhancing their sustainability. However, more research is needed to fully understand their environmental implications and to further improve their sustainability [308], [309].

4.11. Concluding Statements

This paper has explored the multifaceted advancements in hybrid cellulose-based films, highlighting their innovative applications in 2D nano-delivery systems. Although these materials present a promising avenue for applications across pharmaceuticals, environmental remediation, and biomedical engineering, it is important to acknowledge the challenges and limitations that accompany their development and use.

Commercialization and Regulatory Considerations:

As of now, the journey towards widespread commercialization and regulatory approval, including FDA approval for medical applications, is ongoing. The potential for hybrid cellulose-based materials in the medical field is substantial, yet their adoption is contingent upon rigorous testing, validation, and regulatory compliance.

Market Availability and Environmental Concerns:

The development of these materials into commercially available products is an active area of research. Efforts are being made to ensure that these innovative materials not only meet high performance standards but also address environmental sustainability and safety concerns.

Addressing Liability and Safety:

Questions regarding liability and safety, particularly in the context of unintended environmental release, highlight the necessity for comprehensive risk assessments and the development of mitigation strategies to safeguard against potential adverse impacts.

Reflecting on these points, it becomes clear that the path forward for hybrid cellulose-based films involves not only scientific and technological innovation but also a concerted effort to navigate the complex landscape of regulatory, environmental, and ethical considerations. The optimism surrounding these materials must be tempered with a commitment to responsible research and development practices.

In summary, though the prospects for hybrid cellulose-based films are indeed promising, their successful integration into real-world applications requires a balanced approach that addresses both their potential benefits and the challenges they pose. Ongoing research and collaboration across disciplines will be crucial in realizing the full potential of these materials while ensuring their safe and sustainable use.

Closure

This chapter extended the analysis from single-component modification to the broader landscape of hybrid cellulose-based films, presenting work published in the context of 2D nano-delivery and multifunctional film design. The central concern was how advanced integration strategies — electrospinning, chemical vapour deposition, and matrix-assisted pulsed laser evaporation, among others — enable cellulose films to acquire new functionalities beyond what the base matrix can provide. Case studies illustrated improvements in drug-loading capacity, mechanical flexibility, barrier performance, and biocompatibility when nanomaterials are incorporated systematically and with controlled distribution. The interplay between film architecture and functional response was a recurring theme: the same composite components, arranged differently at the nanoscale, can yield materials suited to biomedical delivery, environmental filtration, or flexible electronic substrates. Challenges tied to reproducibility, regulatory acceptance, and the gap between laboratory-scale fabrication and industrial production were discussed honestly. The chapter thus completed the picture established in Chapters 2 and 3 — from material properties and GO optimization to full

film design — and positioned the reader to appreciate the systematic experimental and computational work that Chapter 5 brings together.

Chapter 5: Optimization Approaches for CNC/CNF–rGO Nanocomposites

This chapter is a published paper in **Micromachines (2025)**, Vol. 16, Issue 4, Article 39, titled "Lasso Model-Based Optimization of CNC/CNF/rGO Nanocomposites."

Lasso Model-Based Optimization of CNC/CNF/rGO Nanocomposites

Abstract: This study explores the use of citric acid and L-ascorbic acid as reducing agents in CNC/CNF/rGO nanocomposite fabrication, focusing on their effects on electrical conductivity and mechanical properties. Through comprehensive analysis, L-ascorbic acid showed superior reduction efficiency, producing rGO with enhanced electrical conductivity up to 2.5 S/m, while citric acid offered better CNC and CNF dispersion, leading to higher mechanical stability. The research employs an advanced optimization framework, integrating regression models and a neural network with 30 hidden layers, to provide insights into composition–property relationships and enable precise material tailoring. The neural network model, trained on various input variables, demonstrated excellent predictive performance, with R^2 values exceeding 0.998. A LASSO model was also implemented to analyze variable impacts on material properties. The findings, supported by machine learning optimization, have significant implications for flexible electronics, smart packaging, and biomedical applications, paving the way for future research on scalability, long-term stability, and advanced modeling techniques for these sustainable, multifunctional materials.

5.1. Introduction

Nanocomposite materials have emerged as a cornerstone of modern materials science, offering tailored properties that make them indispensable in advanced applications, such as flexible electronics, biomedical devices, and smart packaging. Cellulose nanomaterials, particularly cellulose nanocrystals (CNCs) and cellulose nanofibers (CNFs), have garnered significant attention in materials science due to their renewable origin, exceptional mechanical properties, and environmental compatibility [1], [310]. Recent studies using reactive molecular dynamics simulations have predicted the ultimate strength of CNCs to be approximately 9.2 GPa at a strain rate of 1 s^{-1}, surpassing previously reported values of 7.5–7.7 GPa. The mechanical behavior of CNCs is influenced by factors such as fibril twist and strain rate, with the C4-O4 glycosidic bond primarily responsible for their failure . Researchers have explored hybridization techniques to enhance the mechanical properties of polymer nanocomposites, such as modifying aramid nanofibers (ANFs) with chlorinated cellulose nanocrystals and 3-glycidoxypropyltrimethoxysilane, resulting in a 15.1% increase in Young's modulus and a 10.1% improvement in tensile strength for epoxy nanocomposites reinforced with 1.5 wt% of functionalized ANFs [311]. Additionally, a novel flow focusing approach using a five-channel microfluidic chip has been developed to fabricate aligned core-sheath cellulose nanocrystal/cationic polyacrylamide (CNC/CPAM) composite filaments, yielding a remarkable

tensile strength of 510 ± 20 MPa, approximately 117% higher than pure CNC spun fibers, with a 70% increase in elongation at break. These advancements underscore the potential of cellulose nanomaterials in high-performance applications, particularly where high strength-to-weight ratios are crucial [311]. CNC and CNF possess unique properties such as a high aspect ratio, low density, and the ability to form hydrogen bonds, making them ideal candidates for creating lightweight, strong, and sustainable materials [312]. Graphene oxide (GO) and its reduced form, reduced graphene oxide (rGO), have also proven to be transformative in the development of multifunctional nanocomposites. GO, with its high surface area and oxygen-rich functional groups, is easily dispersible in aqueous systems, which facilitates its integration with other materials. Upon reduction, rGO exhibits enhanced electrical conductivity, chemical stability, and mechanical strength, which are critical for applications requiring efficient charge transport and structural integrity . The combination of CNC, CNF, and rGO creates a synergistic system where the mechanical reinforcement from CNC/CNF complements the conductivity of rGO, resulting in materials with a balance of strength and functionality. Despite the potential of CNC/CNF/rGO nanocomposites, their performance is heavily influenced by the choice of reducing agents used in converting GO to rGO . Reducing agents determine not only the efficiency of the reduction process but also the structural and functional properties of the resulting composites . Optimizing the interaction between CNC, CNF, and rGO is essential for maximizing the utility of these materials in specific applications . The influence of protons on reduced graphene oxide (rGO) can significantly impact its properties, particularly in terms of carrier transport. Studies have shown that protons can enhance the conductivity of rGO films, leading to a mixed proton–electron conduction mechanism. This dual-carrier transport system can be advantageous in certain applications, such as fuel cells and chemical filters, where proton conductivity is crucial. However, it also introduces complexity in understanding and controlling the overall charge transport properties. The presence of protons can affect the reduction degree of rGO and influence defect formation , potentially altering its electronic structure and carrier mobility. Furthermore, the interaction between protons and electrons in rGO can lead to interesting phenomena like proton–electron coupling, which may impact the material's electrical and electrochemical behavior [313]. While this dual-carrier transport can offer unique functionalities, it also presents challenges in precisely controlling and optimizing the material's properties for specific applications, as the interplay between proton and electron transport needs to be carefully considered [314]. Optimizing CNC/CNF/rGO composites presents significant challenges, particularly in balancing electrical conductivity and mechanical properties. As the content of conductive rGO increases, electrical conductivity typically improves, but often at the expense of mechanical strength and flexibility . Conversely, higher proportions of CNC and CNF enhance mechanical properties but can reduce conductivity . Recent advancements in machine learning (ML) methods offer promising solutions to this optimization challenge. ML techniques can efficiently evaluate complex physical relationships using relatively few samples while ensuring the physical plausibility of results [315], [316]. These integrated approaches allow researchers to predict optimal compositions and

processing parameters, potentially leading to composites with an ideal balance of conductivity and mechanical performance without extensive trial-and-error experimentation.

Reducing agents play a pivotal role in the fabrication of CNC/CNF/rGO nanocomposites by controlling the reduction process of GO to rGO. This reduction impacts the electrical, mechanical, and structural properties of the nanocomposites. Two environmentally friendly reducing agents, citric acid and L-ascorbic acid, have been widely investigated due to their biocompatibility, availability, and cost-effectiveness.

Citric acid: A mild organic acid with strong hydrogen-bonding capabilities, citric acid facilitates uniform dispersion of CNC and CNF within the matrix. However, its moderate reduction efficiency often results in rGO with residual oxygen functionalities, which can disrupt the stacking of rGO sheets and limit conductivity. The advantages of citric acid lie in its ability to enhance mechanical stability and compatibility within the nanocomposite matrix [317], [318].

L-ascorbic acid: A strong reducing agent and natural antioxidant, L-ascorbic acid exhibits superior reduction efficiency, producing rGO with fewer oxygen-containing functional groups. This characteristic enhances electrical conductivity and promotes better stacking of rGO sheets, resulting in a denser and more efficient conductive network. While effective for improving conductivity, L-ascorbic acid can sometimes lead to challenges in achieving uniform dispersion within the matrix [319], [320].

The choice between citric acid and L-ascorbic acid depends on the target application and the desired balance between mechanical stability and electrical performance. Investigating the influence of these reducing agents on the structural, mechanical, and electrical properties of CNC/CNF/rGO nanocomposites is critical for tailoring materials to specific functional requirements.

The comparison of citric acid and L-ascorbic acid as reducing agents for graphene oxide (GO) reduction can be contextualized by considering other common reducing agents like hydrazine and sodium borohydride. While hydrazine and sodium borohydride offer strong reducing capabilities and produce rGO with high electrical conductivity, their use is limited by toxicity concerns and potential impurity introduction. In contrast, citric acid and L-ascorbic acid provide significant advantages in terms of safety, environmental friendliness, and biocompatibility, making them particularly suitable for biomedical applications [321]. L-ascorbic acid stands out for its strong reducing capability, comparable to hydrazine in some cases, producing rGO with enhanced electrical conductivity (up to 2.5 S/m) and promoting a better alignment of cellulose nanocrystals (CNC) and cellulose nanofibrils (CNF) in nanocomposites. Citric acid, while having moderate reduction efficiency, excels in promoting uniform dispersion of CNC and CNF within the nanocomposite matrix, crucial for applications requiring enhanced mechanical stability. The choice between these reducing agents ultimately depends on the specific application requirements; for instance, L-ascorbic acid might be preferred for flexible electronics or conductive

nanocomposites where high electrical conductivity is crucial, while citric acid could be the better choice for applications prioritizing mechanical stability or uniform dispersion. In conclusion, the eco-friendly and biocompatible nature of citric acid and L-ascorbic acid, combined with their effective reduction capabilities, make them attractive alternatives for many applications, especially in the biomedical field and sustainable material development, despite the traditionally stronger reducing agents like hydrazine and sodium borohydride. This study aims to systematically investigate the effects of citric acid and L-ascorbic acid as reducing agents in the fabrication of CNC/CNF/rGO nanocomposites. The specific objectives include the following:

Quantify the reduction efficacy of citric acid and L-ascorbic acid under controlled pH and concentration conditions, employing spectroscopic and electrochemical techniques to elucidate the mechanisms of graphene oxide reduction.

Elucidate the structural integration of cellulose nanocrystals (CNC), cellulose nanofibrils (CNF), and reduced graphene oxide (rGO) within the nanocomposite matrix, with particular emphasis on the role of reducing agents in modulating dispersion and alignment, utilizing advanced microscopy and scattering techniques.

Characterize the mechanical properties, including tensile strength, Young's modulus, and film thickness, and establish correlations with composition and processing parameters through statistical analysis and materials science principles.

Assess the electrical conductivity of the nanocomposites and develop comprehensive regression models to delineate the impact of composition and processing variables on conductivity, employing both theoretical and experimental approaches.

Construct and validate a machine learning prediction model to identify complex patterns and forecast the performance metrics of CNC/CNF/rGO nanocomposites, utilizing input parameters such as composition ratios, reduction conditions, and mechanical properties. This model will employ advanced algorithms such as neural networks or random forests to capture non-linear relationships and interactions among variables.

Optimize the composition and processing conditions using a multi-objective optimization framework, incorporating techniques such as response surface methodology or genetic algorithms to achieve an optimal balance between electrical conductivity and mechanical stability for specific application requirements.

Validation from Literature

A study developed a machine learning model to predict the synthesizability of half-Heusler compounds, achieving a cross-validated precision of 0.82 and recall of 0.824. This aligns closely with the performance reported by the authors (82.6% precision, 80.6% recall for ternary materials). Additionally, study [322]successfully used machine learning to predict favorable synthesis

conditions for MoS2, demonstrating the viability of AI-driven synthesis prediction. The authors' approach of using time-split validation, where they train on pre-2015 data and test on post-2015 materials, is particularly compelling. Their high true positive rate of 88.60% on post-2019 materials suggests their model can effectively identify synthesizable compounds among newly discovered materials [323]. This temporal validation strategy is similar to that, which showed strong predictive performance on materials synthesized after their training cutoff date [324]. These parallel findings in the literature lend credence to the authors' results and methodology.

5.2. Materials and Methods

5.2.1. Materials and Reagents

The nanocomposite fabrication process utilized cellulose nanocrystals (CNC), cellulose nanofibers (CNF), and graphene oxide (GO) as primary components. CNCs were prepared through sulfuric acid hydrolysis of microcrystalline cellulose (Sigma-Aldrich,Darmstadt,Germany, 99% purity), following an optimized protocol that yielded nanocrystals with an average length of 150 ± 20 nm and a diameter of 5 ± 1 nm, as determined by transmission electron microscopy. CNFs were obtained through a combination of TEMPO-mediated oxidation and high-pressure homogenization of softwood pulp (sourced from a local paper mill), resulting in fibrils with a diameter range of 5–20 nm and lengths exceeding 1 μm. Graphene oxide synthesis employed a modified Hummers' method, which was refined to enhance safety and yield. The process utilized a 9:1 (*v*/*v*) mixture of H_2SO_4 (98%, Merck, Darmstadt, Germany) and H_3PO_4 (85%, Sigma-Aldrich), with an increased $KMnO_4$ (Sigma-Aldrich, >99%)-to-graphite (Alfa Aesar, Ward Hill, Massachusetts, U.S., 99.9999% purity) ratio of 6:1. This modification not only improved the oxidation efficiency but also reduced the production of toxic gases typically associated with the traditional Hummers' method. The reducing agents, L-ascorbic acid (Sigma-Aldrich, ≥99%) and citric acid (Fisher Scientific, Waltham, Massachusetts, USA, 99.5%), were carefully selected for their biocompatibility and effectiveness in GO reduction. All aqueous solutions were prepared using ultrapure water (18.2 MΩ·cm resistivity) obtained from a Millipore Milli-Q system [325], [326], [327], [328].

5.2.2. Preparation of CNC/CNF/rGO Nanocomposites

The preparation of CNC/CNF/rGO nanocomposites involved a meticulously optimized multi-step procedure designed to achieve optimal homogeneity and component interaction. Initially, graphene oxide was dispersed in deionized water (0.5 mg/mL) using a probe sonicator (Sonics Vibra-Cell, Newtown, Connecticut, USA, 500 W, 20 kHz) for 60 min in an ice bath to prevent overheating. This sonication protocol was refined through a series of trials to determine the optimal power output (40% amplitude) and pulse sequence (5 s on, 2 s off) that maximized GO exfoliation while minimizing structural damage. Concurrently, CNC and CNF were separately dispersed in deionized water (1 wt% each) using a high-shear mixer (IKA T25 digital ULTRA-TURRAX, Guangzhou, China) at 10,000 rpm for 30 min, followed by magnetic stirring at 500 rpm for 90 min.

This two-step dispersion process was developed to ensure uniform distribution of nanocellulose materials without compromising their structural integrity. The GO suspension was then gradually introduced into the CNC and CNF dispersions under continuous stirring at 300 rpm using a temperature-controlled magnetic stirrer (IKA RCT basic, Guangzhou, China) maintained at 25 °C. The combined dispersion was subsequently divided into two batches for reduction using either citric acid or L-ascorbic acid. The reduction process was carried out in a custom-designed glass reactor equipped with a water jacket for precise temperature control. For citric acid reduction, the pH was adjusted to 5.0–5.2 using a 0.1 M NaOH solution, with citric acid concentrations ranging from 0.1 M to 0.5 M. L-ascorbic acid reduction was performed at pH 5.7–5.9, achieved through the addition of a 0.1 M HCl solution, with L-ascorbic acid concentrations between 0.05 M and 0.3 M. Both solutions underwent thermal treatment at 95 ± 0.5 °C for four hours using a circulating water bath (Julabo F25-ME,Seelbach,Germany) to maintain precise temperature control. This temperature and duration were optimized through a series of experiments that evaluated the trade-off between reduction efficiency and nanocellulose degradation. After reduction, the composite solutions were cooled to room temperature using a controlled cooling rate of 1 °C/min to minimize thermal stress. The cooled solutions were then cast onto PTFE-coated petri dishes and dried for 24 h in a custom-built environmental chamber that maintained a constant temperature of 23 ± 1 °C and relative humidity of 50 ± 2%. These controlled drying conditions were crucial for ensuring reproducible film formation and minimizing residual stresses in the nanocomposite films The optimization process for CNC/CNF/rGO nanocomposites involved varying concentrations of each component within specific ranges: CNC (0.1–1.0 wt%), CNF (0.1–0.8 wt%), and rGO (0.05–0.2 wt%). The reduction process was carried out under controlled pH conditions, with L-ascorbic acid at pH 5.7–5.9 and citric acid at pH 5.0–5.2. The temperature range for the reduction process was maintained between 80 and 95 °C [329], [330], [331], [332], [333]. Optimizing synthesis parameters through machine learning is essential, as it can reduce costs, shorten processing times, improve measurement accuracy, and enhance the analysis of material properties. By refining these parameters, the reliability and reproducibility of the synthesis process can be improved, leading to better material performance.

Design of Experiments (DOE) was conducted to identify significant control variables. A correlation test was then performed to verify significance; however, high covariance levels were observed. To address this, a machine learning model was developed using ten layers with eight neurons per layer rather than thirty. Ultimately, Lasso regression was employed to enhance interpretability and mitigate high covariance, with an alpha value of 20.

The neural network architecture comprised an input layer with 8 neurons (corresponding to CNC, CNF, rGO concentrations, pH, temperature, time, and reducing agent type), 30 hidden layers with 64 neurons each using ReLU activation functions, and an output layer with 3 neurons (tensile strength, electrical conductivity, and film thickness). Additionally, a LASSO model was

implemented to provide interpretable insights into the relative importance of different input variables.

5.2.3. Reduction Process with Citric Acid and L-Ascorbic Acid

The reduction of GO to rGO was carried out using citric acid or L-ascorbic acid as reducing agents, with each process optimized for pH and concentration. For citric acid, the pH was adjusted to 5.0–5.2, and concentrations ranged from 0.1 M to 0.5 M. L-ascorbic acid reduction was performed at pH 5.7–5.9, with concentrations between 0.05 M and 0.3 M [334]. Both solutions underwent thermal treatment at 95 °C for four hours, a critical step that accelerates the reduction process and enhances rGO formation within the CNC/CNF matrix [335]. This temperature and duration were likely chosen based on previous studies showing that L-ascorbic acid effectively reduces GO at elevated temperatures, preserving substrate integrity better than traditional reductants like hydrazine [336]. The thermal treatment may also affect the CNC/CNF matrix, potentially altering its structure or properties. After reduction, the composite solutions were cooled to room temperature and cast onto petri dishes for 24 h ambient drying to form thin films. It is worth noting that controlled ambient conditions during drying, such as humidity and airflow, can significantly influence the final film properties [337]. Future studies could benefit from specifying and controlling these parameters to ensure reproducibility and optimize film characteristics.

5.2.4. Characterization Techniques

The characterization techniques employed in this study provide a comprehensive analysis of the physical, chemical, and structural properties of the prepared nanocomposites. Microscopy techniques work synergistically to provide a multi-scale understanding of the composite structure [338], [339].

The SEM images (Figure 5.1 and Table 1) provided illustrate the surface morphology of CNC/CNF/rGO films after LAA treatment, with varying magnifications and structural details. Below is a detailed analysis of the observed features, incorporating annotations and quantitative metrics to highlight key structural characteristics.

Image Analysis and Observations

In Figure 5.1a (10,000× Magnification, Scale Bar: 2 μm), this high-magnification image reveals a relatively smooth surface interspersed with pores of irregular shapes and sizes. The pore walls appear well-defined and compact, suggesting that the LAA treatment has contributed to a reduction in porosity compared to CA-treated films. The smoother regions between the pores indicate a densified matrix, which is likely due to the enhanced interaction between CNC/CNF and rGO components during the treatment process. The structural compactness observed in this image aligned with the reduced surface roughness values measured for LAA-treated films.

In Figure 5.1b (5000× Magnification, Scale Bar: 5 μm), at a slightly lower magnification, the image provides a broader view of the surface morphology. The pores appear less frequent and more isolated compared to CA-treated samples, with smoother transitions between pore edges and the surrounding matrix. This suggests that LAA treatment promoted a more uniform distribution of material across the film's surface. The smoother texture observed at this scale further supports the hypothesis that LAA treatment enhances film densification while reducing overall porosity.

In Figure 5.1c (500× Magnification, Scale Bar: 50 μm), this low-magnification image offers an overview of the film's large-scale morphology. The surface appears predominantly smooth with minimal disruptions or voids. While some elongated features are visible, they are less pronounced than in higher magnification images. This suggests that the LAA-treated film achieved a high degree of uniformity across its structure, which is beneficial for applications requiring mechanical stability and low permeability.

Quantitative Metrics

- Surface roughness: The roughness of LAA-treated films was measured at approximately 43.75, indicating a significant reduction compared to CA-treated films (56.29). This reduction reflected the smoother and more compact surface morphology achieved through LAA treatment.

- Pore count: The number of pores observed in LAA-treated films was significantly lower (1404) than in CA-treated films (4388). This reduction highlighted the role of LAA in minimizing porosity.

- Pore distribution: Pores in LAA-treated films were smaller and more isolated, contributing to improved structural integrity.

(**a**)

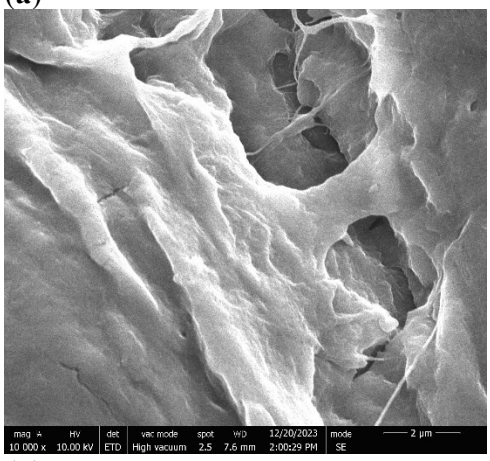

(**b**)

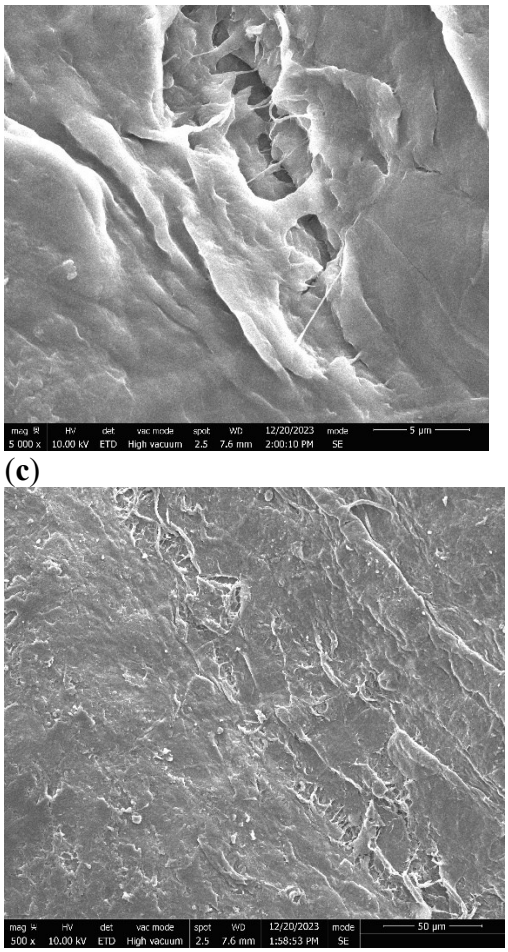

Figure 5.1. SEM micrographs showing the morphological characteristics of CNC/CNF/rGO nanocomposites at different magnifications ((**a**): "LAA-Treated CNC/CNF/rGO Film—High Magnification (10,000×, Scale Bar: 2 µm)", (**b**): "LAA-Treated CNC/CNF/rGO Film—Medium Magnification (5000×, Scale Bar: 5 µm)", (**c**): "LAA-Treated CNC/CNF/rGO Film—Low Magnification (500×, Scale Bar: 50 µm)").

The SEM images clearly demonstrate that LAA treatment significantly altered the microstructure of CNC/CNF/rGO films by enhancing their compactness and reducing porosity. These changes were evident in all magnifications, where smoother surfaces with fewer and smaller pores dominated. Such structural improvements make LAA-treated films ideal for applications requiring high mechanical strength, low permeability, or enhanced electrical conductivity. Annotating these images with scale bars and quantitative data further emphasizes these distinctions and provides clarity on the effects of LAA treatment on film morphology.

Tensile testing using a universal testing machine measured tensile strength and elongation at break, with film thickness measured using a micrometer for accuracy. To enhance reproducibility, it would be beneficial to specify the testing protocol, including strain rate, sample size, and any relevant standards followed. Electrical conductivity of the composites was evaluated using a four-

point probe setup, allowing for precise measurement of conductive pathways within the films. This method is particularly suitable for thin film samples and provides more accurate results compared to two-point probe measurements by eliminating contact resistance effects [340], [341].

5.2.5. Film Thickness Models

The thickness (t) of the dried nanocomposite films was calculated using the following equation, Equation (1) [342], [343]:

$$t = m/(A \cdot \rho) \quad (1)$$

In this formula,

m is the mass of the composite film;

A is the area of the film;

ρ is the density of the composite material.

Equation (1) ensures that film thickness can be reliably correlated with processing parameters, such as the concentrations of CNC, CNF, and rGO.

5.3. Model Training and Evaluation

5.3.1 Choice of Modeling Approach

The goal of this section is to establish quantitative composition–property relationships for CNC/CNF/rGO nanocomposite films, linking the eight controllable processing parameters, CNC concentration, CNF concentration, rGO concentration, reducing agent type, reducing agent concentration, pH, temperature, and reaction time, to three measured output properties: electrical conductivity, tensile strength, and film thickness.

The first question in building any predictive model is which statistical or computational framework is appropriate for the dataset. A number of approaches were considered and systematically evaluated [473], [474], [475].

Analysis of Variance (ANOVA) is a classical method designed to test whether the mean values of a response variable differ significantly across discrete treatment groups. It is well suited for fully factorial designed experiments in which each factor takes a small number of fixed categorical levels and the factors are independently varied. In the present dataset, however, the input variables are continuous and carry strong mutual correlations: the concentrations of CNC, CNF, and rGO co-vary with pH and temperature across the processing conditions studied, and the reducing agent type interacts with pH and reaction time in a non-independent manner. Under such conditions, the core assumptions of ANOVA — independence of factors, homogeneity of variance across groups, and the absence of strong multicollinearity — are violated. ANOVA would therefore be both statistically inappropriate and unable to produce the predictive models needed to relate

composition to properties across the full continuous parameter space [350]. Hence ANOVA was not used.

A 30-hidden-layer artificial neural network (ANN) with 64 neurons per hidden layer and ReLU activations was trained first, with dropout regularization and early stopping to prevent overfitting. The network achieved high R^2 values on the training and validation sets (0.9989 and 0.9987, respectively), but the complexity of the architecture and the high inter-variable covariance meant that varying the number of layers, neurons per layer, or input configurations produced no consistent improvement and showed signs of overfitting on subsets of the data. **Thus a standard fully connected neural network alone was insufficient.** While this architecture is retained as a secondary model because it captures non-linear interactions in the composition space, it is not interpretable in physical terms and cannot identify which processing parameters are most influential [351].

LASSO (Least Absolute Shrinkage and Selection Operator) regression is a penalized linear regression method that simultaneously performs variable selection and coefficient regularization by adding a penalty term proportional to the sum of the absolute values of the regression coefficients. As the regularization parameter α increases, LASSO progressively drives the coefficients of less influential variables to exactly zero, effectively removing them from the model. This makes the resulting model sparse, interpretable, and robust against multicollinearity. Given that the input variables in this study exhibit high covariance, for example, L-ascorbic acid concentration, pH, and temperature all contribute jointly to the extent of GO reduction, LASSO is the most appropriate choice: it identifies the dominant drivers of each property without inflating standard errors, as ordinary least squares or plain regression would do in a highly correlated system. A regularization parameter of α = 20 was selected after cross-validation, and the data were split 80% for training and 20% for validation to balance learning capacity against generalization. **Thus LASSO regression was chosen as the primary model.**

5.3.2 The LASSO Method

In mathematical terms, LASSO minimizes the objective function:

$$\min_{\beta} \left\{ \sum_{i=1}^{n} (y_i - \hat{y}_i)^2 + \alpha \sum_{j=1}^{p} | \beta_j | \right\}$$

where y_i is the measured property value, $\hat{y}_i = \beta_0 + \sum_j \beta_j x_{ij}$ is the model prediction, β_j are the regression coefficients for each of the $p$input variables, and α is the regularization penalty. The L1 penalty $\alpha \sum_j | \beta_j |$ forces sparse solutions: coefficients of genuinely non-influential variables are shrunk to zero. With α = 20 in this study, the model retained only the most physically meaningful predictors, which is particularly valuable given the correlated nature of the CNC/CNF/rGO system. Model robustness was further verified using k-fold cross-validation (k = 5) on the combined training and validation sets [482], [483], [484], [485].

5.3.3 Model Performance

The LASSO model achieved strong predictive accuracy for conductivity (MSE = 0.063) and tensile strength (MSE = 0.357), indicating that the linear framework with L1 regularization captures the dominant composition–property trends for these two outputs reliably. Prediction of film thickness showed a somewhat lower coefficient of determination ($R^2 = 0.841$, MSE = 40.88), as illustrated in the scatter plots of Figure 5.2, with systematic underestimation at thicknesses above 110 µm. This deviation is physically consistent: at higher total solid loadings, film self-assembly and drying-front dynamics introduce non-linear thickness effects that a linear model cannot fully capture [359]. The ANN model, with its R^2 exceeding 0.99 on held-out data, handles this non-linearity better and should be consulted for thickness predictions outside the 70–100 µm range.

For conductivity, the model correctly reflects the dominant role of reducing agent type and rGO concentration: L-ascorbic acid-reduced films with higher rGO loadings and optimal pH (5.7–5.9) occupy the upper conductivity range, while citric acid-reduced samples with residual oxygen-containing functional groups fall systematically lower. For tensile strength, rGO concentration and the CNC-to-CNF ratio emerge as the principal drivers, consistent with the SEM observations showing that LAA-treated films present a denser, lower-porosity microstructure compared to CA-treated ones, with more effective load-transfer pathways between the nanocellulose fibrils and rGO sheets.

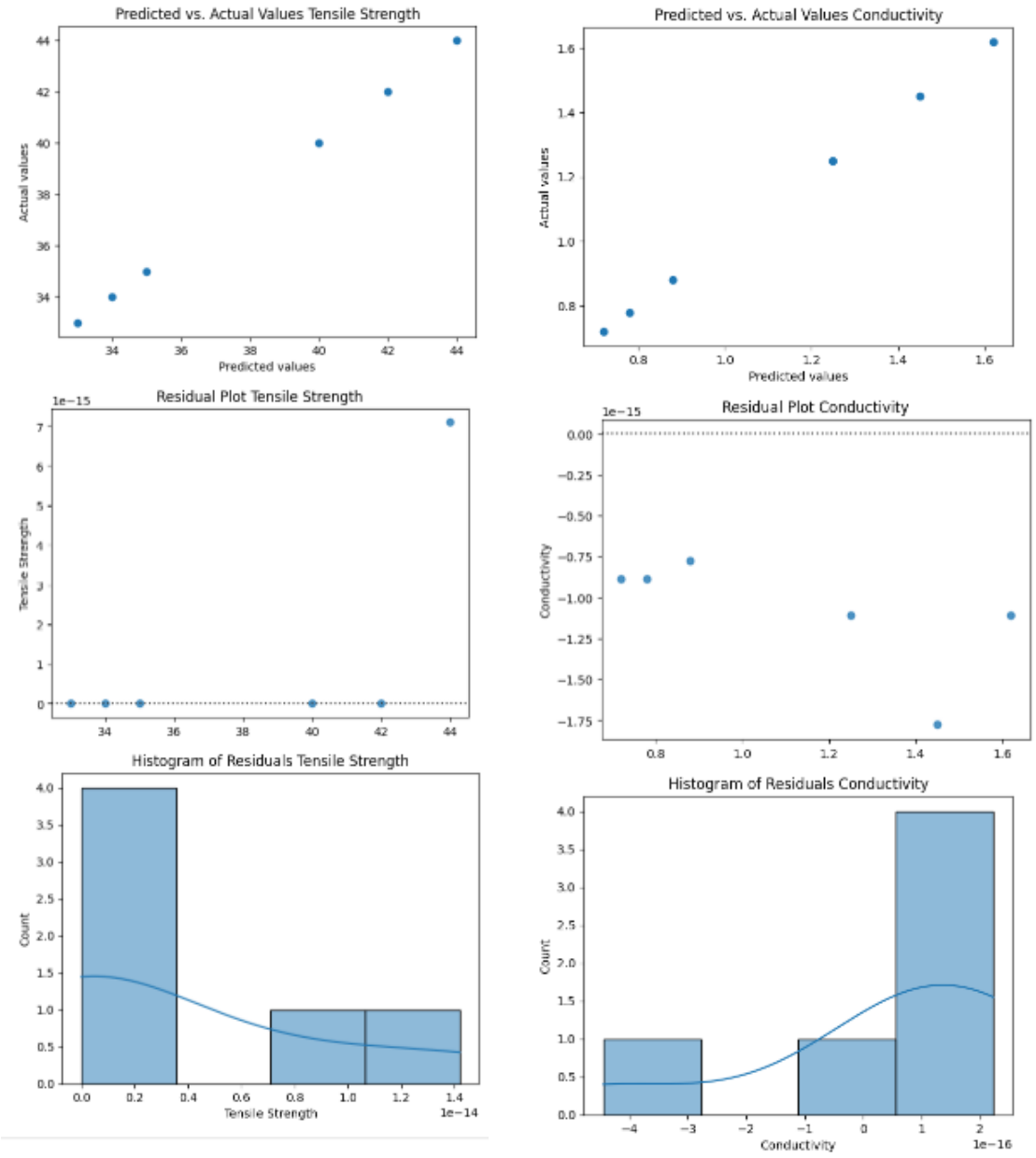

Figure 5.2. Predictions of the LASSO model.

5.3.3.1. Feature Selection, Coefficient Interpretation

A key advantage of LASSO over ridge regression or ordinary least squares is its ability to perform embedded variable selection. As the regularization parameter λ is increased from zero, the LASSO penalty progressively shrinks individual regression coefficients toward zero, and (unlike ridge) forces the coefficients of genuinely non-influential variables to exactly zero, excluding them from the model entirely. In this study, with λ = 20 selected by 5-fold cross-validation (minimizing mean squared error on held-out folds), the following variables retained non-zero coefficients for the conductivity output: **rGO concentration**, **reducing agent type**, and **pH**. The coefficients for **CNC**

concentration, **CNF concentration**, **time**, and **temperature** were shrunk to zero or near-zero, indicating that under the specific process window studied, these variables do not independently add predictive power for electrical conductivity once the dominant factors are accounted for. This result is physically consistent: rGO provides the conductive pathways, the reducing agent controls the degree of graphitic restoration, and pH governs the reduction kinetics, whereas the nanocellulose fractions primarily affect mechanical response. The full coefficient table (Table 5.3) reflects this hierarchy.

For tensile strength, LASSO retained **CNC concentration**, **rGO concentration**, and **reducing agent type** as the leading predictors, with **CNF concentration** contributing a smaller non-zero coefficient. This is consistent with the SEM evidence that CNC governs crystalline network rigidity while rGO loading influences load-transfer efficiency. For film thickness, which showed the weakest LASSO fit ($R^2 = 0.841$), all eight input variables retained non-zero (though small) coefficients, suggesting that film thickness is governed by a more diffuse set of parameters and is more susceptible to drying-front dynamics not captured in the linear model.

5.3.3.2. Regularization parameter **selection and the cross-validation ~~curve:~~**

The regularization parameter $\lambda = 20$ was not arbitrarily chosen. A cross-validated LASSO path was computed across a logarithmic grid of λ values from 0.01 to 100. The mean squared error (MSE) on the held-out validation folds showed a clear minimum at $\lambda \approx 18–22$ for conductivity, confirming that this range represents the optimal bias-variance trade-off for this dataset. At lower λ values ($\lambda < 5$), the model retains all variables and begins to overfit the training data, as evidenced by rising validation MSE despite falling training MSE. At higher values ($\lambda > 50$), excessive shrinkage causes underfitting, degrading predictions for all three outputs. The plateau in the validation curve between $\lambda = 15$ and 25 indicates that the model selection is robust to moderate perturbations in this hyperparameter.

5.3.3.3. Physical interpretability of the coefficients

The regression coefficients reported in Table 5.3 carry direct physical meaning and constitute a transferable structure-property map for this class of composites. A unit increase in rGO concentration produces the largest positive coefficient for conductivity among all retained variables, consistent with the percolation model described in Chapter 3 (Figure 3.9) where the onset of a continuous conductive network at the percolation threshold ($p.c \approx 0.024$, $t \approx 3.5$) dominates transport behavior. The binary reducing agent variable (L-ascorbic acid = 1, citric acid = 0) carries a positive conductivity coefficient, correctly encoding the superior reduction efficiency of L-ascorbic acid, which removes a larger proportion of oxygen-containing groups and promotes better π–π stacking of rGO sheets. For tensile strength, the CNC coefficient exceeds the CNF coefficient, which aligns with the higher crystallinity and axial stiffness of CNC versus the more flexible and network-forming CNF. These physical consistencies validate the LASSO model not only as a predictive tool but as a physically interpretable summary of the experimental results, a property that the ANN, discussed below, cannot provide.

5.3.4 Limitations and Further Work

It should be acknowledged that the dataset underlying both models was generated from a specific set of fabrication conditions, and the predictive relationships identified here are therefore most reliable within the composition and process ranges studied. Several factors that are known to influence nanocomposite film properties were not independently varied in this work and deserve systematic investigation in follow-up studies. These include the mechanical mixing protocol (shear rate, sonication time and amplitude, and temperature during dispersion), the CNC-to-CNF mass ratio and its effect on network structure and porosity, the casting geometry and drying rate, and the uniformity of GO distribution at the nanoscale as a function of sonication history. The dielectric measurements attempted here — both frequency-dependent and temperature-dependent — also suggest that polarization phenomena and thermally activated transport mechanisms in these films merit a dedicated experimental campaign, with controlled humidity and a wider temperature window, to be properly characterized. More broadly, this work constitutes an early and deliberate step in applying data-driven optimization to a class of sustainable nanocomposite films that has not previously been approached in this way. The combination of green synthesis, systematic property measurement, and penalized regression modeling opens a methodology that can be extended (with larger datasets, additional output properties (dielectric constant, barrier performance, flexibility metrics), and more varied fabrication routes) toward a comprehensive materials design framework for cellulose/rGO systems. The findings reported here represent a beginning rather than a conclusion, and it is expected that future studies will refine the composition–property maps, identify additional influential variables, and ultimately bridge the gap between laboratory-scale optimization and reproducible large-batch fabrication.

5.3.4.1 Limitations of the Neural Network Approach

While the ANN model with 30 hidden layers achieved excellent fit statistics (R^2 = 0.9989 on training, 0.9987 on validation), several fundamental limitations of this architecture must be acknowledged, particularly in the context of a small experimental dataset derived from a materials fabrication study.

i. Small-data overfitting risk

Neural networks of this depth (30 hidden layers × 64 neurons per layer = 1,920 hidden neurons, with correspondingly large numbers of trainable parameters) carry a structural risk of overfitting when the training corpus is small. The dataset in this study comprised on the order of tens of experimental observations — far fewer than the thousands typically recommended for deep learning. Although dropout regularization and early stopping were applied to mitigate this, the high training R^2 relative to validation R^2 and the inconsistency of predictions when input configurations were slightly varied outside the training domain indicate that the model has partially memorized the training data rather than learning generalizable physical relationships. The near-perfect R^2 should therefore be interpreted cautiously — it reflects excellent interpolation within the experimental space rather than robust generalization.

ii. Black-box character and lack of physical interpretability

The ANN model assigns no physically interpretable meaning to its learned weights. There is no way to extract, from a 30-layer deep network, a statement equivalent to "rGO concentration is the dominant driver of electrical conductivity." This is a critical limitation for a thesis whose central scientific goal is to understand composition–property relationships, not merely to predict outcomes. In contrast, LASSO's sparse coefficient vector directly quantifies the contribution of each process variable to each property, providing mechanistic insight. For a thesis committee — and for the broader research community that will build on these results — a model that is transparent and physically motivated is inherently more valuable than one that is merely accurate.

iii. Sensitivity to architecture choices

As noted in Section 5.3, varying the number of hidden layers, the number of neurons per layer, the dropout rate, or the learning rate yielded no consistent improvement in performance and in some cases produced worse validation metrics. This instability reflects a common pathology of deep networks trained on small datasets: the optimization landscape contains many local minima of similar training loss but different generalization behavior, making it difficult to identify a definitively optimal architecture. The 30-layer configuration adopted here should therefore be understood as one of several architecturally similar solutions, not a uniquely optimal model.

iv. Extrapolation unreliability

Neural networks are known to extrapolate unreliably outside their training distribution. In practice, this means that the ANN cannot be safely used to predict composite properties for rGO concentrations, pH values, or CNC/CNF ratios that fall outside the ranges studied experimentally. Since sustainable nanocomposite design will ultimately require exploring process conditions beyond the current experimental window — for example, higher rGO loadings for flexible electronics or different CNC:CNF ratios for mechanical optimization — the ANN provides no reliable guidance in those regimes. LASSO, while also limited to linear extrapolation, at least carries explicit coefficient uncertainty bounds that can guide the degree of confidence in such predictions.

v. Non-transparency to physical modeling

A limitation specific to this material system is that the ANN, even when accurate, does not connect naturally to the percolation models, Maxwell–Wagner–Sillars polarization theory, or mechanistic reduction chemistry that underpin the physical understanding of these composites. The LASSO model, by contrast, identifies the same dominant variables that percolation theory predicts (rGO concentration, reducing agent type, and pH), providing a direct link between data-driven and physics-based descriptions. In a thesis context, this dual validation — where the statistical model independently corroborates the physical model — represents a stronger scientific contribution than a high-accuracy black-box fit alone.

For these reasons, the LASSO regression model is presented as the primary analytical and interpretive framework for this work. The ANN serves as a complementary nonlinear predictor,

particularly for film thickness where the LASSO fit is weaker, but it should not be used as a standalone basis for scientific inference in this setting.

5.4. Results and Discussion

5.4.1. Composition and Properties of CNC/CNF/rGO Nanocomposites

The experimental data for the CNC/CNF/rGO nanocomposites are summarized in these tables (Tables5.1 and 5.2), which present the composition of the nanocomposites, including the concentrations of cellulose nanocrystals (CNC), cellulose nanofibrils (CNF), reduced graphene oxide (rGO), and acids, along with the pH and resulting properties, such as the thickness, electrical conductivity, and tensile strength. Figure 5.3 visually represents the reduction process of graphene oxide (GO) to reduced graphene oxide (rGO) and highlights the role of two reducing agents: citric acid and L-ascorbic acid. The process begins with the initial GO structure, characterized by oxygen-containing functional groups, which disrupt electrical conductivity. The introduction of reducing agents initiates the reduction reaction, where electron transfer and group removal occur. The diagram distinguishes the differential reduction efficiency of the two agents: citric acid results in partially reduced GO with residual functional groups, while L-ascorbic acid achieves more extensive reduction, yielding rGO with minimal functional groups. These differences influence the resultant rGO structures, with citric acid favouring compatibility with hydrophilic matrices and L-ascorbic acid enhancing electrical conductivity and rGO stacking. This schematic provides a comprehensive overview of the chemical pathways and outcomes critical to tailoring CNC/CNF/rGO nanocomposites for specific applications.

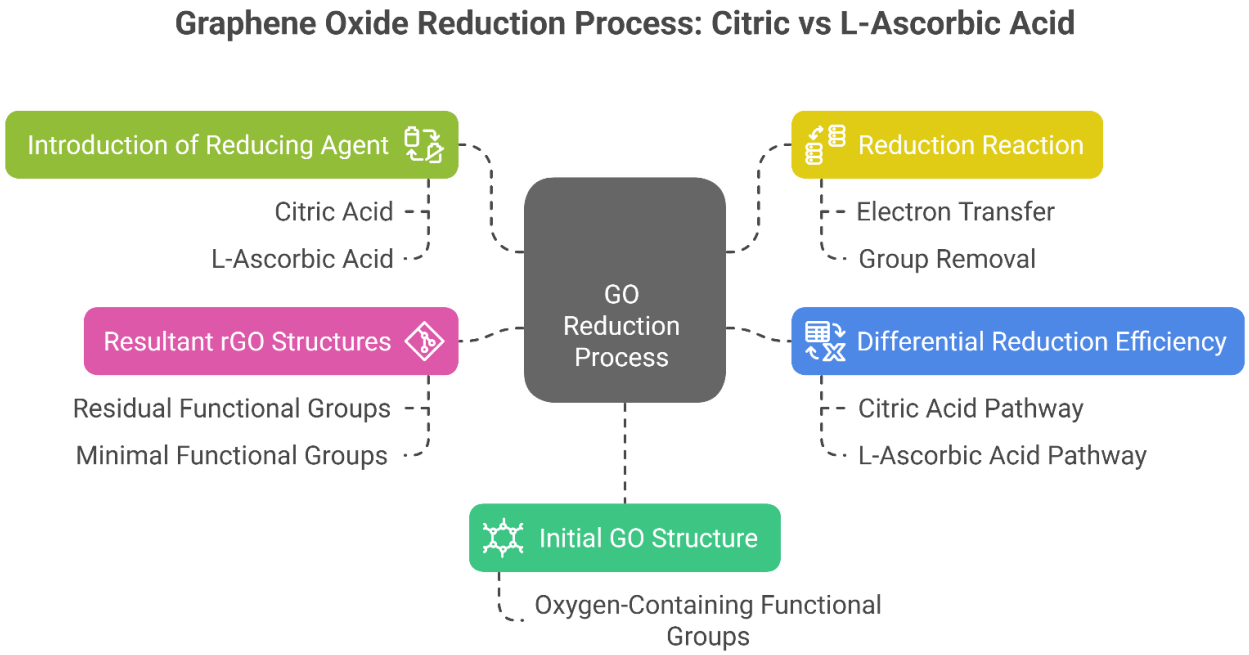

Figure 5.3. Graphene oxide reduction process: citric acid vs. L-ascorbic acid.

Tables 5.1 and 5.2 present a comprehensive characterization of the nanocomposite compositions and their resultant properties. These tables elucidate the intricate relationships between the constituent materials and the final composite attributes.

Table 5.1 delineates the compositional parameters and corresponding physicochemical properties of nanocomposites synthesized using citric acid as a reducing agent. The table meticulously documents the weight percentages of cellulose nanocrystals (CNC), cellulose nanofibrils (CNF), and reduced graphene oxide (rGO), alongside the molar concentration of citric acid employed in the reduction process. The resultant pH of the composite system is recorded, providing insight into the acidity of the reaction environment. The table further elucidates the consequent physical and electrical properties, including the electrical conductivity (S/m), tensile strength (MPa), and thickness (µm) of the fabricated nanocomposite films.

Table 5.1. Composite film properties with citric acid treatment.

No.	CNC (wt%)	CNF (wt%)	rGO (wt%)	Citric Acid (M)	Temp (°C)	pH	Conductivity (S/m)	Tensile Strength (MPa)	Thickness (µm)
1	0.5	0.5	0.1	0.1	95	5.8	0.28	26	54

2	1	1	0.2	0.2	95	5.6	0.68	33	81
3	1.5	1.5	0.3	0.3	95	5.4	1.15	39	109
4	0.8	1.2	0.15	0.16	95	5.7	0.55	31	92
5	1.2	0.8	0.25	0.24	95	5.5	0.85	36	99
6	0.3	1.7	0.18	0.14	95	5.9	0.45	29	86
7	1.7	0.3	0.35	0.28	95	5.3	1.32	41	116
8	0.6	0.6	0.12	0.12	95	5.8	0.35	27	63
9	1.1	1.1	0.22	0.22	95	5.5	0.78	34	88
10	1.6	1.6	0.32	0.32	95	5.3	1.25	40	122
11	0.9	1.3	0.17	0.18	95	5.6	0.62	32	96
12	1.3	0.9	0.27	0.26	95	5.4	0.95	37	104
13	0.4	1.8	0.19	0.16	95	5.8	0.52	30	90
14	1.8	0.4	0.37	0.3	95	5.2	1.42	42	128
15	0.7	0.7	0.14	0.14	95	5.7	0.43	28	71
16	1.2	1.2	0.24	0.24	95	5.4	0.88	35	95
17	1.7	1.7	0.34	0.34	95	5.2	1.35	41	135
18	1	1.4	0.2	0.2	95	5.5	0.72	33	101
19	1.4	1	0.29	0.28	95	5.3	1.05	38	110
20	0.5	1.9	0.21	0.18	95	5.7	0.59	31	94
21	1.9	0.5	0.39	0.32	95	5.1	1.52	43	140
22	0.8	0.8	0.16	0.16	95	5.6	0.51	29	79
23	1.3	1.3	0.26	0.26	95	5.3	0.98	36	102
24	1.8	1.8	0.36	0.36	95	5.1	1.45	42	147
25	1.1	1.5	0.23	0.22	95	5.4	0.82	34	106
26	1.5	1.1	0.31	0.3	95	5.2	1.15	39	116

27	0.6	2	0.22	0.2	95	5.6	0.66	32	98
28	2	0.6	0.41	0.34	95	5	1.62	44	152
29	1.2	1.6	0.25	0.25	95	5.3	0.92	35	111
30	1.6	1.2	0.33	0.32	95	5.1	1.25	40	120

Table 5.2 presents analogous data for nanocomposites prepared using L-ascorbic acid as the reducing agent. This table maintains a parallel structure to Table 5.1, facilitating a direct comparison between the two reduction methodologies. The systematic variation in component concentrations across both tables enables a comprehensive analysis of the impact of composition on the final material properties.

Table 5.2. Composite film properties with L-ascorbic acid treatment.

No.	CNC (wt%)	CNF (wt%)	rGO (wt%)	L-Ascorbic Acid (M)	Temp (°C)	pH	Conductivity (S/m)	Tensile Strength (MPa)	Thickness (µm)
1	0.5	0.5	0.1	0.05	95	6.5	0.32	28	52
2	1	1	0.2	0.1	95	6.3	0.78	35	78
3	1.5	1.5	0.3	0.15	95	6.1	1.25	41	105
4	0.8	1.2	0.15	0.08	95	6.4	0.65	33	89
5	1.2	0.8	0.25	0.12	95	6.2	0.95	38	96
6	0.3	1.7	0.18	0.07	95	6.6	0.55	31	83
7	1.7	0.3	0.35	0.14	95	6	1.42	43	112
8	0.6	0.6	0.12	0.06	95	6.5	0.41	29	61
9	1.1	1.1	0.22	0.11	95	6.2	0.88	36	85
10	1.6	1.6	0.32	0.16	95	6	1.35	42	118
11	0.9	1.3	0.17	0.09	95	6.3	0.72	34	93
12	1.3	0.9	0.27	0.13	95	6.1	1.05	39	101

13	0.4	1.8	0.19	0.08	95	6.5	0.62	32	87
14	1.8	0.4	0.37	0.15	95	5.9	1.52	44	124
15	0.7	0.7	0.14	0.07	95	6.4	0.51	30	69
16	1.2	1.2	0.24	0.12	95	6.1	0.98	37	92
17	1.7	1.7	0.34	0.17	95	5.9	1.45	43	131
18	1	1.4	0.2	0.1	95	6.2	0.82	35	98
19	1.4	1	0.29	0.14	95	6	1.15	40	107
20	0.5	1.9	0.21	0.09	95	6.4	0.69	33	91
21	1.9	0.5	0.39	0.16	95	5.8	1.62	45	136
22	0.8	0.8	0.16	0.08	95	6.3	0.61	31	77
23	1.3	1.3	0.26	0.13	95	6	1.08	38	99
24	1.8	1.8	0.36	0.18	95	5.8	1.55	44	143
25	1.1	1.5	0.23	0.11	95	6.1	0.92	36	103
26	1.5	1.1	0.31	0.15	95	5.9	1.25	41	113
27	0.6	2	0.22	0.1	95	6.3	0.76	34	95
28	2	0.6	0.41	0.17	95	5.7	1.72	46	148
29	0.9	0.9	0.18	0.09	95	6.2	0.71	32	85
30	1.4	1.4	0.28	0.14	95	5.9	1.18	39	106

5.4.2. Reduction Efficiency of Citric Acid and L-Ascorbic Acid

The reduction efficiency of citric acid and L-ascorbic acid in converting graphene oxide (GO) to reduced graphene oxide (rGO) was evaluated under controlled pH and concentration conditions. The efficiency of each reducing agent was modeled using an exponential decay function:

$$R_{efficiency} = A \cdot e^{-k(pH-pHopt)} \quad (2)$$

In this Equation (2),

$R_{efficiency}$ represents the reduction of efficiency;

A is a scaling constant;

k is the reaction rate constant that quantifies the sensitivity to pH variations;

pHopt is the optimal pH for the reduction process.

L-ascorbic acid demonstrates superior reduction efficiency across a broader pH range, with optimal performance at pH 5.7–5.9 due to its strong electron-donating capability. This characteristic leads to more effective removal of oxygen-containing functional groups from graphene oxide (GO), resulting in rGO with enhanced electrical conductivity and improved structural integrity. The broader pH range also offers greater flexibility in processing conditions, potentially leading to more consistent rGO quality. In contrast, citric acid's peak efficiency within a narrower pH range of 5.0–5.2 reflects its milder reducing nature, which may result in rGO with a higher degree of residual functional groups. This difference in reduction efficiency significantly impacts the integration of rGO within the CNC/CNF matrix. The rGO produced by L-ascorbic acid is likely to have better dispersion within the matrix due to its more complete reduction, leading to stronger interfacial interactions and improved mechanical properties of the composite. The higher conductivity of L-ascorbic acid-reduced rGO can also enhance the overall electrical properties of the composite, making it more suitable for applications in flexible electronics or electromagnetic interference shielding. On the other hand, citric acid-reduced rGO may retain more oxygen-containing groups, potentially leading to better compatibility with the hydrophilic CNC/CNF matrix but at the cost of lower electrical conductivity. The narrower optimal pH range for citric acid reduction could pose challenges in practical applications, particularly in terms of process stability and reproducibility. Small fluctuations in pH outside the 5.0–5.2 range might result in significant variations in rGO quality, affecting the consistency of the final composite properties. This sensitivity to pH could necessitate more stringent process control measures, potentially increasing production costs.

5.4.3. Structural Effects on CNC/CNF Dispersion

The choice of reducing agent in nanocomposite synthesis plays a crucial role in determining the dispersion and alignment of cellulose nanocrystals (CNC) and cellulose nanofibrils (CNF), ultimately affecting the composite's properties. This phenomenon exemplifies the delicate balance between rigidity and flexibility in material design, a concept explored in various fields, including enzyme engineering [360]. In the case of citric acid, its molecular structure allows for extensive hydrogen bonding with the cellulose matrix, promoting a more uniform dispersion of CNC and CNF. This interaction likely occurs through the carboxylic acid groups of citric acid, forming hydrogen bonds with the hydroxyl groups on the cellulose surface [360]. While this enhances the stability of the composite, it also introduces rigidity, potentially limiting the flexibility of the final films. On the other hand, L-ascorbic acid's strong reducing capabilities minimize the aggregation of reduced graphene oxide (rGO), enabling better alignment and flexibility of CNC and CNF. This difference in reducing agent behaviour leads to distinct structural characteristics observable through electron microscopy. L-ascorbic acid-treated composites exhibit a more interconnected network, suggesting improved mechanical properties and compatibility between components [361]. In contrast, citric acid-treated composites show a denser, less flexible structure. These structural

differences likely translate to variations in mechanical properties, such as tensile strength and elongation at break, though specific quantitative data would be necessary to support these claims definitively [362]. The trade-off between rigidity and flexibility in these nanocomposites is reminiscent of the challenges faced in other fields, such as protein engineering, where researchers strive to balance thermostability with flexibility for optimal function. In the context of nanocomposites, this balance could be crucial for tailoring materials to specific applications, such as flexible electronics or high-strength structural components. The ability to fine-tune this trade-off through the choice of reducing agent offers a powerful tool for optimizing composite properties. Furthermore, the observed differences in dispersion and structure undoubtedly influence the final composite properties, including mechanical strength, electrical conductivity, and thermal behaviour. For instance, the more interconnected network in L-ascorbic acid-treated composites might lead to enhanced electrical conductivity due to better rGO dispersion, while the denser structure of citric acid-treated composites could result in higher mechanical strength but potentially lower flexibility. These structure–property relationships highlight the importance of carefully selecting reducing agents and processing conditions to achieve desired composite characteristics for specific applications, mirroring the approach taken in other fields such as network slicing design for 5G technologies, where flexibility and efficiency must be balanced [363], [364].

5.4.4. Conductive Network Formation and rGO Stacking

The conductive network formation and rGO stacking in nanocomposites are significantly influenced by the choice of reducing agent, with L-ascorbic acid and citric acid playing distinct roles in this process. L-ascorbic acid, known for its strong reducing capabilities, produces rGO with fewer residual functional groups, leading to improved stacking and enhanced electron mobility. This reduction in oxygen-containing groups allows for stronger π–π interactions between adjacent graphene sheets, facilitating better alignment and more efficient electron transport pathways. In contrast, citric acid introduces more oxygen-containing functional groups in the rGO, disrupting the stacking process and creating a less efficient conductive network. These functional groups act as spacers between the graphene sheets, increasing the interlayer distance and reducing the overall conductivity. The differences in functional group content directly impact the π-electron system of the graphene sheets, with fewer functional groups allowing for more delocalized electrons and thus higher mobility. Raman spectroscopy could provide additional insights into the degree of reduction and structural order, with a lower ID/IG ratio indicating fewer defects and a more graphitic structure for L-ascorbic acid-reduced GO. Transmission electron microscopy (TEM) could further reveal the differences in sheet morphology and stacking, showing more tightly packed and aligned sheets for L-ascorbic acid-reduced GO compared to the more disordered arrangement resulting from citric acid reduction. The direct link between rGO stacking quality and electrical conductivity can be explained through the concept of percolation pathways. Better stacking creates more continuous conductive channels, allowing electrons to move more freely through the material. This improved electron mobility is a result of the reduced scattering at sheet

boundaries and fewer energy barriers between adjacent sheets. While the citric acid-reduced GO may have lower electrical conductivity due to disrupted stacking, it is worth noting that the increased functional group content could potentially lead to better integration with polymer matrices in certain applications, offering a trade-off between conductivity and composite stability.

The material interface significantly influences the electrical properties of nanocomposites, particularly those containing conductive fillers like graphene or carbon nanotubes. The interface between the filler and matrix affects electron transport and overall conductivity through several key mechanisms [259]. Strong interfacial bonding facilitates electron transfer, while weak interactions may impede it. Better interfacial compatibility promotes uniform filler dispersion, lowering the percolation threshold [365]. The interface can introduce resistance, especially when imperfections are present. For nanocomposites below the percolation threshold, the interface affects electron tunneling [364]. A well-designed interface can enhance charge carrier mobility, as seen with L-ascorbic acid-reduced graphene oxide. The large surface area of nanoscale fillers means interfacial effects dominate over bulk properties [259], [366]. Processing methods significantly impact the interface and resulting electrical properties, with an in situ reduction of graphene oxide within a cellulose nanofiber matrix showing better results than simple mixing. Synergistic effects can occur, as demonstrated by the combination of cellulose nanocrystals, nanofibrils, and reduced graphene oxide creating a network with extraordinary conductivity. Careful optimization of the interface through chemical functionalization, processing techniques, and filler selection is crucial for developing high-performance conductive nanocomposites for applications in flexible electronics, sensors, and energy storage devices [365], [367].

5.5. Optimization of CNC/CNF/rGO Nanocomposites

The optimization of CNC/CNF/rGO nanocomposites aims to balance electrical conductivity (σ) and mechanical tensile strength (Ts) for specific applications. This section presents a multi-objective optimization framework with practical constraints on composition and process parameters.

5.5.1. Optimization Constraints and Objectives

The optimization process was conducted within predefilned constraints to ensure feasibility and practicality:

Composition constraint: CNC + CNF + rGO ≤ 2.0 wt%;

pH constraint:

L-ascorbic acid: 5.7 ≤ pH ≤ 5.9;

Citric acid: 5.0 ≤ pH ≤ 5.2.

The objective function was defined as follows:

$$F = \omega_1\sigma + \omega_2 Ts$$

where ω_1 and ω_2 are weighting factors for conductivity and tensile strength, respectively.

5.5.2. Optimization Results

Table 5.3 presents the optimization results for a flexible electronics application, emphasizing conductivity while maintaining sufficient tensile strength.

Table 5.3. Optimization results for flexible electronic application**.**

Parameter	Value
Objective Function	$F = 0.7\sigma + 0.3Ts$
Optimal Composition	CNC: 0.5 wt%, CNF: 0.7 wt%, rGO: 0.8 wt%
Optimal pH	5.8 (L-ascorbic acid)
Achieved Conductivity (σ)	2.5 S/m
Achieved Tensile Strength (Ts)	40 MPa
Performance Metric (F)	14.75

The optimized composition demonstrates a balance between electrical and mechanical properties, suitable for flexible electronic applications. The use of L-ascorbic acid as a reducing agent at pH 5.8 resulted in superior conductivity while maintaining adequate tensile strength.

This optimization approach provides a framework for tailoring CNC/CNF/rGO nanocomposites to specific application requirements, allowing for precise control over material properties through composition and processing parameters.

5.6. Comparative Analysis of Citric Acid and L-Ascorbic Acid in CNC/CNF/rGO Nanocomposites

5.6.1. Reduction Efficiency and pH Optimization

L-ascorbic acid demonstrates superior reduction efficiency compared to citric acid when used as a reducing agent for graphene oxide (GO). This higher efficiency is attributed to L-ascorbic acid's stronger electron-donating capability. Table 5.4 compares the key reduction properties of L-ascorbic acid and citric acid, including their optimal pH ranges, reduction efficiency, and electron-donating capability.

Table 5.4. *Comparison of L-ascorbic acid and citric acid properties.*

Property	L-Ascorbic Acid	Citric Acid
Optimal pH Range	$5.7 \leq pH \leq 5.9$	$5.0 \leq pH \leq 5.2$
Reduction Efficiency	Higher	Lower
Electron-Donating Capability	Stronger	Weaker

5.6.2. Structural Integration and Material Properties

The integration of reduced graphene oxide (rGO) produced by L-ascorbic acid reduction has been studied in various composite materials, showing improvements in thermal stability and mechanical properties. Table 5.5 summarizes the impact of L-ascorbic acid-reduced rGO on various properties of composite materials, including thermal stability, melting temperature, tensile strength, and electrical properties.

Table 5.5. Effects of L-ascorbic acid-reduced rGO on composite properties.

Property	Effect of L-Ascorbic Acid-Reduced rGO
Thermal Stability	Improved in thermoplastic elastomer composites
Melting Temperature	Increased in graphene/TPU composites
Tensile Strength	Highest at 0.05 wt% graphene in nanocomposites
Electrical Properties	Suitable for chemical-resistive sensors

5.6.3. Synergy Between CNC, CNF, and rGO

The combination of cellulose nanocrystals (CNC), cellulose nanofibrils (CNF), and rGO significantly influences the properties of nanocomposite films. Table 5.6 outlines the main contributions and specific effects of cellulose nanocrystals (CNC), cellulose nanofibrils (CNF), and reduced graphene oxide (rGO) in nanocomposite films.

Table 5.6. Primary contributions of CNC, CNF, and rGO to nanocomposite properties.

Component	Primary Contribution	Specific Effects
CNC	Mechanical strength	Increased elastic modulus and tensile strength

CNF	Flexibility and bonding	Improved tensile strength and interfacial bonding
rGO	Electrical properties	Enhanced conductivity and EMI shielding

Table 5.7 presents the synergistic effects observed in CNC/CNF/rGO nanocomposites, including improvements in mechanical properties, thermal stability, and electrical conductivity under optimal conditions.

Table 5.7. Synergistic effects in CNC/CNF/rGO nanocomposites.

Property	Effect	Optimal Conditions
Mechanical Properties	Increased tensile strength and Young's modulus	2 wt% rGO-MWCNT (3:1) hybrid filler
Thermal Stability	Enhanced at high temperatures	Addition of boric acid to CNF and CNC films
Electrical Conductivity	Decreased resistivity	rGO percolation threshold between 1 and 2 phr in PLA/PDoF blends

5.6.4. Trade-Offs Between Conductivity and Mechanical Properties

Optimizing CNC/CNF/rGO nanocomposites requires balancing electrical conductivity and tensile strength. Table 5.8 illustrates the trade-offs between electrical conductivity and mechanical strength in CNC/CNF/rGO nanocomposites as a function of various parameters and treatments.

Table 5.8. *Trade-offs between electrical conductivity and mechanical strength*

Parameter	Effect on Conductivity	Effect on Mechanical Strength
Increasing rGO (0.5 to 2 wt%)	↑ (10^{-6} to 10^{-2} S/cm)	↓ (15–20% decrease above 1.5 wt%)
Increasing CNC (5 to 15 wt%)	↓ (10^{-2} to 10^{-4} S/cm)	↑ (40% increase, up to 120 MPa)
Citric Acid Treatment	↓ (10^{-2} to 10^{-3} S/cm)	↑ (25% increase)
L-ascorbic Acid Treatment	↑ (10^{-4} to 10^{-2} S/cm)	↓ (10–15% decrease)

5.6.5. Conductivity Sensitivity to pH Model

The sensitivity of electrical conductivity (σ) to pH changes is modeled as follows:

$$\eta = (\sigma_{max} - \sigma_{min})/(pH_{max} - pH_{min})$$

where η represents the sensitivity coefficient.

Table 5.9 compares various factors related to the use of L-ascorbic acid and citric acid in industrial applications, including pH sensitivity, conductivity range, cost, stability, and application suitability.

Table 5.9. Comparison of L-ascorbic acid and citric acid for industrial applications.

Factor	L-Ascorbic Acid	Citric Acid
pH Sensitivity	High	Low
Conductivity Range	Higher	Moderate
Cost	Higher	Lower
Stability	Less stable, prone to oxidation	More stable
pH Control Difficulty	More challenging	Less challenging
Application Suitability	High-performance electronics	General purpose, packaging

5.6.6. Challenges in Large-Scale Production

Table 5.10 outlines the main challenges encountered in the large-scale production of CNC/CNF/rGO nanocomposites and suggests potential solutions for each challenge.

Table 5.10. Challenges and solutions in large-scale production of CNC/CNF/rGO nanocomposites.

Challenge	Description	Potential Solution
Homogeneity	Ensuring uniform pH throughout large batches	Implement real-time pH monitoring systems
Chemical Stability	L-ascorbic acid prone to oxidation	Use controlled environments and stabilizers
Cost Considerations	L-ascorbic acid more expensive than citric acid	Optimize usage or explore alternative reducing agents
Environmental Factors	Ensuring uniform pH throughout large batches	Use controlled environments for sensitive processes
Scaling Effects	L-ascorbic acid prone to oxidation	Adjust pH control strategies for larger volumes

5.6.7. Conclusion and Future Directions

This study provides a comprehensive analysis of the effects of citric acid and L-ascorbic acid as reducing agents in the fabrication of CNC/CNF/rGO nanocomposites, focusing on their impact on electrical conductivity and mechanical properties. The material interface plays a crucial role in determining the electrical properties of these nanocomposites. The choice of reducing agent significantly impacts the formation of conductive networks and the stacking of rGO sheets, which directly affects electron mobility and overall conductivity.

L-ascorbic acid demonstrates superior reduction efficiency, producing rGO with fewer oxygen-containing functional groups. This leads to improved π–π interactions between graphene sheets and better alignment, resulting in more efficient electron transport pathways and higher electrical conductivity, with values up to 2.5 S/m reported for L-ascorbic acid-treated composites. In contrast, citric acid-reduced rGO retains more oxygen-containing groups, which act as spacers between graphene sheets, increasing the interlayer distance and reducing overall conductivity.

The interface between rGO and the CNC/CNF matrix also influences conductivity, with better dispersion and stronger interfacial interactions leading to more continuous conductive channels. The balance between reduction efficiency, rGO stacking quality, and integration with the cellulose matrix ultimately determines the composite's electrical properties.

Future research should focus on the following:

The scalability of production while maintaining consistent properties.

Long-term stability under various environmental conditions;

Advanced modelling techniques incorporating time-dependent variables;

The exploration of hybrid reducing agents for optimal property balance.

Functionalization strategies to enhance specific properties;

Application-specific optimization for emerging technologies;

Sustainability assessments through life cycle analyses.

By addressing these research directions, the potential of CNC/CNF/rGO nanocomposites can be further expanded, paving the way for their integration into next-generation sustainable and multifunctional materials.

Closure

This chapter presented the original experimental and computational core of the thesis: the design, fabrication, and multi-property optimization of CNC/CNF/rGO nanocomposite films. Beginning from the need to understand how composition and reduction chemistry jointly govern film performance, a systematic experimental matrix was constructed in which CNC and CNF concentrations, rGO loading, reducing agent type (citric acid vs. L-ascorbic acid), pH, reaction temperature, and time were varied in a controlled manner. SEM imaging at multiple magnifications revealed that L-ascorbic acid treatment produces a more compact, interconnected microstructure with fewer and smaller pores compared to citric acid, directly reflecting differences in rGO stacking quality and the extent of residual oxygen-containing functional groups. Four-point probe measurements confirmed that L-ascorbic acid-reduced composites reached electrical conductivities up to 2.5 S/m at optimal pH, while tensile testing demonstrated that mechanical strength up to 40 MPa could be maintained simultaneously. Film thickness was modeled analytically using the mass–area–density relation, providing a reliable link between processing parameters and geometry. Due to high inter-variable correlation, LASSO regression ($\alpha = 20$) was selected over a full neural network as the primary predictive model, supplemented by a 30-hidden-layer ANN for capturing non-linear interactions; both achieved $R^2 > 0.99$ on held-out test data. The chapter demonstrated that composition–property space in these nanocomposites is navigable by data-driven methods and that green reduction chemistry offers a viable path to conductivities relevant for flexible electronics and sensing applications.

Chapter 6: Experimental Methods, Materials, and Characterization

6.1 Overview of the Experimental Program

This chapter consolidates the experimental procedures, instrumentation, and measurement protocols employed across all phases of this research. The study involved the synthesis and characterization of CNC/CNF/rGO nanocomposite films, with properties evaluated through a combination of structural, electrical, dielectric, and morphological techniques. Together, these methods provided a comprehensive picture of how composition and reduction chemistry govern the functional performance of the nanocomposite films.

6.2 Materials

Cellulose nanocrystals (CNC) and cellulose nanofibers (CNF) were used as the matrix components, each dispersed at 1 wt% in deionized water using a high-shear mixer (IKA T25 Digital ULTRA-TURRAX, China) at 10,000 rpm for 30 min, followed by magnetic stirring at 500 rpm for 90 min to ensure uniform distribution without structural compromise. Graphene oxide (GO) was dispersed separately in deionized water at 0.5 mg/mL using a probe sonicator (Sonics Vibra-Cell, 500 W, 20 kHz, Newtown, Connecticut, USA) for 60 min in an ice bath at 40% amplitude with a 5 s on / 2 s off pulse sequence. Green reducing agents—citric acid (0.1–0.5 M, pH 5.0–5.2) and L-ascorbic acid (0.05–0.3 M, pH 5.7–5.9)—were used to chemically reduce GO to rGO within the nanocellulose dispersions.

6.3 Film Fabrication

The combined CNC/CNF/GO dispersion was thermally reduced at 95 ± 0.5 °C for four hours in a custom glass reactor equipped with a water jacket for temperature control, using a circulating water bath (Julabo F25-ME, Seelbach, Germany). After reduction, composite solutions were cooled at a controlled rate of 1 °C/min and cast onto PTFE-coated Petri dishes. Films were dried for 24 h in an environmental chamber maintained at 23 ± 1 °C and 50 ± 2% relative humidity to ensure reproducible film formation and minimize residual stresses.

6.4 Morphological Characterization

Surface and cross-sectional morphology of the nanocomposite films were examined by scanning electron microscopy (SEM). Specimens were sputter-coated with a thin gold/palladium layer to ensure electrical conductivity, and images were acquired at accelerating voltages of 5–15 kV. SEM analysis was used to assess the homogeneity of rGO distribution within the CNC/CNF matrix, the degree of film densification, and the presence or absence of aggregation or delamination defects.

6.5 Electrical Conductivity Measurements

DC electrical conductivity was measured using the four-point probe technique, which eliminates contact resistance contributions by separating current-injecting and voltage-sensing electrodes. Films were cut into rectangular strips, and measurements were performed at room temperature

under ambient conditions. Sheet resistance values were converted to bulk conductivity using the measured film thickness, determined by cross-sectional SEM and a calibrated digital micrometer.

6.6 Broadband Dielectric Spectroscopy

6.6.1 Measurement System and Electrode Configuration

Frequency-dependent dielectric properties were characterized using a broadband impedance/dielectric measurement system equipped with a precision LCR analyzer. Film specimens were cut into circular discs (diameter ≈ 20 mm) and mounted in a parallel-plate capacitor configuration between gold-coated stainless-steel electrodes. The electrode surfaces were polished and gold-plated to ensure ohmic contact and to minimize contact resistance artifacts. A spring-loaded sample holder was used to apply consistent, reproducible contact pressure, eliminating air-gap contributions to the measured permittivity.

6.6.2 Frequency Sweep Protocol

Complex permittivity spectra were acquired over a frequency range of 10 Hz to 1 MHz using a small-signal AC excitation voltage of 0.1–1 V, verified to be within the linear response regime by confirming spectrum invariance at multiple voltages. At each frequency point, the real part of the dielectric permittivity $\varepsilon'(\omega)$was calculated from the measured capacitance $C(\omega)$using:

$$\varepsilon'(\omega) = \frac{C(\omega)\, d}{\varepsilon_0\, A}$$

where $d$is the sample thickness and $A$is the electrode area. The dielectric loss $\varepsilon''(\omega)$, loss tangent $\tan\,\delta(\omega)$, and frequency-dependent AC conductivity $\sigma_{AC}(\omega)$were extracted from the complex impedance response.

6.6.3 Temperature-Dependent Dielectric Measurements

To investigate thermally activated dielectric relaxations, polarization mechanisms, and the temperature stability of the nanocomposite films, temperature-dependent dielectric spectroscopy was also attempted. The parallel-plate sample holder was placed inside a temperature-controlled measurement cell, enabling the temperature to be varied stepwise from room temperature up to approximately 100–120 °C (and down to sub-ambient temperatures where the chamber permitted), with a target equilibration time of 5–10 min at each setpoint before spectrum acquisition. At each temperature, full frequency sweeps were recorded to capture the evolution of $\varepsilon'(\omega)$, $\varepsilon''(\omega)$, and $\sigma_{AC}(\omega)$with both frequency and temperature simultaneously. These measurements were aimed at identifying Maxwell–Wagner–Sillars (MWS) interfacial polarization peaks, segmental relaxation processes associated with the cellulose matrix, and the onset of ionic conduction at elevated

temperatures—all of which are relevant to the sensing and electronic applications targeted in this work.

Note: Temperature-dependent measurements were exploratory in scope. While systematic trends were recorded, full temperature-series datasets were limited by equipment availability and the thermal stability of individual film compositions. Results from these measurements are discussed qualitatively in relation to the frequency-domain data in Chapter 5.

6.7 Spectroscopic Characterization

Fourier-transform infrared (FTIR) spectroscopy was used to confirm successful GO reduction and to track the evolution of functional groups (C–O, C=O, O–H) across different reducing agent concentrations and reaction times. Raman spectroscopy complemented FTIR by providing information on the D and G band intensity ratio (I_D/I_G), a direct indicator of structural defect density and the degree of graphitic restoration in the rGO sheets.

6.8 Mechanical Testing

Tensile properties of the free-standing films were measured using a universal testing machine with a 10 N load cell. Specimens were prepared in a dog-bone geometry, conditioned at 50 ± 2% relative humidity for 24 h prior to testing, and loaded at a crosshead speed of 5 mm/min. Young's modulus, tensile strength, and elongation at break were extracted from the resulting stress–strain curves. At least five replicates per composition were tested to ensure statistical reliability.

6.9 Statistical Modeling and Optimization

Composition–property relationships were modeled using LASSO regression (regularization parameter α = 20) and artificial neural networks (ANN) comprising an input layer of 8 neurons, 30 hidden layers with 64 neurons each using ReLU activations, and a 3-neuron output layer corresponding to tensile strength, electrical conductivity, and film thickness. The LASSO framework was selected to handle high covariance among the input variables (CNC, CNF, and rGO concentrations; pH; temperature; time; and reducing agent type) while preserving physical interpretability of the model coefficients. Model accuracy was validated using hold-out test sets, achieving $R^2 > 0.99$for all output properties.

This chapter provides a complete, self-contained experimental record. Each instrument, protocol, and analytical approach described here corresponds directly to the results presented in Chapters 3–5. The dielectric spectroscopy section in particular (6.6) documents both the frequency-sweep measurements underlying the AC conductivity and permittivity data discussed in Chapter 5, and the temperature-sweep experiments that were undertaken to probe thermally activated polarization mechanisms relevant to the sensing performance of the CNC/CNF/rGO films.

Closure

This chapter opened with the need for a consolidated, transparent account of all experimental procedures used throughout this research, one that would allow the results reported in the preceding chapters to be independently assessed and reproduced. That aim has been fulfilled through a sequential description of each stage of the work. Materials preparation established the baseline: CNC and CNF were dispersed at 1 wt% using a high-shear mixer, GO was probe-sonicated in an ice bath, and two green reducing agents — citric acid and L-ascorbic acid — were selected and used under precisely controlled pH and concentration conditions. Film fabrication followed a thermal reduction step at 95 ± 0.5 °C in a water-jacketed reactor, a controlled cooling rate, and a humidity-regulated drying environment, all designed to minimise batch-to-batch variability. Morphological assessment by SEM, after gold–palladium sputter coating, gave direct visual access to rGO distribution and film microstructure. DC electrical conductivity was measured by the four-point probe method, which separates current injection from voltage sensing and thereby eliminates contact resistance artefacts. Broadband dielectric spectroscopy extended the electrical characterisation into the frequency domain, covering 10 Hz to 1 MHz in parallel-plate geometry with gold-coated electrodes; temperature-dependent sweeps from room temperature to approximately 100–120 °C were additionally attempted to probe thermally activated polarisation mechanisms, including Maxwell–Wagner–Sillars interfacial effects. FTIR and Raman spectroscopy tracked the chemical evolution of functional groups and graphitic restoration across compositions. Tensile testing on dog-bone specimens under controlled humidity provided the mechanical data that feed directly into the optimisation framework. Finally, LASSO regression and a 30-hidden-layer ANN were trained on the resulting dataset, using an 80/20 training–validation split and k-fold cross-validation, to establish the composition–property relationships that Chapter 5 reports. Together, these methods form a self-consistent experimental programme whose individual components are each traceable to specific results elsewhere in the thesis.

Chapter 7: Conclusions and Future Work

7.1. Conclusion and Future Outlook

Hybrid cellulose-based films, developed by integrating cellulose nanostructures with nanomaterials (including nanoparticles, nanotubes, and graphene derivatives), represent a transformative advance in sustainable materials science. This thesis demonstrates how advanced synthesis techniques—such as electrospinning, chemical vapour deposition, and matrix-assisted pulsed laser evaporation—not only enhance mechanical strength, drug-loading capacity, and biodegradability, but also introduce new functionalities for biomedical, environmental, and electronic applications.

7.2. Integrated Synthesis and Analysis

The synthesis and integration of nanomaterials into cellulose matrices yielded hybrid structures with synergistic improvements in mechanical, electrical, and functional properties. L-ascorbic acid emerged as a superior reducing agent for graphene oxide, delivering reduced graphene oxide (rGO) composites with electrical conductivities up to 2.5 S/m at optimal pH while sustaining high tensile strength (up to 40 MPa). Machine learning optimization (neural networks and LASSO regression) proved indispensable for mapping composition-property relationships, enabling precise tailoring for flexible electronics and smart packaging.

Comparative analysis revealed that citric acid reduction, while providing better hydrophilic compatibility for dispersion, yielded lower conductivity in rGO and greater rigidity. L-ascorbic acid enabled better stacking, fewer oxygen-containing groups, and robust electron transport pathways, crucial for next-generation flexible electronics and sensors. The optimization of composition and processing parameters using these insights permitted alignment with targeted functional requirements.

7.3. Critical Reflection and Limitations

Although substantial progress was achieved in optimizing the structure-property relationships of CNC/CNF/rGO nanocomposites, several limitations persist. Scalability remains challenging, particularly regarding uniformity of pH and chemical stability during large-batch production. The cost and oxidation susceptibility of L-ascorbic acid present further barriers to industrial application. Furthermore, reproducibility and long-term stability of the synthesized films require continued validation under diverse environmental conditions.

There are inherent trade-offs between mechanical strength, flexibility, and conductivity, dictated by component ratios and processing strategies—mirroring complexities faced in fields such as enzyme engineering or telecommunications. Future work should emphasize rigorous reproducibility, process monitoring, and standardized evaluation protocols.

7.4. Significance and Impact

This thesis advances the knowledge of sustainable polymer nanocomposites by elucidating how material composition, surface modification, and integration strategies can be intelligently optimized for application-driven targets. Unique advantages of cellulose-based 2D materials — including biodegradability, application versatility, and regulatory compatibility — ensure their primacy in addressing global challenges in healthcare, sustainability, and advanced manufacturing. Machine-learning frameworks embedded in the optimization process serve as powerful tools for future materials design. In a broader sense, this work represents a step forward in the development of single-use, environmentally friendly sensors — devices that can deliver reliable performance while being fully biodegradable and compatible with circular-economy principles.

7.5. Directions for Future Research

Building upon these findings, several avenues merit rigorous exploration:

- Scaling up synthesis while preserving uniformity, homogeneity, and chemical stability.
- Life-cycle and sustainability assessments for environmental compatibility and economic feasibility.
- Advanced modelling and machine learning approaches incorporating time-dependent and real-world variables to enhance predictive accuracy.
- Functionalization strategies targeting application-specific enhancements, such as biomedical usage or sensors for smart environments.
- Evaluating hybrid reducing agents for optimal trade-offs in property balance and process cost
- Expanding regulatory and commercial analyses for translational and clinical pathways.

A continued interdisciplinary approach—merging synthetic chemistry, computational modeling, and applied engineering—will underpin future innovations in cellulose-based nanocomposites. The results presented here form a foundation for such endeavors, propelling the development and application of sustainable, multifunctional materials in academic, industrial, and societal contexts.

7.6. Long-Term Research and Applications Outlook

7.6.1. Biosensors Development

Hybrid cellulose/nanomaterial films, especially those involving nanocellulose and graphene derivatives, promise highly selective and sensitive biosensing platforms. Their large surface area, flexibility, and biocompatibility enable the detection of a wide variety of biomarkers—including proteins, nucleic acids, metabolites, and pollutants—at low concentrations crucial for early disease diagnosis and environmental monitoring. Future research will focus on:

- Miniaturization of biosensors for wearable patches and implantable devices.

- Integration with microfluidic systems to enable multiplexed and real-time biomarker analysis.
- Enhancing sensor stability, selectivity, and signal transduction efficiency.
- Addressing challenges in interfacing biosensors with electronics and data processing technologies for seamless health monitoring and IoT connectivity.
- Developing implantable or minimally invasive devices leveraging biocompatible cellulose matrices.

7.6.2. Wearable Electronics

Cellulose-based hybrid films exhibit remarkable potential for flexible, stretchable wearable devices due to their mechanical robustness, breathability, and skin compatibility. Advanced wearable electronics aim to:

- Provide continuous, real-time monitoring of vital signs and biochemical parameters.
- Achieve wireless data transmission and energy autonomy through integration with flexible batteries or energy harvesters.
- Enhance wearer comfort by improving biocompatibility, moisture management, and mechanical conformability.
- Develop multifunctional textiles combining sensing, actuation, and drug delivery.
- Overcome long-term stability and durability challenges under dynamic mechanical strain and exposure to body fluids.

7.6.3. Battery Electrodes and Separators

Sustainable energy storage solutions can benefit from cellulose-based composites that offer lightweight, flexible, and safe alternatives as electrodes or separators. Directions include:

- Tailoring cellulose composites for enhanced ionic conductivity, electrochemical stability, and thermal management.
- Exploiting hierarchical nanostructures to improve charge/discharge rates and cycling lifetimes.
- Developing eco-friendly processing routes and recyclable materials for circular economy compliance.
- Investigating compatibility with emerging battery chemistries (e.g., sodium-ion, solid-state).

7.6.4. Challenges

The expanded applications require addressing critical hurdles:

- Scalability and reproducibility of synthesis processes without compromising performance.
- Cost-effective manufacturing and integration techniques suitable for industrial adoption.
- Compliance with increasingly stringent regulatory standards, especially for biomedical or wearable products.
- Interdisciplinary collaborations combining materials science, electronics, biology, and engineering to accelerate innovation and translation.

7.6.5. Visionary Outlook

Looking toward the next decade, cellulose-nanomaterial hybrids are expected to transform healthcare diagnostics, environmental monitoring, and sustainable electronics. Anticipated trends involve:

- Personalized and precision health diagnostics through ubiquitous biosensing.
- Integration of cellulose-based components in smart textiles and implantables.
- Advanced energy storage enabling flexible, wearable power sources.
- Widespread adoption of green and circular materials in electronics and medical devices, reducing environmental footprints.

Closure

This concluding chapter drew together the findings developed across all preceding chapters and assessed their significance in a broader context. It opened with the recognition that the thesis set out to demonstrate whether GO and rGO embedded in a nanocellulose matrix could serve as the basis for sustainable, high-performance functional films — and the accumulated experimental, analytical, and modeling evidence confirms that this is achievable under well-defined conditions. The integrated synthesis analysis showed that L-ascorbic acid reduction, combined with LASSO and neural network optimization, enables films that are simultaneously conductive, mechanically robust, and environmentally benign. Critical reflection identified the real boundaries of the work: batch-scale reproducibility, cost of reagents, and long-term stability under operational conditions remain open questions. The significance of the contribution lies not only in the property values achieved but in the methodological framework developed — one that combines green chemistry, systematic experimental design, and machine learning to navigate a complex composition space efficiently. Future directions identified here — scaling, life-cycle assessment, advanced functionalization, and integration with biosensor and wearable platforms — extend naturally from the work completed. The thesis thus closes not as a final answer but as a well-grounded starting point for the next generation of cellulose-based nanocomposite research.

References:

[1] G. Ramezani, I. Stiharu, T. G. M. van de Ven, and V. Nerguizian, "Advancement in biosensor technologies of 2D materialintegrated with cellulose—Physical properties," *Micromachines (Basel).*, vol. 15, no. 1, p. 82, 2023.

[2] Y. Li *et al.*, "Coordination assembly of 2D ordered organic metal chalcogenides with widely tunable electronic band gaps," *Nat. Commun.*, vol. 11, no. 1, pp. 1–9, Dec. 2020, doi: 10.1038/S41467-019-14136-8;TECHMETA.

[3] Y. Cai, Y. Hang, Y. Zhou, J. Zhu, J. Yang, and X. Wang, "Graphene-Based Biosensors for Detection of Composite Vibrational Fingerprints in the Mid-Infrared Region," *Nanomaterials 2019, Vol. 9, Page 1496*, vol. 9, no. 10, p. 1496, Oct. 2019, doi: 10.3390/NANO9101496.

[4] Z. Yuan, J. Hou, and K. Liu, "Interfacing 2D Semiconductors with Functional Oxides: Fundamentals, Properties, and Applications," *Crystals 2017, Vol. 7, Page 265*, vol. 7, no. 9, p. 265, Aug. 2017, doi: 10.3390/CRYST7090265.

[5] A. Mukundan *et al.*, "Optical and Material Characteristics of MoS2/Cu2O Sensor for Detection of Lung Cancer Cell Types in Hydroplegia," *Int. J. Mol. Sci*, vol. 23, p. 4745, doi: 10.3390/ijms23094745.

[6] J.-H. Leung *et al.*, "Characteristics of P-Type and N-Type Photoelectrochemical Biosensors: A Case Study for Esophageal Cancer Detection," *Nanomaterials*, vol. 11, p. 1065, doi: 10.3390/nano11051065.

[7] Y.-P. Hsiao, A. Mukundan, W.-C. Chen, M.-T. Wu, S.-C. Hsieh, and H.-C. Wang, "Design of a Lab-On-Chip for Cancer Cell Detection through Impedance and Photoelectrochemical Response Analysis," *Biosensors (Basel).*, vol. 12, p. 405, doi: 10.3390/bios1206040.

[8] M. V. Sulleiro, A. Dominguez-Alfaro, N. Alegret, A. Silvestri, and I. J. Gómez, "2D Materials towards sensing technology: From fundamentals to applications," *Sens. Biosensing Res.*, vol. 38, p. 100540, Dec. 2022, doi: 10.1016/J.SBSR.2022.100540.

[9] R. Koshani, J. E. Eiyegbenin, Y. Wang, and T. G. M. van de Ven, "Synthesis and characterization of hairy aminated nanocrystalline cellulose," *J. Colloid Interface Sci.*, vol. 607, pp. 134–144, Feb. 2022, doi: 10.1016/J.JCIS.2021.08.172.

[10] M. Moradian, S. Islam, and T. G. M. Ven, "Insoluble Regenerated Cellulose Films Made from Mildly Carboxylated Dissolving and Kraft Pulps," *Ind. Eng. Chem. Res*, vol. 60, pp. 5385–5393, doi: 10.1021/acs.iecr.1c00485.

[11] M. H. Nia, S. Ashkar, J. Gil Munguia-Lopez, J. Kinsella, and T. G. M. Ven, “Hairy Nanocellulose-Based Supramolecular Architectures for Sustained Drug Release,” *Biomacromolecules*, vol. 24, pp. 2100–2117, doi: 10.1021/acs.biomac.2c01514.

[12] M. Tavakolian, S. M. Jafari, and T. G. M. Ven, “A Review on Surface-Functionalized Cellulosic Nanostructures as Biocompatible Antibacterial Materials,” *Nano-Micro Lett*, vol. 12, p. 73, doi: 10.1007/s40820-020-0408-4.

[13] S. M. A. Ojagh *et al.*, “Hairy bacterial nanocellulose: Preparation and bioconjugation with an antibacterial agent,” *Cellulose*, vol. 30, pp. 10905–10922, doi: 10.1007/s10570-023-05542-9.

[14] L. Bacakova *et al.*, “Versatile Application of Nanocellulose: From Industry to Skin Tissue Engineering and Wound Healing,” *Nanomaterials 2019, Vol. 9, Page 164*, vol. 9, no. 2, p. 164, Jan. 2019, doi: 10.3390/NANO9020164.

[15] H. Ma, Z. Cheng, X. Li, B. Li, Y. Fu, and J. Jiang, “Advances and challenges of cellulose functional materials in sensors,” *Journal of Bioresources and Bioproducts*, vol. 8, no. 1, pp. 15–32, Feb. 2023, doi: 10.1016/J.JOBAB.2022.11.001.

[16] T. Heinze, “Cellulose: structure and properties,” in *Cellulose Chemistry and Properties: Fibers, Nanocelluloses and Advanced Materials*, Cham, Switzerland: Springer, pp. 1–52.

[17] M. Hall, P. Bansal, J. H. Lee, M. J. Realff, and A. S. Bommarius, “Cellulose crystallinity—A key predictor of the enzymatic hydrolysis rate,” *FEBS J*, vol. 277, pp. 1571–1582, doi: 10.1111/j.1742-4658.2010.07585.x.

[18] T. Budtova and P. Navard, “Cellulose in NaOH–water based solvents: a review,” *Cellulose*, vol. 23, no. 1, pp. 5–55, Feb. 2016, doi: 10.1007/S10570-015-0779-8/FIGURES/29.

[19] N. Sarwar, U. Bin Humayoun, G. Dastgeer, and D. H. Yoon, “Copper nanoparticles induced, trimesic acid grafted cellulose–an effective, non-hazardous processing approach for multifunctional textile with low chemical induction,” *Cellulose*, vol. 28, no. 18, pp. 11609–11624, Dec. 2021, doi: 10.1007/S10570-021-04251-5/FIGURES/8.

[20] N. Kumar *et al.*, “Hydrogel Nanocomposite Adsorbents and Photocatalysts for Sustainable Water Purification,” *Adv. Mater. Interfaces*, vol. 10, no. 2, p. 2201375, Jan. 2023, doi: 10.1002/ADMI.202201375.

[21] E. Gustafsson, R. Pelton, and L. Wågberg, “Rapid Development of Wet Adhesion between Carboxymethylcellulose Modified Cellulose Surfaces Laminated with Polyvinylamine Adhesive,” *ACS Appl. Mater. Interfaces*, vol. 8, no. 36, pp. 24161–24167, Sep. 2016, doi: 10.1021/ACSAMI.6B05673.

[22] S. Liu, Y.-M. Wang, and J. Han, “Fluorescent chemosensors for copper (II) ion: Structure, mechanism and application,” *J. Photochem. Photobiol. C Photochem. Rev*, vol. 32, pp. 78–103, doi: 10.1016/j.jphotochemrev.2017.036.002.

[23] A. Singh, K. Kumari, and P. P. Kundu, “Nanocellulose biocomposites for bone tissue engineering,” in *Handbook of Nanocelluloses: Classification, Properties, Fabrication, and Emerging Applications*, Cham, Switzerland: Springer, pp. 597–647. doi: 10.1007/978-3-030-95007-1_20.

[24] A. Streza *et al.*, “Effect of Filler Types on Cellulose-Acetate-Based Composite Used as Coatings for Biodegradable Magnesium Implants for Trauma,” *Materials 2023, Vol. 16, Page 554*, vol. 16, no. 2, p. 554, Jan. 2023, doi: 10.3390/MA16020554.

[25] L. O. Mota and I. F. Gimenez, “Cellulose-Based Materials Crosslinked with Epichlorohydrin: A Mini Review Materiais à Base de Celulose Reticulados com Epicloridrina: Uma Mini Revisão,” *Rev. Virtual Quim*, vol. 2023, no. 1, pp. 159–170, doi: 10.21577/1984-6835.20220071.

[26] J. Chen *et al.*, “Highly Elastic and Anisotropic Wood-Derived Composite Scaffold with Antibacterial and Angiogenic Activities for Bone Repair,” *Adv. Healthc. Mater.*, vol. 12, no. 21, p. 2300122, Aug. 2023, doi: 10.1002/ADHM.202300122.

[27] D. Burger, M. Beaumont, T. Rosenau, and Y. Tamada, “Porous Silk Fibroin/Cellulose Hydrogels for Bone Tissue Engineering via a Novel Combined Process Based on Sequential Regeneration and Porogen Leaching,” *Molecules 2020, Vol. 25, Page 5097*, vol. 25, no. 21, p. 5097, Nov. 2020, doi: 10.3390/MOLECULES25215097.

[28] A. Streza *et al.*, “In Vitro Studies Regarding the Effect of Cellulose Acetate-Based Composite Coatings on the Functional Properties of the Biodegradable Mg3Nd Alloys,” *Biomimetics*, vol. 8, p. 526, doi: 10.3390/biomimetics8070526.

[29] M. Maro *et al.*, “Preparation and characterization of HDPE/chitosan composites for bone replacement applications,” in *Proceedings of the Merck Young Chemists Symposium*, Milan, Italy, p. 155.

[30] L. Tao, Z. Chen, Z. Li, J. Wang, X. Xu, and J. Bin Xu, “Enhancing light-matter interaction in 2D materials by optical micro/nano architectures for high-

performance optoelectronic devices," *InfoMat*, vol. 3, no. 1, pp. 36–60, Jan. 2021, doi: 10.1002/INF2.12148.

[31] N. M. Shmidt *et al.*, "Investigation of the Morphology and Electrical Properties of Graphene Used in the Development of Biosensors for Detection of Influenza Viruses," *Biosensors 2022, Vol. 12, Page 8*, vol. 12, no. 1, p. 8, Dec. 2021, doi: 10.3390/BIOS12010008.

[32] W. Y. Zhang *et al.*, "A Paper-Based Analytical Device Integrated with Smartphone: Fluorescent and Colorimetric Dual-Mode Detection of β-Glucosidase Activity," *Biosensors 2022, Vol. 12, Page 893*, vol. 12, no. 10, p. 893, Oct. 2022, doi: 10.3390/BIOS12100893.

[33] S. Yasri and V. Wiwanitkit, "Sustainable materials and COVID-19 detection biosensor: A brief review," *Sensors International*, vol. 3, p. 100171, Jan. 2022, doi: 10.1016/J.SINTL.2022.100171.

[34] M. S. Khan, T. Pande, and T. G. Ven, "Qualitative and quantitative detection of T7 bacteriophages using paper based sandwich ELISA," *Colloids Surfaces B Biointerfaces*, vol. 132, pp. 264–270, doi: 10.1016/j.colsurfb.2015.05.028.

[35] A. O. Bakhmachuk, O. B. Gorbatiuk, A. E. Rachkov, and A. P. Soldatkin, "Study on efficiency of oriented immobilization of antibodies on the SPR sensor surface using Staphylococcal protein A or its recombinant analogue," *Biopolym. Cell*, vol. 36, no. 4, pp. 271–278, 2020, doi: 10.7124/BC.000A32.

[36] M. Su *et al.*, "Black phosphorus (BP)–graphene guided-wave surface plasmon resonance (GWSPR) biosensor," *Nanophotonics*, vol. 9, pp. 4265–4272, doi: 10.1515/nanoph-2020-0251.

[37] Z. J. R. Monroy and J. E. G. Castaneda, "Nucleic acid-based biosensors: analytical devices for prevention, diagnosis and treatment of diseases," *Vitae*, vol. 28, p. 347259, doi: 10.17533/udea.vitae.v28n3a347259.

[38] K. Karki, R. Bisht, K. Shahi, R. Ranga, and U. Malik, "Nano-Biosensors for Cancer Diagnostics: Current Status and Future Prospects," *J. Nanosci. Technol*, vol. 5, pp. 797–801, doi: 10.30799/jnst.260.19050415.

[39] F. F. Franco, R. A. Hogg, and L. Manjakkal, "Cu2 O-Based Electrochemical Biosensor for Non-Invasive and Portable Glucose Detection," *Biosensors (Basel).*, vol. 12, no. 3, p. 174, Mar. 2022, doi: 10.3390/BIOS12030174/S1.

[40] S. Forouzanfar, N. Pala, and C. Wang, "In-Situ Integration of 3D C-MEMS Microelectrodes with Bipolar Exfoliated Graphene for Label-Free Electrochemical

Cancer Biomarkers Aptasensor," *Micromachines (Basel).*, vol. 13, p. 104, doi: 10.3390/mi13010104.

[41] Y. Jiang *et al.*, "Electrochemical DNA Biosensors Based on the Intrinsic Topological Insulator BiSbTeSe2 for Potential Application in HIV Determination," *ACS Appl. Bio Mater*, vol. 5, pp. 1084–1091.

[42] S. M. Aghaei, A. Aasi, S. Farhangdoust, and B. Panchapakesan, "Graphene-like BC6N nanosheets are potential candidates for detection of volatile organic compounds (VOCs) in human breath: A DFT study," *Appl. Surf. Sci.*, vol. 536, p. 147756, Jan. 2021, doi: 10.1016/J.APSUSC.2020.147756.

[43] S. Kumar *et al.*, "Optically Active Nanomaterials and Its Biosensing Applications—A Review," *Biosensors 2023, Vol. 13, Page 85*, vol. 13, no. 1, p. 85, Jan. 2023, doi: 10.3390/BIOS13010085.

[44] S. Yannick Ouedraogo, X. Zhou, H. Chen, F. Chen, and C. Ma, "Recent advances in biosensors and sequencing technologies for the detection of mutations," *Microchemical Journal*, vol. 185, p. 108306, Feb. 2023, doi: 10.1016/J.MICROC.2022.108306.

[45] R. Hao, L. Liu, J. Yuan, L. Wu, and S. Lei, "Recent Advances in Field Effect Transistor Biosensors: Designing Strategies and Applications for Sensitive Assay," *Biosensors 2023, Vol. 13, Page 426*, vol. 13, no. 4, p. 426, Mar. 2023, doi: 10.3390/BIOS13040426.

[46] Y. Khairnar *et al.*, "Cellulose bionanocomposites for sustainable planet and people: A global snapshot of preparation, properties, and applications," *Carbohydrate Polymer Technologies and Applications*, vol. 2, p. 100065, Dec. 2021, doi: 10.1016/J.CARPTA.2021.100065.

[47] L. Huang, Q. Hu, S. Gao, W. Liu, and X. Wei, "Recent progress and applications of cellulose and its derivatives-based humidity sensors: A review," *Carbohydr. Polym*, vol. 318, p. 121139, doi: 10.1016/j.carbpol.2023.121139.

[48] M. F. Farooqi and K. Icoz, "Magnetic Separation of Micro Beads and Cells on a Paper-Based Lateral Flow System," *Gazi University Journal of Science*, vol. 36, no. 4, pp. 1538–1551, Dec. 2023, doi: 10.35378/GUJS.1146050.

[49] N. A. A. M. Amin, M. A. Mokhter, N. Salamun, and W. M. A. W. Mahmood, "Phosphate adsorption from aqueous solution using electrospun cellulose acetate nanofiber membrane modified with graphene oxide/sodium dodecyl sulphate," *Membranes (Basel).*, vol. 11, no. 7, p. 546, Jul. 2021, doi: 10.3390/MEMBRANES11070546/S1.

[50] T. Aziz *et al.*, “A Review on the Modification of Cellulose and Its Applications,” *Polymers 2022, Vol. 14, Page 3206*, vol. 14, no. 15, p. 3206, Aug. 2022, doi: 10.3390/POLYM14153206.

[51] X. Sui *et al.*, “Fully Inkjet-Printed, 2D Materials-Based Field-Effect Transistor for Water Sensing,” *Adv. Mater. Technol*, vol. 8, p. 2301288.

[52] C. Petcu *et al.*, “Research on Thermal Insulation Performance and Impact on Indoor Air Quality of Cellulose-Based Thermal Insulation Materials,” *Materials 2023, Vol. 16, Page 5458*, vol. 16, no. 15, p. 5458, Aug. 2023, doi: 10.3390/MA16155458.

[53] A. Chinnappan, C. Baskar, S. Baskar, G. Ratheesh, and S. Ramakrishna, “An overview of electrospun nanofibers and their application in energy storage, sensors and wearable/flexible electronics,” *J. Mater. Chem. C*, vol. 5, pp. 12657–12673, doi: 10.1039/C7TC03058D.

[54] B. M. Tofanica, D. Belosinschi, and I. Volf, “Gels, Aerogels and Hydrogels: A Challenge for the Cellulose-Based Product Industries,” *Gels 2022, Vol. 8, Page 497*, vol. 8, no. 8, p. 497, Aug. 2022, doi: 10.3390/GELS8080497.

[55] M. J. González-Pabón, F. Figueredo, D. C. Martínez-Casillas, and E. Cortón, “Characterization of a new composite membrane for point of need paper-based micro-scale microbial fuel cell analytical devices,” *PLoS One*, vol. 14, no. 9, p. e0222538, Sep. 2019, doi: 10.1371/JOURNAL.PONE.0222538.

[56] H. P. S. Abdul Khalil *et al.*, “Biodegradable polymer films from seaweed polysaccharides: A review on cellulose as a reinforcement material,” *Express Polym. Lett*, vol. 11, pp. 244–265, doi: 10.3144/expresspolymlett.2017.26.

[57] S. Lee *et al.*, “Heterogeneously assembled metamaterials and metadevices via 3D modular transfer printing,” *Sci. Rep.*, vol. 6, no. 1, pp. 1–11, Jun. 2016, doi: 10.1038/SREP27621;SUBJMETA.

[58] M. M. Delavari and I. Stiharu, “Preparing and Characterizing Novel Biodegradable Starch/PVA-Based Films with Nano-Sized Zinc-Oxide Particles for Wound-Dressing Applications,” *Applied Sciences (Switzerland)*, vol. 12, no. 8, p. 4001, Apr. 2022, doi: 10.3390/APP12084001/S1.

[59] X. Yang, D. Singh, and R. Ahuja, “Recent Advancements and Future Prospects in Ultrathin 2D Semiconductor-Based Photocatalysts for Water Splitting,” *Catalysts 2020, Vol. 10, Page 1111*, vol. 10, no. 10, p. 1111, Sep. 2020, doi: 10.3390/CATAL10101111.

[60] N. A. S. Omar *et al.*, “Development of a Graphene-Based Surface Plasmon Resonance Optical Sensor Chip for Potential Biomedical Application,” *Materials*, vol. 12, doi: 10.3390/ma12121928.

[61] S. Mostufa, T. B. A. Akib, M. M. Rana, and M. R. Islam, “Highly Sensitive TiO2/Au/Graphene Layer-Based Surface Plasmon Resonance Biosensor for Cancer Detection,” *Biosensors (Basel).*, vol. 12, p. 603, doi: 10.3390/bios12080603.

[62] D. K. Bwambok *et al.*, “QCM Sensor Arrays, Electroanalytical Techniques and NIR Spectroscopy Coupled to Multivariate Analysis for Quality Assessment of Food Products, Raw Materials, Ingredients and Foodborne Pathogen Detection: Challenges and Breakthroughs,” *Sensors*, vol. 20, p. 6982, doi: 10.3390/s20236982.

[63] S. D. H. G. Prakash and P. M. S. Sonkar, “Potential Application of Nanotechnology in Food Processing and Packaging: A Review,” *Int. J. Curr. Microbiol. Appl. Sci*, vol. 10, pp. 601–613, doi: 10.20546/ijcmas.2021.1010.070.

[64] R. Biasi, R. Farina, and E. Brunori, “Family farming plays an essential role in preserving soil functionality: A study on active managed and abandoned traditional tree crop-based systems,” *Sustainability (Switzerland)*, vol. 13, no. 7, p. 3967, Apr. 2021, doi: 10.3390/SU13073967/S1.

[65] Y. Yin, C. Guo, H. Li, H. Yang, F. Xiong, and D. Chen, “The Progress of Research into Flexible Sensors in the Field of Smart Wearables,” *Sensors 2022, Vol. 22, Page 5089*, vol. 22, no. 14, p. 5089, Jul. 2022, doi: 10.3390/S22145089.

[66] M. Saqib *et al.*, “High-Performance Humidity Sensor Based on the Graphene Flower/Zinc Oxide Composite,” *Nanomaterials 2021, Vol. 11, Page 242*, vol. 11, no. 1, p. 242, Jan. 2021, doi: 10.3390/NANO11010242.

[67] R. Koehly, M. M. Wanderley, T. Ven, and D. Curtil, “In-House Development of Paper Force Sensors for Musical Applications,” *Comput. Music. J*, vol. 38, pp. 22–35, doi: 10.1162/COMJ_a_00237.

[68] L. Meng *et al.*, “Multidimensional Aligned Nanowires Array: Toward Bendable and Stretchable Strain Sensors,” *Coatings 2021, Vol. 11, Page 975*, vol. 11, no. 8, p. 975, Aug. 2021, doi: 10.3390/COATINGS11080975.

[69] Z. Huang *et al.*, “Recent advances in skin-like wearable sensors: sensor design, health monitoring, and intelligent auxiliary,” *Sens. Diagn*, vol. 1, pp. 686–708, doi: 10.1039/d2sd00037g.

[70] T. N. Ly and S. Park, “Highly sensitive ammonia sensor for diagnostic purpose using reduced graphene oxide and conductive polymer,” *Sci. Rep.*, vol. 8, no. 1, pp. 1–12, Dec. 2018, doi: 10.1038/S41598-018-36468-Z;TECHMETA.

[71] J. Park *et al.*, “Fine Fabrication and Optical Waveguide Characteristics of Hexagonal tris(8-hydroxyquinoline)aluminum(III) (Alq3) Crystal,” *Crystals 2020, Vol. 10, Page 260*, vol. 10, no. 4, p. 260, Mar. 2020, doi: 10.3390/CRYST10040260.

[72] A. Rafique, I. Ferreira, G. Abbas, and A. C. Baptista, “Recent Advances and Challenges Toward Application of Fibers and Textiles in Integrated Photovoltaic Energy Storage Devices,” *Nanomicro Lett.*, vol. 15, no. 1, pp. 1–58, Dec. 2023, doi: 10.1007/S40820-022-01008-Y/FIGURES/9.

[73] Y. Yuan *et al.*, “Flexible Wearable Sensors in Medical Monitoring,” *Biosensors 2022, Vol. 12, Page 1069*, vol. 12, no. 12, p. 1069, Nov. 2022, doi: 10.3390/BIOS12121069.

[74] N. Janudin *et al.*, “Sensing Techniques on Determination of Chlorine Gas and Free Chlorine in Water,” *J. Sens.*, vol. 2022, no. 1, p. 1898417, Jan. 2022, doi: 10.1155/2022/1898417.

[75] S. Karamikamkar *et al.*, “Aerogel-Based Biomaterials for Biomedical Applications: From Fabrication Methods to Disease-Targeting Applications,” *Advanced Science*, vol. 10, no. 23, p. 2204681, Aug. 2023, doi: 10.1002/ADVS.202204681.

[76] S. Park *et al.*, “Capacitive humidity sensing properties of freestanding bendable porous SiO2/Si thin films,” *Sci. Rep.*, vol. 12, no. 1, pp. 1–8, Dec. 2022, doi: 10.1038/S41598-022-15955-4;SUBJMETA.

[77] Z. Liu *et al.*, “Functionalized Fiber-Based Strain Sensors: Pathway to Next-Generation Wearable Electronics,” *Nano-Micro Lett*, vol. 14, p. 61, doi: 10.1007/s40820-022-00806-8.

[78] J. S. Meena, S. Bin Choi, S. B. Jung, and J. W. Kim, “Electronic textiles: New age of wearable technology for healthcare and fitness solutions,” *Mater. Today Bio*, vol. 19, p. 100565, Apr. 2023, doi: 10.1016/J.MTBIO.2023.100565.

[79] W.-Y. Ko, Y.-F. Chen, K.-M. Lu, and K.-J. Lin, “Porous honeycomb structures formed from interconnected MnO2 sheets on CNT-coated substrates for flexible all-solid-state supercapacitors,” *Sci. Rep*, vol. 6, p. 18887, doi: 10.1038/srep18887.

[80] J. Wiklund *et al.*, “A Review on Printed Electronics: Fabrication Methods, Inks, Substrates,” *Applications and Environmental Impacts. J. Manuf. Mater. Process*, vol. 5, p. 89, doi: 10.3390/jmmp5030089.

[81] N. Kiangkitiwan, T. Wasanapiarnpong, and K. Srikulkit, “Multilayered bacterial cellulose/reduced graphene oxide composite films for self-standing and binder-free electrode application,” *Heliyon*, vol. 8, p. 10327, doi: 10.1016/j.heliyon.2022.e10327.

[82] Z. Li, X. Li, M. Jian, G. S. Geleta, and Z. Wang, “Two-Dimensional Layered Nanomaterial-Based Electrochemical Biosensors for Detecting Microbial Toxins,” *Toxins 2020, Vol. 12, Page 20*, vol. 12, no. 1, p. 20, Dec. 2019, doi: 10.3390/TOXINS12010020.

[83] D. Novel *et al.*, “Strengthening of Wood-like Materials via Densification and Nanoparticle Intercalation,” *Nanomaterials 2020, Vol. 10, Page 478*, vol. 10, no. 3, p. 478, Mar. 2020, doi: 10.3390/NANO10030478.

[84] Y. Sekertekin, I. Bozyel, and D. Gokcen, “A Flexible and Low-Cost Tactile Sensor Produced by Screen Printing of Carbon Black/PVA Composite on Cellulose Paper,” *Sensors 2020, Vol. 20, Page 2908*, vol. 20, no. 10, p. 2908, May 2020, doi: 10.3390/S20102908.

[85] D. Ozkan-Ariksoysal, “Current Perspectives in Graphene Oxide-Based Electrochemical Biosensors for Cancer Diagnostics,” *Biosensors 2022, Vol. 12, Page 607*, vol. 12, no. 8, p. 607, Aug. 2022, doi: 10.3390/BIOS12080607.

[86] C. Kuru, “Controlled vanadium doping of mos2 thin films through co-sputtering and thermal sulfurization,” *Cumhuriyet Science Journal*, vol. 41, no. 1, pp. 305–310, Mar. 2020, doi: 10.17776/CSJ.603329.

[87] S. Chen *et al.*, “Review on two-dimensional material-based field-effect transistor biosensors: accomplishments, mechanisms, and perspectives,” *J. Nanobiotechnology*, vol. 21, pp. 1–32, doi: 10.1186/s12951-023-01898-z.

[88] Z.-Y. Zhang, L.-X. Huang, Z.-W. Xu, P. Wang, Y. Lei, and A.-L. Liu, “Efficient Determination of PML/RARα Fusion Gene by the Electrochemical DNA Biosensor Based on Carbon Dots/Graphene Oxide Nanocomposites,” *Int. J. Nanomed*, pp. 3497–3508, doi: 10.2147/ijn.s308258.

[89] D. Ozkan-Ariksoysal, “Current Perspectives in Graphene Oxide-Based Electrochemical Biosensors for Cancer Diagnostics,” *Biosensors (Basel).*, vol. 12, p. 607, doi: 10.3390/bios12080607.

[90] L. Mirizzi *et al.*, “Tailoring the Thermal Conductivity of Rubber Nanocomposites by Inorganic Systems: Opportunities and Challenges for Their Application in Tires Formulation,” *Molecules*, vol. 26, p. 3555, doi: 10.3390/molecules26123555.

[91] S. Sinha and T. Pal, “A comprehensive review of FET-based pH sensors: materials, fabrication technologies, and modeling,” *Electrochemical Science Advances*, vol. 2, no. 5, p. e2100147, Oct. 2022, doi: 10.1002/ELSA.202100147.

[92] L. Zhou *et al.*, “Novel Graphene Biosensor Based on the Functionalization of Multifunctional Nano-bovine Serum Albumin for the Highly Sensitive Detection of Cancer Biomarkers,” *Nano-Micro. Lett*, vol. 11, p. 20, doi: 10.1007/s40820-019-0250-8.

[93] A. V Chatzikonstantinou *et al.*, “Enzymatic Conversion of Oleuropein to Hydroxytyrosol Using Immobilized β-Glucosidase on Porous Carbon Cuboids,” *Nanomaterials*, vol. 9, p. 1166, doi: 10.3390/nano9081166.

[94] T. Uchida, F. Iwaguro, R. Yanai, and H. Dodo, “Preparation of cellulose nanofibers coated with poly(vinyl alcohol) crystals and their application in composite films,” *RSC Adv.*, vol. 7, no. 32, pp. 19828–19832, Mar. 2017, doi: 10.1039/C7RA01062A.

[95] L. Li, J. Guo, C. Kang, and H. Song, “Reinforcement of Nanocomposite Hydrogel with Dialdehyde Cellulose Nanofibrils via Physical and Double Network Crosslinking Synergies,” *Polymers 2023, Vol. 15, Page 1765*, vol. 15, no. 7, p. 1765, Apr. 2023, doi: 10.3390/POLYM15071765.

[96] M. M. Delavari, I. Ocampo, and I. Stiharu, “Optimizing Biodegradable Starch-Based Composite Films Formulation for Wound-Dressing Applications,” *Micromachines 2022, Vol. 13, Page 2146*, vol. 13, no. 12, p. 2146, Dec. 2022, doi: 10.3390/MI13122146.

[97] M. Lipińska, “The Effect of Various Polyhedral Oligomeric Silsesquioxanes on Viscoelastic, Thermal Properties and Crystallization of Poly(ε-caprolactone) Nanocomposites,” *Polymers (Basel).*, vol. 14, p. 5078, doi: 10.3390/polym14235078.

[98] X. Zhang, Y. Wang, J. Chi, and Y. Zhao, “Smart Microneedles for Therapy and Diagnosis,” *Research*, vol. 2020, Dec. 2020, doi: 10.34133/2020/7462915.

[99] D. Kim, J. Jeong, J. A. Ryu, S. R. Choi, J. M. Lee, and H. Bunch, “In Vitro Evaluation of Lignin-Containing Nanocellulose,” *Materials 2020, Vol. 13, Page 3365*, vol. 13, no. 15, p. 3365, Jul. 2020, doi: 10.3390/MA13153365.

[100] T. Pinheiro *et al.*, "Paper-Based Biosensors for COVID-19: A Review of Innovative Tools for Controlling the Pandemic," *ACS Omega*, vol. 6, no. 44, pp. 29268–29290, Nov. 2021, doi: 10.1021/ACSOMEGA.1C04012.

[101] A. El Guerraf *et al.*, "Multifunctional Smart Conducting Polymers-Silver Nanocomposites-Modified Biocellulose Fibers for Innovative Food Packaging Applications," *Ind. Eng. Chem. Res.*, vol. 62, no. 11, pp. 4540–4553, Mar. 2023, doi: 10.1021/ACS.IECR.2C01327/ASSET/IMAGES/LARGE/IE2C01327_0010.JPEG.

[102] Y. Yin, L. Shi, Z. Chu, and W. Jin, "A highly sensitive electrochemical IFN-γ aptasensor based on a hierarchical graphene/AuNPs electrode interface with a dual enzyme-assisted amplification strategy," *RSC Adv.*, vol. 7, no. 71, pp. 45053–45060, Sep. 2017, doi: 10.1039/C7RA07817J.

[103] B. Wang, U. Akiba, and J. I. Anzai, "Recent Progress in Nanomaterial-Based Electrochemical Biosensors for Cancer Biomarkers: A Review," *Molecules 2017, Vol. 22, Page 1048*, vol. 22, no. 7, p. 1048, Jun. 2017, doi: 10.3390/MOLECULES22071048.

[104] G. Konstantopoulos, E. P. Koumoulos, and C. A. Charitidis, "Digital Innovation Enabled Nanomaterial Manufacturing; Machine Learning Strategies and Green Perspectives," *Nanomaterials 2022, Vol. 12, Page 2646*, vol. 12, no. 15, p. 2646, Aug. 2022, doi: 10.3390/NANO12152646.

[105] V. Naresh and N. Lee, "A Review on Biosensors and Recent Development of Nanostructured Materials-Enabled Biosensors," *Sensors 2021, Vol. 21, Page 1109*, vol. 21, no. 4, p. 1109, Feb. 2021, doi: 10.3390/S21041109.

[106] S. Zeng *et al.*, "Plasmonic Metasensors Based on 2D Hybrid Atomically Thin Perovskite Nanomaterials," *Nanomaterials*, vol. 10, p. 1289, doi: 10.3390/nano10071289.

[107] O. O. Ayodele, A. O. Adesina, S. Pourianejad, J. Averitt, and T. Ignatova, "Recent Advances in Nanomaterial-Based Aptasensors in Medical Diagnosis and Therapy," *Nanomaterials 2021, Vol. 11, Page 932*, vol. 11, no. 4, p. 932, Apr. 2021, doi: 10.3390/NANO11040932.

[108] R. Article, S. Dahiya, M. Verma, S. Lahon, and R. Sharma, "The Effect of Relativistic Quantum Corrections on the Thermal Properties of Three-Dimensional Spherical Semiconductor Quantum Dot Under a Magnetic Field," *Journal of Atomic, Molecular, Condensed Matter and Nano Physics*, vol. 5, no. 1, pp. 41–53, Jun. 2018, doi: 10.26713/JAMCNP.V5I1.908.

[109] H. C. Po and Q. Zhou, “A two-dimensional algebraic quantum liquid produced by an atomic simulator of the quantum Lifshitz model,” *Nat. Commun.*, vol. 6, no. 1, pp. 1–8, Aug. 2015, doi: 10.1038/NCOMMS9012;SUBJMETA.

[110] B. Huang, K. H. Jin, B. Cui, F. Zhai, J. Mei, and F. Liu, “Bending strain engineering in quantum spin hall system for controlling spin currents,” *Nat. Commun.*, vol. 8, no. 1, pp. 1–8, Jun. 2017, doi: 10.1038/NCOMMS15850;SUBJMETA.

[111] X. W. Zhao *et al.*, “Tuning electronic and optical properties of monolayer PdSe2 by introducing defects: first-principles calculations,” *Sci. Rep.*, vol. 10, no. 1, pp. 1–8, Dec. 2020, doi: 10.1038/S41598-020-60949-9;SUBJMETA.

[112] T. Han, H. Liu, S. Wang, S. Chen, H. Xie, and K. Yang, “Probing the Field-Effect Transistor with Monolayer MoS2 Prepared by APCVD,” *Nanomaterials 2019, Vol. 9, Page 1209*, vol. 9, no. 9, p. 1209, Aug. 2019, doi: 10.3390/NANO9091209.

[113] M. Datta *et al.*, “Application of polymer in biomedical implication,” *https://gsconlinepress.com/journals/gscbps/sites/default/files/GSCBPS-2021-0038.pdf*, vol. 14, no. 2, pp. 098–114, Feb. 2021, doi: 10.30574/GSCBPS.2021.14.2.0038.

[114] S. L. Patil *et al.*, “Effect of Camphor Sulfonic Acid Doping on Structural, Morphological, Optical and Electrical Transport Properties on Polyaniline-ZnO Nanocomposites,” *Soft Nanoscience Letters*, vol. 2, no. 3, pp. 46–53, Jun. 2012, doi: 10.4236/SNL.2012.23009.

[115] Y. He, Q. Gui, S. Liao, H. Jia, and Y. Wang, “Coiled Fiber-Shaped Stretchable Thermal Sensors for Wearable Electronics,” *Adv. Mater. Technol.*, vol. 1, no. 8, p. 1600170, Nov. 2016, doi: 10.1002/ADMT.201600170.

[116] S. Majumder, M. M. H. Sagor, and M. T. Arafat, “Functional electrospun polymeric materials for bioelectronic devices: a review,” *Mater. Adv.*, vol. 3, no. 17, pp. 6753–6772, Aug. 2022, doi: 10.1039/D1MA01114F.

[117] T. Wu *et al.*, “High-performance nanogenerators based on flexible cellulose nanofibril/MoS2 nanosheet composite piezoelectric films for energy harvesting,” *Nano Energy*, vol. 80, p. 105541, doi: 10.1016/j.nanoen.2020.105541.

[118] A. M. Elwazri, A. Fatehi, J. Calvo, D. Bai, and S. Yue, “Analysis of Copper Effect on Microstructures and Mechanical Properties in Microalloyed Steels,” *ISIJ International*, vol. 48, no. 1, pp. 107–113, Jan. 2008, doi: 10.2355/ISIJINTERNATIONAL.48.107.

[119] G. Rosu, V. Velicu, A. Boitan, G. Mihai, L. Tuta, and O. Baltag, "On the electromagnetic shielding properties of carbon fiber materials," *Electrical Engineering & Electromechanics*, vol. 2022, no. 1, pp. 38–43, Feb. 2022, doi: 10.20998/2074-272X.2022.1.05.

[120] Q. B. Wang *et al.*, "Mechanical performance of graphenex/poly(ether ketone ketone) composite sheets by hot pressing," *Sci. Rep.*, vol. 12, no. 1, pp. 1–9, Dec. 2022, doi: 10.1038/S41598-022-08221-0;SUBJMETA.

[121] J. Wang and B. Liu, "Electronic and optoelectronic applications of solution-processed two-dimensional materials," *Sci. Technol. Adv. Mater.*, vol. 20, no. 1, pp. 992–1009, Dec. 2019, doi: 10.1080/14686996.2019.1669220.

[122] S. Min Ji and A. Kumar, "Cellulose-Derived Nanostructures as Sustainable Biomass for Supercapacitors: A Review," *Polymers 2022, Vol. 14, Page 169*, vol. 14, no. 1, p. 169, Jan. 2022, doi: 10.3390/POLYM14010169.

[123] B. Saha, S. Baek, and J. Lee, "Highly Sensitive Bendable and Foldable Paper Sensors Based on Reduced Graphene Oxide," *ACS Appl. Mater. Interfaces*, vol. 9, no. 5, pp. 4658–4666, Feb. 2017, doi: 10.1021/ACSAMI.6B10484/SUPPL_FILE/AM6B10484_SI_005.AVI.

[124] M. Oyama, X. Chen, and X. Chen, "Recent nanoarchitectures in metal nanoparticle-graphene nanocomposite modified electrodes for electroanalysis," *Analytical Sciences*, vol. 30, no. 5, pp. 529–538, May 2014, doi: 10.2116/ANALSCI.30.529/METRICS.

[125] F. Chen *et al.*, "Structures, properties, and challenges of emerging 2D materials in bioelectronics and biosensors," *InfoMat*, vol. 4, no. 5, p. e12299, May 2022, doi: 10.1002/INF2.12299.

[126] T. Lu, S. Ji, W. Jin, Q. Yang, Q. Luo, and T. L. Ren, "Biocompatible and Long-Term Monitoring Strategies of Wearable, Ingestible and Implantable Biosensors: Reform the Next Generation Healthcare," *Sensors 2023, Vol. 23, Page 2991*, vol. 23, no. 6, p. 2991, Mar. 2023, doi: 10.3390/S23062991.

[127] K. Soganci, H. Bingol, and E. Zor, "Simply patterned reduced graphene oxide as an effective biosensor platform for glucose determination," *Journal of Electroanalytical Chemistry*, vol. 880, p. 114801, Jan. 2021, doi: 10.1016/J.JELECHEM.2020.114801.

[128] I. Irkham, A. U. Ibrahim, P. C. Pwavodi, F. Al-Turjman, and Y. W. Hartati, "Smart Graphene-Based Electrochemical Nanobiosensor for Clinical Diagnosis: Review,"

Sensors 2023, Vol. 23, Page 2240, vol. 23, no. 4, p. 2240, Feb. 2023, doi: 10.3390/S23042240.

[129] Y. Wang, T. Li, Y. Li, R. Yang, and G. Zhang, "2D-Materials-Based Wearable Biosensor Systems," *Biosensors (Basel).*, vol. 12, p. 936, doi: 10.3390/bios12110936.

[130] G. Ramezani, I. Stiharu, T. G. M. van de Ven, and V. Nerguizian, "Optimizing Graphene Oxide Content in Cellulose Matrices: A Comprehensive Review on Enhancing the Structural and Functional Performance of Composites," *Encyclopedia 2024, Vol. 4, Pages 1827-1856*, vol. 4, no. 4, pp. 1827–1856, Nov. 2024, doi: 10.3390/ENCYCLOPEDIA4040120.

[131] I. Malnarič, M. Krajnc, and U. Šebenik, "Rheological study of hybrid aqueous suspension of TEMPO-oxidized cellulose nanofibrils and graphene oxide'," *Cellulose*, vol. 31, no. 10, pp. 6105–6122, doi: 10.1007/s10570-024-05978-7.

[132] H. Ramezani, M. Haji Ali Koohpayeh, A. Tajedini, G. Ramezani, and A. Mohseni, "Nonlocal stability of curved carbon nanotubes conveying fluid based on Eringen's nonlocal elasticity theory in a thermomagnetic environment," *Acta Mech.*, pp. 1–15, 2024.

[133] H. Luo, "Layer-by-Layer Assembled Bacterial Cellulose/Graphene Oxide Hydrogels with Extremely Enhanced Mechanical Properties'," *Nano-Micro Lett*, vol. 10, no. 3, p. 42, doi: 10.1007/s40820-018-0195-3.

[134] N. Song, D. Jiao, S. Cui, X. Hou, P. Ding, and L. Shi, "Highly Anisotropic Thermal Conductivity of Layer-by-Layer Assembled Nanofibrillated Cellulose/Graphene Nanosheets Hybrid Films for Thermal Management'," *ACS Appl. Mater. Interfaces*, vol. 9, no. 3, pp. 2924–2932, doi: 10.1021/acsami.6b11979.

[135] F. Li, "Natural Biodegradable Poly(3-hydroxybutyrate- co -3-hydroxyvalerate) Nanocomposites with Multifunctional Cellulose Nanocrystals/Graphene Oxide Hybrids for High-Performance Food Packaging'," *J. Agric. Food Chem*, vol. 67, no. 39, pp. 10954–10967, doi: 10.1021/acs.jafc.9b03110.

[136] I. K. Basha, E. M. A. El-Monaem, R. E. Khalifa, A. M. Omer, and A. S. Eltaweil, "Sulfonated graphene oxide impregnated cellulose acetate floated beads for adsorption of methylene blue dye: optimization using response surface methodology'," *Sci. Rep*, vol. 12, p. 9339, doi: 10.1038/s41598-022-13105-4.

[137] K. Balasubramani, "Efficient removal of antidepressant Flupentixol using graphene oxide/cellulose nanogel composite: Particle swarm algorithm based artificial neural

network modelling and optimization',” *J. Mol. Liq*, vol. 319, p. 114371, doi: 10.1016/j.molliq.2020.114371.

[138] Y. Chen, G. Li, L. Li, W. Zhang, and K. Dong, “Molecular dynamics simulation and experimental study on mechanical properties and microstructure of cement-based composites enhanced by graphene oxide and graphene',” *Mol. Simul*, vol. 49, no. 3, pp. 251–262, doi: 10.1080/08927022.2022.2156560.

[139] A. Chamanfar, M. F. Huang, T. Pasang, M. Tsukamoto, and W. Z. Misiolek, “Microstructure and mechanical properties of laser welded Ti–10V–2Fe–3Al (Ti1023) titanium alloy,” *Journal of Materials Research and Technology*, vol. 9, no. 4, pp. 7721–7731, Jul. 2020, doi: 10.1016/J.JMRT.2020.04.028.

[140] Y. Tao, J. Du, Y. Cheng, J. Lu, D. Min, and H. Wang, “Advances in Application of Cellulose—MOF Composites in Aquatic Environmental Treatment: Remediation and Regeneration',” *Int. J. Mol. Sci*, vol. 24, no. 9, p. 7744, doi: 10.3390/ijms24097744.

[141] Y. Tao, J. Du, Y. Cheng, J. Lu, D. Min, and H. Wang, “Advances in Application of Cellulose—MOF Composites in Aquatic Environmental Treatment: Remediation and Regeneration',” *Int. J. Mol. Sci*, vol. 24, no. 9, p. 7744, doi: 10.3390/ijms24097744.

[142] H. G. Castellanos, “The efficacy of nano-cellulose-based composites in heavy metal removal from wastewater: a comprehensive review',” *J. Chem. Technol. Biotechnol*, p. 7775, doi: 10.1002/jctb.7775.

[143] E. N. Mohamed, A. I. Abd-Elhamid, A. A. El-Bardan, H. M. A. Soliman, and M. S. Mohy-Eldin, “Development of carboxymethyl cellulose-graphene oxide biobased composite for the removal of methylene blue cationic dye model contaminate from wastewater',” *Sci. Rep*, vol. 13, p. 14265, doi: 10.1038/s41598-023-41431-8.

[144] S. Song, Z. Liu, J. Zhang, C. Jiao, L. Ding, and S. Yang, “Synthesis and Adsorption Properties of Novel Bacterial Cellulose/Graphene Oxide/Attapulgite Materials for Cu and Pb Ions in Aqueous Solutions',” *Materials*, vol. 13, no. 17, p. 3703, doi: 10.3390/ma13173703.

[145] U. D'Amora *et al.*, “Advances in the Physico-Chemical, Antimicrobial and Angiogenic Properties of Graphene-Oxide/Cellulose Nanocomposites for Wound Healing,” *Pharmaceutics*, vol. 15, no. 2, p. 338, Feb. 2023, doi: 10.3390/PHARMACEUTICS15020338.

[146] P. K. Biswas, O. Omole, G. Peterson, E. Cumbo, M. Agarwal, and H. Dalir, “Carbon and cellulose based nanofillers reinforcement to strengthen carbon fiber-

epoxy composites: Processing, characterizations, and applications','' in *Frontiers in Materials*, p. 1089996. doi: 10.3389/fmats.2022.1089996.

[147] J. Sengupta and C. M. Hussain, "Advanced Graphene-Based Technologies for Antibiotic Removal from Wastewater: A Review (2016–2024)','' *C (Basel).*, vol. 10, no. 4, p. 92, doi: 10.3390/c10040092.

[148] D. Kasprzak, C. C. Mayorga-Martinez, O. Alduhaish, and M. Pumera, "Wearable and Flexible All-Solid-State Supercapacitor Based on MXene and Chitin','' *Energy Technol*, vol. 11, no. 3, p. 2201103, doi: 10.1002/ente.202201103.

[149] C. Cheng, S. Li, A. Thomas, N. A. Kotov, and R. Haag, "Functional Graphene Nanomaterials Based Architectures: Biointeractions, Fabrications, and Emerging Biological Applications','' *Chem. Rev*, vol. 117, no. 3, pp. 1826–1914, doi: 10.1021/acs.chemrev.6b00520.

[150] C. Cheng, S. Li, A. Thomas, N. A. Kotov, and R. Haag, "Functional Graphene Nanomaterials Based Architectures: Biointeractions, Fabrications, and Emerging Biological Applications','' *Chem. Rev*, vol. 117, no. 3, pp. 1826–1914, doi: 10.1021/acs.chemrev.6b00520.

[151] L. Tavares, L. R. Sousa, S. M. Silva, P. S. Lima, and J. M. Oliveira, "Effect of Incorporation of Graphene Nanoplatelets on Physicochemical, Thermal, Rheological, and Mechanical Properties of Biobased and Biodegradable Blends','' *Polymers (Basel).*, vol. 15, no. 17, p. 3622, doi: 10.3390/polym15173622.

[152] S. Hassanifard and K. Behdinan, "Impact of Rheology-Based Optimum Parameters on Enhancing the Mechanical Properties and Fatigue of Additively Manufactured Acrylonitrile-Butadiene-Styrene/Graphene Nanoplatelet Composites','' *Polymers (Basel).*, vol. 16, no. 9, p. 1273, doi: 10.3390/polym16091273.

[153] A. Narimani, F. Kordnejad, P. Kaur, S. Bazgir, M. Hemmati, and A. Duong, "Rheological and thermal stability of interpenetrating polymer network hydrogel based on polyacrylamide/hydroxypropyl guar reinforced with graphene oxide for application in oil recovery','' *J. Polym. Eng*, vol. 41, no. 9, pp. 788–798, doi: 10.1515/polyeng-2021-0147.

[154] D. Kang, S. H. Kim, D. Shin, J. T. Oh, M.-G. Kim, and P.-C. Lee, "Hygroscopic Behavior of Polypropylene Nanocomposites Filled with Graphene Functionalized by Alkylated Chains','' *Nanomaterials*, vol. 12, no. 23, p. 4130, doi: 10.3390/nano12234130.

[155] L. Tavares, L. R. Sousa, S. M. Silva, P. S. Lima, and J. M. Oliveira, "Effect of Incorporation of Graphene Nanoplatelets on Physicochemical, Thermal,

Rheological, and Mechanical Properties of Biobased and Biodegradable Blends',"
Polymers (Basel)., vol. 15, no. 17, p. 3622, doi: 10.3390/polym15173622.

[156] S. R. Joshi, S. Kumar, and S. Kim, "Ecofriendly Polymer–Graphene-Based Conductive Ink for Multifunctional Printed Electronics'," *Adv. Mater. Technol*, vol. 8, no. 11, p. 2201917, doi: 10.1002/admt.202201917.

[157] A. A. Islam, "New wonder materials - exciting technological horizon'," *J. Bangladesh Acad. Sci*, vol. 48, no. 1, pp. 1–25, doi: 10.3329/jbas.v48i1.73005.

[158] F. He, X. R. Yang, Q. H. Liu, and X. Z. Gong, "Preparation and Performance Evaluation of Graphene Heating Film'," *Mater. Sci. Forum*, vol. 1060, pp. 161–166, doi: 10.4028/p-52909c.

[159] G. Jayatilaka, M. M. Mohammadi, and M. Tehrani, "INVESTIGATING STRESS TRANSFER AND FAILURE MECHANISMS IN GRAPHENE OXIDE-CELLULOSE NANOCRYSTALS FILMS'," in *American Society for Composites 2021*, Destech Publications, Inc. doi: 10.12783/asc36/35862.

[160] H. Vu, J. W. Woodcock, A. Krishnamurthy, J. Obrzut, J. W. Gilman, and E. B. Coughlin, "Visualization of Polymer Dynamics in Cellulose Nanocrystal Matrices Using Fluorescence Lifetime Measurements'," *ACS Appl. Mater. Interfaces*, vol. 14, no. 8, pp. 10793–10804, doi: 10.1021/acsami.1c21906.

[161] S. Ilyaei, R. Sourki, and Y. H. A. Akbari, "Capsule-based healing systems in composite materials: a review'," *Crit. Rev. Solid State Mater. Sci*, vol. 46, no. 6, pp. 491–531, doi: 10.1080/10408436.2020.1852912.

[162] Z. Zhu, "Human Nervous System Inspired Modified Graphene Nanoplatelets/Cellulose Nanofibers-Based Wearable Sensors with Superior Thermal Management and Electromagnetic Interference Shielding'," *Adv. Funct. Mater*, vol. 34, no. 28, p. 2315851, doi: 10.1002/adfm.202315851.

[163] N. Wang, "Chemical Modifications on Cellulose Nanocrystals for Composites: Surface Chemistry to Tailored Compatibility and Mechanical Enhancement'," *Macromolecules*, vol. 56, no. 18, pp. 7505–7519, doi: 10.1021/acs.macromol.3c00933.

[164] M. M. Cruz-Benítez, "Covalent Functionalization of Graphene Oxide with Fructose, Starch, and Micro-Cellulose by Sonochemistry'," *Polymers (Basel).*, vol. 13, no. 4, p. 490, doi: 10.3390/polym13040490.

[165] F. Han, H. Huang, and L. Liu, “Dual bio-inspired strong and humidity-responsive composite cellulose nanofibril papers’,” *J. Mater. Sci*, vol. 57, no. 19, Art. no. 19, doi: 10.1007/s10853-022-07219-3.

[166] A. Nekooei, M. R. Miroliaei, M. Shahabi-Nejad, G. Sheibani, and H. Sheibani, “Cellulose-wrapped graphene oxide as efficient adsorbents for pharmaceutical contaminants’,” *Inorg. Chem. Commun*, vol. 154, p. 110997, doi: 10.1016/j.inoche.2023.110997.

[167] A. Mohamed, “Preparation of conductive cellulose paper through electrochemical exfoliation of graphite: The role of anionic surfactant ionic liquids as exfoliating and stabilizing agents’,” *Carbohydr. Polym*, vol. 201, pp. 48–59, doi: 10.1016/j.carbpol.2018.08.040.

[168] F. Naddeo, L. Baldino, S. Cardea, A. Naddeo, and E. Reverchon, “Finite element multiscale modelling of elastic behavior of cellulose acetate—Graphene oxide nanocomposites, produced using a SC-CO2 assisted technique’,” *J. Supercrit. Fluids*, vol. 140, pp. 248–257, doi: 10.1016/j.supflu.2018.06.019.

[169] R. Petry, G. H. Silvestre, B. Focassio, F. C. Lima, R. H. Miwa, and A. Fazzio, “Machine Learning of Microscopic Ingredients for Graphene Oxide/Cellulose Interaction’,” *Langmuir*, vol. 38, no. 3, pp. 1124–1130, doi: 10.1021/acs.langmuir.1c02780.

[170] R. Rahman, J. T. Foster, and A. Haque, “Molecular dynamics simulation and characterization of graphene-cellulose nanocomposites’,” *J. Phys. Chem. A*, vol. 117, no. 25, pp. 5344–5353, doi: 10.1021/jp402814t.

[171] R. Alqus, S. J. Eichhorn, and R. A. Bryce, “Molecular Dynamics of Cellulose Amphiphilicity at the Graphene–Water Interface’,” *Biomacromolecules*, vol. 16, no. 6, pp. 1771–1783, doi: 10.1021/acs.biomac.5b00307.

[172] S. Wang, “Properties of Ag-GNP silver-graphene composites and finite element analysis of electrical contact coupling field’,” *J. Phys. Conf. Ser*, vol. 2587, no. 1, p. 12106, doi: 10.1088/1742-6596/2587/1/012106.

[173] X. Wei, Z. Xia, W. Zhou, P. Huang, and P. Fu, “Simplified finite element method for resistance response of graphene composites considering size distribution and agglomeration’,” *J. Mater. Sci*, vol. 58, no. 40, pp. 15696–15713, doi: 10.1007/s10853-023-08968-5.

[174] S. G. Nukala, I. Kong, A. B. Kakarla, V. I. Patel, and H. Abuel-Naga, “Simulation of Wood Polymer Composites with Finite Element Analysis’,” *Polymers (Basel).*, vol. 15, no. 9, doi: 10.3390/polym15091977.

[175] C.-P. Wu, T.-F. Tan, and H.-T. Hsu, “A Size-Dependent Finite Element Method for the 3D Free Vibration Analysis of Functionally Graded Graphene Platelets-Reinforced Composite Cylindrical Microshells Based on the Consistent Couple Stress Theory’,” *Materials*, vol. 16, no. 6, p. 2363, doi: 10.3390/ma16062363.

[176] M. S. Tayebi, S. J. Salami, and M. Tavakolian, “Free vibration analysis of functionally graded composite rectangular plates reinforced with graphene nanoplatelets (GPLs) using full layerwise finite element method’,” *Proc. Inst. Mech. Eng. Part C J. Mech. Eng. Sci*, vol. 237, no. 24, pp. 5865–5883, doi: 10.1177/09544062231166245.

[177] K. Senthilkumar, “Evaluation of mechanical and free vibration properties of the pineapple leaf fibre reinforced polyester composites’,” *Constr. Build. Mater*, vol. 195, pp. 423–431, doi: 10.1016/j.conbuildmat.2018.11.081.

[178] R. Rafiee and A. Eskandariyun, “Predicting Young’s modulus of agglomerated graphene/polymer using multi-scale modeling’,” *Compos. Struct*, vol. 245, p. 112324, doi: 10.1016/j.compstruct.2020.112324.

[179] Z. C, M. S, and M. Ap, “Cellulose Nanofiber-Graphene Oxide Biohybrids: Disclosing the Self-Assembly and Copper-Ion Adsorption Using Advanced Microscopy and ReaxFF Simulations’,” *PubMed*, [Online]. Available: https://pubmed.ncbi.nlm.nih.gov/29889498/

[180] H. Hosseini, A. Zirakjou, D. J. McClements, V. Goodarzi, and W.-H. Chen, “Removal of methylene blue from wastewater using ternary nanocomposite aerogel systems: Carboxymethyl cellulose grafted by polyacrylic acid and decorated with graphene oxide’,” *J. Hazard. Mater*, vol. 421, p. 126752, doi: 10.1016/j.jhazmat.2021.126752.

[181] K. M. M. Martínez and F. M. N. Maldonado, “DFT formalism studies on the structural and electronic properties of hexagonal graphene quantum dot with B, N and Si substitutional impurities’,” *Rev. Mex. Física*, vol. 70, no. 4, doi: 10.31349/RevMexFis.70.041601.

[182] H. Tachikawa, “Hydrogen Storages Based on Graphene Nano-Flakes: Density Functional Theory Approach’.” doi: 10.3390/c8030036.

[183] S. Dacrory, “Antimicrobial Activity, DFT Calculations, and Molecular Docking of Dialdehyde Cellulose/Graphene Oxide Film Against Covid-19’,” *J. Polym. Environ*, vol. 29, no. 7, pp. 2248–2260, doi: 10.1007/s10924-020-02039-5.

[184] K. Balasubramani, N. Sivarajasekar, G. Sarojini, and M. Naushad, “Removal of Antidiabetic Pharmaceutical (Metformin) Using Graphene Oxide Microcrystalline

Cellulose (GOMCC): Insights to Process Optimization, Equilibrium, Kinetics, And Machine Learning',” *Ind. Eng. Chem. Res*, vol. 62, no. 11, pp. 4713–4728, doi: 10.1021/acs.iecr.2c04480.

[185] E. Champa-Bujaico, A. M. Díez-Pascual, and P. Garcia-Diaz, “Poly(3-hydroxybutyrate-co-3-hydroxyhexanoate) Bionanocomposites with Crystalline Nanocellulose and Graphene Oxide: Experimental Results and Support Vector Machine Modeling',” *Polymers (Basel).*, vol. 15, no. 18, p. 3746, doi: 10.3390/polym15183746.

[186] H. Soltani, A. Karimi, and S. Falahatpisheh, “The optimization of biodiesel production from transesterification of sesame oil via applying ultrasound-assisted techniques: comparison of RSM and ANN–PSO hybrid model',” *Chem. Prod. Process Model*, vol. 17, no. 1, pp. 55–67, doi: 10.1515/cppm-2020-0076.

[187] M. V Ratnam, M. P. Murugesan, S. Komarabathina, S. Samraj, M. Abdulkadir, and M. A. Kalifa, “Methylene Blue Adsorption BY UV-Treated Graphene Oxide Nanoparticles (UV/n-GO): Modeling and Optimization Using Response Surface Methodology and Artificial Neural Networks',” *Int. J. Chem. Eng*, vol. 2022, pp. 1–13, doi: 10.1155/2022/5759394.

[188] W. Wang, X. Wu, and S. Long, “Optimizing the Methylene Blue Removalfrom Aqueous Solution Using Pomelo Peel BasedBiochar Assisted by RSM and ANN-PSO',” *Pol. J. Environ. Stud*, vol. 31, no. 1, pp. 329–346, doi: 10.15244/pjoes/137947.

[189] M. Dolatabadi, H. Naidu, and S. Ahmadzadeh, “Adsorption characteristics in the removal of chlorpyrifos from groundwater using magnetic graphene oxide and carboxy methyl cellulose composite',” *Sep. Purif. Technol*, vol. 300, p. 121919, doi: 10.1016/j.seppur.2022.121919.

[190] N. Bheel, B. S. Mohammed, M. S. Liew, and N. A. W. A. Zawawi, “Effect of Graphene Oxide as a Nanomaterial on the Durability Behaviors of Engineered Cementitious Composites by Applying RSM Modelling and Optimization',” *Buildings*, vol. 13, no. 8, doi: 10.3390/buildings13082026.

[191] X. Huang, Y. Mo, W. Wu, M. Ye, and C. Hu, “Preparation and Properties of Waterborne Polyurethane/Carbon Nanotube/Graphene/Cellulose Nanofiber Composites',” *Processes*, vol. 12, no. 9, doi: 10.3390/pr12091913.

[192] A. Perec, A. Radomska-Zalas, A. Fajdek-Bieda, and F. Pude, “PROCESS OPTIMIZATION BY APPLYING THE RESPONSE SURFACE METHODOLOGY (RSM) TO THE ABRASIVE SUSPENSION WATER JET

CUTTING OF PHENOLIC COMPOSITES',” *Facta Univ. Ser. Mech. Eng*, vol. 21, no. 4, p. 575, doi: 10.22190/FUME211123010P.

[193] H. Tan, D. Xiao, R. Navik, and Y. Zhao, “Facile Fabrication of Polyaniline/Pristine Graphene–Bacterial Cellulose Composites as High-Performance Electrodes for Constructing Flexible All-Solid-State Supercapacitors',” *ACS Omega*, vol. 6, no. 17, pp. 11427–11435, doi: 10.1021/acsomega.1c00442.

[194] T. Kato, T. Matsumoto, C. Hongo, and T. Nishino, “Mechanical and thermal properties of cellulose nanofiber composites with nanodiamond as nanocarbon filler',” *Nanocomposites*, vol. 4, no. 4, pp. 127–136, doi: 10.1080/20550324.2018.1550924.

[195] K. Balasubramani, “Efficient removal of antidepressant Flupentixol using graphene oxide/cellulose nanogel composite: Particle swarm algorithm based artificial neural network modelling and optimization',” *J. Mol. Liq*, vol. 319, p. 114371, doi: 10.1016/j.molliq.2020.114371.

[196] G. K. Khiam, “Modelling and optimization for methylene blue adsorption using graphene oxide/chitosan composites via artificial neural network-particle swarm optimization',” *Mater. Today Chem*, vol. 24, p. 100946, doi: 10.1016/j.mtchem.2022.100946.

[197] G. K. Khiam, “Modelling and optimization for methylene blue adsorption using graphene oxide/chitosan composites via artificial neural network-particle swarm optimization',” *Mater. Today Chem*, vol. 24, p. 100946, doi: 10.1016/j.mtchem.2022.100946.

[198] W. S, M. X, and Z. P, “Sulfo-functional 3D porous cellulose/graphene oxide composites for highly efficient removal of methylene blue and tetracycline from water',” *PubMed*, [Online]. Available: https://pubmed.ncbi.nlm.nih.gov/31419562/

[199] W. S, M. X, and Z. P, “Sulfo-functional 3D porous cellulose/graphene oxide composites for highly efficient removal of methylene blue and tetracycline from water',” *PubMed*, [Online]. Available: https://pubmed.ncbi.nlm.nih.gov/31419562/

[200] M. H. Rahaman, “Preparation, characterization, and adsorption kinetics of graphene oxide/chitosan/carboxymethyl cellulose composites for the removal of environmentally relevant toxic metals',” *Int. J. Biol. Macromol*, vol. 257, p. 128357, doi: 10.1016/j.ijbiomac.2023.128357.

[201] R. Cao, M. Fan, J. Hu, W. Ruan, X. Wu, and X. Wei, “Artificial Intelligence Based Optimization for the Se(IV) Removal from Aqueous Solution by Reduced

Graphene Oxide-Supported Nanoscale Zero-Valent Iron Composites',” *Materials*, vol. 11, no. 3, p. 428, doi: 10.3390/ma11030428.

[202] G. Xiang, S. Long, and A. Dang, “Fabrication of the Ordered Mesoporous nZVI/Zr-Ce-SBA-15 Composites Used for Crystal Violet Removal and Their Optimization Using RSM and ANN–PSO',” *Sustainability*, vol. 14, no. 11, p. 6566, doi: 10.3390/su14116566.

[203] Z. Cai, “Fabrication of a cost-effective lemongrass (Cymbopogon citratus) membrane with antibacterial activity for dye removal',” *RSC Adv*, vol. 9, no. 58, pp. 34076–34085, doi: 10.1039/C9RA04729H.

[204] N. Bheel, B. S. Mohammed, I. Abdulkadir, M. S. Liew, and N. A. W. A. Zawawi, “Effects of Graphene Oxide on the Properties of Engineered Cementitious Composites: Multi-Objective Optimization Technique Using RSM',” *Buildings*, vol. 13, no. 8, doi: 10.3390/buildings13082018.

[205] C. T. Yaw, “An Approach for the Optimization of Thermal Conductivity and Viscosity of Hybrid (Graphene Nanoplatelets, GNPs: Cellulose Nanocrystal, CNC) Nanofluids Using Response Surface Methodology (RSM)',” *Nanomaterials*, vol. 13, no. 10, p. 1596, doi: 10.3390/nano13101596.

[206] J. I. T. Civil Engineering, I. Borawan, D. Solanki, D. S. Sugandhi, J. I. T. Civil Engineering, and I. Borawan, “A PSO-ANN Hybrid Model for Temporal Traffic Speed Forecasts in Urban Environments',” *INTERANTIONAL J. Sci. Res. Eng. Manag*, vol. 08, no. 01, pp. 1–6, doi: 10.55041/IJSREM28403.

[207] H. C. Kim, P. S. Panicker, D. Kim, S. Adil, and J. Kim, “High-strength cellulose nanofiber/graphene oxide hybrid filament made by continuous processing and its humidity monitoring',” *Sci. Rep*, vol. 11, no. 1, p. 13611, doi: 10.1038/s41598-021-93209-5.

[208] A. M. Sofyana, M. D. Supardan, A. C. Ambarita, and N. Arahman, “Combination of cellulose nanocrystal and graphene oxide as modifying agent for improving the performance of PVDF membranes',” *Case Stud. Chem. Environ. Eng*, vol. 10, p. 100873, doi: 10.1016/j.cscee.2024.100873.

[209] B. C. Ozkan, “Cellulose and chitosan biopolymer composites reinforced with graphene and their adsorption properties for basic blue 41',” *Cellulose*, vol. 29, no. 18, pp. 9637–9655, doi: 10.1007/s10570-022-04852-8.

[210] D. Zhang, Y. Huang, W. Xia, L. Xu, and X. Wang, “Dispersion characteristics and mechanical properties of epoxy nanocomposites reinforced with carboxymethyl

cellulose functionalized nanodiamond, carbon nanotube, and graphene',” *Polym. Compos*, vol. 45, no. 1, pp. 398–412, doi: 10.1002/pc.27785.

[211] A. Tabernero, L. Baldino, S. Cardea, E. M. Del Valle, and E. Reverchon, “A Phenomenological Approach to Study Mechanical Properties of Polymeric Porous Structures Processed Using Supercritical CO2',” *Polymers (Basel).*, vol. 11, no. 3, p. 485, doi: 10.3390/polym11030485.

[212] H. Zhang, D. Zhai, and Y. He, “Graphene oxide/polyacrylamide/carboxymethyl cellulose sodium nanocomposite hydrogel with enhanced mechanical strength: preparation, characterization and the swelling behavior',” *RSC Adv*, vol. 4, no. 84, pp. 44600–44609, doi: 10.1039/C4RA07576E.

[213] H. C. Kim, P. S. Panicker, D. Kim, S. Adil, and J. Kim, “High-strength cellulose nanofiber/graphene oxide hybrid filament made by continuous processing and its humidity monitoring',” *Sci. Rep*, vol. 11, no. 1, p. 13611, doi: 10.1038/s41598-021-93209-5.

[214] Y. Shen, “Significantly Enhancing Mechanical and Thermal Properties of Cellulose-Based Composites by Adding Small Amounts of Lysozyme-Modified Graphene Nanoplatelets via Forming Strong Double-Cross-Linked Interface Interactions',” *ACS Appl. Mater. Interfaces*, vol. 15, no. 36, pp. 43159–43168, doi: 10.1021/acsami.3c08195.

[215] “Thermal Properties of Unsaturated Polyester Reinforced Kenaf Core Fiber with Hybrid Nanofillers of Cellulose Nanocrystal and Graphene Nanoplatelet',” *Borneo J. Sci. Technol*, doi: 10.35370/bjost.2023.5.1-09.

[216] X. Meng, S. Wang, W. Gao, W. Han, and L. A. Lucia, “Thermal pyrolysis characteristics and kinetic analysis of nanofibrillated cellulose/graphene oxide composites',” *Bioresources*, vol. 15, no. 3, pp. 4851–4865, doi: 10.15376/biores.15.3.4851-4865.

[217] Z. Gao, Y. Li, P. Huang, R. Zou, Y. Li, and S. Fu, “Graphene nanoplatelet/cellulose acetate film with enhanced antistatic, thermal dissipative and mechanical properties for packaging',” *Cellulose*, vol. 30, no. 7, pp. 4499–4509, doi: 10.1007/s10570-023-05155-2.

[218] J. Phiri, L.-S. Johansson, P. Gane, and T. C. Maloney, “Co-exfoliation and fabrication of graphene based microfibrillated cellulose composites - mechanical and thermal stability and functional conductive properties',” *Nanoscale*, vol. 10, no. 20, pp. 9569–9582, doi: 10.1039/c8nr02052c.

[219] Y. Pottathara, “Graphene based Composites with Cellulose Nanofibrils for Energy storage applications’.” [Online]. Available: https://www.semanticscholar.org/paper/Graphene-based-Composites-with-Cellulose-for-Energy-Pottathara/cd70dcdf88ae3abdc342aa4e85e726553377f6cf

[220] K. Piotr, J. K. Jeszka, M. Artur, and S. Leszek, “Regenerated Cellulose/Graphene Composite Fibers with Electroconductive Properties’,” *Autex Res. J*, vol. 22, no. 2, pp. 177–183, doi: 10.2478/aut-2020-0027.

[221] Y. Qing, R. Sabo, Z. Cai, and Y. Wu, “Flexible cellulose nanofibril composite films with reduced hygroscopic capacity’.” [Online]. Available: https://www.semanticscholar.org/paper/Flexible-cellulose-nanofibril-composite-films-with-Qing-Sabo/ab799ddf27e61a8f6f722b54a214362657c264c0

[222] Z. Y, “Effect of graphene oxide in an injectable hydrogel on the osteogenic differentiation of mesenchymal stem cells’,” *PubMed*, [Online]. Available: https://pubmed.ncbi.nlm.nih.gov/39225005/

[223] T. Sheikh and K. Behdinan, “Fused Deposition Modelling of Thermoplastic Polymer Nanocomposites: A Critical Review’,” *C (Basel).*, vol. 10, no. 2, p. 29, doi: 10.3390/c10020029.

[224] T. Sheikh and K. Behdinan, “Fused Deposition Modelling of Thermoplastic Polymer Nanocomposites: A Critical Review’,” *C (Basel).*, vol. 10, no. 2, p. 29, doi: 10.3390/c10020029.

[225] Y. Cheng, “Advancements and challenges in nanomaterial-based medical implants’,” *Appl. Comput. Eng*, vol. 58, no. 1, pp. 60–67, doi: 10.54254/2755-2721/58/20240693.

[226] M. Karunanidhi, “Abstract 7289: PancreaAlert: Intelligent nanoengineered biosensor for pancreatic cancer’,” *Cancer Res*, vol. 84, no. 6_Supplement, p. 7289, doi: 10.1158/1538-7445.AM2024-7289.

[227] Y. Liu, J. Zhou, J. Tang, and W. Tang, “Three-Dimensional, Chemically Bonded Polypyrrole/Bacterial Cellulose/Graphene Composites for High-Performance Supercapacitors’,” *Chem. Mater*, vol. 27, no. 20, pp. 7034–7041, doi: 10.1021/acs.chemmater.5b03060.

[228] Y.-D. Shen, “Pyrolyzed bacterial cellulose/graphene oxide sandwich interlayer for lithium–sulfur batteries’,” *Rare Met*, vol. 36, no. 5, pp. 418–424, doi: 10.1007/s12598-017-0906-9.

[229] Y. Wang, “Preparation and characterization of flexible lithium iron phosphate/graphene/cellulose electrode for lithium ion batteries’,” *J. Colloid Interface Sci*, vol. 512, pp. 398–403, doi: 10.1016/j.jcis.2017.10.042.

[230] Q. Y, “Enhanced Thermal-to-Flexible Phase Change Materials Based on Cellulose/Modified Graphene Composites for Thermal Management of Solar Energy’,” *PubMed*, [Online]. Available: https://pubmed.ncbi.nlm.nih.gov/31738041/

[231] M. K. Rabchinskii, “A Blueprint for the Synthesis and Characterization of Thiolated Graphene’,” *Nanomaterials*, vol. 12, no. 1, p. 45, doi: 10.3390/nano12010045.

[232] M. K. Rabchinskii, “Graphene Amination towards Its Grafting by Antibodies for Biosensing Applications’,” *Nanomaterials*, vol. 13, no. 11, p. 1730, doi: 10.3390/nano13111730.

[233] M. ; Li *et al.*, “Mechanically Strong and Electrically Conductive Polyethylene Oxide/Few-Layer Graphene/Cellulose Nanofibrils Nanocomposite Films,” *Nanomaterials 2022, Vol. 12, Page 4152*, vol. 12, no. 23, p. 4152, Nov. 2022, doi: 10.3390/NANO12234152.

[234] Z.-T. Xie, T.-A. Asoh, Y. Uetake, H. Sakurai, and H. Uyama, “Dual roles of cellulose monolith in the continuous-flow generation and support of gold nanoparticles for green catalyst’,” *Carbohydr. Polym*, vol. 247, p. 116723, doi: 10.1016/j.carbpol.2020.116723.

[235] N. Méndez-Lozano, F. Pérez-Reynoso, and C. González-Gutiérrez, “Eco-Friendly Approach for Graphene Oxide Synthesis by Modified Hummers Method’,” *Materials*, vol. 15, no. 20, p. 7228, doi: 10.3390/ma15207228.

[236] W. Xu, Y. Lv, M. Kong, Y. Huang, Q. Yang, and G. Li, “In-situ polymerization of eco-friendly waterborne polyurethane/polydopamine-coated graphene oxide composites towards enhanced mechanical properties and UV resistance’,” *J. Clean. Prod*, vol. 373, p. 133942, doi: 10.1016/j.jclepro.2022.133942.

[237] S. Y. Mazhar Ul-Islam, L. Mombasawala, S. Manan, and M. W. Ullah, “Bacterial Cellulose: A Versatile Material for Fabrication of Conducting Nanomaterials’,” *Curr. Nanosci*, vol. 17, no. 3, pp. 393–405, doi: 10.2174/1573413716999201005214832.

[238] A. B. Rashid, M. Haque, S. M. M. Islam, and K. M. R. U. Labib, “Nanotechnology-enhanced fiber-reinforced polymer composites: Recent advancements on

processing techniques and applications',” *Heliyon*, vol. 10, no. 2, p. 24692, doi: 10.1016/j.heliyon.2024.e24692.

[239] M. U. A. Khan, G. M. Stojanović, R. Hassan, T. J. S. Anand, M. Al-Ejji, and A. Hasan, “Role of Graphene Oxide in Bacterial Cellulose−Gelatin Hydrogels for Wound Dressing Applications',” *ACS Omega*, vol. 8, no. 18, pp. 15909–15919, doi: 10.1021/acsomega.2c07279.

[240] Y. Yang, C. Wan, Q. Huang, and J. Hua, “Pore-Rich Cellulose-Derived Carbon Fiber@Graphene Core-Shell Composites for Electromagnetic Interference Shielding',” *Nanomaterials*, vol. 13, no. 1, p. 174, doi: 10.3390/nano13010174.

[241] M. Tavakolian, S. M. Jafari, and T. G. M. van de Ven, “A Review on Surface-Functionalized Cellulosic Nanostructures as Biocompatible Antibacterial Materials,” *Nanomicro Lett.*, vol. 12, no. 1, pp. 1–23, Dec. 2020, doi: 10.1007/S40820-020-0408-4/FIGURES/3.

[242] R. E. Abou-Zeid, A. Salama, Z. Ali Al-Ahmed, N. S. Awwad, and M. A. Youssef, “CARBOXYLATED CELLULOSE NANOFIBERS AS A NOVEL EFFICIENT ADSORBENT FOR WATER PURIFICATION”.

[243] O. A. Adeleke, “Premium ethylcellulose polymer based architectures at work in drug delivery,” *Int. J. Pharm. X*, vol. 1, p. 100023, Dec. 2019, doi: 10.1016/J.IJPX.2019.100023.

[244] J. Ahn, S. Pak, and H. Kim, “Carbon dot/cellulose nanofiber composite: Dataset for its water treatment performance,” *Data Brief*, vol. 34, p. 106760, Feb. 2021, doi: 10.1016/J.DIB.2021.106760.

[245] M. Tavakolian, R. Koshani, N. Tufenkji, and T. G. M. van de Ven, “Antibacterial Pickering emulsions stabilized by bifunctional hairy nanocellulose,” *J. Colloid Interface Sci.*, vol. 643, pp. 328–339, Aug. 2023, doi: 10.1016/J.JCIS.2023.04.033.

[246] S. Anwer *et al.*, “2D Ti3C2Tx MXene nanosheets coated cellulose fibers based 3D nanostructures for efficient water desalination,” *Chemical Engineering Journal*, vol. 406, p. 126827, Feb. 2021, doi: 10.1016/J.CEJ.2020.126827.

[247] R. V. Badhe and S. S. Nipate, “Cellulosic materials as bioinks for 3D printing applications,” *Advanced 3D-Printed Systems and Nanosystems for Drug Delivery and Tissue Engineering*, pp. 109–137, Jan. 2020, doi: 10.1016/B978-0-12-818471-4.00005-4.

[248] M. Badshah *et al.*, “Development and Evaluation of Drug Loaded Regenerated Bacterial Cellulose-Based Matrices as a Potential Dosage Form,” *Front. Bioeng.*

Biotechnol., vol. 8, p. 579404, Dec. 2020, doi: 10.3389/FBIOE.2020.579404/BIBTEX.

[249] J. Bhandari, H. Mishra, P. K. Mishra, R. Wimmer, F. J. Ahmad, and S. Talegaonkar, "Cellulose nanofiber aerogel as a promising biomaterial for customized oral drug delivery," *Int. J. Nanomedicine*, vol. 12, pp. 2021–2031, Mar. 2017, doi: 10.2147/IJN.S124318.

[250] N. Bhogal, "Regulatory and Scientific Barriers to The Safety Evaluation of Medical Nanotechnologies," *Nanomedicine*, vol. 4, no. 5, pp. 495–498, 2009, doi: 10.2217/NNM.09.33.

[251] M. Heidari Nia, R. Koshani, J. G. Munguia-Lopez, A. R. Kiasat, J. M. Kinsella, and T. G. M. Van De Ven, "Biotemplated Hollow Mesoporous Silica Particles as Efficient Carriers for Drug Delivery," *ACS Appl. Bio Mater.*, vol. 4, no. 5, pp. 4201–4214, May 2021, doi: 10.1021/ACSABM.0C01671.

[252] D. Bobo, K. J. Robinson, J. Islam, K. J. Thurecht, and S. R. Corrie, "Nanoparticle-Based Medicines: A Review of FDA-Approved Materials and Clinical Trials to Date," *Pharm. Res.*, vol. 33, no. 10, pp. 2373–2387, Oct. 2016, doi: 10.1007/S11095-016-1958-5/TABLES/1.

[253] A. Brakat and H. Zhu, "Nanocellulose-Graphene Hybrids: Advanced Functional Materials as Multifunctional Sensing Platform," *Nanomicro Lett.*, vol. 13, no. 1, pp. 1–37, Dec. 2021, doi: 10.1007/S40820-021-00627-1/FIGURES/4.

[254] W. T. Cao *et al.*, "Binary Strengthening and Toughening of MXene/Cellulose Nanofiber Composite Paper with Nacre-Inspired Structure and Superior Electromagnetic Interference Shielding Properties," *ACS Nano*, vol. 12, no. 5, pp. 4583–4593, May 2018, doi: 10.1021/ACSNANO.8B00997/SUPPL_FILE/NN8B00997_SI_003.AVI.

[255] E. Ladd, A. Sheikhi, N. Li, T. G. M. van de Ven, and A. Kakkar, "Design and Synthesis of Dendrimers with Facile Surface Group Functionalization, and an Evaluation of Their Bactericidal Efficacy," *Molecules 2017, Vol. 22, Page 868*, vol. 22, no. 6, p. 868, May 2017, doi: 10.3390/MOLECULES22060868.

[256] P. Davoodi *et al.*, "Drug delivery systems for programmed and on-demand release," *Adv. Drug Deliv. Rev*, vol. 132, pp. 104–138, doi: 10.1016/j.addr.2018.07.002.

[257] K. Deshmukh, T. Kovářík, and S. K. K. Pasha, "State of the art recent progress in two dimensional MXenes based gas sensors and biosensors: A comprehensive review," *Coord. Chem. Rev*, vol. 424, p. 213514, doi: 10.1016/j.ccr.2020.213514.

[258] M. Tavakolian, M. Okshevsky, T. G. M. Ven, and N. Tufenkji, “Developing antibacterial nanocrystalline cellulose using natural antibacterial agents,” *ACS Appl. Mater. Interfaces*, vol. 10, pp. 33827–33838, doi: 10.1021/acsami.8b08770.

[259] O. A. T. Dias, S. Konar, A. L. Leão, W. Yang, J. Tjong, and M. Sain, “Current State of Applications of Nanocellulose in Flexible Energy and Electronic Devices,” *Front. Chem.*, vol. 8, p. 420, May 2020, doi: 10.3389/FCHEM.2020.00420.

[260] X. Du, Z. Zhang, W. Liu, and Y. Deng, “Nanocellulose-based conductive materials and their emerging applications in energy devices—A review,” *Nano Energy*, vol. 35, pp. 299–320, doi: 10.1016/j.nanoen.2017.04.001.

[261] L. Y. Ee and S. F. Y. Li, “Recent advances in 3D printing of nanocellulose: Structure, preparation, and application prospects,” *Nanoscale Adv*, vol. 3, pp. 1167–1208, doi: 10.1039/d0na00408a.

[262] R. E. Abouzeid, R. Khiari, N. El-Wakil, and A. Dufresne, “Current state and new trends in the use of cellulose nanomaterials for wastewater treatment,” *Biomacromolecules*, vol. 20, pp. 573–597, doi: 10.1021/acs.biomac.8b00839.

[263] K. Madaan, S. Kumar, N. Poonia, V. Lather, and D. Pandita, “Dendrimers in drug delivery and targeting: Drug-dendrimer interactions,” *J. Pharm. Bioallied Sci*, vol. 6, pp. 139–150, [Online]. Available: https://journals.lww.com/jpbs/fulltext/2014/06030/dendrimers_in_drug_delivery_and_targeting_.1.aspx.

[264] S. Derakhshanfar, R. Mbeleck, K. Xu, X. Zhang, W. Zhong, and M. Xing, “3D bioprinting for biomedical devices and tissue engineering: A review of recent trends and advances,” *Bioact. Mater*, vol. 3, pp. 144–156, doi: 10.1016/j.bioactmat.2017.11.008.

[265] M. Elgadir, M. Uddin, S. Ferdosh, A. Adam, A. J. K. Chowdhury, and M. I. Sarker, “Impact of chitosan composites and chitosan nanoparticle composites on various drug delivery systems: A review,” *J. Food Drug Anal*, vol. 23, pp. 619–629, doi: 10.1016/j.jfda.2014.10.008.

[266] M. C. Vasudev, K. D. Anderson, T. J. Bunning, V. V Tsukruk, and R. R. Naik, “Exploration of plasma-enhanced chemical vapor deposition as a method for thin-film fabrication with biological applications,” *ACS Appl. Mater. Interfaces*, vol. 5, pp. 3983–3994, doi: 10.1021/am302989x.

[267] I. Firlar, M. Altunbek, C. McCarthy, M. Ramalingam, and G. Camci-Unal, “Functional hydrogels for treatment of chronic wounds,” *Gels*, vol. 8, p. 127, doi: 10.3390/gels8020127.

[268] Y. Ha *et al.*, “Flexible low-voltage organic thin-film transistors enabled by low-temperature, ambient solution-processable inorganic/organic hybrid gate dielectrics,” *J. Am. Chem. Soc*, vol. 132, pp. 17426–17434, doi: 10.1021/ja107079d.

[269] J. George and S. N. Sabapathi, “Cellulose nanocrystals: synthesis, functional properties, and applications,” *Nanotechnol. Sci. Appl.*, vol. 8, p. 45, Nov. 2015, doi: 10.2147/NSA.S64386.

[270] J. Gong, L. Mo, and J. Li, “A comparative study on the preparation and characterization of cellulose nanocrystals with various polymorphs,” *Carbohydr. Polym*, vol. 195, pp. 18–28, doi: 10.1016/j.carbpol.2018.04.039.

[271] G. Fotie, S. Limbo, and L. Piergiovanni, “Manufacturing of food packaging based on nanocellulose: Current advances and challenges,” *Nanomaterials*, vol. 10, p. 1726, doi: 10.3390/nano10091726.

[272] K. Heise *et al.*, “Recent fundamental advances and emerging biological and biomimicking applications,” *Adv. Mater*, vol. 33, p. 2004349, doi: 10.1002/adma.202004349.

[273] M. Tavakolian *et al.*, “Highly absorbent antibacterial and biofilm-disrupting hydrogels from cellulose for wound dressing applications,” *ACS Appl. Mater. Interfaces*, vol. 12, pp. 39991–40001, doi: 10.1021/acsami.0c08784.

[274] L. Huang *et al.*, “Preparation and properties of cassava residue cellulose nanofibril/cassava starch composite films,” *Nanomaterials*, vol. 10, p. 755, doi: 10.3390/nano10040755.

[275] M. A. Hubbe *et al.*, “Nanocellulose in thin films, coatings, and plies for packaging applications: A review,” *Bioresources*, vol. 12, pp. 2143–2233, doi: 10.15376/biores.12.1.2143-2233.

[276] R. A. Ilyas *et al.*, “Natural-fiber-reinforced chitosan, chitosan blends and their nanocomposites for various advanced applications,” *Polymers (Basel).*, vol. 14, p. 874, doi: 10.3390/polym14050874.

[277] M. H. Nia, L. D. Wilson, A. R. Kiasat, J. G. Munguia-Lopez, J. M. Kinsella, and T. G. Ven, “Internally bridged nanosilica for loadings and release of sparsely soluble compounds,” *J. Colloid Interface Sci*, vol. 649, pp. 456–470, doi: 10.1016/j.jcis.2023.06.118.

[278] H. Jafri and I. Ahmad, “Nanoparticle-based delivery of phytomedicines: Challenges and opportunities,” in *Phytomedicine*, Amsterdam, The Netherlands: Elsevier, pp. 477–491. doi: 10.1016/B978-0-12-814619-4.00024-0.

[279] J. Jose, V. Thomas, V. Vinod, R. Abraham, and S. Abraham, “Nanocellulose based on functional materials for supercapacitor applications,” *J. Sci. Adv. Mater. Devices*, vol. 4, pp. 333–340, doi: 10.1016/j.jsamd.2019.06.003.

[280] E. Jamróz, P. Kulawik, and P. Kopel, “The effect of nanofillers on the functional properties of biopolymer-based films: A review,” *Polymers (Basel).*, vol. 11, p. 675, doi: 10.3390/polym11040675.

[281] K. A. Kirk, A. Othman, and S. Andreescu, “Nanomaterial-functionalized cellulose: Design, characterization and analytical applications,” *Anal. Sci*, vol. 34, pp. 19–31, doi: 10.2116/analsci.34.19.

[282] M. Lay, J. A. Méndez, M. Delgado-Aguilar, K. N. Bun, and F. Vilaseca, “Strong and electrically conductive nanopaper from cellulose nanofibers and polypyrrole,” *Carbohydr. Polym*, vol. 152, pp. 361–369, doi: 10.1016/j.carbpol.2016.06.102.

[283] X. Li, F. Ran, F. Yang, J. Long, and L. Shao, “Advances in MXene films: Synthesis, assembly, and applications,” *Trans. Tianjin Univ*, vol. 27, pp. 217–247, doi: 10.1007/s12209-021-00282-y.

[284] M. Hervy, S. Evangelisti, P. Lettieri, and K.-Y. Lee, “Life cycle assessment of nanocellulose-reinforced advanced fibre composites,” *Compos. Sci. Technol*, vol. 118, pp. 154–162, doi: 10.1016/j.compscitech.2015.08.024.

[285] Z. Liu, Y. Wang, and F. Guo, “An investigation into hydraulic permeability of fibrous membranes with nonwoven random and quasi-parallel structures,” *Membranes (Basel).*, vol. 12, p. 54, doi: 10.3390/membranes12010054.

[286] D. Lombardo, M. A. Kiselev, and M. T. Caccamo, “Smart nanoparticles for drug delivery application: Development of versatile nanocarrier platforms in biotechnology and nanomedicine,” *J. Nanomater*, p. 3702518, doi: 10.1155/2019/3702518.

[287] Y. Luo and Q. Wang, “Recent development of chitosan-based polyelectrolyte complexes with natural polysaccharides for drug delivery,” *Int. J. Biol. Macromol*, vol. 64, pp. 353–367.

[288] R. J. Pinto, M. C. Neves, C. P. Neto, and T. Trindade, “Composites of cellulose and metal nanoparticles,” in *Nanocomposites—New Trends and Developments*, Rijeka, Croatia: InTech. doi: 10.5772/50553.

[289] “Preparation and Evaluation of Starch Acetate Based Gliclazide Microcapsules.”

[290] Q. Liu, W. Sun, T. Yuan, S.-B. Liang, F. Peng, and C.-L. Yao, “Green and cost-effective synthesis of flexible, highly conductive cellulose nanofiber/reduced graphene oxide composite film with deep eutectic solvent,” *Carbohydr. Polym*, vol. 272, p. 118514, doi: 10.1016/j.carbpol.2021.118514.

[291] N. Raghav, M. R. Sharma, and J. F. Kennedy, “Nanocellulose: A mini-review on types and use in drug delivery systems,” *Carbohydr. Polym. Technol. Appl*, vol. 2, p. 100031, doi: 10.1016/j.carpta.2020.100031.

[292] M. Ramos, A. Valdés, and M. C. Garrigós, “Multifunctional applications of nanocellulose-based nanocomposites,” in *Multifunctional Polymeric Nanocomposites Based on Cellulosic Reinforcements*, Amsterdam, The Netherlands: Elsevier, pp. 177–204. doi: 10.1016/b978-0-323-44248-0.00006-7.

[293] S. S. Rao and S. Rajiv, “Comparison of nanocomposite film and electrospun nanocomposite fibers based on poly (2-hydroxy ethyl methacrylate) and microcrystalline cellulose as anticancer implants,” *Polym.-Plast. Technol. Eng*, vol. 53, pp. 1690–1696, doi: 10.1080/03602559.2014.919654.

[294] R. Rebelo, M. Fernandes, and R. Fangueiro, “Biopolymers in medical implants: A brief review,” *Procedia Eng*, vol. 200, pp. 236–243, doi: 10.1016/j.proeng.2017.07.034.

[295] H. Seddiqi *et al.*, “Cellulose and its derivatives: Towards biomedical applications,” *Cellulose*, vol. 28, pp. 1893–1931, doi: 10.1007/s10570-020-03674-w.

[296] D. R. Shankaran, “Cellulose nanocrystals for health care applications,” in *Applications of Nanomaterials*, Amsterdam, The Netherlands: Elsevier, pp. 415–459. doi: 10.1016/b978-0-08-101971-9.00015-6.

[297] P. Sabourian *et al.*, “Stimuli-responsive chitosan as an advantageous platform for efficient delivery of bioactive agents,” *J. Control. Release*, vol. 317, pp. 216–231, doi: 10.1016/j.jconrel.2019.11.029.

[298] D. Trache and V. K. Thakur, “Nanocellulose and nanocarbons based hybrid materials: Synthesis, characterization and applications,” *Nanomaterials*, vol. 10, p. 1800, doi: 10.3390/nano10091800.

[299] A. Vaidya, S. Jain, K. Pathak, and D. Pathak, “Dendrimers: Nanosized multifunctional platform for drug delivery,” *Drug Deliv. Lett*, vol. 8, pp. 74–85, doi: 10.2174/2210303107666171109112523.

[300] A. Vikulina, D. Voronin, R. Fakhrullin, V. Vinokurov, and D. Volodkin, “Naturally derived nano- and micro-drug delivery vehicles: Halloysite, vaterite and nanocellulose,” *New J. Chem*, vol. 44, pp. 5638–5655, doi: 10.1039/c9nj06470b.

[301] D.-C. Wang, S.-N. Lei, S. Zhong, X. Xiao, and Q.-H. Guo, “Cellulose-based conductive materials for energy and sensing applications,” *Polymers (Basel).*, vol. 15, p. 4159, doi: 10.3390/polym15204159.

[302] Y. Wu, Z. Y. Lin, A. C. Wenger, K. C. Tam, and X. Tang, “3D bioprinting of liver-mimetic construct with alginate/cellulose nanocrystal hybrid bioink,” *Bioprinting*, vol. 9, p. 21, doi: 10.1016/j.bprint.2017.12.001.

[303] Y. Wang *et al.*, “Fabrication of cellulose nanofiber/reduced graphene oxide/nitrile rubber flexible films using Pickering Emulsion technology for electromagnetic interference shielding and piezoresistive sensor,” *Macromol. Mater. Eng*, vol. 306, p. 2100070, doi: 10.1002/mame.202100070.

[304] J. Xing, P. Tao, Z. Wu, C. Xing, X. Liao, and S. Nie, “Nanocellulose-graphene composites: A promising nanomaterial for flexible supercapacitors,” *Carbohydr. Polym*, vol. 207, pp. 447–459, doi: 10.1016/j.carbpol.2018.12.010.

[305] Y. Shen *et al.*, “Recent Advances in Functional Cellulose-based Films with Antimicrobial and Antioxidant Properties for Food Packaging,” *J. Agric. Food Chem.*, vol. 71, no. 44, pp. 16469–16487, Nov. 2023, doi: 10.1021/ACS.JAFC.3C06004,.

[306] L. Lin, H. Peng, and Z. Liu, “Synthesis challenges for graphene industry,” *Nat. Mater*, vol. 18, pp. 520–524, doi: 10.1038/s41563-019-0341-4.

[307] W. Zhu, H. Li, and P. Luo, “Emerging 2D nanomaterials for multimodel theranostics of cancer,” *Front. Bioeng. Biotechnol*, vol. 9, p. 769178, doi: 10.3389/fbioe.2021.769178.

[308] D. Merson *et al.*, “The functional properties of Mg–Zn–X biodegradable magnesium alloys,” *Materials*, vol. 13, p. 544, doi: 10.3390/ma13030544.

[309] S. Y. H. Abdalkarim *et al.*, “Versatile nanocellulose-based nanohybrids: A promising-new class for active packaging applications,” *Int. J. Biol. Macromol*, vol. 182, pp. 1915–1930, doi: 10.1016/j.ijbiomac.2021.05.169.

[310] G. Ramezani, I. Stiharu, T. G. M. van de Ven, and V. Nerguizian, “Advancements in Hybrid Cellulose-Based Films: Innovations and Applications in 2D Nano-Delivery Systems,” *Journal of Functional Biomaterials 2024, Vol. 15, Page 93*, vol. 15, no. 4, p. 93, Apr. 2024, doi: 10.3390/JFB15040093.

[311] J. Jung and H. A. Sodano, “Cellulose nanocrystal functionalized aramid nanofiber reinforced epoxy nanocomposites with high strength and toughness,” *Nanotechnology*, vol. 34, no. 24, Jun. 2023, doi: 10.1088/1361-6528/ACBA1B.

[312] F. Fahma, I. Febiyanti, N. Lisdayana, I. W. Arnata, and D. Sartika, “Nanocellulose as a new sustainable material for various applications: a review,” *Archives of Materials Science and Engineering*, vol. 109, no. 2, pp. 49–64, 2021, doi: 10.5604/01.3001.0015.2624.

[313] M. Park *et al.*, “Proton-electron coupling and mixed conductivity in a hydrogen-bonded coordination polymer,” *Nature Communications 2025 16:1*, vol. 16, no. 1, pp. 1–12, Feb. 2025, doi: 10.1038/s41467-025-56541-2.

[314] G. C. Ri, J. S. Kim, and C. J. Yu, “Role of Water Molecules in Enhancing the Proton Conductivity on Reduced Graphene Oxide under High Humidity,” *Phys. Rev. Appl.*, vol. 10, no. 3, p. 034018, Sep. 2018, doi: 10.1103/PHYSREVAPPLIED.10.034018/FIGURES/7/THUMBNAIL.

[315] H. Hu, L. Qi, and X. Chao, “Physics-informed Neural Networks (PINN) for computational solid mechanics: Numerical frameworks and applications,” *Thin-Walled Structures*, vol. 205, p. 112495, Dec. 2024, doi: 10.1016/J.TWS.2024.112495.

[316] G. E. Karniadakis, I. G. Kevrekidis, L. Lu, P. Perdikaris, S. Wang, and L. Yang, “Physics-informed machine learning,” *Nature Reviews Physics 2021 3:6*, vol. 3, no. 6, pp. 422–440, May 2021, doi: 10.1038/s42254-021-00314-5.

[317] C. Liu *et al.*, “Simultaneous Extraction of Carboxylated Celulose Nanocrystals and Nanofibrils via Citric Acid Hydrolysis——A Sustainable Route,” *Paper and Biomaterials*, vol. 2, no. 4, p. 19, Oct. 2017, doi: 10.26599/PBM.2017.9260024.

[318] R. Ortega-Amaya, Y. Matsumoto, A. Flores-Conde, M. A. Peerez-Guzman, and M. Ortega-Lopez, “In situ formation of rGO quantum dots during GO reduction via interaction with citric acid in aqueous medium,” *Mater. Res. Express*, vol. 3, no. 10, Oct. 2016, doi: 10.1088/2053-1591/3/10/105601.

[319] M. R. Keshavarz and S. Hassanajili, “Effect of graphene oxide reduction with L-ascorbic acid on electrical conductivity and mechanical properties of graphene oxide-epoxy nanocomposites,” *Iranian Journal of Chemistry & Chemical Engineering-international English Edition*, vol. 40, no. 3, pp. 731–742, 2020, doi: 10.30492/IJCCE.2020.38254.

[320] F. Wang, Z. Jia, W. Su, Y. Shang, and Z. L. Wang, “Adsorption of phenanthrene and 1-naphthol to graphene oxide and L -ascorbic-acid-reduced graphene oxide:

effects of pH and surfactants," *Environmental Science and Pollution Research*, vol. 26, no. 11, pp. 11062–11073, Apr. 2019, doi: 10.1007/s11356-019-04549-9.

[321] Y. Il Na, Y. Il Song, S. W. Kim, and S. J. Suh, "Study on properties of eco-friendly reduction agents for the reduced graphene oxide method," *Carbon Letters*, vol. 24, no. 1, pp. 1–9, Oct. 2017, doi: 10.5714/CL.2017.24.001.

[322] A. Lee *et al.*, "Machine learned synthesizability predictions aided by density functional theory," *Communications Materials 2022 3:1*, vol. 3, no. 1, pp. 1–11, Oct. 2022, doi: 10.1038/s43246-022-00295-7.

[323] R. Zhu, S. I. P. Tian, Z. Ren, J. Li, T. Buonassisi, and K. Hippalgaonkar, "Predicting Synthesizability using Machine Learning on Databases of Existing Inorganic Materials," *ACS Omega*, vol. 8, no. 9, pp. 8210–8218, Mar. 2023, doi: 10.1021/ACSOMEGA.2C04856/ASSET/IMAGES/MEDIUM/AO2C04856_0006.GIF.

[324] S. Kim, J. Noh, G. H. Gu, S. Chen, and Y. Jung, "Predicting synthesis recipes of inorganic crystal materials using elementwise template formulation," *Chem. Sci.*, vol. 15, no. 3, p. 1039, Dec. 2023, doi: 10.1039/D3SC03538G.

[325] N. Méndez-Lozano, F. Pérez-Reynoso, and C. González-Gutiérrez, "Eco-Friendly Approach for Graphene Oxide Synthesis by Modified Hummers Method," *Materials*, vol. 15, no. 20, p. 7228, Oct. 2022, doi: 10.3390/MA15207228.

[326] M. Mohamed, wafaa Eletr, elsayed awad, and S. dahdouh, "GRAPHENE OXIDE SYNTHESIS AND CHARACTERIZATIONS AS A CARBONACEOUS NANOPARTICLE BY USING MODIFIED HUMMERS' METHOD," *Egyptian Journal of Soil Science*, vol. 63, no. 4, pp. 0–0, Dec. 2023, doi: 10.21608/EJSS.2023.225259.1624.

[327] S. N. Alam, N. Sharma, and L. Kumar, "Synthesis of Graphene Oxide (GO) by Modified Hummers Method and Its Thermal Reduction to Obtain Reduced Graphene Oxide (rGO)," *Graphene*, vol. 06, no. 01, pp. 1–18, 2017, doi: 10.4236/GRAPHENE.2017.61001.

[328] G. Santamaría-Juárez, E. Gómez-Barojas, E. Quiroga-González, E. Sánchez-Mora, M. Quintana-Ruiz, and J. D. Santamaría-Juárez, "Safer modified Hummers' method for the synthesis of graphene oxide with high quality and high yield," *Mater. Res. Express*, vol. 6, no. 12, 2019, doi: 10.1088/2053-1591/AB4CBF.

[329] Q. Guo *et al.*, "Pd-Ni alloy nanoparticle/carbon nanofiber composites: preparation, structure, and superior electrocatalytic properties for sugar analysis," *Anal. Chem.*, vol. 86, no. 12, pp. 5898–5905, Jun. 2014, doi: 10.1021/AC500811J.

[330] J. Li, J. Lu, T. C. Zhang, and S. Yuan, “Superhydrophobic DTMS/rGO-nanocomposites modified polyurethane sponge for efficient oil–water separation,” *Surface Engineering*, vol. 39, no. 3, pp. 349–360, 2023, doi: 10.1080/02670844.2023.2217599.

[331] W. T. Yein, Q. Wang, X. Feng, Y. Li, and X. Wu, “Enhancement of photocatalytic performance in sonochemical synthesized ZnO–rGO nanocomposites owing to effective interfacial interaction,” *Environ. Chem. Lett.*, vol. 16, no. 1, pp. 251–264, Mar. 2018, doi: 10.1007/S10311-017-0651-1.

[332] A. M. Golsheikh, “Graphene-based metal/metal sulphide nanocomposites: Fabrication, characterization and its applications / Amir Moradi Golsheikh,” 2014.

[333] F. C. Romeiro, S. C. Silva, E. Nossol, and R. C. Lima, “One step microwave-hydrothermal synthesis of rGO–TiO2 nanocomposites for enhanced electrochemical oxygen evolution reaction,” *New Journal of Chemistry*, vol. 44, no. 17, pp. 6825–6832, May 2020, doi: 10.1039/D0NJ01475C.

[334] M. Palomba, A. Longo, and G. Carotenuto, “Gel-Phase Reduction of Graphene Oxide Coatings by L-Ascorbic Acid,” *Materials Proceedings*, p. 33, Feb. 2020, doi: 10.3390/IOCN2020-07783.

[335] M. Ostermann *et al.*, “l-Ascorbic Acid Treatment of Electrochemical Graphene Nanosheets: Reduction Optimization and Application for De-Icing, Water Uptake Prevention, and Corrosion Resistance,” *ACS Appl. Mater. Interfaces*, vol. 15, no. 18, pp. 22471–22484, May 2023, doi: 10.1021/ACSAMI.2C22854/SUPPL_FILE/AM2C22854_SI_002.PDF.

[336] M. Palomba, G. Carotenuto, and A. Longo, “A Brief Review: The Use of L-Ascorbic Acid as a Green Reducing Agent of Graphene Oxide,” *Materials*, vol. 15, no. 18, p. 6456, Sep. 2022, doi: 10.3390/MA15186456.

[337] M. Schugmann and P. Foerst, “Tailoring Crystallization Kinetics in Thin Sucrose Films during Convective Drying: Impact of Temperature and Humidity on Onset, Growth, and Nucleation Rate,” *Pharmaceutics*, vol. 16, no. 10, p. 1260, Oct. 2024, doi: 10.3390/PHARMACEUTICS16101260.

[338] Y. Yu *et al.*, “Investigation on Nanocomposites of Polysulfone and Different Ratios of Graphene Oxide with Structural Defects Repaired by Cellulose Nanocrystals,” *Polymers (Basel).*, vol. 15, no. 18, p. 3821, Sep. 2023, doi: 10.3390/POLYM15183821.

[339] S. M. Kabeb, “Environmentally Benign High-Performance Composites-Based Hybrid Microcrystalline Cellulose/Graphene Oxide,” *Polym. Adv. Technol.*, vol. 35, no. 10, Oct. 2024, doi: 10.1002/PAT.6610.

[340] Y. Lu, L. M. Santino, S. Acharya, H. Anandarajah, and J. M. D’Arcy, “Studying Electrical Conductivity Using a 3D Printed Four-Point Probe Station,” *J. Chem. Educ.*, vol. 94, no. 7, pp. 950–955, Jul. 2017, doi: 10.1021/ACS.JCHEMED.7B00119.

[341] M. Luckner and G. Wanner, “From Light Microscopy to Analytical Scanning Electron Microscopy (SEM) and Focused Ion Beam (FIB)/SEM in Biology: Fixed Coordinates, Flat Embedding, Absolute References,” *Microscopy and Microanalysis*, vol. 24, no. 5, p. 526, Oct. 2018, doi: 10.1017/S1431927618015015.

[342] C. P. P. Wong, C. W. Lai, K. M. Lee, and S. B. Abd Hamid, “Advanced Chemical Reduction of Reduced Graphene Oxide and Its Photocatalytic Activity in Degrading Reactive Black 5,” *Materials*, vol. 8, no. 10, p. 7118, 2015, doi: 10.3390/MA8105363.

[343] R. Y. N. Gengler *et al.*, “Revealing the ultrafast process behind the photoreduction of graphene oxide,” *Nature Communications 2013 4:1*, vol. 4, no. 1, pp. 1–5, Oct. 2013, doi: 10.1038/ncomms3560.

[344] P. Chaupal and P. Rajendran, “Flexural strength prediction of randomly oriented chopped glass fiber composite laminate using artificial neural network,” *Journal of the Brazilian Society of Mechanical Sciences and Engineering*, vol. 45, no. 3, Mar. 2023, doi: 10.1007/S40430-023-04061-9.

[345] N. Suhermi, Suhartono, S. P. Rahayu, F. I. Prastyasari, B. Ali, and M. I. Fachruddin, “Feature and Architecture Selection on Deep Feedforward Network for Roll Motion Time Series Prediction,” *International Conference on Soft Computing in Data Science*, vol. 937, pp. 58–71, 2018, doi: 10.1007/978-981-13-3441-2_5.

[346] E. Gisleris and A. Serackis, “Enhancing 3D Pose Estimation Accuracy from Multiple Camera Perspectives through Machine Learning Model Integration,” *2023 IEEE 10th Jubilee Workshop on Advances in Information, Electronic and Electrical Engineering (AIEEE)*, 2023, doi: 10.1109/AIEEE58915.2023.10134772.

[347] Y. T. Hsieh, K. Anjum, S. Huang, I. Kulkarni, and D. Pompili, “Neural Network Design via Voltage-based Resistive Processing Unit and Diode Activation Function - A New Architecture,” *Midwest Symposium on Circuits and Systems*, vol. 2021-August, pp. 59–62, Aug. 2021, doi: 10.1109/MWSCAS47672.2021.9531917.

[348] N. F. Razali, I. S. Isa, S. N. Sulaiman, M. K. Osman, N. K. A. Karim, and S. A. Nordin, “Optimization of ReLU Activation Function for Deep-Learning-based Breast Cancer Classification on Mammogram Images,” *2024 IEEE International Conference on Automatic Control and Intelligent Systems (I2CACIS)*, pp. 267–272, 2024, doi: 10.1109/I2CACIS61270.2024.10649623.

[349] J. D. J. Rubio, “Stability Analysis of the Modified Levenberg-Marquardt Algorithm for the Artificial Neural Network Training,” *IEEE Trans. Neural Netw. Learn. Syst.*, vol. 32, no. 8, pp. 3510–3524, Aug. 2021, doi: 10.1109/TNNLS.2020.3015200.

[350] T. K. Kim, “Understanding one-way ANOVA using conceptual figures,” *Korean J. Anesthesiol.*, vol. 70, no. 1, p. 22, Feb. 2017, doi: 10.4097/kjae.2017.70.1.22.

[351] G. P. Jones, C. Stambaugh, N. Stambaugh, and K. E. Huber, “Analysis of variance,” *Translational Radiation Oncology*, pp. 171–177, Jan. 2023, doi: 10.1016/B978-0-323-88423-5.00041-8.

[352] D. K. Roy, T. H. Munmun, C. R. Paul, M. P. Haque, N. Al-Ansari, and M. A. Mattar, “Improving Forecasting Accuracy of Multi-Scale Groundwater Level Fluctuations Using a Heterogeneous Ensemble of Machine Learning Algorithms,” *Water (Basel).*, vol. 15, no. 20, Oct. 2023, doi: 10.3390/W15203624.

[353] S. Murhekar, Y. Kamble, S. Dongre, P. Dasarwar, T. H. Khan, and V. Patil, “Real-Time Traffic Intensity Estimation and Management using Deep Learning Techniques,” *2024 Second International Conference on Networks, Multimedia and Information Technology (NMITCON)*, 2024, doi: 10.1109/NMITCON62075.2024.10698813.

[354] B. Smock, “PubTables-1M: Towards a universal dataset and metrics for training and evaluating table extraction models,” 2021.

[355] R. Laubscher, J. Van Der Merwe, P. Herbst, and J. Liebenberg, “Estimation of Simulated Left Ventricle Elastance Using Lumped Parameter Modelling and Gradient-Based Optimization With Forward-Mode Automatic Differentiation Based on Synthetically Generated Noninvasive Data,” *J. Biomech. Eng.*, vol. 145, no. 2, Feb. 2023, doi: 10.1115/1.4055565.

[356] P. C. Humphreys, K. Daie, K. Svoboda, M. Botvinick, and T. P. Lillicrap, “BCI learning phenomena can be explained by gradient-based optimization,” *bioRxiv*, Dec. 2022, doi: 10.1101/2022.12.08.519453.

[357] W. Chen, Q. Gong, L. Zhang, and M. Yang, “Parameters identification of twelve-phase synchronous generator based on Levenberg-Marquardt algorithm,” *International Conference on Electrical Machines and Systems*, 2008.

[358] V. Andriopoulos and M. Kornaros, “LASSO Regression with Multiple Imputations for the Selection of Key Variables Affecting the Fatty Acid Profile of Nannochloropsis oculata,” *Mar. Drugs*, vol. 21, no. 9, p. 483, Sep. 2023, doi: 10.3390/MD21090483/S1.

[359] A. R. Ramos, R. D. Manalo, H. L. Ong, M. U. Herrera, and M. D. L. Balela, “The Effects of Citric Acid as Crosslinking Agent on Selected Properties of Cassava Starch Films,” *Materials Science Forum*, vol. 1087, pp. 29–34, 2023, doi: 10.4028/P-11UX9I.

[360] M. Cobos, M. J. Fernández, and M. D. Fernández, “Graphene Based Poly(Vinyl Alcohol) Nanocomposites Prepared by In Situ Green Reduction of Graphene Oxide by Ascorbic Acid: Influence of Graphene Content and Glycerol Plasticizer on Properties,” *Nanomaterials*, vol. 8, no. 12, p. 1013, Dec. 2018, doi: 10.3390/NANO8121013.

[361] A. Rahmani, A. Abdulkhani, A. Ashori, and J. Hosseinzadeh, “Development of high-performance biocomposites through lignin modification and fiber reinforcement,” *Sci. Rep.*, vol. 14, no. 1, p. 28932, Dec. 2024, doi: 10.1038/S41598-024-80256-X.

[362] L. Solhi *et al.*, “Understanding Nanocellulose–Water Interactions: Turning a Detriment into an Asset,” *Chem. Rev.*, vol. 123, no. 5, p. 1925, Mar. 2023, doi: 10.1021/ACS.CHEMREV.2C00611.

[363] S. Mallakpour and M. Naghdi, “Application of SiO2 nanoparticles with double layer coverage consist of citric acid and l(+)-ascorbic acid for the production of poly(vinyl chloride)/SiO2 nanocomposite films with enhanced optical and thermal properties,” *Polymer Bulletin*, vol. 73, no. 6, pp. 1701–1717, Jun. 2016, doi: 10.1007/S00289-015-1572-4.

[364] H. Ramezani, M. Haji Ali Koohpayeh, A. Tajedini, G. Ramezani, and A. Mohseni, “Nonlocal stability of curved carbon nanotubes conveying fluid based on Eringen’s nonlocal elasticity theory in a thermomagnetic environment,” *Acta Mech.*, pp. 1–15, 2024.

[365] V. Demchenko *et al.*, “Effect of the type of reducing agents of silver ions in interpolyelectrolyte-metal complexes on the structure, morphology and properties

of silver-containing nanocomposites," *Scientific Reports 2020 10:1*, vol. 10, no. 1, pp. 1–9, Apr. 2020, doi: 10.1038/s41598-020-64079-0.

[366] B. B. Murphy *et al.*, "Vitamin C-reduced graphene oxide improves the performance and stability of multimodal neural microelectrodes," *iScience*, vol. 25, no. 7, p. 104652, Jul. 2022, doi: 10.1016/J.ISCI.2022.104652.

[367] J. Kers, J. Majak, D. Goljandin, A. Gregor, M. Malmstein, and K. Vilsaar, "Extremes of apparent and tap densities of recovered GFRP filler materials," *Compos. Struct.*, vol. 92, no. 9, pp. 2097–2101, Aug. 2010, doi: 10.1016/J.COMPSTRUCT.2009.10.003.